



## **Terms and Conditions of Use of Digitised Theses from Trinity College Library Dublin**

### **Copyright statement**

All material supplied by Trinity College Library is protected by copyright (under the Copyright and Related Rights Act, 2000 as amended) and other relevant Intellectual Property Rights. By accessing and using a Digitised Thesis from Trinity College Library you acknowledge that all Intellectual Property Rights in any Works supplied are the sole and exclusive property of the copyright and/or other IPR holder. Specific copyright holders may not be explicitly identified. Use of materials from other sources within a thesis should not be construed as a claim over them.

A non-exclusive, non-transferable licence is hereby granted to those using or reproducing, in whole or in part, the material for valid purposes, providing the copyright owners are acknowledged using the normal conventions. Where specific permission to use material is required, this is identified and such permission must be sought from the copyright holder or agency cited.

### **Liability statement**

By using a Digitised Thesis, I accept that Trinity College Dublin bears no legal responsibility for the accuracy, legality or comprehensiveness of materials contained within the thesis, and that Trinity College Dublin accepts no liability for indirect, consequential, or incidental, damages or losses arising from use of the thesis for whatever reason. Information located in a thesis may be subject to specific use constraints, details of which may not be explicitly described. It is the responsibility of potential and actual users to be aware of such constraints and to abide by them. By making use of material from a digitised thesis, you accept these copyright and disclaimer provisions. Where it is brought to the attention of Trinity College Library that there may be a breach of copyright or other restraint, it is the policy to withdraw or take down access to a thesis while the issue is being resolved.

### **Access Agreement**

By using a Digitised Thesis from Trinity College Library you are bound by the following Terms & Conditions. Please read them carefully.

I have read and I understand the following statement: All material supplied via a Digitised Thesis from Trinity College Library is protected by copyright and other intellectual property rights, and duplication or sale of all or part of any of a thesis is not permitted, except that material may be duplicated by you for your research use or for educational purposes in electronic or print form providing the copyright owners are acknowledged using the normal conventions. You must obtain permission for any other use. Electronic or print copies may not be offered, whether for sale or otherwise to anyone. This copy has been supplied on the understanding that it is copyright material and that no quotation from the thesis may be published without proper acknowledgement.



**NITRATE-BARBITURATE COMPOUNDS INHIBIT  
MATRIX METALLOPROTEINASE-9 IN IN-VITRO AND IN-  
VIVO MODELS OF INTESTINAL INFLAMMATION**

by

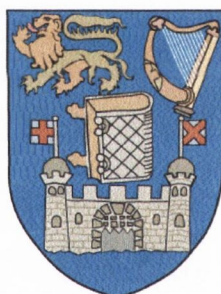
**Shane O'Sullivan**

being a thesis submitted for the degree of Doctor of Philosophy

(Pharmacology)

at

**Trinity College Dublin**



Under the supervision and direction of

**Dr Carlos Medina and Dr John Gilmer**

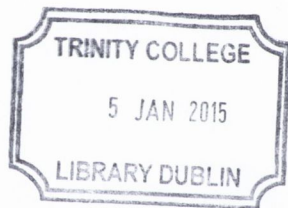
**School of Pharmacy and Pharmaceutical Sciences**

**Trinity College Dublin**

Submitted February 2014

## Declaration

This thesis is submitted by the undersigned to the University of Dublin, Trinity College, for examination for the degree of doctor of philosophy. It has not been submitted as an exercise for a degree at this or any other university. I have carried out all the practical work except where duly acknowledged. I agree that the library may lend or copy this thesis upon request.



*Shane O'Sullivan*

**Shane O'Sullivan**

*Thesis 10793*

## Summary

Inflammatory bowel disease is characterised by a dysregulated immune response and a compromised epithelial barrier. The enzyme matrix metalloproteinase-9 (MMP-9) is upregulated in an inflammatory setting and is believed to contribute to the pathogenesis of the disease. Nitric oxide is a gaseous signalling molecule with an, as of yet, unknown regulatory effect on MMP-9. Organic nitrates have been used as NO donors or mimetics to take advantage of NO's pharmacological effects, but never as part of a hybrid to inhibit an MMP. The aims of my project were to synthesise and test the ability of a series of nitrate-barbiturate compounds to inhibit MMP-9 in both *in-vitro* and *in-vivo* models of intestinal inflammation and to determine the contribution of the nitrate moiety in this inhibition.

The compounds were first tested in TNF- $\alpha$  and IL-1 $\beta$  stimulated Caco-2 cells, where MMP-9 activity was measured by gelatin zymography and the gene expression by qPCR. The effect of the nitrate-barbiturates was compared to both the alcohol-barbiturate analogues and nitrate side-chains to determine the contribution of the nitrate group. The NO-donors SNAP and DETA-NONOate were also tested in the same model. DSS induced colitis in Wistar rats was used to test the *in-vivo* efficacy of the compounds, which were administered twice daily by rectal enema. The disease activity index with histological measures of colitis were used to determine the ability of the compounds to reduce the severity of the inflammation and MMP-9 levels in the distal colon were measured using gelatin zymography and qPCR. TaqMan inflammatory array cards were used to screen for changes in expression of other inflammatory mediators in the colon.

Nitrate-barbiturate hybrids were found to inhibit MMP-9 gene transcription to a greater extent than the alcohol-barbiturates or the nitrate-side chains alone in an *in-vitro* model of



intestinal inflammation. The NO-donors, SNAP and DETA-NONOate, were also capable of inhibiting MMP-9. The inhibition of MMP-9 expression was found to be dependent on cGMP where the sGC inhibitor, ODQ, abolished the effect of the compounds, but the cGMP analogue, 8-Br-cGMP, restored the inhibitory effects of the compounds. In a DSS induced model of colitis in rats, a representative nitrate-barbiturate compound, **1a**, was capable of reducing the severity of the DSS induced colitis as measured by the disease activity index. Histological measures of inflammation were also reduced by compound **1a** and expression of MMP-9 in the distal colon significantly correlated with the level of inflammation. PCR-array cards identified several other genes whose transcription is affected by the compound including KLK7 (kalikrein related peptidase 7), Anxa3 (annexin A3), Pla2g2a (phospholipase A2 group IIA), IL1r11 (interleukin 1 receptor-like 1) and IL1r2 (interleukin 1 receptor 2).

Our results demonstrate the potential for nitrate-barbiturates as MMP inhibitors where the barbiturate scaffold serves as a zinc-binding group and active site inhibitor where the nitrate group can inhibit the expression of MMP-9 in a cGMP dependent manner. The dinitrate-barbiturate **1a** can protect against DSS induced colitis in rats which highlights the compounds potential application in inflammatory bowel disease.

## Table of Contents

List of Figures .....	ix
List of Tables .....	xiii
Acknowledgements.....	xv
List of abbreviations .....	xvi

### **1. Introduction and Background ..... 1**

1.1. Matrix Metalloproteinases .....	1
1.1.1. Structure.....	4
1.1.1.1. Pre-domain .....	4
1.1.1.2. Pro-domain .....	5
1.1.1.3. Catalytic domain.....	5
1.1.1.4. The hinge region.....	6
1.1.1.5. The hemopexin domain .....	7
1.1.2. Regulation of MMPs.....	8
1.1.2.1. Transcriptional regulation .....	8
1.1.2.2. Secretion of MMPs.....	10
1.1.2.3. Activation of MMPs .....	11

1.1.2.4.	Endogenous inhibitors of MMPs.....	13
1.1.3.	Synthetic inhibitors of MMPs.....	15
1.1.3.1.	Hydroxamic Acids.....	17
1.1.3.2.	Newer generation of hydroxamate inhibitors .....	19
1.1.3.3.	Carboxylic acid inhibitors .....	20
1.1.3.4.	Thiol-based inhibitors.....	23
1.1.3.5.	Phosphorous containing inhibitors .....	25
1.1.3.6.	Tetracycline inhibitors.....	27
1.1.3.7.	Barbiturate (pyrimidinetrione) inhibitors .....	28
1.1.3.8.	Non zinc-binding inhibitors.....	30
1.1.3.9.	Other approaches to MMP inhibition.....	33
1.1.4.	Inflammatory bowel disease and the implication of MMPs.....	33
1.1.5.	Pathological implications of MMP-9.....	39
1.1.5.1.	MMP-9 and cardiovascular disease.....	39
1.1.5.2.	MMP-9 and diabetes.....	40
1.1.5.3.	MMP-9 and cancer .....	40
1.1.5.4.	MMP-9 and other diseases .....	41
1.2.	Nitric Oxide.....	42
1.2.1.	The role of NO in IBD .....	45
1.2.2.	NO as therapeutic (nitrate-barbiturate hybrids) .....	46
1.3.	Project aims.....	48



<b>2. Materials and methods .....</b>	<b>50</b>
2.1. Reagents and materials.....	50
2.2. Chemistry Methods .....	50
2.2.1. Synthesis of barbiturate compounds .....	51
2.3. Cell Culture .....	52
2.4. Dextran sulphate sodium (DSS) induced colitis .....	54
2.4.1. Histological assessment of colon samples .....	56
2.4.1.1. Haematoxylin and Eosin (H&E) Stain .....	57
2.4.1.2. Histopathological Scoring .....	58
2.4.1.3. Imaging and crypt length measurements.....	59
2.5. Biological Methods .....	60
2.5.1. MTT assay .....	60
2.5.2. Annexin V flow cytometry .....	61
2.5.3. MMP-2 and MMP-9 fluorogenic assay .....	62
2.5.4. Bradford protein assay .....	63
2.5.5. Gelatin Zymography .....	64
2.5.6. RNA isolation .....	65
2.5.7. RNA quantification.....	66
2.5.8. Reverse transcription .....	67
2.5.9. Real time quantitative polymerase chain reaction (qPCR).....	68

2.5.10.	TaqMan low density array (TLDA) cards.....	71
2.5.11.	Nitrate and nitrite quantification – modified Griess assay .....	75
2.5.12.	NF-κB (p65) binding activity.....	77
2.5.12.1.	Nuclear extraction.....	77
2.5.12.2.	NF-κB (p65) transcription factor assay.....	78
2.6.	Statistical analysis .....	79

### **3. Synthesis and in-vitro assessment of barbiturate based inhibitors. ..82**

3.1.	Introduction and background .....	82
3.1.1.	Selective inhibition of MMP-9 .....	82
3.1.2.	Effects of NO on activation of pro-MMP-9.....	84
3.1.2.1.	NO activates pro-MMP-9.....	84
3.1.2.2.	NO indirectly activates MMP-9 .....	85
3.1.2.3.	NO-mediated inhibition of MMP-9.....	86
3.1.3.	Effect of NO on MMP-9 release and distribution.....	88
3.1.4.	Effect of NO on expression of MMP-9 .....	91
3.1.4.1.	NO inhibits MMP-9 Expression.....	91
3.1.4.2.	NO promotes MMP-9 Expression .....	92
3.1.5.	Understanding the interactions of NO and MMP-9.....	93
3.2.	Results.....	97

3.2.1.	Synthesis of nitrate-barbiturates .....	97
3.2.2.	Effect of the nitrate-barbiturate compounds on cell viability .....	98
3.2.2.1.	MTT assay .....	98
3.2.2.2.	Annexin V flow cytometry .....	102
3.2.3.	Effect of nitrate-barbiturate compounds and corresponding non-nitrates and nitrate side-chains on the expression and activity of MMP-9 .....	105
3.2.3.1.	Effect of the compounds on MMP-9 activity .....	107
3.2.3.2.	Effect of the compounds on MMP-9 expression .....	110
3.3.	Discussion .....	115

**4. NO donors and mechanism of action of nitrate-barbiturate compounds ..... 121**

4.1.	Introduction and background .....	121
4.1.1.	NO, MMP-9 and NF- $\kappa$ B .....	121
4.1.2.	NO, MMP-9 and AP-1 .....	123
4.1.3.	NO, MMP-9 and cGMP/ PKG.....	124
4.1.4.	NO, MMP-9 and MAP Kinases/ PKC .....	127
4.1.5.	NO and its effects on MMP-9 mRNA stability .....	128
4.1.6.	NO-donors .....	131
4.2.	Results .....	135



4.2.1.	The effect of NO-donors on MMP-9 in Caco-2 cells .....	135
4.2.2.	The role of the NF- $\kappa$ B pathway in the downregulation of MMP-9 by the nitrate-barbiturate compounds.....	143
4.2.3.	The role of the cGMP pathway in the downregulation of MMP-9 by the nitrate-barbiturate compounds.....	146
4.3.	Discussion .....	150

## **5. In-vivo assessment of dinitrate-barbiturate and corresponding alcohol-barbiturate and side chain ..... 156**

5.1.	Introduction and background .....	156
5.1.1.	Impact of IBD .....	156
5.1.2.	In-vivo models of IBD .....	157
5.1.2.1.	Chemically induced colitis .....	158
5.1.2.2.	Congenetic or transgenic models of colitis .....	161
5.1.2.3.	Gene KO models of colitis .....	163
5.1.2.4.	Cell transfer models.....	166
5.1.3.	Experimental design .....	166
5.2.	Results.....	169
5.2.1.	Clinical and histological assessment.....	169
5.2.2.	The effect of compound <i>1a</i> on MMP-9 and a gene expression analysis in the distal colon.....	174

5.3. Discussion .....	189
<b>6. Future directions .....</b>	<b>196</b>
<b>7. References .....</b>	<b>199</b>
<b>8. Appendix I .....</b>	<b>235</b>
8.1. Compound characterisation.....	236
8.1.1. 5-(4-phenoxyphenyl)-5-(bis-(2-nitrooxy-ethyl)-amino)pyrimidine- 2,4,6(1H,3H,5H)-trione (1a).....	236
8.1.2. 5-(4-phenoxyphenyl)-5-(bis-(2-hydroxyethyl)-amino)pyrimidine- 2,4,6(1H,3H,5H)-trione (2a).....	236
8.1.3. Bis-(2-nitrooxy-ethyl)-amine (3a) .....	237
8.1.4. 5-(4-phenoxyphenyl)-5-(methyl-(2-nitrooxy-ethyl)-amino)pyrimidine- 2,4,6(1H,3H,5H)-trione (1b) .....	237
8.1.5. 5-(4-phenoxyphenyl)-5-(N-(2-hydroxyethyl-N-methylamino)pyrimidine- 2,4,6(1H,3H,5H)-trione (2b) .....	238
8.1.6. Methyl-(2-nitrooxy-ethyl)-amine (3b).....	239
8.1.7. 5-(4-phenoxyphenyl)-5-(4-(2-nitrooxy-ethyl)piperazin-1-yl)pyrimidine- 2,4,6(1H,3H,5H)-trione (1c).....	239

8.1.8.	5-(4-phenoxyphenyl)-5-(4-(2-hydroxyethyl)piperazin-1-yl)pyrimidine-2,4,6(1H,3H,5H)-trione (2c).....	240
8.1.9.	(2-nitrooxy-ethyl)-piperazine (3c) .....	240
8.1.10.	5-(4-phenoxyphenyl)-5-(4-(2-nitrooxy-ethyl)piperidin-1-yl)pyrimidine-2,4,6(1H,3H,5H)-trione (1d) .....	241
8.1.11.	5-(4-phenoxyphenyl)-5-(4-(2-hydroxyethyl)piperidin-1-yl)pyrimidine-2,4,6(1H,3H,5H)-trione (2d) .....	242
8.1.12.	4-(2-nitrooxy-ethyl)-piperidine (3d) .....	243
8.1.13.	5-(4-phenoxyphenyl)-5-(4-(1-nitrooxy-methyl)piperidin-1-yl)pyrimidine-2,4,6(1H,3H,5H)-trione (1e).....	243
8.1.14.	5-(4-phenoxyphenyl)-5-(4-(hydroxymethyl)piperidin-1-yl)pyrimidine-2,4,6(1H,3H,5H)-trione (2e).....	244
8.1.15.	4-(1-nitrooxy-methyl)-piperidine (3e) .....	245
8.1.16.	5-(4-phenoxyphenyl)-5-(3-(1-nitrooxy-methyl)piperidin-1-yl)pyrimidine-2,4,6(1H,3H,5H)-trione (1f) .....	245
8.1.17.	5-(4-phenoxyphenyl)-5-(3-(hydroxymethyl)piperidin-1-yl)pyrimidine-2,4,6(1H,3H,5H)-trione (2f) .....	246
8.1.18.	3-(1-nitrooxy-methyl)-piperidine (3f).....	247

## **9. Appendix II..... 248**

9.1.	Presentation of work .....	249
9.2.	Publications .....	250



## List of Figures

Figure 1.1: The catalytic domain. ....	6
Figure 1.2: MMP classification according to domains structure.....	8
Figure 1.3: Representation of the regulatory elements in the promoter regions of human MMP genes drawn in the direction of 5'-3'. ....	10
Figure 1.4: Diagram representing MMP-9 activation by other MMPs.....	12
Figure 1.5: Representation of Batimastat binding to an MMP .....	16
Figure 1.6: Factors in the pathogenesis of IBD .....	36
Figure 1.7: Summary of cells involved in release of MMPs in the gut. ....	38
Figure 1.8: Biological reactions of NO.....	44
Figure 2.1: Layout of rat inflammatory array card with gene symbols. ....	73
Figure 3.1: Synthesis of bromide intermediate.. ....	83
Figure 3.2: Preparation of the nitrate side-chains using the commercially available corresponding alcohols. ....	97
Figure 3.3: Preparation of 5-phenoxyphenyl barbiturate-5-aminoalkyl nitrates (1a-f) and aminoalkylalcohols (2a-f). ....	98
Figure 3.4: Cleavage of MTT by mitochondrial enzymes.....	99
Figure 3.5: MTT assay of nitrate-barbiturate compounds.. ....	100
Figure 3.6: MTT assay of alcohol-barbiturate compounds.....	101
Figure 3.7: Representative traces from annexin V flow cytometry analysis with nitrate- barbiturate compounds at 10 $\mu$ M in Caco-2 cells.....	102

Figure 3.8: Histogram of Annexin V flow cytometry in Caco-2 cells..	103
Figure 3.9: Representative traces from annexin V flow cytometry analysis with nitrate-barbiturate compounds at 10 $\mu$ M.....	104
Figure 3.10: Histogram of Annexin V flow cytometry in HT1080 cells.....	105
Figure 3.11: Gelatin-zymography of conditioned media from Caco-2 cells treated with the nitrate-barbiturate compounds (1 a-f).....	108
Figure 3.12: Gelatin-zymography of conditioned media from Caco-2 cells treated with the alcohol-barbiturate compounds (2 a-f) .....	109
Figure 3.13: Gelatin-zymography of conditioned media from Caco-2 cells treated with the nitrate side-chains (3 a-f). .....	110
Figure 3.14: Relative quantitation of MMP-9 mRNA following treatment with nitrate-barbiturate compounds.....	112
Figure 3.15: Relative quantitation of MMP-9 mRNA following treatment with alcohol-barbiturate compounds.....	113
Figure 3.16: Relative quantitation of MMP-9 mRNA following treatment with nitrate side chains. ....	114
Figure 3.17: Intestinal epithelial cells play an important role in chronic inflammation....	116
Figure 4.1: Activation of the NF- $\kappa$ B pathway..	122
Figure 4.2: NO and the activation of the cGMP pathway .....	125
Figure 4.3: Representation of some of the pathways involved in the transcriptional upregulation of MMP-9 and the possible impacts of NO and peroxynitrite (ONOO <sup>-</sup> )..	130
Figure 4.4: Crude classification of NO-donors according to pathway of NO generation..	131
Figure 4.5: The effects of SNAP on MMP-9 potential activity from Caco-2 cells .....	135

Figure 4.6: Relative quantitation of MMP-9 mRNA following treatment with SNAP.....	136
Figure 4.7: Measurements of nitrate and nitrite concentrations as breakdown products of NO by the Griess assay on the conditioned media of Caco-2 cells after 24 hours with SNAP .....	137
Figure 4.8: The effects of DETA-NONOate on MMP-9 potential activity from Caco-2 cells. ....	138
Figure 4.9: Relative quantitation of MMP-9 mRNA following treatment with DETA-NONOate .....	139
Figure 4.10: Measurements of nitrate and nitrite concentrations as breakdown products of NO by the Griess assay on the conditioned media of Caco-2 cells after 24 hours with DETA-NONOate .....	140
Figure 4.11: Expression of iNOS and NO <sub>x</sub> <sup>-</sup> production following treatment of Caco-2 cells with the nitrate-barbiturates (1a-f) at 10μM .....	142
Figure 4.12: p65 nuclear binding .....	144
Figure 4.13: Relative quantitation of mRNA of RelA, IκBKG and NF-κB1 following treatment with nitrate-barbiturate compounds.....	145
Figure 4.14: MMP-9 gelatin zymography (left) and qPCR (right) following co-incubation of stimulated Caco-2 cells with nitrate-barbiturates and ODQ.....	147
Figure 4.15: MMP-9 gelatin zymography (left) and qPCR (right) following co-incubation of stimulated Caco-2 cells with nitrate-barbiturates, ODQ and 8-Br-cGMP.. .....	148
Figure 5.1: Experimental design.....	167
Figure 5.2: Progression of disease activity over the course of the experiment as measured by the DAI. ....	169



Figure 5.3: Representative images of H&E stained distal colon samples from four different animals from each group.....	171
Figure 5.4: Histological measures of inflammation.....	172
Figure 5.5: Correlations of histological measures of inflammation and the DAI scores...	173
Figure 5.6: Gene expression and activity of MMP-9 in the distal colon.....	174
Figure 5.7: Correlation of MMP-9 activity and expression with DAI score and histological scores of inflammation.....	175
Figure 5.8: Gene expression and activity of TNF- $\alpha$ and IL-1 $\beta$ in the distal colon.....	177
Figure 5.9: Correlation matrix of samples used in gene profiling experiment.....	178
Figure 5.10: Heatmap of expression profiles of distal colon samples with clustering of samples and genes.....	180
Figure 5.11: Venn diagrams of commonly downregulated genes. ....	182
Figure 5.12: Venn diagrams of commonly upregulated genes. ....	183
Figure 5.13: Relative quantitation of mRNA of genes commonly upregulated in the sham and 1a treated group compared to the DSS group. ....	184
Figure 5.14: Correlation of $\Delta C_T$ values of MMP-9 and KLK7 and KLK7 $\Delta C_T$ values with DAI score.....	185
Figure 5.15: Relative quantitation of mRNA of genes commonly downregulated in the sham and 1a treated group compared to the DSS group.....	186
Figure 5.16: Graphs of genes where the 1a group is statistically significantly downregulated compared with the DSS group and correlation with MMP-9 $\Delta C_T$ value ..	187



## List of Tables

Table 1.1: Classification of MMPs .....	4
Table 1.2: A summary of endogenous inhibitors of MMPs .....	15
Table 1.3: Early hydroxamic acid based MMP inhibitors .....	18
Table 1.4: Newer generation of hydroxamate based MMP inhibitors.....	19
Table 1.5: Carboxylic acid based MMP inhibitors. ....	22
Table 1.6: Thiol based MMP inhibitors.....	24
Table 1.7: Phosphorous containing MMP inhibitors .....	26
Table 1.8: Tetracycline MMP inhibitors.....	28
Table 1.9: Barbiturate MMP inhibitors.....	30
Table 1.10: Non zinc-binding MMP inhibitor. ....	32
Table 2.1: Criteria for scoring DAI .....	55
Table 2.2: Criteria for scoring of tissue inflammation.....	58
Table 2.3: Criteria for scoring of crypt damage.....	59
Table 2.4: Components of High Capacity cDNA Reverse Transcription kit and volumes required per reaction. ....	68
Table 2.5: Components of TaqMan gene expression assay and volumes per well. ....	69
Table 2.6: Gene symbols and assay IDs of TaqMan gene expression assays used. ....	70
Table 2.7: Master mix and sample components per reservoir .....	71
Table 2.8: Assay ID and gene symbol for the assays pre-loaded onto the TaqMan Rat inflammation array cards .....	75
Table 3.1: Studies of the effects of NO on activation or expression of MMP-9 .....	96
Table 3.2: IC <sub>50</sub> values (nM) with 95% confidence interval for nitrate-barbiturate hybrids (1a-f) and alcohol-barbiturates (2a-f). ....	106

Table 4.1: Representations of commonly used NO-donor compounds and their expected half-lives. ....	134
Table 5.1: Models of chemically induced colitis with features.. ....	159
Table 5.2: Models of congenic or transgenic colitis with features.....	162
Table 5.3: Models of gene KO colitis with features. ....	164

## Acknowledgements

I would firstly like to thank Dr Carlos Medina and Dr John Gilmer whom I consider myself very fortunate to have had as supervisors. I appreciate you taking me on as a PhD student and giving me the opportunity to undertake this research project. I feel very lucky to have been able to join the group and your positivity, support and guidance on all matters has made this a hugely enjoyable experience.

I would like to acknowledge Dr Maria Jose Santos-Martinez and Dr Jun Wang for all their help with my experiments, day to day issues and making the lab a nice place to work. I would also like to recognise the help of Dr Shona Harmon, Dr Lorraine O'Driscoll, Dr Marek Radomski, Dr Neil Docherty and Dr Noreen Boyle with various technical aspects of the project as well as all the students that I worked with over the past few years. My thanks also go to all the technical and administrative staff of the school of pharmacy and pharmaceutical sciences.

My gratitude goes to all the past and present students of the school who have been my friends and have made it the last few years enjoyable and memorable.

I would like to thank my girlfriend Maggie for all her support and for being the holiday in my week.

I would finally like to thank my parents for encouraging me to do what I wanted and their continuous support with everything since. It is greatly appreciated.

## List of abbreviations

ADAM	A disintegrin and metalloproteinase
ADAMT	A disintegrin and metalloproteinase with thrombospondin motifs
AGRE	AG rich element
ALDH-2	Mitochondrial aldehyde dehydrogenase
ALOX12	Arachidonate 12 lipoxygenase
AMPA	Aminophenylmercuric acetate
AP	Activator protein
ARE-BP	ARE-binding proteins
AREs	Adenylate and uridylate-rich elements
bFGF	Basic fibroblast growth factor
bp	Base pair
bZIP	Basic region-leucine zipper proteins
C/EBP	CCAAT-enhancer-binding protein
CBFA1	Core binding factor 1
CD	Crohn's disease
cGMP	Cyclic guanosine monophosphate
CI	Confidence interval
CIZ	CAS interacting zinc-finger protein
CMTs	Chemically modified tetracyclines
COX	Cyclooxygenase
CREB	Cyclic AMP response-element binding protein
C <sub>T</sub>	Threshold cycle



CTFB	Complete transcription factor binding assay buffer
CV	Cardiovascular
DAI	Disease activity index
ddH <sub>2</sub> O	Double distilled water
DEA NONOate	Diethylamine NONOate
DETA-NONOate	Diethylene triamine NONOate
dNTP	Deoxyribonucleotide triphosphate
DSS	Dextran sulfate sodium
DTH	Delayed-type hypersensitivity
DTT	Dithiothreitol
ECM	Extracellular Matrix
EGF	Epidermal-growth factor
EGR1	Early growth response-1
ELISA	Enzyme Linked Immunosorbent Assay
EMMPRIN	Extracellular matrix metalloproteinase inducer
EMSA	Electrophoretic mobility shift assay
eNOS	Endothelial NOS
ERK	Extracellular signal-regulated kinase
ESI-MS	Electrospray ionization mass spectrometry
FACS	Fluorescence-activated cell sorting
FBS	Foetal bovine serum
GPI	Glycosylphosphatidylinositol
GSNO	S-nitrosoglutathione
GST	Glutathione S-transferase
GTN	Glyceryl trinitrate

H&E	Haematoxylin and eosin
HGF	Hepatocyte growth factor
HMF	Hazardous materials facility
HMG-CoA	3-hydroxy-3-methylglutaryl coenzyme A
HRP	Horseradish peroxidase
IBD	Inflammatory bowel disease
ICAM-1	Intercellular adhesion molecule-1
IEC	Intestinal epithelial cell
IFN	Interferon
IKK	I $\kappa$ B kinase
IL	Interleukin
iNOS	Inducible NOS
IR	Infrared
ISE	Immortalization-sensitive elements
ISMN	Isosorbide mononitrate
I $\kappa$ B	Inhibitor of $\kappa$ B
JAK	Janus kinase
JNK	c-Jun N-terminal kinase
kb	Kilobase
KLK	Kalikrein
KO	Knock out
KRE	Keratinocyte differentiation-factor responsive element
LADH	Liver alcohol dehydrogenase
LC	Liquid chromatography
LFA-1	Leukocyte function-associated antigen-1

LPS	Lipopolysaccharide
LRP	Low density lipoprotein receptor-related protein
MAPKs	Mitogen activated protein kinases
MEM	Minimum Essential Media
MHC	Major histocompatibility complex
MKK	MAPK kinases
MKKK	MKK kinases
MKP-1	Mitogen activated protein kinase phosphatase-1
MMPI	MMP inhibitors
MMPs	Matrix metalloproteinases
MP	Melting point
mRNA	Messenger ribonucleic acid
MSS	Musculoskeletal syndrome
MT-MMPs	Membrane type-MMPs
MUC	Mucin
MW	Molecular weight
NADPH	Nicotinamide adenine dinucleotide phosphate
NED	N-1-(naphthyl) ethylenediamine
NF- $\kappa$ B	Nuclear Factor-kappa B
NMR	Nuclear magnetic resonance
nNOS	Neuronal NOS
NO	Nitric oxide
NOS	Nitric oxide synthase
ODQ	1H-[1,2,4]oxadiazolo[4,3-a]quinoxalin-1-one
PAI-1	Plasminogen activator inhibitor-1

PBS	Phosphate buffered saline
PCPE	Procollagen C-terminal proteinase enhancer protein
PDE	Phosphodiesterases
PDGF	Platelet-derived growth factor
PEA3	Polyomavirus enhancer-A-binding –protein-3
PI	Propidium iodide
PI 3-kinase	Phosphatidylinositide 3-kinases
PKA	Protein Kinase A
PKC	Protein kinase C
PKG	Protein Kinase G
PLA2	Phospholipase A2
PS	Phosphatidylserine
Ptger2	Prostaglandin E receptor 2
Ptgir	Prostaglandin I2 receptor
PTGS2	Prostaglandin endoperoxide synthase 2
qPCR	Quantitative polymerase chain reaction
RARE	Retinoic-acid response element
RCE	Retinoblastoma control element
RECK	Reversion-inducing cysteine-rich protein with Kazal motifs
ROS	Reactive oxygen species
RPHPLC	Reverse phase high performance liquid chromatography
RT	Room temperature
sGC	Soluble guanylate cyclase
siRNA	Small interfering RNA
SNAP	<i>S</i> -Nitroso- <i>N</i> -acetylpenicillamine



SNP	Single neucleotide polymorphism
SOC	Store-operated calcium entry
SOD	Superoxide dismutase
SP	Specificity protein
SAPK	Stress activated protein kinase
SPRE	Stromelysin-1 platelet-derived growth factor- $\beta$ responsive element
STAT	Signal transducer and activator of transcription
TACE	TNF- $\alpha$ converting enzyme
TATA	TATA-box
TBS	Translocation-ETS-leukaemia binding site
TBXAS1	Thromboxane A synthase 1
TCF	T-cell factor
Tg	Transgenic
TGF	Transforming growth factor
TIE	Transforming growth factor- $\beta$ inhibitory element
TIMP	Tissue inhibitor of metalloproteinase
TLC	Thin layer chromatography
TNBS	Trinitrobenzene sulfonic acid
TNF	Tumor necrosis factor
TPA	12- <i>O</i> -Tetradecanoylphorbol-13-acetate
TSP	Thrombospodin
UC	Ulcerative colitis
UTR	Untranslated region
VCAM-1	Vascular cell adhesion molecule-1
VEGFR1	Vascular endothelial growth factor receptor-1

VLA-4	Very late antigen 4
WT1	Wilms tumor 1
ZBG	Zinc-binding group
ZBP-89	89kDa zinc-binding protein

## **Chapter 1: Introduction and background**

# 1. Introduction and Background

## 1.1. Matrix Metalloproteinases

Matrix metalloproteinases (MMPs) are a group of structurally similar endopeptidases with a  $Zn^{2+}$  ion in the active site. All are capable of digesting components of the extracellular matrix including collagens, laminins, fibronectin, elastin, and proteoglycans. MMPs play a key role in controlling homeostasis of all extracellular matrix (ECM) proteins. They regulate cell function, growth and division, host defences, ECM synthesis, morphogenesis, wound healing, tissue repair, skeletal formation, apoptosis, as well as cleavage of transmembrane proteins and bioactive molecules. Dysregulation of the MMPs has been implicated in tumour angiogenesis, invasion and metastasis, inflammatory bowel disease (IBD), arthritis, atherosclerosis, respiratory and heart disease and may also play other diverse pathological roles [1-6].

The first study of an MMP was in 1967 where a collagenase was reported in the metamorphosis of a tadpole to frog. At the time, as the paper noted, "there is little evidence in animal tissues for specific enzyme systems functioning in the removal of particular structural components" [7]. From that point until 2014, the study of MMPs has grown hugely year upon year with more and more diverse implications. The search term "matrix metalloproteinase" in pubmed now yields nearly 44,000 results.

At present, 24 human MMPs have been discovered, five of which are a shorter isoform [8, 9]. MMPs can digest almost all components of the ECM and were historically classified



according to the substrate preference. This grouped the enzymes as collagenases, gelatinases, stromelysins and matrilysins; however, this classification is now viewed as somewhat arbitrary due to overlapping substrate specificities [1, 10]. The MMPs are given a sequential numbering system and are now often grouped according to their domain structure [1, 5, 11] as shown in Table 1.1. Closely related to the MMPs are the families of metalloendopeptidases the ADAMs (a disintegrin and metalloproteinase) and the ADAMTs (a disintegrin and metalloproteinase with thrombospondin motifs), whose members play important roles in development, cell signalling and contribute to pathologies such as inflammation and cancer [12].

<b>MMP Designation</b>	<b>Structural class</b>	<b>Common Name</b>
<b>MMP-1</b>	Simple hemopexin domain	Collagenase-1, interstitial collagenase, fibroblast collagenase, tissue collagenase
<b>MMP-2</b>	Gelatin-binding	Gelatinase-A, 72-kDa gelatinase, 72-kDa type IV collagenase, neutrophil gelatinase
<b>MMP-3</b>	Simple hemopexin domain	Stromelysin-1, transin-1, proteoglycanase, procollagenase-activating protein
<b>MMP-7</b>	Minimal domain	Matrilysin, matrin, PUMP1, small uterine metalloproteinase
<b>MMP-8</b>	Simple hemopexin domain	Collagenase-2, neutrophil collagenase, PMN collagenase, granulocyte collagenase
<b>MMP-9</b>	Gelatin-binding	Gelatinase B, 92-kDa gelatinase, 92-kDa type IV collagenase
<b>MMP-10</b>	Simple hemopexin domain	Stromelysin-2, transin-2
<b>MMP-11</b>	Furin-activated and secreted	Stromelysin-3
<b>MMP-12</b>	Simple hemopexin domain	Metalloelastase, macrophage elastase, macrophage metalloelastase
<b>MMP-13</b>	Simple hemopexin domain	Collagenase-3
<b>MMP-14</b>	Transmembrane	MT1-MMP, MT-MMP1
<b>MMP-15</b>	Transmembrane	MT2-MMP, MT-MMP2
<b>MMP-16</b>	Transmembrane	MT3-MMP, MT-MMP3
<b>MMP-17</b>	GPI-linked	MT4-MMP, MT-MMP4
<b>MMP-18</b>	Simple hemopexin domain	Collagenase-4 (Xenopus; no human homologue known)
<b>MMP-19</b>	Simple hemopexin domain	RASI-1, MMP-18
<b>MMP-20</b>	Simple hemopexin domain	Enamelysin
<b>MMP-21</b>	Vitronectin-like insert	Homologue of Xenopus XMMP
<b>MMP-22</b>	Simple hemopexin domain	CMMP (chicken; no human

		homologue known
<b>MMP-23</b>	Type II transmembrane	Cysteine array MMP (CA-MMP), femalysin, MIFR, MMP-21/MMP22
<b>MMP-24</b>	Transmembrane	MT5-MMP, MT-MMP5
<b>MMP-25</b>	GPI-linked	MT6-MMP, MT-MMP6, leukolysin
<b>MMP-26</b>	Minimal domain	Endometase, matrilysin-2
<b>MMP-27</b>	Simple hemopexin domain	
<b>MMP-28</b>	Furin-activated and secreted	Epilysin
<b>No designation</b>	Simple hemopexin domain	Mcol-A (Mouse)
<b>No designation</b>	Simple hemopexin domain	Mcol-B (Mouse)
<b>No designation</b>	Gelatin-binding	75-kDa gelatinase (chicken)

Table 1.1: Classification of MMPs including sequential numbering, domain structure or common names. Adapted from [11].

### 1.1.1. Structure

While the members of the MMP family are structurally different, they share many similarities. They all possess a pre-domain, a pro-domain, a conserved catalytic domain, and with the exception of MMP-7, MMP-23 and MMP-26, a hemopexin-like domain which is linked to the catalytic domain by a short linker or hinge region [13]. The domain structures of the main groups of MMPs are shown in Figure 1.2. Most of the MMPs are secreted, but the membrane-type-MMPs (MT-MMPs) are associated with the cell membrane as a type I transmembrane protein [14] or a glycosylphosphatidylinositol (GPI)-anchored protein [15, 16].

#### 1.1.1.1. Pre-domain

All the MMPs contain an N-terminal pre-domain which is required for their correct secretion [5]. This pre-domain is viewed as a signalling domain which directs the protein



synthesis towards the endoplasmic reticulum and is subsequently cleaved prior to secretion of the enzyme [11].

#### **1.1.1.2. Pro-domain**

The pro-domain of about 80 amino acids is also conserved in all MMPs with the exception of MMP-23 and remains unchanged following post-translational processing and secretion [13]. This pro-domain maintains the MMP in a latent form and is secreted as an inactive zymogen. A thiol group from a cysteine residue in the pro-domain, part of a consensus sequence PRCGXPD, coordinates with the  $Zn^{2+}$  ion in the catalytic domain and confers latency. Disruption of this thiol bond and replacement with a water molecule results in a catalytically active enzyme and is known as the "cysteine switch" [17, 18].

#### **1.1.1.3. Catalytic domain**

All members of the MMP family possess a catalytic domain of about 165 – 170 amino acids which is essential for proteolysis [13, 19]. It contains a defining zinc atom coordinated by three histidine residues as part of a consensus sequence HExxHxxGxxH and also a strictly conserved methionine-containing tight 1,4 beta turn forming a hydrophobic cleft for the catalytic zinc ion which is known as the "Met turn" [20]. The significance of this Met turn is unknown, however, serine or leucine mutants show unchanged proteolytic efficiency or structural integrity [21]. This catalytic domain is made up of a five stranded  $\beta$ -sheet (four parallel and one anti-parallel) and two or three  $\alpha$ -helices forming an "open sandwich" [22, 23] with two or three calcium ions bound for stability and correct architecture [2, 19, 24].



The structure of the domain varies slightly in groove depth as well as the depth and accessibility of six side pockets along the side of the central cleft of the catalytic domain. These pockets flank the  $Zn^{2+}$  ion and are referred to as unprimed or left-handed pockets with the designations S3, S2 and S1 and primed or right handed pockets with the designations S1', S2' and S3'. The S1' pocket has the greatest variation amongst the MMPs in both depth and amino acid make-up, whereas the S2' and S3' are more solvent exposed [25]. These differences account in part for the differing substrate specificities [13, 26].

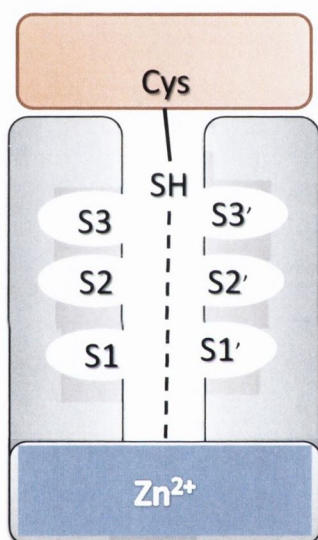


Figure 1.1: The catalytic domain. Simplified representation of the catalytic domain with six-side pockets and the catalytic zinc ion. The pro-peptide domain, which confers latency, blocks the active site cleft and is held in place through bonding of a conserved cysteine residue and the zinc ion. The enzyme is activated through disruption of this bond or partial or complete cleavage of the pro-domain.

#### 1.1.1.4. *The hinge region*

The hinge region of the MMPs usually links the catalytic domain to the hemopexin domain and so is absent in MMP-7, MMP-23 and MMP-26, which have no hemopexin domain and MMP-21, whose catalytic domain is connected to the hemopexin domain without a linker

[27]. It is a potentially flexible proline rich section that is variable in length. The exact function of the region is not fully understood but it does appear to be more than just a linker. Its involvement in collagen binding and destabilisation has been hypothesised [28]. Replacement of the proline to alanine residues in the hinge region in mutant variants shows collagenolytic activity drop to 1.5% and a reduction in stability [29]. Further mutant studies illustrate the hinge region's involvement in correct autocatalytic processing of MT1-MMP [30].

#### **1.1.1.5. The hemopexin domain**

The C-terminal domain is present in most MMPs with the exception of the matrilysins (MMP-7, MMP-26) and MMP-23 [11]. It consists of a 200 amino acid peptide making up a four blade propeller structure stabilised by a disulphide bond. The four blades of the propeller are made up of antiparallel, four-stranded  $\beta$  sheets arranged around a hollow which contains a number of calcium and chloride ions [13]. The primary functions of the domain are believed to be substrate recognition and binding [31]. Collagenolytic activity of MMP-1 has been shown to require the hemopexin domain where the C-terminal contributes to the collagen cleavage specificity along with the catalytic domain [32]. It has also been shown that tissue inhibitor of metalloproteinase (TIMP) binding to MMP-1 is, in part, dependent on the hemopexin domain [33]. While binding of TIMPs to MMPs is at the N-terminal, the rate of this binding has been shown to be dependent on initial interactions of the TIMPs with the C-terminal [34]. Similarly, the cell surface activation of certain MMPs including MMP-2 and MMP-13 is dependent on the presence of the hemopexin domain [13]. It can also interact with integrins on the cell surface to anchor MMPs and has been shown to trigger anti-apoptotic signalling pathways in B-cell chronic lymphocytic leukaemia [35].

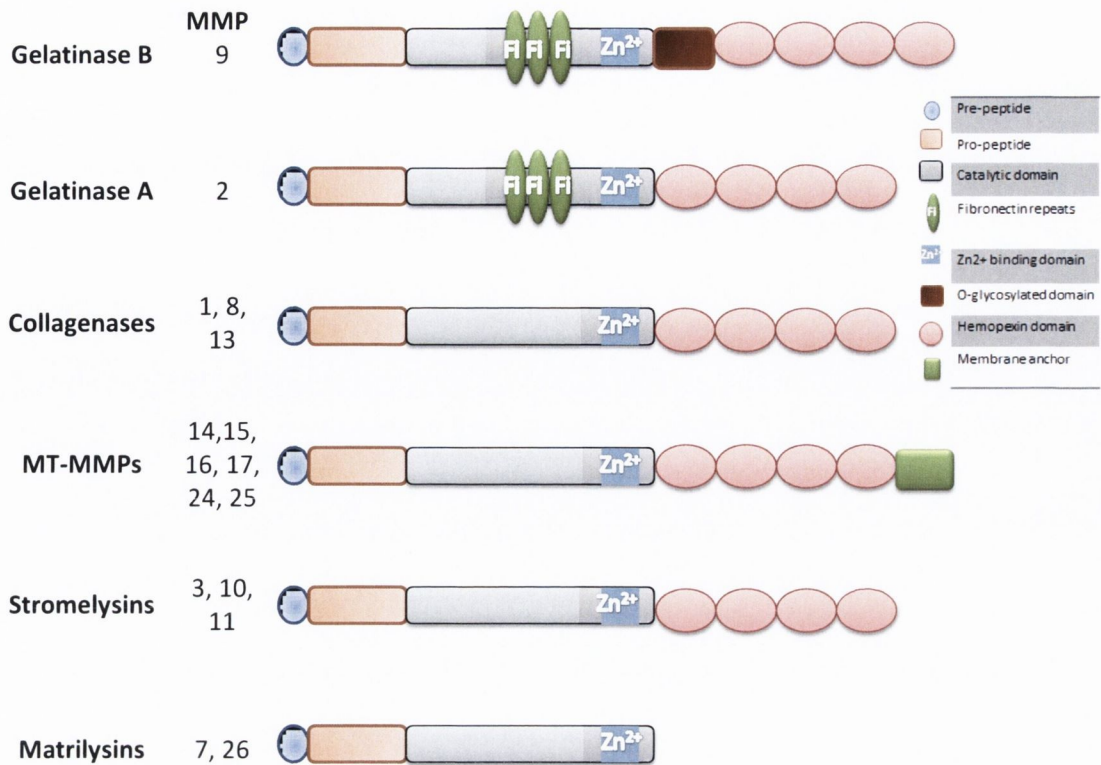


Figure 1.2: MMP classification according to domains structure. The main structural domains of the MMPs are shown, many of which are conserved for all MMPs including the pre and pro-peptide, and catalytic domain. Adapted from [1] and [36].

### 1.1.2. Regulation of MMPs

MMPs are all differentially regulated at multiple levels including transcription, secretion, activation, as well as cell surface and inhibitor interactions.

#### 1.1.2.1. Transcriptional regulation

With the notable exception of the constitutively expressed MMP-2 [37], *De novo* synthesis of large amounts of MMPs can be rapidly induced by various factors including epidermal-growth factor (EGF), platelet-derived growth factor (PDGF), hepatocyte growth factor



(HGF), basic fibroblast growth factor (bFGF), transforming growth factor (TGF- $\alpha$  and  $\beta$ ), amphiregulin, tumor necrosis factor (TNF-  $\alpha$ ), interleukin (IL-1  $\alpha$  and  $\beta$ , 2, 8, 15, 17), interferon (IFN- $\alpha$  and  $\gamma$ ), RANTES, bacterial lipopolysaccharide (LPS) and phorbol esters (e.g. PMA) [38-41]. Physical interactions of certain cells with the ECM or other cells can also induce MMP expression and have been shown to be mediated through extracellular matrix metalloproteinase inducer (EMMPRIN)(Basigin)[42], various integrins [43], leukocyte function-associated antigen-1 (LFA-1) interaction with intercellular adhesion molecule-1 (ICAM-1) [44], very late antigen 4 (VLA-4) interaction with vascular cell adhesion molecule-1 (VCAM-1) [45] and gp39-CD40 interaction [46]. Mechanical stress and alterations in cell shape have also been implicated in transcriptional upregulation of some MMPs. The transcription of each MMP is independently controlled depending on the cell type, the stimulating factors and therefore the signal transduction pathways that are activated, although many MMPs share common cis-acting elements in their promoter and are co-expressed. One of the main group of signalling molecules involved are the mitogen activated protein kinases (MAPK) which are made up of c-Jun N-terminal kinases (JNK) 1/2, extracellular signal regulated kinase (ERK) 1/2 and p38. These may induce or inhibit synthesis depending on the cell type [47]. Many of these signalling pathways converge at Jun and Fos oncoprotein activation which heterodimerize to bind to the activator protein-1 (AP-1) binding site which accounts for a general mechanism of MMP upregulation [8, 11]. Variation in transcription may be accounted for by the combination of factors binding in MMP promoters. ETS oncoproteins bind to PEA3 sites [48], Nuclear Factor-kappa B (NF- $\kappa$ B), specificity protein (SP)-1, Janus kinase/signal transducer and activator of transcription (JAK/STAT) and Smad are some of the contributors to MMP transcriptional regulation [47] which are laid out in Figure 1.3.



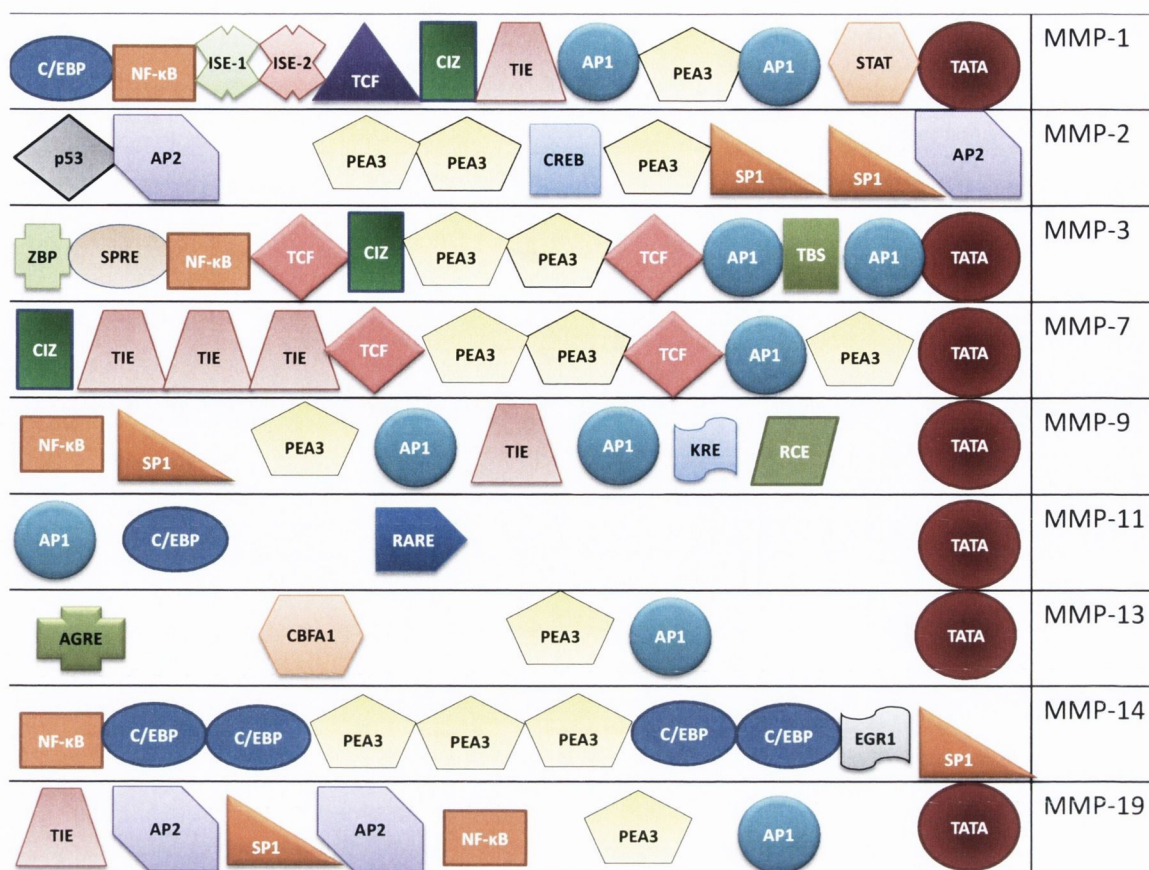


Figure 1.3: Representation of the regulatory elements in the promoter regions of human MMP genes drawn in the direction of 5'-3' and adapted from [8]. AG rich element (AGRE), activator proteins (AP)-1 and 2, core binding factor 1 (CBFA1), CCAAT-enhancer-binding protein (C/EBP), CAS interacting zinc-finger protein (CIZ), cyclic AMP response-element binding protein (CREB), early growth response-1 (EGR1), immortalization-sensitive elements (ISE)-1, and -2, keratinocyte differentiation-factor responsive element (KRE), NF-κB, polyomavirus enhancer-A-binding-protein-3 (PEA3), retinoic-acid response element (RARE), retinoblastoma control element (RCE), stromelysin-1 platelet-derived growth factor-β responsive element (SPRE), signal transducer and activator of transcription (STAT), TATA-box (TATA), translocation-ETS-leukaemia binding site (TBS), T-cell factor (TCF) site, transforming growth factor-β inhibitory element (TIE), binding site for 89kDa zinc-binding protein (ZBP-89).

### 1.1.2.2. Secretion of MMPs

While most MMPs are constitutively secreted upon synthesis, there are some notable exceptions. Neutrophils synthesise and store MMP-9 and MMP-8 in tertiary granules which then release within an hour upon stimulation [49] which is in contrast to other cell types where stimulation of the cell results in transcriptional upregulation of the enzyme and a lag of 6-12 hours before release of MMP-9 [36]. Macrophages can also secrete MMP-12 following protein kinase C (PKC) stimulation by thrombin or plasmin without altering the rate of transcription through pre-formed MMP-12 release [50].

### 1.1.2.3. *Activation of MMPs*

Like many other proteases, MMPs are secreted in the "pro" form as inactive zymogens. Latency is conferred by the pro-domain which masks the active-site cleft and prevents hydration of the catalytic zinc ion. An interaction of a sulphhydryl group on a conserved cysteine residue in the pro-domain and the zinc ion forms this "cysteine switch" [17, 51]. Activation of the enzyme therefore requires either proteolytic removal of the propeptide domain, or disruption of the zinc-cysteine bond. The zinc ion then interacts with a water molecule which can attack the peptide bonds of MMP targets [18]. Activation of MMPs can be carried out by multiple mechanisms, where it is common that the activated protease may, in turn, activate the zymogen of its activator [52]. The most common activators of MMPs are proteases such as serine proteinases, plasmin, trypsin, chymase, and other MMPs [8], but also by conformational perturbants such as heat denaturation, substrate binding, heavy metals and organomercurials such as aminophenylmercuric acetate (APMA), oxidants and alkylating agents [18, 53-56]. Most MMPs are activated outside the cell however, MMP-11, MMP-28 and the MT-MMPs can be activated by intracellular furin-like serine proteases before reaching the cell surface [57, 58]. An interesting example of MMP activation is that of the gelatinases. In this cascade, tissue inhibitor of metalloproteinase (TIMP)-2 binds and inhibits MT1-MMP with its N-terminal domain and the C-terminal domain of the same TIMP-2 molecule binds the hemopexin-like domain of pro-MMP-2 forming a ternary complex [59, 60]. A free adjacent MT1-MMP then cleaves an Asn<sup>37</sup>-Leu<sup>38</sup> bond on a surface exposed loop of the pro-domain known as a "bait" region to release a 64kDa intermediate [61]. This intermediate is then further processed through cleavage of the Asn<sup>80</sup>-Tyr<sup>81</sup> bond by an activating enzyme such as MMP-3, MMP-1, MMP-7 or an already activated MMP-2 [62]. There is evidence to suggest that the urokinase plasminogen activator (uPA) can activate several pro-MMPs including pro-



MMP-2, 3, 9, 13 [63-66]. Binding of uPA to its receptor uPAR causes plasminogen to be cleaved to plasmin which in turn cleaves pro-MMP-3 [62, 67]. MMP-3 can then activate pro-MMP-9 as shown in Figure 1.4. In addition, thrombin has been shown to induce MMP-9 activation and association with  $\beta$ 1-integrin in a human osteosarcoma cell line through a phosphatidylinositide 3-kinase (PI-3K) -dependent pathway is a key step in thrombin-induced tumour invasion [68].

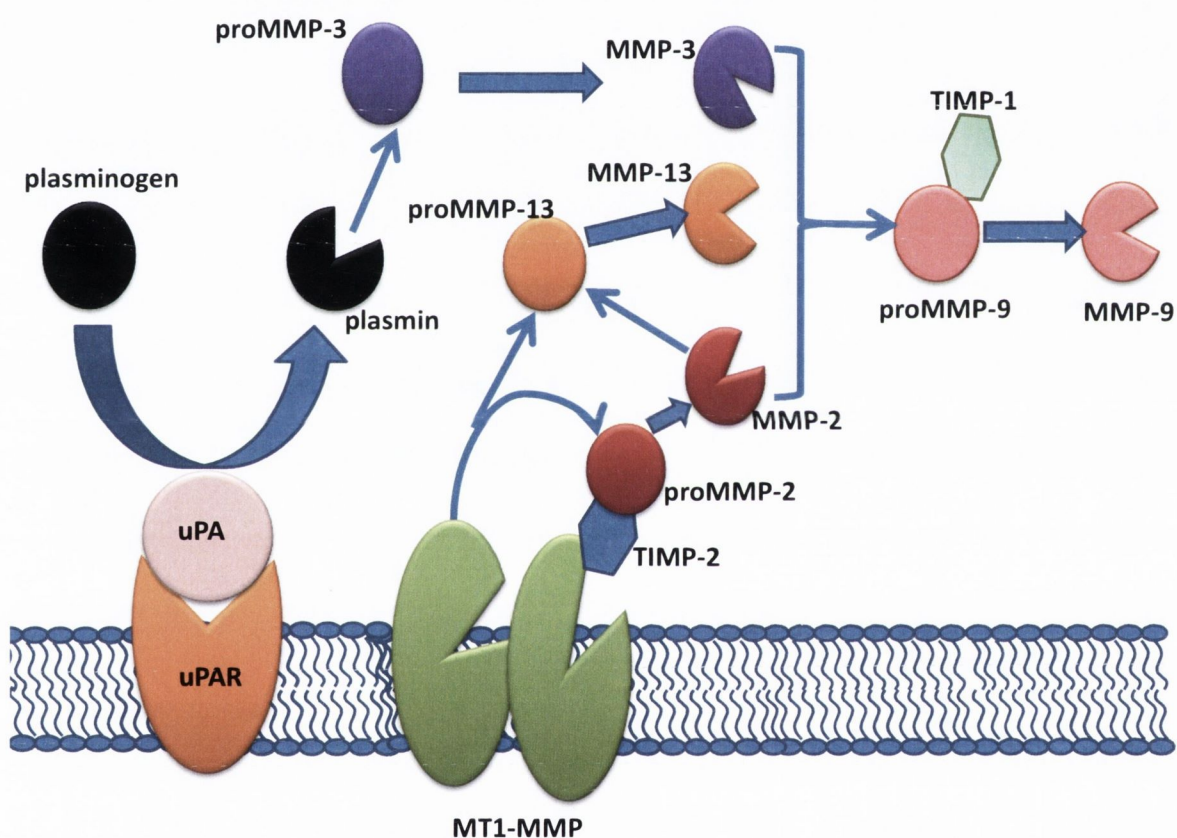


Figure 1.4: Diagram representing MMP-9 activation by other MMPs. TIMP-2 can bind both MT1-MMP and pro-MMP-2 which is then activated by an uninhibited MT1-MMP. Both activated MMP-2 and MT1-MMP can both activate pro-MMP-13. The urokinase plasminogen activator (uPA) bound to the urokinase plasminogen activator receptor (uPAR) converts plasminogen to plasmin which can in turn activate pro-MMP-3. MMP-2, MMP-13 and MMP-3 can all activate pro-MMP-9.

#### 1.1.2.4. *Endogenous inhibitors of MMPs*

There is a large list of physiological inhibitors of MMPs which serve to regulate MMP activity and proteolysis, some of which are summarised in Table 1.2.  $\alpha$ 2-Macroglobulin is an abundant plasma protein and the main inhibitor of MMPs in tissue fluids [69].

Inhibition occurs when limited proteolysis at a 'bait' region by the enzyme results in a conformational change in the macroglobulin which then traps or encloses the enzyme [70].

It is a general proteinase inhibitor but may only bind to activated MMPs which are then irreversibly cleared by endocytosis following binding to a scavenger receptor [71].

The TIMPs are a more specific inhibitor of MMPS. They are a family of at least four 20–29-kDa secreted proteins (TIMPs 1–4) that reversibly inhibit the MMPs in a 1:1 stoichiometric fashion [72, 73]. TIMPs share 12 invariant cysteine residues that form six intrachain disulphide bridges to yield a conserved six-loop, two-domain structure [11]. While both domains are involved in enzyme binding, it seems that TIMP's inhibitory capacity resides almost entirely in the N-terminal domain which interacts with the catalytic domain of MMPs [74, 75]. The four TIMPs can inhibit all MMPs however they show varying specificities. For example, TIMP-2 and TIMP-3 inhibit MT1- MMP, whereas TIMP-1 does not. Likewise, TIMP1 is a relatively poor inhibitor of MT3-MMP, and TIMP3 appears to be a more potent inhibitor of MMP-9 than other TIMPs [11]. TIMP-1 inhibits MMP-9 with a high affinity, whereas TIMP-2 inhibits MMP-2 [76, 77]. The physiological role of the TIMPs is not fully understood but is not limited to MMP inhibition. Studies of TIMP-2 knockout mice reveals that its primary function is activation of pro-MMP-2 [78] by formation of a complex as described previously in section 1.1.2.3. These inhibitors have also been shown to inhibit tumour cell apoptosis, promote or inhibit cell growth and angiogenesis [79-81] independently of MMP inhibition. Examples of other reported roles include stimulation of steroidogenesis in rat testis and ovary *in-vitro* [82],



TIMP-3 inhibition of the metalloproteinase responsible for the cleavage and release of TNF- $\alpha$ , known as TNF- $\alpha$ -converting enzyme (TACE, ADAM-17) [83], IL-6 receptor shedding [84] and interestingly, stimulation of fibroblasts to produce MMP-1 [85].

There is a large list of proteins with MMP regulatory properties with more being discovered all the time. Some of the known proteins with MMP inhibiting properties include the C-terminal fragment of the procollagen C-terminal proteinase enhancer protein (PCPE), albeit a less potent inhibitor than the TIMPs [86]. The noncollagenous NC1 domain of type IV collagen also shares structural similarities with TIMPs and has been shown to have MMP inhibiting properties [87], a serine protease inhibitor named tissue factor pathway inhibitor-2 [88], and a collagen XVIII derived proteolytic fragment named endostatin which can block the activation of MMP-2, MMP-9 and MMP-13 as well the catalytic activity of MMP-2 and MT1-MMP [89, 90]. Thrombospondin-1 (TSP-1) is an extracellular 450kDa glycoprotein that directly binds pro-MMP-2 and -9 and inhibits their activation [91, 92]. Thrombospondin-2 (TSP-2) is thought to bind MMP-2 and MMP-9 and facilitate a low density lipoprotein receptor-related protein (LRP)-mediated endocytosis and clearance in a manner similar to  $\alpha$ 2-macroglobulin [89, 93]. Reversion-inducing cysteine-rich protein with Kazal motifs (RECK protein) is a 110-kDa glycoprotein expressed in many normal tissues and is the only known membrane bound MMP inhibitor [94, 95]. Finally, fatty acids have been shown to inhibit gelatinase activity but only weakly other MMPs. Activity was dependent on carbon chain length and presence of unsaturation and inhibition involved binding to the fibronectin type II module of the gelatinases [96].

<b>Inhibitor</b>	<b>Method of Inhibition</b>	<b>Targets</b>	<b>Ref.</b>
<b>TIMP-1</b>	Catalytic activity	Most MMPs, ADAM-10, ADAMTS-4	[1]
<b>TIMP-2</b>	Catalytic activity	Most MMPs, ADAMTS-4	[1]
<b>TIMP-3</b>	Catalytic activity	Most MMPs, ADAM-10, -12, -17, ADAMTS-4, -5	[1]
<b>TIMP-4</b>	Catalytic activity	Most MMPs	[1]
<b><math>\alpha</math>2-macroglobulin</b>	Catalytic activity, clearance	Most proteases	[69]
<b>C-terminal of PCPE</b>	Catalytic activity	MMP-2, MMP-9	[86]
<b>Tissue factor pathway inhibitor-2</b>	Catalytic activity, activation	Serine proteases, other MMPs	[88]
<b>NC1 domain of type IV collagen</b>	Catalytic activity	MMP-2, -3	[87]
<b>Endostatin</b>	Catalytic activity, activation	MMP-2, -9, -13, MT1-MMP	[89]
<b>TSP-1</b>	Inhibition of activation	MMP-2, -9	[1]
<b>TSP-2</b>	Facilitates clearance	MMP-2, -9	[1]
<b>RECK proteins</b>	Catalytic activity	MMP-2, -9, MT1-MMP	[94]

Table 1.2: A summary of endogenous inhibitors of MMPs including mechanism of inhibition and known targets.

### 1.1.3. Synthetic inhibitors of MMPs

Since the discovery of MMPs and the growing understanding of the role their dysregulation plays in various pathological conditions, targeted inhibition has been an active goal. Over the past three decades, numerous small molecule MMP inhibitors (MMPIs) have been designed and synthesised without ever delivering on the hopes for

great success. Early MMPi mimicked the structure of the peptide substrates of the MMPs with an incorporated zinc-binding group (ZBG) to chelate the catalytic zinc ion and inactivate the enzyme. The first generation inhibitors such as Batimastat were potent but showed little selectivity for individual MMPs [97]. With the determination of the crystal structure and NMR studies of more and more MMPs since 1994, the next generation of inhibitors sought to exploit the subtle differences in the catalytic domain of the enzymes and achieve this selectivity [98].

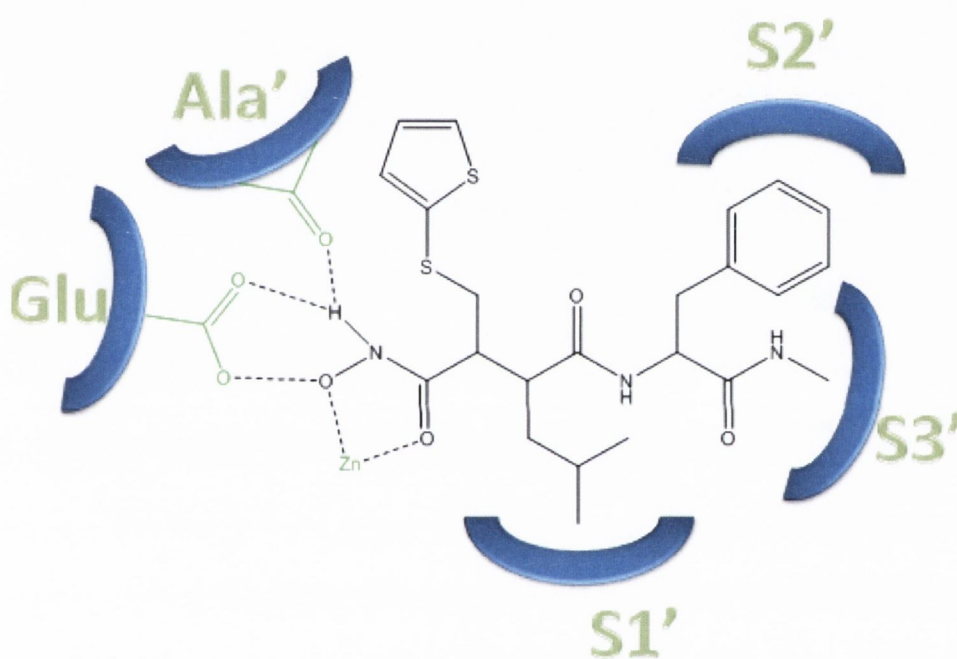


Figure 1.5: Representation of Batimastat binding to an MMP where the two hydroxamate oxygen atoms coordinate the active site Zn<sup>2+</sup>, hydrogen bonding to conserved Ala and Glu residues of the catalytic domain and the distribution of the substituents into the primed pockets of the enzyme [99].

A large number of MMPi have been designed and synthesised and many are peptidomimetic. The newer inhibitors were modifications of the original hydroxamic acid ZBG that better target the pockets of the active site cleft of the MMP in question. Other approaches in small molecule inhibitors include the use of ZBGs other than the traditional hydroxamic acid, non-zinc binding inhibitors and mechanism-based covalent inhibitors.



### 1.1.3.1. *Hydroxamic Acids*

Hydroxamic acids were the first ZBGs to be used and are still one of the most popular due to their ability to potently bind the  $Zn^{2+}$  ion in MMPs and ease of synthesis. In these inhibitors, the hydroxamate provides two oxygen atoms to displace the coordinated water molecule and binds to zinc at the catalytic site while the nitrogen atom binds to the alanine residue on the enzyme [97]. The substitutions on the hydroxamate can fit into the different pockets of the active site to improve the binding affinity and selectivity. Batimastat is shown bound in the catalytic domain of an MMP in Figure 1.5.

Early hydroxamic acid based structures such as those shown in Table 1.3 had many inherent problems, of which, lack of selectivity was considered of central importance. These inhibitors generally reduced the activity of all MMPs as well as off target proteinases such as the ADAMs which was seen as a major contributor to the observed side effects, although the lack of selectivity between MMPs may not necessarily go hand in hand with the use of a strong chelator as was once believed [100]. Though potent inhibitors of MMPs, these compounds caused a dose-limiting musculoskeletal syndrome (MSS) which is characterised by joint stiffness, pain, inflammation and tendinitis [101-103]. These side effects are thought to be caused by the broad-spectrum of inhibition causing disruption to physiological processes. These compounds were further limited by poor oral bioavailability [97, 102, 104], and the fact that the ZBG was metabolically labile. The functional group can be metabolised by dehydroxylation or may be cleaved by exopeptidases to release hydroxylamine [104].



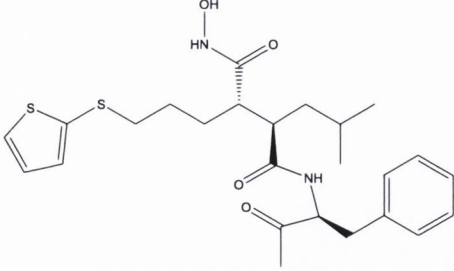
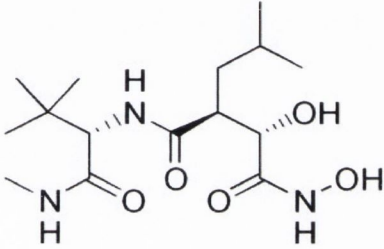
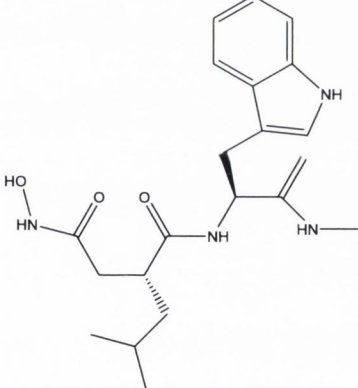
Representative compound	Compound name	Activity (IC <sub>50</sub> unless otherwise stated)	Ref.
	Batimastat, BB-94	3nM (MMP-1) 4nM (MMP-2) 20nM (MMP-3) 10nM (MMP-8) 10nM (MMP-9)	[99]
	Marimastat	5nM (MMP-1) 6nM (MMP-2) 230nM (MMP-3) 16nM (MMP-7) 3nM (MMP-9)	[105]
	Ilomastat, GM6001, Galardin, CS-610	Ki values  0.4nM (MMP-1) 0.39nM (MMP-2) 26nM (MMP-3) 0.18nM (MMP-8) 0.57nM (MMP-9)	[106]

Table 1.3: Early hydroxamic acid based MMP inhibitors. Table shows compound structure, name and IC<sub>50</sub> or Ki value for a given MMP.

Despite promising lab results, clinical trial results were disappointing including dose limiting side-effects (phase I trials) and lack of appropriate end point measures and efficacy (phase II/III) [101]. This led to a closer look at MMP inhibition with the aim of improving selectivity.

### 1.1.3.2. Newer generation of hydroxamate inhibitors

Several selective hydroxamate inhibitors have been developed and involve modification of the molecule backbone in order to target the pockets of the catalytic domain of specific MMPs. This is achieved with the aid of crystal structures and computer modelling to attempt to find best fit molecules for the S1' pocket in particular.

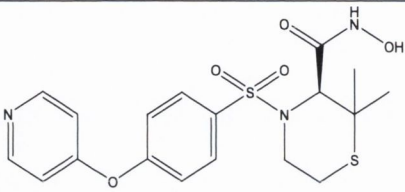
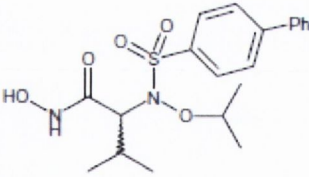
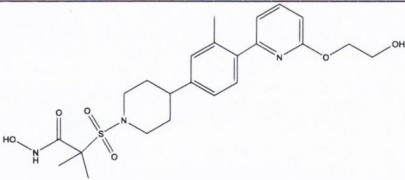
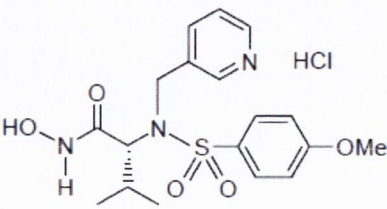
Representative compound	Compound name	Activity (IC <sub>50</sub> unless otherwise stated)	Ref
	Prinomastat, AG3340	Ki values  8.3nM (MMP-1) 0.05nM (MMP-2) 0.3nM (MMP-3) 54nM (MMP-7) 0.26nM (MMP-9) 0.03nM (MMP-13) 0.33nM (MMP-14)	[107]
	N-i-Propoxy-N-biphenylsulfonylaminobutylhydroxamic acid	0.147μM (MMP-1) 0.00009μM (MMP-2) 0.050μM (MMP-3) >1μM (MMP-7) 0.0016μM (MMP-8) 0.0067μM (MMP-9) 0.0098μM (MMP-14)	[108]
	Selective MMP-3 sulfonamide based compound 27	14μM (MMP-1) 0.529μM (MMP-2) 0.001μM (MMP-3) 2.42μM (MMP-9) 20.1μM (MMP-14)	[109]
	CGS-27023A	Ki values  33nM (MMP-1) 20nM (MMP-2) 43nM (MMP-3) 8nM (MMP-9)	[110]

Table 1.4: Newer generation of hydroxamate based MMP inhibitors. Table shows compound structure, name and IC<sub>50</sub> or Ki value for a given MMP.

With the belief that MMP-1 inhibition may be the cause of the unwanted MSS, many of the new molecules developed aimed to spare the MMP-1 enzyme. This is seen in many of the structures in Table 1.4, where lengthy side chains, often comprising of two phenyl rings with various linker groups make up a backbone that would be too large to fit into the shallow pocket of MMP-1 and direct towards the deeper pockets of the gelatinases. More recent studies dispute this theory of MMP-1 inhibition being the sole cause of these side-effects and seem to prove it inaccurate [111]. Prinomastat is a succinate based hydroxamate inhibitor along with marimastat, barimastat, MMI-270 and Cipemastat, and is one of the most studied. It showed evidence that increased MMP-9 specificity correlated with MMP inhibitor efficacy [112]. The *N*-*i*-Propoxy-*N*-biphenylsulfonylaminobutylhydroxamic acid shown in Table 1.4 is a highly specific MMP-2 inhibitor and is shown to decrease angiogenesis and invasion in HUVEC cells. Selectivity is improved with the addition of alkyl groups to the carbon adjacent to the hydroxamic acid group [108]. The third molecule in the table is an example of a highly selective MMP-3 inhibitor. The steric bulk of the sulphur containing moiety close to the hydroxamic acid group favours the larger opening of the S1' pocket of MMP-3 [109]. The methoxyphenyl group of CGS-27023A fits into the S1' pocket of the stromelysins and the pyridine ring points to the S2' pocket. The isopropyl substituent is able to protect the hydroxamic acid from metabolic deactivation [110].

### **1.1.3.3. Carboxylic acid inhibitors**

The carboxylic acids are synthetic precursors to the hydroxamic acids and may have been the reason that many were tested as MMP inhibitors [113]. This group of compounds are functionally similar to their hydroxamate counterparts in that the oxygen atoms of the functional groups coordinate the  $Zn^{2+}$  and form hydrogen bonds with the conserved Glu or



Ala residues. However, examination suggests that the carboxylic acid ZBG is coordinated in a monodentate fashion to the catalytic zinc ion. In most cases this difference results in a lower potency as seen when the hydroxamic acid moiety of CGS 27023 seen in Table 1.4 is changed to a carboxylic acid leading to a 50-fold increase of the  $IC_{50}$  value for MMP-13 [114]. While in many cases the carboxylic acids are less potent than their hydroxamic acid equivalents, more favourable pharmacokinetics have been reported. In a series of biphenylsulfonyl derivatives of D-amino acids, a potent hydroxamic acid inhibitor of MMP-2 and MMP-9 showed 40 times the inhibitory effect of the carboxylic acid but was found to be unstable *in-vivo* and poorly absorbed in contrast to the carboxylic acid [115]. Another group synthesised a series of biphenylsulfonamide derivatives (shown in Table 1.5), including a carboxylic acid analogue, as selective inhibitors against MMP-2, MMP-3 and MMP-13. Surprisingly, the corresponding hydroxamic acid showed a decreased biological activity as well as a less favourable pharmacokinetic profile with active site binding also shown to be dependent on the enantiomer used [116, 117].



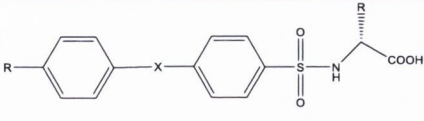
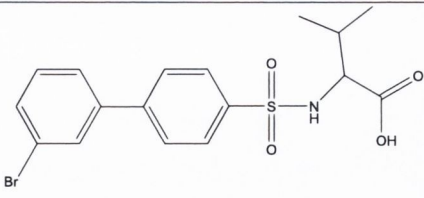
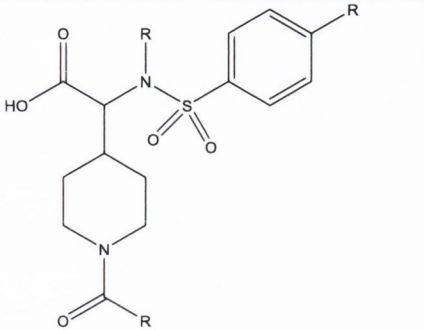
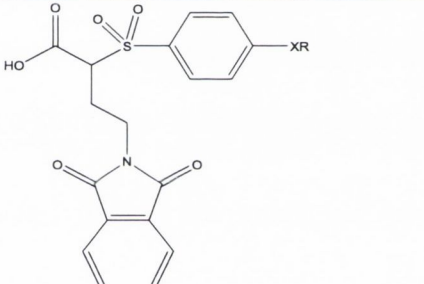
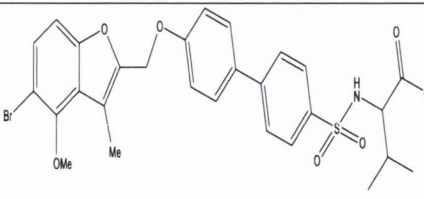
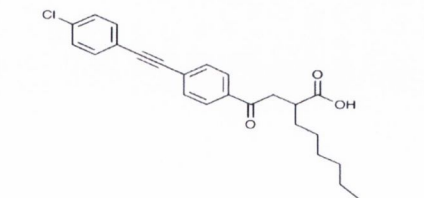
Representative compound	Compound name	Activity (IC <sub>50</sub> )	Ref
	Representative of N-Sulfonylamino Acid Derivatives	2.7 nM (MMP-9) 2.6 nM (MMP-2)	[115]
	PD 166793	6 μM (MMP-1) 4 nM (MMP-2) 7 nM (MMP-3) 7.2 μM (MMP-9) 8 nM (MMP-13)	[116]
	Representative of a group of carboxylic-acid based inhibitors	1370 nM (MMP-1) <0.4 nM (MMP-2) 33.7 nM (MMP-3) 3660 nM (MMP-7) 1.5 nM (MMP-8) 6.6 nM (MMP-9) 0.4 nM (MMP-13)	[118]
	Representative of a group of α-sulfonylcarboxylic acids	>1000 nM (MMP-1) 0.7 nM (MMP-2) 28 nM (MMP-3) 0.5 nM (MMP-9) 1.4 nM (MMP-13)	[119]
	Compound 17 of a group of 3,4,5-trisubstituted benzofuran carboxylic acid derivatives	1.4 nM (MMP-13) 136 nM (MMP-2)	[120]
	Representative of a group of γ-keto carboxylic acids (compound 1j)	0.55 μM (MMP-2) 1.51 μM (MMP-9) 0.20 μM (MMP-12)	[121]

Table 1.5: Carboxylic acid based MMP inhibitors. Table shows compound structure, name and IC<sub>50</sub> or Ki value for a given MMP

#### 1.1.3.4. *Thiol-based inhibitors*

Thiol-based MMP inhibitors contain a sulphur group which is able to bind to the  $Zn^{2+}$  of the active site [122]. Most thiol inhibitors have a carbonyl group close to the sulphur atom, which can improve the binding affinity between the inhibitors and protein due to the extra interaction of the zinc with the carbonyl group. Interest in the use of thiol as a ZBG stemmed from the apparent thiophilicity of the  $Zn^{2+}$ , where it is coordinated by a cysteine residue in several proteins including ‘zinc fingers’, liver alcohol dehydrogenase (LADH), metallothioneins [123], and the cysteine switch of MMPs themselves. The thiol zinc binding inhibitor Rebimastat (BMS-275291) shown in Table 1.6, represents one of the earliest non-hydroxamate ZBGs. It is orally active and a potent broad-spectrum MMPI [124]. The compound was designed to spare TACE where it was believed that this sheddase inhibition may contribute to the MSS observed with earlier MMP inhibitors [125]. Mercaptosulphide inhibitors have been developed to improve binding affinity and potency and many have inhibitory activity comparable to that of the hydroxamates [126]. Novel and potent MMP inhibitors of the type YHJ-224 or YHJ-132 (Table 1.6) with a mercaptosulphide zinc-binding functionality have been designed, synthesized, and tested against human MMP-14 along with other MMPs [127].

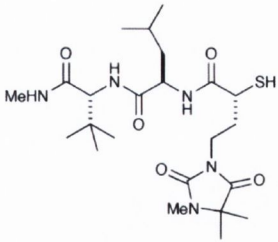
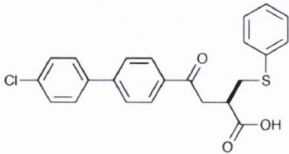
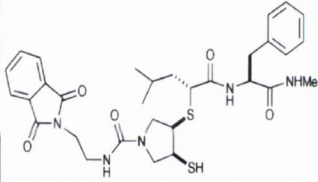
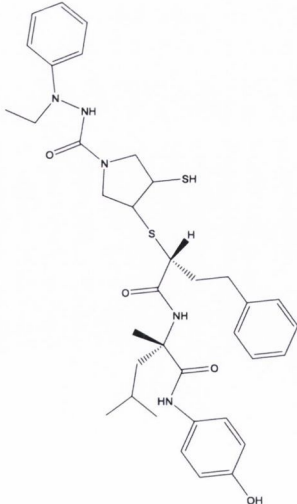
Representative compound	Compound or group name	Activity (IC <sub>50</sub> unless otherwise stated)	Ref
	Rebimastat, BMS-275291, D-2163	9nM (MMP-1) 39nM (MMP-2) 57nM (MMP-3) 23nM (MMP-7) 27nM (MMP-9) 40 nM (MMP-14)	[124]
	Tanomastat, BAY 12-9566	K <sub>i</sub> : 10 nM (MMP-2) 130 nM (MMP-3) 300 nM (MMP-9) >5 μM (MMP- 1) 1.5 μM (MMP-13)	[128]
	YHJ-132	K <sub>i</sub> : 1.2nM (MMP-14) 8.8nM (MMP-1) 0.7nM (MMP-2) 6nM (MMP-3) 6.5nM (MMP-7) 1.1nM (MMP-9)	[127]
	YHJ-224	K <sub>i</sub> : 3.1 nM (MMP-14) >3000 nM (MMP-1) 31 nM (MMP-2) 1.5 nM (MMP-3) 76 nM (MMP-7) 4.6 nM (MMP-9)	[127]

Table 1.6: Thiol based MMP inhibitors. Table shows compound structure, name and IC<sub>50</sub> or K<sub>i</sub> value for a given MMP.



### 1.1.3.5. *Phosphorous containing inhibitors*

Phosphorous-based inhibitors represent another class of ZBG and encompass the phosphonamides, phosphonates, phosphinates and interestingly, the bisphosphonates. Early compounds targeted MMP-11 and -13 and achieved nanomolar potency with optimisation of the substituents [129].

Bisphosphonates are a group of compounds that have been in use for decades for the treatment of bone disease but their potential in cancer was not noticed until relatively recently [130], where their inhibitory effects on bone metastasis were found to be due to MMP inhibition [131]. It is believed that the bisphosphonates work, at least in part by binding to or chelating the zinc ion in MMPs as they do calcium and other heavy metal cations. Zolendronic acid, shown in Table 1.7, which has been shown to be of value as an anti-cancer agent, has the advantage of being well tolerated with a known toxicity profile and can block the expression of MMP-9 [132, 133]. Several phosphonamide compounds have been tested as MMP inhibitors, many with low nanomolar potency and have a mode of action similar to the hydroxamates (Table 1.7). Phosphinates evolved from the phosphonamide compounds where the unstable P-N bond was replaced with a P-CH<sub>2</sub> without, it seems, any loss in potency. A large number of these compounds have been synthesised; many show low nanomolar potency and some with relatively good selectivity. 582311-81-7 is one such potent compound with MMP-1 and MMP-3 sparing characteristics [129]. Phosphonates are another class of phosphorous based MMPi. A series of N-phosphonoalkyl dipeptides were synthesised with different side chains and it was found that having the bicyclic aromatic tryptophan analogue as P2' substituent conferred the greatest potency [134]. Sulphonyl aminophosphonates have also been synthesised based on the structure of earlier carboxylic acids and show good inhibitory action [135].



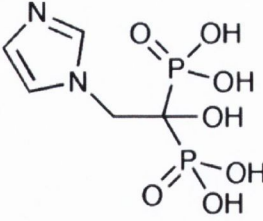
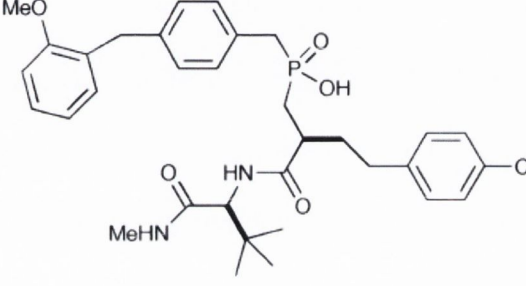
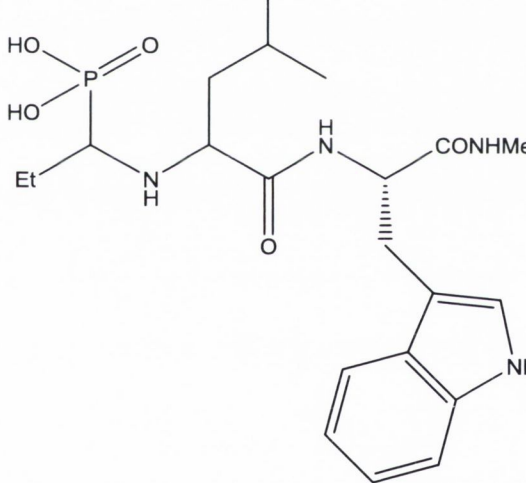
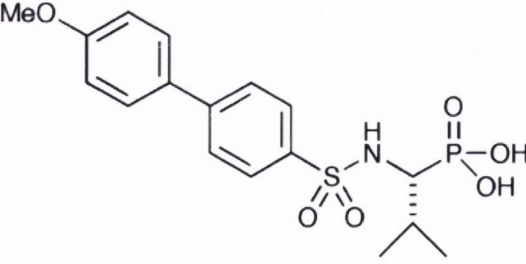
Representative Compound	Compound or group name	Activity (IC <sub>50</sub> unless otherwise stated)	Ref
	Zoledronic acid, zoledronate	NA	[132]
	582311-81-7	1200nM (MMP-1) 7nM (MMP-2) 1600nM (MMP-3) 2nM (MMP-8) 5nM (MMP-12) 5nM (MMP-13)	[129]
	N-phosphonoalkyl dipeptide	50nM (MMP-1)	[134]
	R-sulfonyl aminophosphate 873586-67-5.	Ki 5nM (MMP-2) 40nM (MMP-3) 0.6nM (MMP-8)	[135]

Table I.7: Phosphorous containing MMP inhibitors. Table shows compound structure, name and IC<sub>50</sub> or Ki value for a given MMP

### 1.1.3.6. *Tetracycline inhibitors*

The tetracyclines are a group of compounds better known for their antibiotic activity but also possess inherent MMP inhibitory activity. Similar to the bisphosphonates, this class of compounds appear to have functions beyond simple binding and inhibition of the enzyme which are not fully understood. Two molecules of doxycycline bind weakly to MMP-7 such that the zinc and calcium ions are said to be involved [136]. Despite this weak binding, the tetracyclines display good *in-vivo* and *in-vitro* activity and mechanisms cited include direct or indirect inhibition of expression, accumulation in the matrix acting to bind both pro and active forms of the enzyme, inhibition of oxidative activation, increase in degradation of pro-MMPs, induction of apoptosis, inhibition of production of secretory non-pancreatic phospholipase A2, inhibition of production of TNF- $\alpha$  and IL-8, and reduction of the expression of serine proteinase and trypsinogen-2 [137, 138].

Subantimicrobial doses of doxycycline licensed as periostat for periodontal disease remains the only generally available clinical MMPI [139]. In 1992, Yu et al. synthesised a series of chemically modified tetracyclines (CMTs), which abolished their antibacterial action while retaining the anti-collagenase activity [140]. Metastat (COL-3, CMT-3) shown in Table 1.8 was assessed in clinical trials with some reasonable success [137].

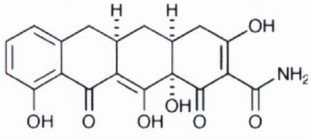
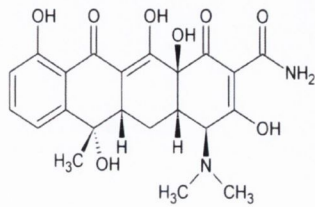
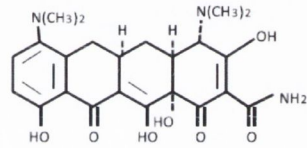
Representative Compound	Compound or group name	Activity (IC <sub>50</sub> unless otherwise stated)	Ref.
	Metastat, CMT-3, COL-3	NA	[137, 141]
	Doxycycline	28μM (MMP-7) 1-10μM (MMP-8) 5-30μM (MMP-13) >200μM (MMP-1)	[136, 142]
	Minocycline	290μM (MMP-3)	[143]

Table 1.8: Tetracycline MMP inhibitors. Table shows compound structure, name and IC<sub>50</sub> or Ki value for a given MMP.

#### 1.1.3.7. Barbiturate (pyrimidinetrione) inhibitors

The barbiturates are a group of compounds that have been commonly used as sedative-hypnotics but in 2001 were found to inhibit MMP-8 in a high throughput screen. Various barbiturates were subsequently found to inhibit MMP-1, -2, -3, -8, -9, and MMP-14 with a general selectivity for gelatinases. The class have good oral bioavailability and activity and were specific for MMPs over other metalloproteinases. The synthesised barbiturate MMPi's departed from the earlier sedative-hypnotic character and were believed to be less likely to exhibit the adverse effects of earlier MMP inhibitors. In the last decade, several new compounds have been synthesised and the structure-activity relationships of the barbiturates have begun to be elucidated.

The inhibitory capacity of this group is primarily due to the interactions of the barbituric acid moiety and the catalytic site of the MMP where they bind the zinc ion in a tridentate manner [144]. As with all MMP inhibitors, binding to the S1' and S2' pockets is key. In the case of the barbiturates, two substituents on the C-5 of the barbiturate ring named P1' and P2' bind in these pockets conferring specificity and potency [145].

Compound Ro 28-2653, shown in Table 1.9 was developed in a search for selective inhibitors for MMP-2, MMP-9 and MMP-14 [144], three enzymes that are consistently upregulated during metastasis and are associated with poor prognosis. A long aromatic P1' substituent ensured selectivity for the deep S1' pockets of these MMPs and improved potency. The compound has shown promise in inhibiting many laboratory models of angiogenesis. A similar compound synthesised by another group also shows great gelatinase selectivity [146]. Addition of a 1,3,4-oxadiazol-2-yl heteroaryl group to the C-4 of the common diphenyl ether side chain conferred selectivity for MMP-13 over MMP-14 [147].



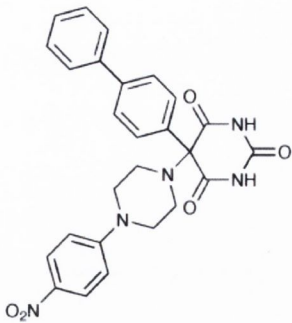
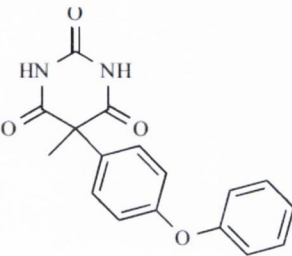
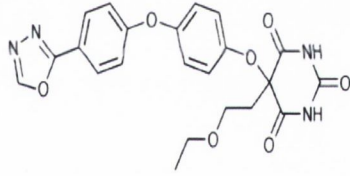
Representative Compound	Compound or group name	Activity (IC <sub>50</sub> unless otherwise stated)	Ref
	Ro 28-2653	16000 nM (MMP-1) 10 nM (MMP-2) 12 nM (MMP-9) 10 nM (MMP-14)	[144]
	Compound 5 (5,5-Disubstitutedpyrimidine-2,4,6-trione)	2000nM (stromelysin) 81 (MMP-2) 52 (MMP-9)	[146]
	420121-84-2	13M (MMP-1) 20nM (MMP-2) 30nM (MMP-8) 30nM (MMP-12) 1nM (MMP-13) 220nM (MMP-14)	[144]

Table 1.9: Barbiturate MMP inhibitors. Table shows compound structure, name and IC<sub>50</sub> or Ki value for a given MMP

### 1.1.3.8. Non zinc-binding inhibitors

All the molecules reviewed to this point possessed a ZBG aiming to chelate the catalytic Zn<sup>2+</sup> of MMPs. Although this strategy has proved effective, selectivity has been difficult to attain owing to the fact that the zinc ion and surrounding region of the protein is the most conserved feature of all MMPs. Other compounds aim to circumvent this problem and attain greater selectivity for certain MMPs. Many of the non-zinc-binding small molecule

inhibitors show selectivity for MMP-13 by binding deep in the S1' pocket and inducing a conformational change. MMP-13 has a deep S1' pocket and is flexible which may account for the preference. It is thought that binding of these inhibitors rigidify the active site to a conformation that is less able to accommodate the substrate [148, 149]. Critical to maintaining the protein-inhibitor interactions is the hydrophobic nature of many of the molecules and so to improve water solubility, carboxylic acids have been positioned to the solvent exposed parts of the compound [150]. The kinetics of many of this group have been shown to be non-competitive [148, 151].

The compound SB-3CT which is shown in Table 1.10 is classed as a mechanism based inhibitor which becomes activated following coordination with the  $Zn^{2+}$  and then forms a covalent bond with the protein which impedes dissociation [152, 153] and long lasting inhibition of the MMP [154].

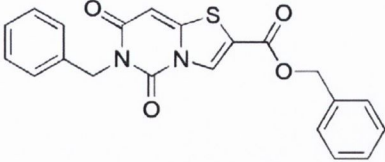
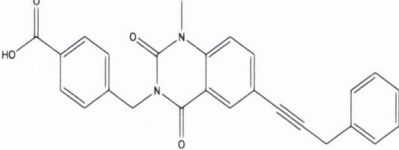
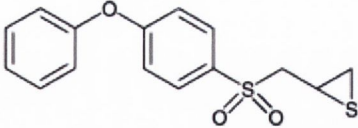
Representative Compound	Compound or group name	Activity (IC <sub>50</sub> unless otherwise stated)	Ref
	Compound 1 (6-benzyl-5,7-dioxo-6,7-dihydro-5 <i>H</i> -thiazolo[3,2- <i>c</i> ]pyrimidine-2-carboxylic acid benzyl ester)	>100μM (MMP-1) >100μM (MMP-2) >100μM (MMP-3) >100μM (MMP-7) >100μM (MMP-8) >100μM (MMP-9) >100μM (MMP-12) 0.03μM (MMP-13) >100μM (MMP-14)	[148]
	Compound 2 (4-[1-methyl-2,4-dioxo-6-(3-phenyl-prop-1-ynyl)-1,4-dihydro-2 <i>H</i> -quinazolin-3-ylmethyl]-benzoic acid)	>30μM (MMP-1) >30μM (MMP-2) >30μM (MMP-3) >30μM (MMP-7) >100μM (MMP-8) >100μM (MMP-9) >100μM (MMP-12) 0.00067μM (MMP-13) >30μM (MMP-14)	[148]
	SB-3CT	73μM (MMP-1) 0.28μM (MMP-2) 4μM (MMP-3) 67μM (MMP-7) 0.4μM (MMP-9) 0.1μM (MMP-14)	[153]

Table 1.10: Non zinc-binding MMP inhibitors. Table shows compound structure, name and IC<sub>50</sub> or K<sub>i</sub> value for a given MMP.

#### **1.1.3.9. Other approaches to MMP inhibition**

With the limited clinical success of traditional small molecule inhibitors, researchers have looked at more novel ways of controlling the upregulation of MMP activity in specific conditions. Many of these approaches look at ways that these enzymes are controlled endogenously in an attempt to exploit these mechanisms.

A huge number of extracellular factors are involved in the regulation of MMP expression making targeting difficult; however, certain approaches show promise. Selective activation of IFN- $\alpha$ , IFN- $\beta$  or INF- $\gamma$  has been shown to downregulate the transcription of several MMPs [155-157]. Similarly, using monoclonal antibodies to inhibit the cytokines or growth factors that upregulate MMP expression such as TNF- $\alpha$ , IL-1 $\beta$  or EGF may be another option for inhibition [158, 159]. Inhibitors of intracellular signalling molecules involved in the transcriptional upregulation of MMPs such as the MAPKs represent another avenue of research [160-162]. A final strategy is to target the nuclear factors that bind to the promoter region of various MMP genes leading to transcriptional upregulation. Much of this focus is aimed at NF- $\kappa$ B [163] and AP-1 [164] at which many signalling pathways converge.

#### **1.1.4. Inflammatory bowel disease and the implication of MMPs**

IBD, which includes both ulcerative colitis (UC) and Crohn's disease (CD), are chronic, relapsing disorders with inflammation and tissue remodelling of the gastrointestinal tract. The disease is characterised by abdominal pain, diarrhoea, rectal bleeding, and fever. UC is



characterised by continuous inflammation involving the rectum and colon which extends proximally. Crypt abscesses from infiltration of neutrophils and ulceration of the mucosa is observed. CD may affect any region of the gastrointestinal tract intermittently with the terminal ileum being the most common. The inflammatory process may extend throughout the intestinal wall narrowing the intestinal lumen and is histologically characterized by the formation of granulomas, fibrosis, and fistulae [165]. There is a strong genetic component to IBD with first degree relatives having a relative risk of up to tenfold [166-168]. NOD2 is a pattern recognition receptor expressed in macrophages, dendritic cells, intestinal epithelial cells and Paneth cells and recognises the peptidoglycan constituent, muramyl dipeptide. Several groups have identified NOD2 (CARD15/IBD1) as a susceptibility gene for CD where presence of common NOD2 single nucleotide polymorphisms (SNPs) can confer as much as a 40-fold increased likelihood of developing ileal CD [169] by affecting host interaction with LPS and triggering NF- $\kappa$ B signalling [170-172]. A collaborative pilot study between our group and the Adelaide and Meath hospital, Dublin of NOD2 mutations G908R, R702W and 10007fs in an Irish cohort found that these NOD2 mutations were more prevalent than previously described in the Celtic population [173]. In addition, stricturing and ileocolonic phenotype and surgery were strongly correlated with a NOD2 mutation [174]. Therefore, NOD2 (SNPs) are associated with complicated CD and may be a useful biomarker for disease severity. Several large genome wide studies have identified loci that are linked to IBD; 16q12 (IBD1), 12q13 (IBD2), 6p21 (IBD3), 14q11 (IBD4), 19p13 (IBD5), 5q31-q33 (IBD6) and Xq21.3 [175-180] and polymorphisms of genes other than NOD2 have been identified as conferring susceptibility including IL23R, which triggers JAK2/STAT3 signalling and ATG16L1, which forms part of a complex essential for autophagy [181-183]. Some recent studies present some preliminary evidence for the implication of MMP SNPs in intestinal inflammation, including MMP-3 SNPs in UC [184-

186], MMP-9 SNPs in collagenous colitis [187], TIMP-1 SNPs were associated with increased susceptibility to CD [188] and finally, SNPs in MMP-3, -8, -10 and -14 were statistically significantly associated with UC in a New-Zealand cohort [189].

There is a body of evidence to suggest that gut microbes are key to the initiation and development of IBD but it is likely that the interaction between the gut flora with the host defences and an impaired barrier function, rather than a specific species, triggers the disease. The fact that antibiotics or some probiotics have shown to be of benefit in treating IBD [190, 191] and gnotobiotic mice do not develop colitis but it rapidly emerges when normal luminal flora are reintroduced [192, 193] are lines of evidence for the important role that bacteria play in the disease.

Tight junctions are essential for proper barrier function and are regulated by cytokines. Barrier integrity is essential for the proper functioning of the gut where increased gut permeability seems to be pre-requisite for development of IBD. The junctional complexes E-cadherin and  $\beta$ -catenin are downregulated in IBD patients [194]. These factors combine in the host to trigger a complex interaction of both immune and non-immune components of the intestinal tract such as epithelium, endothelium, fibroblasts, muscle, lymphoid and nerve cells, and the ECM through surface adhesion molecules as well as soluble factors such as cytokines, proteases, nitric oxide (NO) and reactive oxygen species (ROS)[195, 196]. This interaction of extracellular factors and microbes with the genetically susceptible host to trigger the inflammatory response is summarised in Figure 1.6. There is a body of evidence to implicate the involvement MMPs as key regulators of the disease.



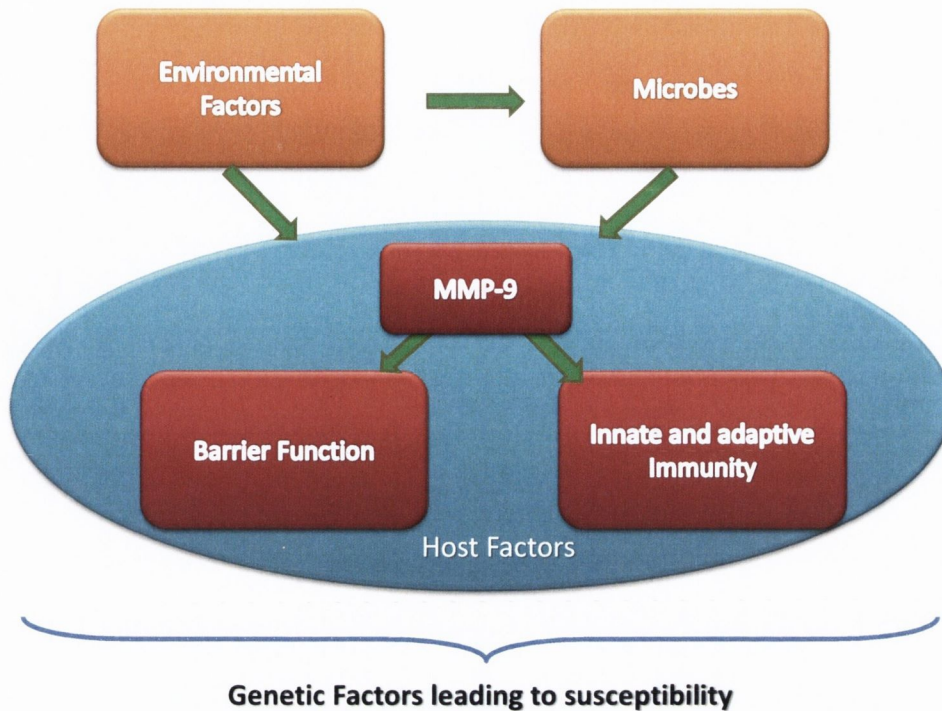


Figure 1.6: Factors in the pathogenesis of IBD. Representation of our current understanding of IBD where a dysregulated inflammatory response is triggered by microbes and other mitogenic factors in genetically susceptible individuals through compromised barrier function and innate and adaptive immunity [169]. This inflammatory response is, in part mediated through upregulation in MMP-9 that can contribute to gut barrier permeability and immune response activation.

As previously discussed, MMPs can be upregulated by various factors including cytokines and growth factors including IL-1 $\beta$  and TNF- $\alpha$  which are markedly increased in IBD [197], and it has been shown that an imbalance between MMPs and TIMPs correlates with the level of inflammation in the bowel [165, 198]. MMP-1, -2, -3 and in particular MMP-9 have all shown to be upregulated in patients with IBD [199] and are implicated in fistulae formation [200]. MMP-1 and MMP-3 are upregulated relative to TIMP-1 in inflamed colons and in mononuclear cells within the mucosa of colitic patients [201, 202]. MMP-13 has recently been shown to mediate inflammation in models of IBD through its ability to cleave and activate pro-TNF [203]. Several other studies conclude that MMPs including MMP-1, MMP-2, MMP-3, MMP-8, MMP-9, MMP-10, MMP-12, and MT1-MMP-1 are

upregulated in IBD and that their upregulation is associated with an increase in disease activity [198, 204-206].

The effect of MMPIs in experimental models of colitis further highlights the role of the endopeptidases. The models used include the dextran sulfate sodium (DSS) and trinitrobenzene sulfonic acid (TNBS) models. TNBS-induced colitis is a hapten-induced model of chronic inflammation characterized by segmental lesions, mucosal ulceration with granulation tissue at the base, and mixed transmural infiltration by neutrophils, lymphocytes and macrophages, and occasionally, small granulomas are observed [207]. The DSS model has similarities with human UC with features of diarrhoea and rectal bleeding, infiltration of inflammatory cells, crypt loss, and extensive mucosal erosions with predominance of distal involvement of the large intestine. Occasionally, crypt abscesses and regenerated epithelium are seen [208]. When used in a rat model of DSS-induced colitis, the MMP inhibitor CGS-27023A significantly reduced the extent and severity of epithelial injury without influencing mucosal repair and MMP-9 was found to be a crucial mediator of colitis [209, 210]. Phenanthroline, a zinc chelating compound with a known MMP inhibitory effect, led to a significant improvement of morphological and histological scores in a rat model of chronic colitis induced by TNBS [211]. Marimastat and Batimastat, hydroxamate inhibitors of MMPs, both dose dependently reduced tissue injury, inflammation and the extent of the disease in a TNBS model of induced colitis [212, 213]. Another hydroxamate MMPI, ONO-4817, has also been tested in DSS-induced colitis in mice and was found to reduce disease activity and infiltration of inflammatory cells [214].

MMP-9 is one of the most abundantly expressed proteases in bowel inflammation. Neutrophils seem to be the primary source [199, 215] where it is stored in zymogen granules and can be released following an inflammatory stimulus [38]. Although basal expression is low in almost all tissues, it is also expressed by macrophages, lymphocytes,



epithelial cells, fibroblastic cells and vascular smooth muscle cells in IBD [11, 206, 216] and is considered pivotal in the pathogenesis of the disease (Figure 1.7) [205]. MMP-9 null mice display significantly reduced inflammation in a DSS model of colitis and the same study showed that exogenous MMP-9 inhibits epithelial cell adhesion and wound healing *in-vitro* [216]. The defective re-epithelialization and reduction in adhesion complex integrity [217, 218], increased endothelial permeability [219], activation of proteins including fibrin(ogen),  $\alpha$ 1-proteinase inhibitor, interleukin-1 $\beta$ , IL-8, transforming growth factor- $\beta$  have all been listed as some of the roles for MMP-9 in the inflammatory response [39, 218, 220].

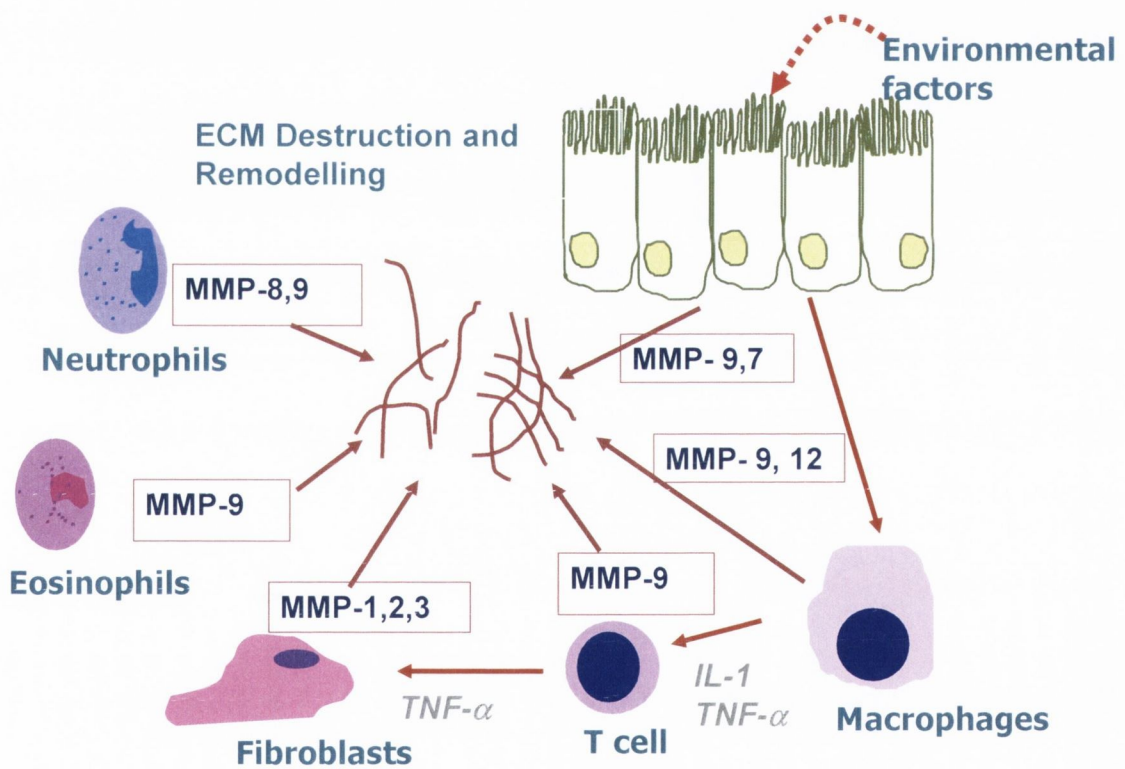


Figure 1.7: Summary of cells involved in release of MMPs in the gut. Microbes or other environmental factors trigger an immune response in genetically susceptible individuals. Release of cytokines, recruitment of inflammatory cells and release of MMPs results in the breakdown of the ECM, activation of pro-inflammatory mediators and increasing epithelial permeability, all potentiating triggers for further inflammation [165].

### 1.1.5. Pathological implications of MMP-9

Of the MMPs, MMP-9 is consistently upregulated in an inflammatory setting. Large amounts of the enzyme are generated in response to various inflammatory mediators despite its basal expression being low. As well as its contributions to IBD that are summarized in 1.1.4, MMP-9 is implicated in a wide range of conditions and represents over 50% of all MMP literature that is published [36]. Cardiovascular (CV) disease, diabetes and cancer are responsible for the majority of human deaths in the developed world and have all been associated with MMP-9 abnormalities.

#### 1.1.5.1. *MMP-9 and cardiovascular disease*

Changes in the CV ECM are regulated by the gelatinases and their tissue inhibitors and, as key components of CV remodeling, are associated with inflammation and reactive, rather than reparative, fibrosis [221, 222]. MMP-2 and MMP-9 knockout models are associated with reduced aortic elastin degradation [223] and protection from pressure overload myocardial hypertrophy, fibrosis and dysfunction [224]. Post-infarction models and models of left ventricular arrhythmogenesis have shown that MMP-9 gene promoters are temporally activated specifically in the region of myocardial injury [225, 226]. The gene promoter region of MMP-9 includes a proximal activator protein-1 (AP-1) site which mediates an enhanced transcriptional response to a wide variety of cytokine and cellular stimuli [227]. In the clinic, independent associations between myocardial remodelling post-MI, left ventricular dysfunction and heart failure, have been identified with markers of inflammation, fibrosis and MMP-9 [222, 228-231].

### **1.1.5.2. MMP-9 and diabetes**

Microvascular and macrovascular complications of diabetes are associated with MMP-9 dysregulation. In an animal model of diabetic retinopathy, increased MMP-9 activity was observed in retinal microvessels and MMP-9 knockout was protective [232]. In patients, increased urinary excretion of MMP-9 supports a role for MMP-9 dysregulation in diabetic renal dysfunction [233] and aortic and coronary arteries of diabetic patients taken at autopsy had higher expression of MMP-9 compared to non-diabetics and were correlated with glycated haemoglobin (HbA1c), a common measure of blood glucose levels, as well as apoptosis [234]. Elevated MMP-9 has also been associated with arterial stiffness in patients with diabetes [235]. Furthermore, human genetic polymorphisms associated with MMP-9 elevation support a role for this enzyme in the pathophysiology of vascular disease. The 1562C>T SNP, which affects the promoter region of MMP-9 gene and increases circulating levels of MMP-9, is significantly associated with vascular disease in type 2 diabetes mellitus [236]. In age and sex matched controls, patients with type 2 diabetes, without and with microangiopathy, T allele frequencies, the portion of CT or TT SNPs relative to CC, were 11.9%, 13.1% and 24.4% respectively ( $p < 0.05$ ).

### **1.1.5.3. MMP-9 and cancer**

MMPs play a central role in cancer cell intravasation and extravasation and their plasma levels are known biomarkers of breast, ovarian, colorectal, renal, pancreas, bladder and lung cancers [237]. MMP-9, in particular, regulates vascular endothelial growth factors, which, in turn, promote tumour growth and angiogenesis [238]. MMP-9 also modulates tumour-associated inflammation via cytokines and their receptors [239] and is involved in endothelial-mesenchymal-transition (EMT) whereby cells acquire migratory characteristics [240].



Upregulation of MMPs by tumours has long been established and it is now known that stromal cells, such as fibroblasts, endothelial cells and leucocytes can play an equally important role by releasing MMP-9 to the tumour microenvironment following activation of growth factors in the ECM by tumour cells, release of cytokines and growth factors, and through direct cell-cell contact with tumours [241, 242]. Tumours and tumour associated stromal cell interactions are incompletely understood, but their recruitment serves to enhance the metastatic efficiency. An interesting study on skin squamous cell carcinoma found that increased expression of stroma-derived MMP-9 occurred exclusively in enhanced malignant tumour transplants [243].

While numerous preclinical studies demonstrate the ability of MMP inhibitors to delay primary tumour growth and block metastasis [244], MMP inhibition in the clinic has been limited by toxicity, including dose-limiting musculoskeletal pain and inflammation [245], while recent research on the development of MMP inhibitors has been focused on selective inhibition of MMPs [246].

#### **1.1.5.4. *MMP-9 and other diseases***

MMP-9 abnormalities have been associated with disease progression in many other key organs. In the liver, MMP-9 has been associated with the fibrotic response to hepatitis C [247] and in models of fulminant liver failure where MMP-9 expression is increased, inhibition of MMP-9 was associated with outcome improvements when used early in the natural history of the disease [248]. In patients with kidney disease, interstitial fibrosis correlated with MMP-9 expression in the atrophic tubular nuclei [249] and elevated MMP-9 is also associated with the vascular complications of chronic kidney disease associated with diabetes [250]. In children with aggressive chronic renal dysfunction, focal segmental

glomerulosclerosis is associated with elevated MMP-9, which may represent an early diagnostic biomarker as well as a therapeutic target [235].

## 1.2. Nitric Oxide

NO is a ubiquitous gaseous and diatomic mediator, transducer and modulator, produced from the conversion of L-arginine to L-citrulline by nitric oxide synthase (NOS). Three NOS isoforms have been discovered and are classified as neuronal NOS (nNOS, NOS1), endothelial NOS (eNOS, NOS3), which are both constitutively expressed, calcium-dependent enzymes producing physiological levels of NO, and inducible NOS (iNOS, NOS2) which produces high levels of NO in a sustained manner. This inducible isoform is transcriptionally upregulated during inflammation in response to bacterial lipopolysaccharide or endotoxin, pro-inflammatory cytokines and other immune complexes through NF- $\kappa$ B signalling pathways. The diverse roles of NO include smooth muscle relaxation, inhibition of platelet aggregation [251], neurotransmission [252] and immune and inflammatory modulation [253, 254]. The NO involvement in many physiological processes is mostly mediated through its activation of the heme iron in soluble guanylate cyclase (sGC). Following activation, sGC can then produce cyclic guanosine monophosphate (cGMP) from guanosine triphosphate (GTP) which activates downstream signalling pathways that trigger these effects. NO can also react directly with signalling proteins and when generated in high amounts such as during inflammation, it can react with superoxide anion to produce peroxynitrite, a much stronger oxidant, with significant pathophysiological/inflammatory contributions. Although NO has a half-life in

the range of seconds, properties such as charge neutrality, a small molecular radius and hydrophobicity, allow for free diffusion through cell membranes. NO reacts with oxygen and with oxygen-derived radicals as well as metal centres in proteins, properties which make it a key signal transducer [255].

The net effect of NO in a given setting depends on its environment and concentration, with iNOS generating the highest local flux. Following transcriptional upregulation of the enzyme, there is a delay of 6-8 hours before NO production begins, but this production is then sustained for hours to days and is 1000 fold greater than those produced by the constitutive NOS isoforms [256]. The presence of molecular oxygen and its derived free radicals in the local environment affect NO concentration because they react at diffusion limited rates. Interestingly, vascular relaxation and vasodilator tone caused by NO is inhibited by superoxide and inhibition of superoxide production may enhance the effects of NO [257]. Therefore, scavengers of superoxide such as superoxide dismutase and oxyhaemoglobin influence NO bioavailability.

The observed effects of NO, especially those that lead to cytotoxicity, have been also attributed to the generation of peroxynitrite from NO and superoxide [258-263]. In addition, NO can react directly with sulfhydryls [264, 265], metal centres including iron/sulphur and  $Zn^{2+}$ -thiolate groups [258, 266, 267] but can also react via metal independent mechanisms through generation of hydroxyl or carboxyl radicals formed from different decomposition reactions [268-270]. This explains the concentration dependent, often biphasic nature of NO where its effects can be separated into cGMP dependent, which tend to occur at lower NO flux, and cGMP independent, occurring at higher concentrations. These cGMP independent effects are often mediated by formation of peroxynitrite [262, 263, 271, 272], leading to direct reaction with proteins to alter their function through S-nitrosylation, tyrosine nitration or oxidation [273]. Indeed,



peroxynitrite often opposes the biological effects of NO [262, 263, 274-276]. The balance of these reactions will often give rise to a threshold in concentration, beyond which the role of NO may change; summarised in Figure 1.8. To further complicate this concentration-dependent role of NO, effects will also be cell- and environment-specific depending on the presence of endogenous antioxidants [277] and other genes involved in regulating a given response. The dichotomy of protective and damaging effects of NO is evident in inflammation, where iNOS is generally considered pro-inflammatory, whereas eNOS and nNOS are considered anti-inflammatory [278] and also in the dual roles of NO in apoptosis [271, 279].

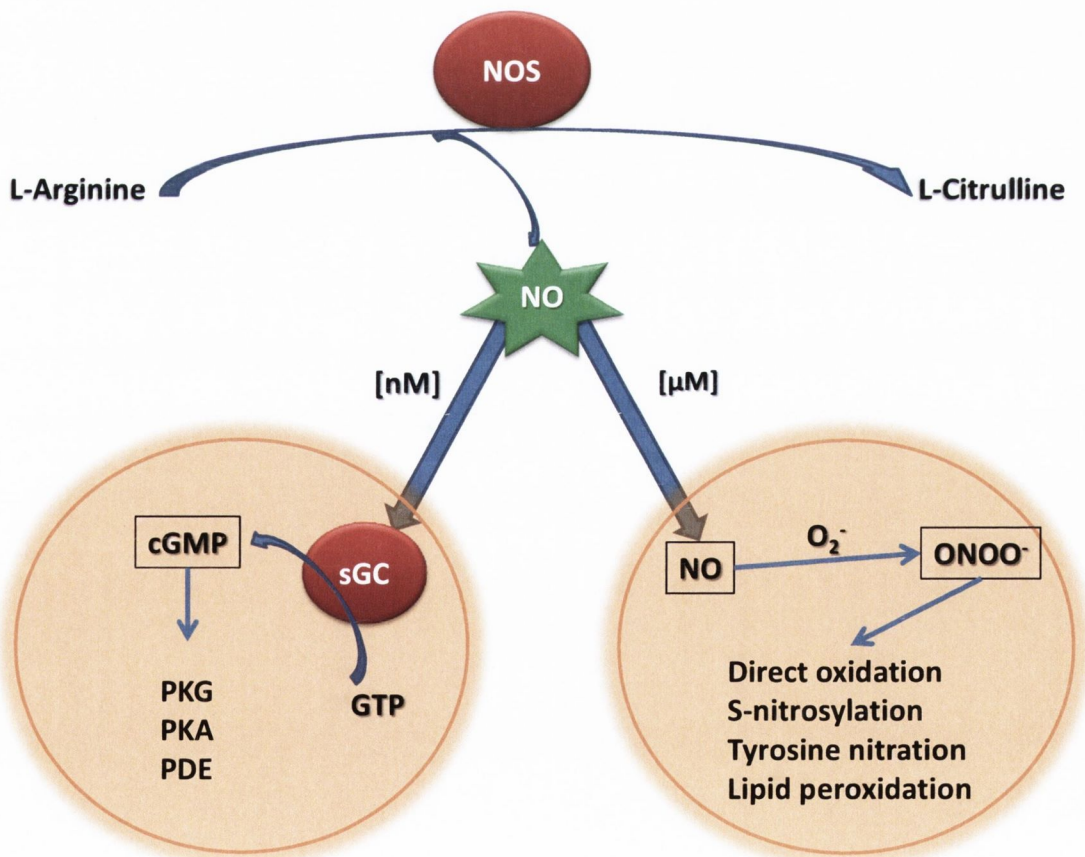


Figure 1.8: Biological reactions of NO. Many of NO's effects are mediated through activation of cGMP which in turn modulates protein kinase G (PKG), protein kinase A (PKA) and the phosphodiesterases (PDE). At higher concentrations of NO and through reaction with superoxide to generate peroxynitrite, it can modulate signalling with direct lipid peroxidation and reaction with proteins through oxidation, S-nitrosylation and tyrosine nitration.

### 1.2.1. The role of NO in IBD

NO is recognised as playing a role in gut homeostasis, maintaining mucosal blood flow, coordination of peristalsis and sphincter action and also in the pathogenesis of IBD. In the gastrointestinal tract, nNOS and eNOS are both continuously expressed by neuronal cell bodies, endothelial cells and enterocytes producing picomolar to nanomolar quantities of NO [280, 281]. Exposure to inflammatory mediators will lead to transcriptional upregulation of iNOS in a variety of cell including neutrophils, monocytes, macrophages, T-lymphocytes, vascular smooth muscle cells and enterocytes [282]. High levels of NO are proposed to be toxic to the gut through potentiation of hyperaemia in the mucosa and submucosa, gut relaxation and peroxynitrite mediated cytotoxic reactions; however many protective roles have also been highlighted including increased blood flow, decreased microvascular permeability, decreased aggregation of platelets and adhesion of leukocytes and inhibition of mast cell degranulation [282]. A study examining the expression and distribution of iNOS and eNOS in UC and CD found that the dominant iNOS expressing cell type in UC was neutrophils and this expression was concentrated in patches of inflammation. In CD, macrophage was the dominant cell type, however, iNOS expression was not localised in inflamed patches [283]. The studies show that the expression patterns of eNOS and iNOS are different in UC and CD and so NO may play different roles in the diseases. Animal models of IBD where NOS inhibitors have been used show conflicting results with the effect of NO being highly dependent on the biological setting. Some studies where treatment with NOS inhibitors commenced after colitis had been induced showed improvements in local inflammation [284-286] whereas increased mucosal inflammation and injury was observed when treatment began with or before the induction of colitis [285, 287, 288]. These results highlight the influence of timing, the type of NO

donor or NOS inhibitors used and the local concentrations. Several studies of IBD models in iNOS knockout mice [289-291] have shown that these animals show a reduction in the severity of inflammation giving weight to the theory that lower concentrations of NO are protective and the higher levels generated by iNOS can potentiate inflammation. The spontaneous generation of peroxynitrite under these settings may be the major contributor to this observation. Addition of peroxynitrite to the gut elicits a severe inflammatory response [292], superoxide dismutase (SOD) mimetics which scavenge superoxide can alleviate the severity of inflammation in a rodent model of colitis [293] and a peroxynitrite scavenger markedly alleviated colonic injury in a TNBS induced colitis [294], all lines of evidence pointing to many of the pro-inflammatory effects of NO being mediated by peroxynitrite.

### 1.2.2. NO-hybrids (nitrate-barbiturates)

The search for clinically successful MMPi has not proven fruitful and many reviews on the subject sight poor selectivity for the different MMPs as being a major contributing factor [37, 295]. In 2001, Hoffman La-Roche reported that certain 5,5-disubstituted pyrimidine-2,4,6,-triones (barbiturates) were effective inhibitors of MMPs and had good selectivity for the gelatinases [97, 144]. These barbiturates did not retain the sedative, hypnotic effects of the classical compounds but did exhibit some of the preferable pharmacokinetic properties such as *in-vivo* stability, which was an advantage over other MMPi. Crystal structure analysis of the human MMP-9 catalytic domain with inhibitors has shown that the ionised barbiturate ring chelates the  $Zn^{2+}$  in a tridentate mode while the C5-substituents were directed to the S1' and S2' pockets [296]. The barbiturates display



broadly similar structure activity relation (SAR) to other MMPiS where the carbonyl groups of the barbiturate ring serve as a ZBG and the long biphenyl or phenoxyphenyl 5-aromatic substituent binds in the deep S1' pocket. The second 5-substituent is directed towards the S2' pocket where C5- piperazine or piperidine have been shown to confer potency [145]. For these reasons, the barbiturates were chosen as the MMPI scaffold for the project and were designed to be potent and selective MMP-9 active site inhibitors.

While the precise role of NO in a given setting may be difficult to measure, several groups have demonstrated benefit in using NO-donors to reduce inflammation and potential for inhibition of MMP-9. Glyceryl trinitrate (GTN) has been used clinically for over 150 years and has a well-established toxicity profile [297]. Its potential use as an MMPI was demonstrated when it reduced plasma MMP-9 levels by increasing the enzyme's membrane binding and inhibited its release [298]. In conflict with these findings, the same compound is reported to activate pro-MMP-9 [299], increasing potential MMP-9 activity through NF- $\kappa$ B activation [300] and increased MMP-9 expression [301] and so setting may be important.

Nitrate groups or other NO-donor groups have been incorporated into several established pharmacological agents as NO-drug hybrids in an effort to enhance efficacy and decrease side-effects of the resultant pharmacological agents. The rationale for these compounds is that they retain the pharmacological action of the parent compound but their effects would also include the biological action of NO. Of these, hybrids of NO with non-steroidal anti-inflammatory drugs (NO-NSAIDS) [302-305] including nitro-aspirins [306], NO-glucocorticoids [307-309], and NO-salbutamol [310-312] have been extensively studied for their anti-inflammatory properties. Despite a significant number of publications relating to the role of NO in mediating MMP-9 [313], an NO-MMPI has not been previously reported.

### 1.3. Project aims

The aims of my PhD were

- 1) To synthesise a series of nitrate-barbiturates and establish their effect on MMP-9 activity and expression in an *in-vitro* model of intestinal inflammation.
- 2) To establish the contribution of the nitrate group in any observed effect.
- 3) To establish possible mechanisms of action for the inhibitors.
- 4) To assess the efficacy of the compounds in an *in-vivo* model of colitis.

## **Chapter 2: Materials and methods**



## 2. Materials and methods

### 2.1. Reagents and materials

All chemicals and biological materials were supplied by Sigma Aldrich<sup>®</sup> unless otherwise stated. Plastic consumables for cell culture were supplied by greiner bio-one<sup>®</sup>. Ethanol and Methanol were supplied by Trinity College hazardous materials facility (HMF) solvent stores.

### 2.2. Chemistry Methods

All reactions were monitored using thin layer chromatography (TLC). Uncorrected melting points were measured on a Stuart Apparatus. Infrared (IR) spectra were acquired on a Perkin-Elmer FT-IR Paragon 1000 spectrometer. <sup>1</sup>H and <sup>13</sup>C nuclear magnetic resonance (NMR) spectra were recorded at 27 °C on a Bruker DPX 400 spectrometer (400.13 MHz, <sup>1</sup>H; 100.61 MHz, <sup>13</sup>C). Coupling constants are reported in hertz. Electrospray ionization mass spectrometry (ESI-MS) was performed in the positive ion mode on a liquid chromatography (LC) time-of-flight mass spectrometer (Micromass LCT, Waters Ltd., Manchester, UK). The samples were introduced into the ion source by an LC system (Waters Alliance 2795, Waters Corporation, USA) in acetonitrile:water (60:40% v/v) at 200µL/min. The capillary voltage of the mass spectrometer was at 3 kV. The sample cone (declustering) voltage was set at 40 V. For exact mass determination, the instrument was externally calibrated for the mass range m/z 100 to m/z 1000. A lock (reference) mass (m/z

556.2771) was used. Mass measurement accuracies of  $< \pm 5$  ppm were obtained. Reverse phase high-performance liquid chromatography (RPHPLC) was used to establish compound purity. The stationary phase was a Waters Xbridge C18, 5 $\mu$ m column (4.6 mm  $\times$  150 mm); the mobile phase consisted of a mixture of methanol and water (60:40 v/v) at a flow rate of 1 mL/min. HPLC was performed using a system consisting of a Waters 600 pump and controller, Waters 717 autosampler and a Waters 996 photodiode array detector controlled by Waters Empower Software. Chromatograms were extracted at 230 nm. All test compounds were  $>95\%$  pure.

### 2.2.1. Synthesis of barbiturate compounds

Synthesis of the nitrate-barbiturate compounds was carried out by substitution of the phenoxyphenyl barbiturate-5 bromide given the designation **3** in Figure 3.1. **3** is synthesised in four steps from methyl 4-hydroxyphenylacetate as previously described by our group [314]. The aminoalkyl nitrate side chains, seen as series **3** in Figure 3.2, were obtained by reacting the corresponding, aminoalkyl alcohols with fuming nitric acid at  $-10^\circ\text{C}$ . The aminoalkyl alcohol in DCM was added to a mixture of DCM and fuming nitric acid ( $-10^\circ\text{C}$ ) dropwise over 20 minutes. After stirring for a further 30 minutes, acetic anhydride was added to the reaction mixture which was left for a further 15 minutes with stirring. If the desired product formed as a white solid precipitate, it was isolated by suction filtration and dried *in vacuo*. Where some of the products did not precipitate, the pH was adjusted to 14 with 7 M NaOH and extracted with DCM. The combined organic layers were washed with water and brine and dried over anhydrous  $\text{Na}_2\text{SO}_4$ . The nitrate-barbiturate inhibitors were synthesised by reacting the intermediate **3** with the nitrate side

chains in triethyl amine and methanol at room temperature (RT) for 24 hours as shown in Figure 3.3. The solvents of the reaction mixture were removed *in vacuo* and residues were purified by flash column chromatography. All structures were confirmed with Mass Spectrometry where IR, NMR and melting point data had previously been obtained.

### 2.3. Cell Culture

*In-vitro* experiments were carried out using Caco-2 and HT1080 cells. Caco-2 cells are a human colorectal epithelial cell line that is commonly used to study colonic inflammation. The intestinal epithelium is actively involved in inflammation and in response to pro-inflammatory cytokines, can release other pro-inflammatory mediators such as MMP-9 [315]. This made the cell line ideal for studying the ability of drug candidates to inhibit MMP-9 in a model of intestinal inflammation. HT1080 is a human epithelial fibrosarcoma cell line and commonly used to study invasion and metastasis. Production of MMPs can be induced by proinflammatory mediators and the cell line is used in our lab to study the ability of drug candidates to inhibit cancer cell invasion [315]. It was used in this study for cytotoxicity analysis of the compounds.

Caco-2 cells were supplied by American type culture collection (ATCC), and were cultured in 75cm<sup>3</sup> flasks (T-75). Cells were cultured in Minimum Essential Media (MEM), 1% sodium pyruvate, sodium bicarbonate 2.2g/L, gentamicin 5mg/L, streptomycin 10mg/L, penicillin G 6mg/L and buffered to pH~7.3. The media was then passed through a 0.22µM filter into a sterile container and sterile foetal bovine serum (FBS) was added to give a final concentration of 20%. Experiments were carried out in FBS free media. Cells were maintained in a 37°C, 5% CO<sub>2</sub> humidified incubator. Media was changed



approximately every second day until the cells reached confluence when they were detached using trypsin, pelleted by centrifugation and split to new flasks. The media was changed the following day. Caco-2 cells were used up to a maximum passage number of 50.

HT1080 cells were supplied by the ATCC and cultured in T-75 flasks. Media used for culture and experiments were as for Caco-2 media but with the exception that the growing media used contained 10% FBS instead of 20%.

For experiments, a cell pellet was resuspended in serum free media and cell numbers were counted using the coulter counter (Beckman) or a haemocytometer. Cells were then seeded into 25cm<sup>3</sup> flasks (T-25), 6-well plates or 96-well plates. Cells were grown until 70-80% confluent. The media was then changed to FBS free media and the cells were incubated with nitrate-barbiturate, alcohol-barbiturate or nitrate side-chain compounds at 100nM or 10µM for 30 minutes. Cytokines TNF- $\alpha$  and IL-1 $\beta$  10ng/mL were then added and the cells were incubated for 24 hours at 37°C in a humidified 5% CO<sub>2</sub> atmosphere. A stimulated flask (FBS free media with TNF $\alpha$  and IL-1 $\beta$ ) and a sham flask (FBS free media) were also prepared and incubated for 24hrs. For NO-donor experiments, solutions of SNAP or DETA-NONOate were prepared daily when needed and incubated at a range of concentrations in the place of the compounds as listed above. For co-incubation experiments with ODQ, this was added with the nitrate-barbiturate compounds to give a concentration in the media of 10µM as with the compounds. The experiments where 8-Br-cGMP was used, this was added with the ODQ and compounds to give a final concentration of 10µM in the media.

## 2.4. Dextran sulphate sodium (DSS) induced colitis

*In-vivo* experiments were carried with ethical approval from the TCD ethics committee using male Wistar rats which were supplied by the bioresources unit of Trinity College Dublin. Animals were maintained in the SCRUBS or the Llyod building bioresources facilities at 23°C with 12 hour: 12 hour light-dark cycles and access to drinking water and food pellets ad libitum. Animals were monitored daily and bedding and cages were changed as required. Upon arrival, all animals were weighed and divided into cages of equal animal numbers and giving approximately equal weights per cage. Animals were given a minimum of 5 days to settle to conditions before any experimental interventions were commenced.

DSS induced colitis is a model frequently used to induce colitis, with similar features to human UC, in rodents. DSS is toxic to colonic epithelial cells and causes an increase in epithelial barrier permeability. Reduction of tight junction proteins and increased pro-inflammatory cytokine production are seen and increased exposure of DSS and luminal contents to the mucosa triggers an inflammatory response [316].

Animals were split up into cages so that all animals in a given cage were part of the same experimental group and so that each cage had approximately the same average animal weight. Solutions of 5% DSS (molecular weight (MW) 40,000) (TdB consultancy, Sweeden) in tap water replaced the drinking water the rats received in all but the sham group starting on day 0 until the end of the experiment on day 5. Animals were given twice daily, 500µL rectal enemas of vehicle (1% cremophor, 5% ethanol in ddH<sub>2</sub>O) or compounds dissolved in the vehicle to give 1.8µM solutions (calculated from an approximate 2mg/kg dose in 500µL for compound **1a**). The rats were weighed each

morning for the duration of the experiment and examined for diarrhoea and evidence of blood in the stool or rectal bleeding. Diarrhoea was defined as the presence of faecal matter adherent to the fur around the anus or tail and rectal bleeding as the visible presence of blood around the rectal area of the rat [214, 317]. The disease activity index (DAI) was calculated by assigning scores to weight change, rectal bleeding or diarrhoea and averaging them as shown in Table 2.1.

<b>DAI score</b>	<b>Weight Loss (%)</b>	<b>Stool Consistency</b>	<b>Presence of Blood</b>
0	<1%	Normal	None
1	1-5%	-	-
2	5-10%	Soft stool	Blood in stool
3	11-15%	-	-
4	>15%	Diarrhoea	Gross rectal bleeding

Table 2.1: Criteria for scoring DAI

At the endpoint of the experiment on day 5, all animals were individually euthanized in a CO<sub>2</sub> chamber at a flow rate of 4 L/minute. Once expired, a mid-laparotomy was performed and the distal colon was removed, opened longitudinally, rinsed with sterile saline and divided into three parts by longitudinal section. One section was snap frozen in liquid nitrogen for zymographical analysis, another was placed in neutral buffered 10% formalin



for 48 hours for fixing and then transferred to 70% ethanol for storage and the other section was added to RNAlater solution (Ambion) and frozen for future isolation of mRNA.

#### **2.4.1. Histological assessment of colon samples**

The fixed colon samples that had been stored in 70% ethanol were placed uncut into labelled embedding cassettes for processing using a Leica TP 1020 automated tissue processor. The samples underwent a pre-treatment protocol prior to embedding. Pre-treatment consisted of 9 consecutive steps as follows; immersion in 70% alcohol, 80% alcohol, 95% alcohol, 100% alcohol 1, 100% alcohol 2, alcohol-xylene mix and xylene for one hour each. Samples were subsequently placed in pure paraffin wax 1 at 61°C for one hour, followed by pure paraffin wax 2 at 61°C for 2 hours.

Following pre-treatment, samples were embedded in molten liquid paraffin to form tissue blocks, on a paraffin embedding station (Leica EG-1150H). Tissue samples were removed from their cassettes after processing. Sections were inserted using a forceps in an upright position into plastic moulds filled with molten paraffin (61°C) using a forceps. To ensure optimal orientation, colon samples were transferred to a cold plate briefly while orientating colons in liquid paraffin. Samples were orientated with the longitudinal axis perpendicular to the base of the mould. Labelled cassettes were positioned on top of wax for identification purposes, pressed down, and filled with more paraffin to completely cover the face of the cassette. The plastic moulds were then transferred to a cold plate for 24

hours to allow the wax to fully solidify. Paraffin wax embedded samples were stored at 4°C.

For sectioning, cold blocks were removed from the moulds and trimmed with a blade to remove excess paraffin. Tissue sections (7µm) were then cut using a rotary microtome. Speed and blade angle (5°) were adjusted to optimise sectioning and obtain cohesive ribbons of tissue. Following sectioning, ribbons of tissue were transferred to a water bath at 50°C (below melting point of wax) with a gentle sweeping action to allow sections to flatten out. Clean, labelled slides, which were subbed in poly-lysine solution, were used to collect the tissue sections from the water bath. Slides were removed vertically to facilitate drainage, and blotted on tissue paper. The surface of the water bath was cleared with tissue between each block to avoid cross-contamination. Slides containing sections were placed on a slide drying hotplate warm plate for 30 minutes.

#### **2.4.1.1. Haematoxylin and Eosin (H&E) Stain**

Routine H&E staining was carried out on 7µm colon tissue sections for detailed histological evaluation. Haematoxylin is a basic dye which stains organelle including nuclei a blue/black colour. Eosin stain is an acidic dye and stains cytoplasmic and extracellular matrix structures varying shades of pink to red.

Slides were mounted onto a linear stainer (Leica ST4020) in which tissue sections were initially deparaffinised in Histoclear for 5 minutes before being passed through a series of rehydration steps in an ethanol gradient (100% and 70%) to ddH<sub>2</sub>O for one minute each. Slides were submerged in Harris haematoxylin for 1 minute and rinsed in running water. Slides were differentiated in 1% acid-alcohol for 1 minute prior to immersion in Eosin Y solution for 1 minute. Slides were rinsed in running water, dehydrated in increasing

concentrations of ethanol (70% and 100%), and cleared in HistoClear. Slides were mounted in Di-N-Butyl Phthalate in Xylene (DPX) mounting medium, cover-slipped and examined by light microscopy.

#### **2.4.1.2. Histopathological Scoring**

Transverse and longitudinal colon sections were analysed at three random locations in order to obtain an indiscriminate representation of tissue state from which to establish histopathological scores.

Histological scoring was based on a modified version of a protocol employed by Cooper et al. [317] to evaluate histopathology in a 5% DSS- induced murine model of colitis. In accordance with this protocol, two histological parameters were employed in order to establish the severity of DSS-induced colitis. Tissue inflammation was graded on a scale of 0-3 as shown in Table 2.2.

<b>Score</b>	<b>Gross Morphology</b>
<b>0</b>	No visible enlargement of lamina propria
<b>1</b>	Mild enlargement of lamina propria
<b>2</b>	Moderate expansion of lamina propria with increased infiltration of nuclei
<b>3</b>	Substantial increase in lamina propria size in addition to heavy infiltration of nuclei into surrounding areas

Table 2.2: Criteria for scoring of tissue inflammation



The second parameter used to assess tissue damage was the crypt damage. This was graded on a scale of 0-4 as set out in Table 2.3.

<b>Score</b>	<b>Gross Morphology</b>
<b>0</b>	Intact crypts extending down to muscularis mucosae
<b>1</b>	Shortening and loss of basal 1/3 of crypt
<b>2</b>	Loss of basal 2/3 of crypts and focal thinning of epithelium
<b>3</b>	Total loss of crypts with retainment of surface epithelium
<b>4</b>	Total loss of crypts with surface erosions

Table 2.3: Criteria for scoring of crypt damage

Based on the criteria outlined above, individual scores were assigned to each area of the section analysed by an examiner who was blind to treatment groups. In cases where the tissue section exhibited varying grades of pathology, the highest score was recorded.

Average scores were then obtained for each sample; reflecting the extent of DSS-induced colonic damage.

#### **2.4.1.3. *Imaging and crypt length measurements.***

Colon sections were digitally scanned (40x magnification) by Slidepath and these images were visualised using Digital Slidebox software. In order to determine the average crypt depth, areas from longitudinal colon sections were measured using the annotation functions across five areas of each sample and averaged.

## 2.5. Biological Methods

### 2.5.1. MTT assay

The MTT assay is widely used to determine the cytotoxicity of drug candidates. It is a colourimetric assay where the mitochondrial enzymes in viable cells will reduce the MTT (3(4,5-dimethylthiazol-2-yl)-2,5-dipenyltetrazolium) bromide) to produce formazan crystals which can be seen as a colour change from pale yellow to purple.

The MTT assay was carried out in Caco-2 and HT1080 cell lines. Cells were seeded into 96-well plates (Caco-2 at  $8 \times 10^3$  cells/well and HT1080 at  $12 \times 10^4$  cells/well) and grown until 70-80% confluent. The cells were serum starved by changing the media to FBS free for 1 hour prior to adding the compounds. The nitrate-barbiturate compounds were then added to the FBS free media at a concentration range of 0.1-200 $\mu$ M and incubated for 24 hours at 37°C. Vehicle was added in place of the compound solutions for the control, and blank wells contained serum free media only. Following this incubation, MTT (3(4,5-dimethylthiazol-2-yl)-2,5-dipenyltetrazolium) bromide) was added at 0.5mg/mL and the plates were incubated for a further 3 hours at 37°C. Supernatants were then aspirated, 100 $\mu$ L of DMSO was added to each well, and the plates were incubated with shaking for 10 minutes in order to lyse the cells and dissolve the purple formazan crystals in the mitochondria of the living cells. The absorbance of each well was then read at 540nm. The percentage cell survival was calculated as  $(A_T - A_B)/(A_V - A_B) \times 100$ , where  $A_T$  is the absorbance of the compound treated wells,  $A_B$  is the absorbance of the blank wells with media only, and  $A_V$  is the absorbance of the vehicle treated cells.

### 2.5.2. Annexin V flow cytometry

Flow cytometry suspends cells in a stream of fluid and passes them through a laser detector. With the use of appropriate antibodies, cells can be sorted according to certain characteristics by fluorescence-activated cell sorting (FACS). We used annexin V and propidium iodide (PI) to identify cells where apoptosis or necrosis had been induced following incubation with the compounds in order to assess their toxicity.

Phosphatidylserine (PS) is a phospholipid that is usually orientated to the cytosolic side of the cell membrane; however, during early apoptosis, it becomes exposed on the cell surface [318]. Annexin V can preferentially bind to PS and so positive staining can indicate that a cell is in early apoptosis or loss of cell membrane integrity as in necrosis. PI is used as a nucleic acid stain and will only stain the cell DNA following disruption of the plasma membrane indicating necrosis of the cells. Therefore, cells that are considered viable are both annexin V and PI negative, while cells that are in early apoptosis are annexin V positive and PI negative, and cells that are in late apoptosis or already dead are both annexin V and PI positive.

Flow cytometry was carried out in Caco-2 and HT1080 cell lines. Cells were grown until 70-80% confluent in T-25 flasks. The media was then changed to FBS free, the inhibitor compounds were added as described previously and the flasks incubated for 24 hours at 37°C. Following the incubation, the cells were detached from the flasks using trypsin and washed with 10x binding buffer (0.1M HEPES (pH 7.4), 1.4M NaCl, 25mM CaCl<sub>2</sub>). The cells were then pelleted by centrifugation and resuspended in 100µL 1x binding buffer. 20µL of the suspension was taken and stained with 5µL Annexin V-FITC and 5 µL of propidium iodide (PI) in 70µL of 1x binding buffer and incubated at room temperature for 15 minutes protected from light. Following incubation, the samples were diluted with



400µL of 1x binding buffer, added to a 96-well plate and analysed within 5 minutes using a BD FACS Array (BD Biosciences, Oxford, UK). Flow cytometry was performed on the stained cell samples (Caco-2 and HT1080). The instrument was set up to measure the size (forward scatter), granularity (side scatter) and cell fluorescence. Antibody binding was measured by analysing individual cells for fluorescence. The data were analysed using BD FACS array software and expressed as percentage of control fluorescence in arbitrary units.

### **2.5.3. MMP-2 and MMP-9 fluorogenic assay**

IC<sub>50</sub> values of the compounds were determined using a fluorogenic assay. This provides an accurate and precise method for testing the potency of compounds and has been widely used for obtaining IC<sub>50</sub> values of MMP inhibitors [319, 320]. Activated recombinant gelatinases are incubated with inhibitors and a suitable fluorescently labelled substrate. Uninhibited protease is capable of cleaving an amide bond between the fluorescent group and quencher group, which causes an increase in fluorescence that can be measured and the inhibition calculated.

Recombinant pro-MMP-2 and -9 (R&D Systems, Ireland) were activated by incubating with 1mM APMA at 37°C for 1 and 24 hours respectively according to manufacturer's protocol. The synthetic broad-spectrum fluorogenic substrate (7-methoxycoumarin-4-yl)-acetyl-pro-Leu-Gly-Leu-(3-(2,4-dinitrophenyl)-L-2,3-diaminopropionyl)-Ala-Arg-NH<sub>2</sub> (R&D Systems, UK) was used to assay MMP-2 and MMP-9 activity. The activated recombinant enzyme was diluted to 0.2ng/µL, 50µL added to a 96 well plate and incubated with the compounds for 30 minutes at 37°C. The substrate was then added to the plate

(50 $\mu$ L of 20 $\mu$ M solution) and the fluorescence was immediately read using the FLOUstar Optima spectrophotometer and Optima software with excitation and emission wavelengths set to 330 and 405 nm, respectively. Readings were repeatedly taken at 1 minute intervals for 10 time points. Fluorescence plotted against time gave a straight line from which the slope was used as a measure of inhibition:  $\text{Inhibition \%} = \left(1 - \frac{\text{Slope (compounds)}}{\text{Slope (control)}}\right) * 100\%$ .

Slope of the compounds is the slope following incubation with a compound and control represents incubation without any compound. This was repeated for six concentrations in the range 0.1nM-10 $\mu$ M for each compound. The IC<sub>50</sub> values were calculated by plotting the logarithm of the concentration versus the %inhibition in the sigmoidal dose-response formula using GraphPad Prism® 4. IC<sub>50</sub> values and 95% confidence intervals were obtained from the readout from the software.

#### **2.5.4. Bradford protein assay**

Protein quantification was required for many experiments and was performed using the Bio-Rad protein assay. A serial dilution of a bovine serum albumin standard was carried out to give the range of 400-25mg/ml. The standards were loaded onto a 96 well plate and ddH<sub>2</sub>O was used as a blank. Most conditioned media and cell lysate samples required a 1 in 4 dilution prior to loading on to the plate. Bio-Rad protein assay dye reagent was added to each well. Absorbance was measured at  $\lambda$  595nm using FLOUstar Optima spectrophotometer and Optima software. The protein concentration of the samples was then determined using the standard curve.

### 2.5.5. Gelatin Zymography

Gelatin zymography is an electrophoretic technique where proteins are separated on a gel according to their size. The gel is impregnated with gelatin, a substrate for MMP-2 and -9 and so following renaturing and incubation steps, the gelatinases can digest the gelatin which becomes visible as bands following staining. This technique can be used to assess the activity of the enzymes in *in-vitro* models.

The conditioned media from cell experiments was removed from all flasks, centrifuged at 13000 rpm for 5 min and the supernatants transferred to 1.5mL tubes. Colon samples of approximately 50mg were added to 2ml tubes with 1ml of lysis buffer (150mM NaCl, 50mM Tris-HCl pH 8.0, 1% v/v NP-40, 50µl/10ml Phosphatase Inhibitor Cocktail I, 50µL/10mL Phosphatase Inhibitor Cocktail II) and the sample was homogenised using a polytron homogeniser. The samples were then centrifuged at 13000 rpm for 15 minutes at 4°C and the supernatants were frozen as 25µL aliquots to avoid freeze-thaw cycles. The total protein concentration of the samples was calculated using the protein assay method described previously and the samples were normalised for protein concentration. Each sample was diluted as required with ddH<sub>2</sub>O to a volume of 18µL and 6 µL of loading buffer (50%v/v stacking buffer (Trizma base 6.05%w/v, SDS 0.4%w/v in ddH<sub>2</sub>O, pH 6.8), 40%v/v glycerol, 8%w/v SDS, 2%w/v bromophenol blue) was then added. The zymography gel consisted of a separating gel (8%w/v acrylamide, 25%v/v resolving buffer (18.2%w/v Trizma base, 0.4%w/v SDS in ddH<sub>2</sub>O, pH 8.8), 2%w/v gelatin, 0.0033% APS and 0.067%v/v TEMED in ddH<sub>2</sub>O) and a stacking gel (4%w/v acrylamide, 25%v/v stacking buffer, 0.05%w/v APS and 0.1%v/v TEMED in ddH<sub>2</sub>O), with wells to load the samples. The prepared samples were loaded onto the stacking gel and electrophoresis was carried out for approximately 2 hours at 300V (Bio-Rad Power Pac HC®) in tank buffer



(0.3%w/v trizma base, 1.44%w/v glycine (Bio-Rad), 0.1% SDS in ddH<sub>2</sub>O, pH 8.3). Gels were washed and placed on a rocker for 20 minutes with 2.5% Triton X. This was repeated three times. The gels were then washed twice and finally incubated with zymography buffer (0.15M NaCl, 5mM CaCl<sub>2</sub>, 0.05% NaN<sub>3</sub>, and 50mM tris-HCl buffer at pH 7.5) at 37°C for approximately 48 hours or until the bands became visible. After incubation, the gels were stained with 0.025% coumassie brilliant blue G250 in 25% methanol, 10% acetic acid, and H<sub>2</sub>O for 3 hours or as required and destained with acetic acid 8%, methanol 4%, and H<sub>2</sub>O until ready to analyse. The gelatinolytic activity of MMP-2 and MMP-9 was detected as a clear band of gelatin digestion against a blue background and was quantified by densitometry using the gel documentation system Bio-RAD, Universal hood II and Quantity One 4.6 software. Snapshots of the gels were transformed so that the bands could be automatically read by the software. Band width and height were detected automatically and adjusted as appropriate. Trace quantity readout was calculated automatically as intensity x mm where intensity was calculated by integrating the average intensity for each row of pixels across the specified band width and height to the baseline and mm is the band height in mm. Results were expressed as a percentage of the stimulated group.

### **2.5.6. RNA isolation**

Following removal of the media in cell samples after an incubation of 24 hours, the RNA was isolated using RNAqueous-4PCR<sup>®</sup> kit from Ambion (Applied Biosystems) according to the manufacturer's protocol. Briefly, 400µL lysis/binding solution was added to the T-25 flasks or wells of a 6-well plate. Cell scrapers and forceful pipetting were used to remove the cells and the suspension was transferred to an RNAase-free 1.5ml tube. For colon

samples, 400 $\mu$ L lysis buffer was added to approximately 50mg of tissue and a polytron homogenizer or a scissors followed by vortexing were used to homogenise the tissue. Any large lumps of tissue were pelleted by centrifugation and the supernatant was transferred to a clean tube. An equal volume of 64% ethanol was added to the lysate samples and the samples were mixed by gentle vortexing. The kit's filter cartridges were assembled to sit on top of the supplied 1.5ml tubes and 450 $\mu$ L of the sample was added to the filter. The lysate/ethanol mixture is passed through the filter by centrifuging at 10,000G for 30 seconds. The filtrate is removed and discarded and the step is repeated so that all lysed sample had passed through the filter. 700 $\mu$ L of wash solution #1 is then added to the filter and drawn through by centrifugation as described previously and discarded. 500 $\mu$ L of wash solution #2/3 was then added to the filter, drawn through and discarded. This step was then repeated. Following removal of the wash solution, another centrifugation step was carried out to remove any residual solution from the filter. The filters were then transferred to fresh, unused tubes supplied with the kit and 40 $\mu$ L of elution solution, which had been heated to 80°C, was added to ensure that the entire surface of the filter is wet. The solution was drawn through the filter by centrifugation as described previously and the draw-through was retained in the tube while the step was repeated. The filters were discarded and the 80 $\mu$ L of RNA solution can be used immediately or stored at -80°C.

### **2.5.7. RNA quantification**

The isolated RNA from each sample was quantified using a NanoDrop ND-1000 spectrophotometer (Fisher Scientific Ireland Ltd, Dublin, Ireland) and ND-1000 software. The optical surfaces of the instrument were cleaned with RNA free wipes and it was

initialized using nuclease-free water (Ambion). The NanoDrop was then blanked using the elution solution. Each sample is measured by loading 1  $\mu$ L onto the lower optical platform and lowering the arm. The surfaces were wiped clean between each measurement. The RNA concentration was automatically calculated by the software from the absorbance at 260nm and given as ng/ $\mu$ L. Purity of the sample was primarily assessed by the 260/280 ratio which was again automatically calculated by the software and for RNA should be approximately 2. A further measure of purity was the 260/230 ratio which should be approximately 2-2.2 and these ratios served as a rule of thumb for purity assessment. All samples were diluted to 1  $\mu$ g/100  $\mu$ L with nuclease free water.

#### **2.5.8. Reverse transcription**

RNA samples were converted to single-stranded cDNA using a High Capacity cDNA Reverse Transcription kit (Applied Biosystems) according to the manufacturer's protocol. The kit components were thawed on ice and for each sample, the quantities required were calculated based on the number of samples as per Table 2.4. Equal volumes of the 2x RT master mix and the diluted RNA samples (10  $\mu$ L) were added to nuclease-free 50  $\mu$ L reaction tubes, inverted several times and centrifuged at 8,000G for 15 seconds.



<b>Kit component</b>	<b>Volume/Reaction (μL)</b>
10x RT buffer	2
25x deoxyribonucleotide triphosphate (dNTP) mix (100mM)	0.8
10x RT random primers	2
Multiscribe™ reverse transcriptase	1
Nuclease free H <sub>2</sub> O	4.2
<b>Total per reaction</b>	<b>10</b>

Table 2.4: Components of High Capacity cDNA Reverse Transcription kit and volumes required per reaction.

The heat cycles required for reverse transcription were carried out using a Realplex<sup>2</sup> Mastercycler (Eppendorf UK Ltd) using the following cycles: step 1, 25°C for 10 minutes, step 2, 37°C for 120 minutes, step 3, 85°C for 5 minutes and step 4, 4°C until samples were collected. The cDNA samples were used immediately or stored at -20°C.

### 2.5.9. Real time quantitative polymerase chain reaction (qPCR)

Real Time qPCR was carried out using pre-designed TaqMan Gene Expression Assays (Applied Biosystems) according to the manufacturer's protocol. 1.5μL of cDNA solution was added to each well of a twin.tec 96 well-plate (eppendorf). Master-mix was made up separately with primers for each of the genes of interest as well as 18S primer which was used as a control and 18.5μL was added to each well as shown in Table 2.5.

<b>Component</b>	<b>Volume/well (μL)</b>
Sample cDNA	1.5
TaqMan universal master mix II no UNG	10
Nuclease-free H <sub>2</sub> O	7.5
Primer	1
<b>Total per reaction</b>	<b>20</b>

Table 2.5: Components of TaqMan gene expression assay and volumes per well.

Each sample was run in duplicate for both the primer of the gene of interest and the internal control 18S (which was used in all cases) and the pre-designed assays that were used are listed in Table 2.6. Heat cycles required for PCR were run on Realplex<sup>2</sup> Mastercycler (Eppendorf UK) and consisted of step 1, 95°C for 10 minutes, step 2, 95°C for 15 seconds, step 3, 60°C for 60 seconds. Steps 2 and 3 were repeated for 40 cycles and the measuring point for the reaction was set at the 60°C step.

<b>Primer</b>	<b>Assay ID</b>
<b>18S</b>	Hs 99999901_s1
<b>MMP-9</b>	Hs 00234579_m1
<b>MMP-2</b>	Hs 01548724_m1
<b>MMP-3</b>	Hs 00968305_m1
<b>MMP-8</b>	Hs 01029057_m1
<b>NOS2</b>	Hs 01075521_m1
<b>NFKB1</b>	Hs 00949904_m1
<b>RelA</b>	Hs 01042014_m1
<b>IKBKG</b>	Hs 01006763_m1
<b>MMP-9</b>	Rn 00579162_m1
<b>IL-1B</b>	Rn 00580432_m1
<b>TNF</b>	Rn 99999017_m1

Table 2.6: Gene symbols and assay IDs of TaqMan gene expression assays used. All primers/probes were commercially available and pre-designed by Applied Biosystems. Assay IDs beginning with the code Hs are human primers used for cell culture experiments and primers with the assay ID beginning in Rn are rat primers and used for gene expression analysis of rat colons.

Real-Time qPCR data were analysed using realplex 1.5 software. Relative quantitation was carried out by the comparative  $C_T$  (threshold cycle) method. The  $C_T$  value of the gene of interest is compared to that of the endogenous control, 18S. This difference is the  $\Delta C_T$  value. Relative quantitation is given by the formula  $2^{-(\Delta\Delta C_T)}$  where  $\Delta\Delta C_T$  is the difference between the  $\Delta C_T$  value of a given sample and that of a reference sample or group such as a stimulated group.



### 2.5.10. TaqMan low density array (TLDA) cards

Rat inflammation microfluidic cards (Applied Biosystems) were used to screen the effect of a selected compound on the expression of 90 different inflammatory related genes (Table 2.8). The cards consist of 384-well plates that use PCR to measure mRNA levels in a given sample. The combined results give a profile of the expression of inflammatory genes in a sample and comparing groups allows us to observe how interventions can affect the expression of these genes.

mRNA was isolated from distal colon samples that had been stored in RNAlater solution using RNAqueous 4-PCR kit as described previously. The samples were normalised for RNA concentration and reverse transcription was carried out as described previously. Each card contained 8 loading ports and pre-loaded primers/probes that were repeated 4 times per card, as shown in Figure 2.1. Two samples were loaded per card with 150ng of cDNA in each of the four fill reservoirs which allowed duplicates of each mRNA. Samples to load were prepared in 1.5mL tubes as shown in Table 2.7 but calculated for 4 reservoirs with excess. The tube was vortexed and briefly centrifuged to mix and remove any bubbles.

Reaction Component	Volume per reservoir ( $\mu$ L)
cDNA sample (150ng) in nuclease free	50
H <sub>2</sub> O	
TaqMan universal master mix II no UNG	50
<b>Total</b>	<b>100</b>

Table 2.7: Master mix and sample components per reservoir

The cards were equilibrated to room temperature prior to opening to prevent condensation. 100 $\mu$ L of prepared sample was loaded into each port with care taken not to puncture the foil bottom or insert air to the port which is shown in Figure 2.1 along with the card layout.

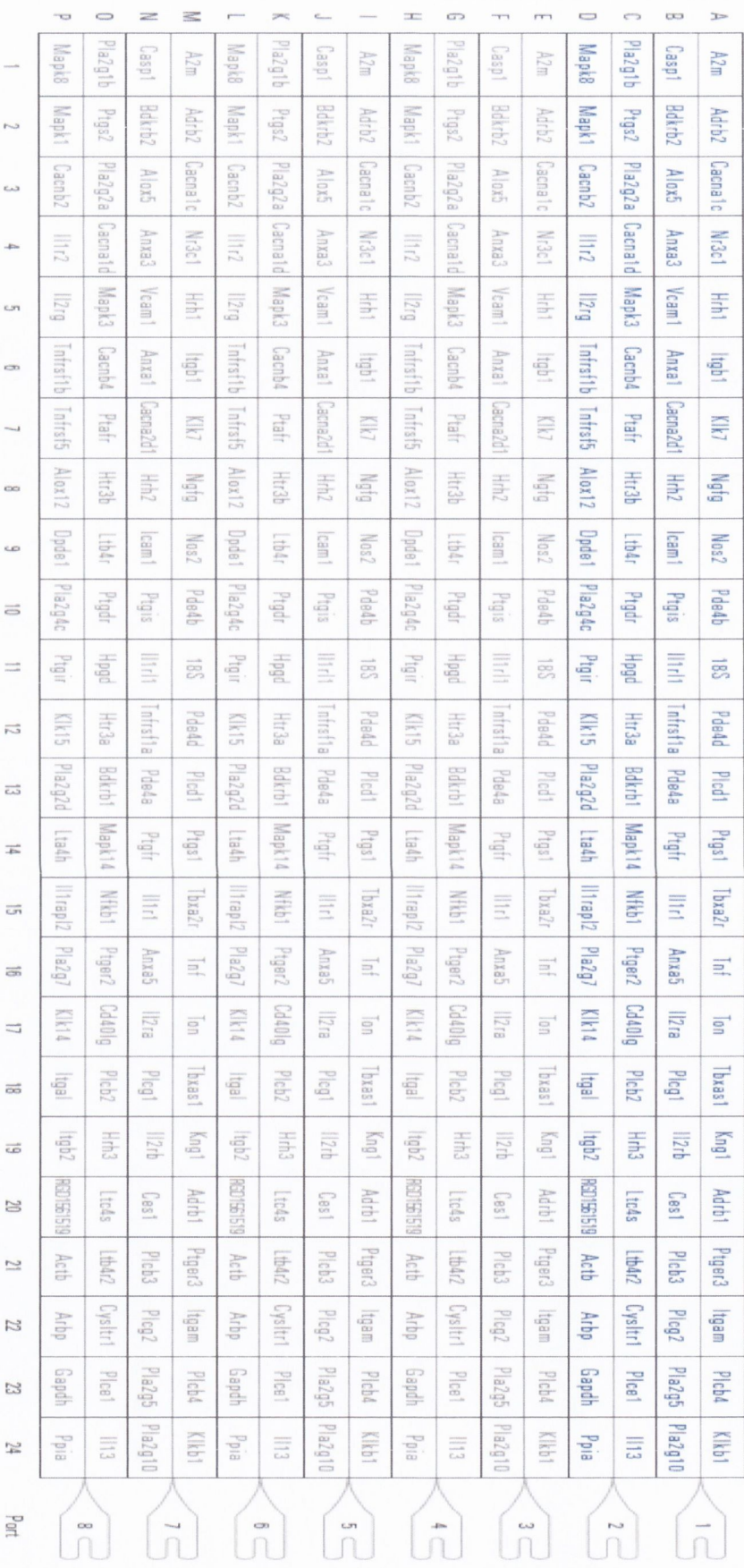


Figure 2.1: Layout of rat inflammatory array card with gene symbols.



Once filled, the cards were placed in a card holder and placed in buckets (Sorvall) for centrifugation. The centrifuge (Quikset, Sorvall) was run twice for 1 minute at 12,000 rpm and ramp 3. Centrifugation draws the sample into the wells and resuspends the dried primers and probes in each well. The cards were then removed and sealed using an array card sealer. The loading ports were cut off and the cards were ready to run on the Viia 7 (Applied Biosystems) using the default settings for 384-well array cards. Quantitation analysis was carried out as described previously using the  $2^{-(\Delta\Delta CT)}$  method relative to a chosen median animal in the DSS group.

Following relative quantitation, a cut-off point of two-fold up or downregulated was chosen. The Venn diagram online software, Venny [321] was used to identify genes that were commonly up or downregulated in all animals of the sham and *Ia* treated groups relative to the DSS group. This was carried out by inputting the names of genes that met the cut-off criteria for each animal in a group and using the diagrams generated to identify commonly regulated genes in at least three of the animals within a group. The names of the genes identified from the previous step were then cross-referenced for the sham and *Ia* treated groups using this same Venn diagram method.

The heatmap and correlation matrix were generated using the dChip software [322]. Fold change data was organised in a Microsoft Excel sheet with the animal group and designation as a column heading and the gene names as row headings. This file was then saved as a text tab-delimited file and opened using the dChip software using the “Get External data” function. The correlation matrix and heatmap were generated using the “sample correlation matrix” and “cluster genes and samples” functions respectively.

Assay ID							
Rn00560589_m1	Rn00560650_s1	Rn00709287_m1	Rn00561369_m1	Rn00566691_s1	Rn00566727_m1	Rn00754920_m1	Rn00824646_m1
Rn00562724_m1	Rn00597384_m1	Rn00563172_m1	Rn00563181_m1	Rn00563627_m1	Rn00563742_m1	Rn01442580_m1	Rn00564216_s1
Rn00580896_m1	Rn01483828_m1	Rn00580999_m1	Rn00568820_m1	Rn00820922_g1	Rn01449787_m1	Rn02132919_s1	Rn00573408_m1
Rn01453358_m1	Rn00671828_m1	Rn00587789_m1	Rn00588589_m1	Rn01752908_g1	Rn00709830_m1	Rn01423590_m1	Rn01461082_m1
Rn00561646_m1	Rn00566785_m1	Hs99999901_s1	Rn00566798_m1	Rn00690481_m1	Rn00566881_m1	Rn00690601_m1	Rn99999017_m1
Rn00564227_m1	Rn00694611_m1	Rn01640664_m1	Rn01492348_m1	Rn00565354_m1	Rn00565423_m1	Rn00565482_m1	Rn00565571_m1
Rn01645597_s1	Rn00824628_m1	Rn00577775_m1	Rn00577803_m1	Rn00578261_m1	Rn00578842_m1	Rn01399583_m1	Rn00579419_m1
Rn01754402_g1	Rn01772640_m1	Rn01764022_m1	Rn01773140_m1	Rn01520520_m1	Rn01503878_m1	Rn01410545_m1	Rn01757268_m1
Rn00820615_m1	Rn00562160_m1	Rn01774062_gH	Rn00824536_s1	Rn00562282_m1	Rn00709342_m1	Rn00577426_m1	Rn01488161_m1
Rn00565865_m1	Rn00566108_m1	Rn00682353_m1	Rn00755849_m1	Rn01453968_m1	Rn00567751_m1	Rn00567782_m1	Rn01424865_g1
Rn00584362_m1	Rn00585063_m1	Rn00585276_m1	Rn01497055_g1	Rn00586282_s1	Rn00586294_s1	Rn00587127_m1	Rn00587615_m1
Rn01476389_m1	Rn01754645_m1	Rn01427948_m1	Rn01482736_m1	Rn00667869_m1	Rn00821065_g1	Rn99999916_s1	Rn00690933_m1
Gene Symbol							
A2m	Adrb2	Cacna1c	Nr3c1	Hrh1	Itgb1	Klk7	Ngfg
Casp1	Bdkrb2	Alox5	Anxa3	Vcam1	Anxa1	Cacna2d1	Hrh2
Pla2g1b	Ptgs2	Pla2g2a	Cacna1d	Mapk3	Cacnb4	Plafr	Htr3b
Mapk8	Mapk1	Cacnb2	Il1r2	Il2rg	Tnfrsf1b	Tnfrsf5	Alox12
Nos2	Pde4b	18S	Pde4d	Plcd1	Ptgs1	Tbxa2r	Tnf
Icam1	Ptgis	Il1r1	Tnfrsf1a	Pde4a	Ptgr	Il1r1	Anxa5
Ltb4r	Ptgd	Hpgd	Htr3a	Bdkrb1	Mapk14	Nfkb1	Ptger2
Dpde1	Pla2g4c	Ptgir	Klk15	Pla2g2d	Lta4h	Il1rapl2	Pla2g7
Ton	Tbxas1	Kng1	Adrb1	Ptger3	Itgam	Plcb4	Klkb1
Il2ra	Plcg1	Il2rb	Ces1	Plcb3	Plcg2	Pla2g5	Pla2g10
Cd40lg	Plcb2	Hrh3	Ltc4s	Ltb4r2	Cysltr1	Plce1	Il13
Klk14	Itgal	Itgb2	RGD1561519	Actb	Arbp	Gapdh	Ppia

Table 2.8: Assay ID and gene symbol for the assays pre-loaded onto the TaqMan Rat inflammation array cards

### 2.5.11. Nitrate and nitrite quantification – modified Griess assay

The Griess assay is a chemical analysis commonly used for determination of nitrites. The Griess reaction is based on the formation of a coloured azo compound by reaction of sulfanilamide with bicyclic amines such as *N*-1-(naphthyl)ethylenediamine (NED) under acid conditions [323]. The absorbance of the azo compound can then be measured. In addition, the concentration of nitrate can also be analysed using the Griess assay by treating samples with reducing metals such as cadmium and Cd/Cu complex [323-325]. A study reported the use of Vanadium (III) for reducing nitrates was better than the metals



due to its short reaction time and less toxicity [323]. NO is notoriously difficult to measure directly owing to the fact that it is a highly reactive gas and so this spectrophotometric method was used to measure the nitrate and nitrite in conditioned media which are common end point products of NO. Combined nitrate and nitrite concentrations would serve as an indirect measure of NO concentration in the conditioned media.

Nitrate and nitrite standards were serially diluted to a range 200 $\mu$ M -1.6 $\mu$ M in ddH<sub>2</sub>O and 200 $\mu$ L of each concentration was added to 12-well plates in duplicate. Nitrate was reduced to nitrite with the addition of 200 $\mu$ L saturated vanadium (III) solution (400mg VCl<sub>3</sub> in 50mL 1M HCl) and then staining of the nitrite was carried out with rapid addition of 100 $\mu$ L sulfanilamide (2% w/v in 5% v/v HCl) and 100 $\mu$ L NED(0.1% w/v in ddH<sub>2</sub>O). The plate was incubated with rocking for 45 minutes and absorbance was read at  $\lambda$  540nm using FLOUstar Optima spectrophotometer and Optima software. Measurement of nitrite standards were carried out as above with ddH<sub>2</sub>O added instead of VCl<sub>3</sub> solution and ddH<sub>2</sub>O was used as a blank for both sets of standards. Conditioned media samples were normalised for protein concentration and 200 $\mu$ L loaded onto 12-well plates in duplicate for both methods described above used to measure the nitrite and nitrate standards. Addition of VCl<sub>3</sub> to the conditioned media samples will give a measure of total NO<sub>2</sub><sup>-</sup> and NO<sub>3</sub><sup>-</sup> given as NO<sub>x</sub><sup>-</sup>. Absorbance values at 540nm were measured following addition of sulphanilamide and NEDD as described previously. Concentrations were calculated by linear regression from the standard curves and NO<sub>3</sub><sup>-</sup> in the samples was calculated by subtracting the NO<sub>2</sub><sup>-</sup> concentration from the NO<sub>x</sub><sup>-</sup> concentration.



## **2.5.12. NF- $\kappa$ B (p65) binding activity**

The NF- $\kappa$ B complex exists as an inactive dimer in the cytoplasm when, upon activation it can migrate to the nucleus. The binding activity of the p65 subunit was measured using an NF- $\kappa$ B (p65) Enzyme Linked Immunosorbent Assay (ELISA) kit (Cayman Chemicals) which first required extraction of the nuclear fraction of the cells. The ELISA plate had a specific NF- $\kappa$ B response element coated to the bottom to which any p65 present in the nuclear fraction would bind to. Following binding, a primary antibody for p65 was added so that the p65 was sandwiched between the plate and the antibody. A secondary antibody conjugated to HRP was then added to bind to the primary antibody and enable detection. The absorbance reading is a measure of the amount of p65 nuclear translocation which is the primary level of NF- $\kappa$ B regulation and thus an indirect measure of NF- $\kappa$ B pathway activation.

### **2.5.12.1. Nuclear extraction**

Extraction of the nuclear fraction was carried out using the nuclear extraction kit (Cayman Chemicals) according to the manufacturer's protocol. Cells were seeded and treated with the nitrate-barbiturate compounds in T-25 flasks, pelleted and each resuspended in 5mL of ice cold phosphate buffered saline (PBS)/phosphatase inhibitor solution (10% nuclear extraction PBS, 88% ddH<sub>2</sub>O, 2% nuclear extraction phosphatase inhibitors) in pre-chilled 15mL tubes. The cell suspensions were centrifuged at 300G for 5 minutes at 4°C and this step was repeated once. The supernatant was discarded and the cells were gently resuspended in 250 $\mu$ L hypotonic buffer (10% nuclear extraction hypotonic buffer, 2%

nuclear extraction phosphatase inhibitors, 1% nuclear extraction protease inhibitors, 87% ddH<sub>2</sub>O). The suspensions were transferred to pre-chilled 1.5mL tubes and were incubated on ice for 15 minutes. 100μL of nonidet P-40 assay reagent was added and gently mixed with pipetting. The suspension was centrifuged at a pulse spin for 30 seconds at 4°C. The supernatant contained the cytosolic fraction and was transferred to a new tube and stored at -80°C. The pellet was resuspended in 50μL ice-cold complete nuclear extraction buffer (nuclear extraction buffer, 1% nuclear extraction protease inhibitors, 2% nuclear extraction phosphatase inhibitors, 10% 10nM dithiothretinol (DTT), 37% ddH<sub>2</sub>O). The samples were vortexed for 15 seconds and then rocked on ice for 15 minutes. The samples were then vortexed again for 30 seconds and rocked on ice for a further 15 minutes. The samples were then centrifuged at 14,000G for 10 minutes at 4°C. The supernatant contained the nuclear fraction and was aliquoted into clean, pre-chilled tubes and flash frozen at -80°C.

#### ***2.5.12.2. NF-κB (p65) transcription factor assay***

The protein concentration of the nuclear extracts was measured as described previously and they were diluted to contain the same protein concentration. The 96-well ELISA plate which contained a specific dsDNA containing the NF κB response element (κB site) immobilised on the bottom was equilibrated to room temperature with all buffers. Blank and non-specific binding wells were loaded with 100μL of complete transcription factor binding assay buffer (CTFB)(73% ddH<sub>2</sub>O, 25% 4x transcription assay binding assay buffer, 1% reagent A, 1% 300mM DTT). Sample and stimulated control wells were loaded with 90μL of CFTB followed by 10μL of the nuclear extract samples for the sample wells and 10μL of the transcription factor NF-κB (human p65) positive control provided with the kit for the positive control wells. All samples and controls were loaded in duplicate, the plate sealed and incubated overnight at 4°C. The following day, the wells were emptied

and washed five times with 200 $\mu$ L wash buffer solution (99.7% ddH<sub>2</sub>O, 0.25% 400x wash buffer concentrate, 0.05% tween 20). The NF $\kappa$ B (p65) primary antibody was diluted 1:100 in antibody binding buffer and 100 $\mu$ L was added to all except the blank wells and incubated for one hour at room temperature without agitation. The wells were then emptied and washed five times with 200 $\mu$ L wash buffer solution. Transcription Factor Goat anti-Rabbit horseradish peroxidase (HRP) conjugate was diluted 1:100 with antibody binding buffer to make the secondary antibody. 100 $\mu$ L of the secondary antibody was then added to all except the blank wells and the plate was sealed and incubated for an hour at room temperature without agitation. The wells were again emptied and washed five times with 200 $\mu$ L wash buffer solution and any residual wash buffer was removed by tapping the plate on a paper towel. 100 $\mu$ L of transcription factor developing solution was added to each well and the plate was protected from light and incubated on a rocker for 15 to 45 minutes or until a medium blue colour developed. Addition of the transcription factor stop solution turned the wells from blue to a yellow colour and the absorbance was measured at  $\lambda$  450nm using FLOUstar Optima spectrophotometer.

## 2.6. Statistical analysis

Analysis of results was carried out using Graph Pad Prism<sup>®</sup> 5 for Windows (Graph Pad software, San Diego, California, USA). All results shown represent  $n = \geq 3$  and analysed using a one way ANOVA and Dunnett's post-test where all groups were compared to the stimulated control unless otherwise stated. Graphs are presented as the mean  $\pm$  the standard error of the mean (SEM) and statistical significance was judged as a P value of  $<0.05$ . A P value  $<0.05$ ,  $>0.01$  is represented as \*, P value of  $<0.01$ ,  $>0.001$  is denoted \*\* and a P



value of  $<0.001$  is denoted as \*\*\* where a group is compared to the stimulated group and a P value  $<0.05, >0.01$  is represented as #, P value of  $<0.01, >0.001$  is denoted ## and a P value of  $<0.001$  is denoted as ### where the stimulated group is compared to the sham group.

**Chapter 3: Synthesis and in-vitro assessment of barbiturate based inhibitors.**

### **3. Synthesis and in-vitro assessment of barbiturate based inhibitors.**

#### **3.1. Introduction and background**

##### **3.1.1. Selective inhibition of MMP-9**

MMPs have failed in clinical trials due to disappointing clinical efficacy results compared to animal trials and dose-limiting side-effects of MSS; but we can now reflect on how little was known of the complex protease network or the net effect of inhibition of certain enzymes in a given setting. The trials added MMPs as co-therapies for patients with invasive or metastatic-cancer which may not have been appropriate considering that metastasis was already established and also, the genetic diversity of the disease [37]. It is now known that the MMPs may play a protective role in tumour progression [326]. Setting will be crucial to the success of MMPs, and so as we understand more about the interactions of the MMP network and the roles of individual MMPs in a given disease setting, we may be better able to appropriately target them for inhibition. While broad spectrum inhibition may be appropriate in certain acute inflammatory settings, selectivity may be important in reducing side-effects in chronic inflammatory conditions.

Understanding that MMP-9 remains an attractive target for inhibition in a variety of inflammatory conditions, our group have synthesised a series of barbiturate based MMP inhibitors with gelatinase selectivity [314].



The synthesis of compounds for this study were all from the key intermediate barbiturate 5-bromide, given the designation **3**. This is prepared from 4-hydroxyphenylacetate in four steps and had been previously carried out by our group and included in the thesis of Dr Jun Wang (Figure 3.1).

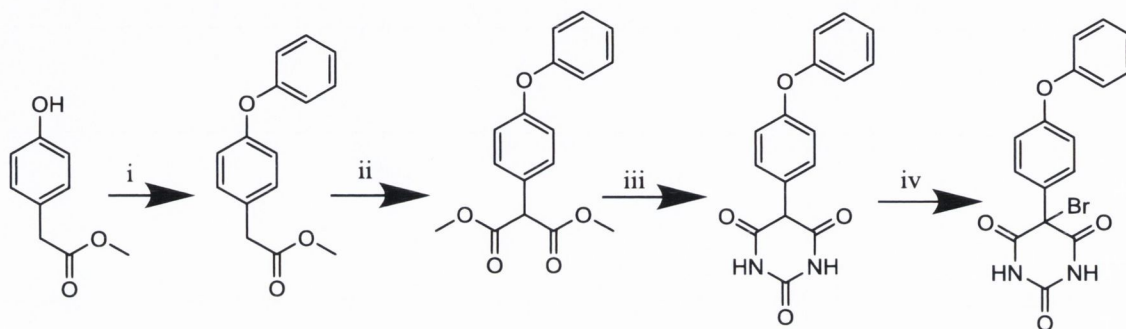


Figure 3.1: Synthesis of bromide intermediate. (i)  $C_6H_5B(OH)_2$ , copper (II) acetate, pyridine, DCM, room temperature (RT), 24 h; (ii)  $(CH_3O)_2CO$ , NaH, dry THF, 105°C, 5 h; (iii) Na, urea, EtOH, 100 °C, 7 h; (iv)  $Br_2$ , HBr,  $H_2O$ , 0 °C, 5 h [314].

From this intermediate, a series of aminoalkyl nitrate-barbiturates were synthesised along with the corresponding group of aminoalkyl alcohol-barbiturates for comparative purposes. The initial synthesis and characterisation of the compounds was carried out by Dr Jun Wang but was also completed by myself during the course of the work.

NO is a crucial second messenger owing to its ability to freely cross biological membranes, and its direct or indirect interactions with proteins and lipids to modify their function. The exact role of NO in a biological setting is extremely complex but taking advantage of the anti-inflammatory role NO may be of therapeutic benefit in certain conditions. NO-hybrids have been shown to be of benefit in a range of conditions including inflammation, cancer

and cardiovascular conditions [327, 328] but their potential as MMPs has yet to be examined. It is evident that NO has a part to play in the modulation of MMP-9 but with iNOS and MMP-9 genes both activated during inflammation and some overlapping pathways, the net effect is difficult to measure in isolation.

### **3.1.2. Effects of NO on activation of pro-MMP-9**

Inflammation leads to concurrent upregulation of iNOS and MMP-9 [329-331], however, the biological outcome of the crosstalk between these two enzymes is not clear. For a detailed review of pro-MMP-9 activation, see Fridman *et al* [59]. It is also worth noting the difficulties in measuring MMP-9 activity. While relative abundance or concentration of the enzyme can be measured using techniques such as Western blot or ELISA, this data does not reveal the activity of the enzyme. Gelatin zymography is a commonly used technique which can separate the pro and active forms of the enzyme but a recent review has highlighted its limitations in providing true activity information [332]. Incomplete refolding of the enzyme following electrophoresis and dissociation of endogenous inhibitors mean that activity data can only be obtained from gelatin zymography when it is combined with a complimentary substrate degradation assay. Let's first review evidence for NO-mediated activation of MMP-9.

#### **3.1.2.1. NO activates pro-MMP-9**

NO could disrupt the Zn-thiolate bond in pro-MMP-9 leading to its activation. There is indirect evidence for this in that NO activates TACE, another metalloproteinase [333].

Furthermore, peroxynitrite has been shown to activate other MMPs [259, 334-336]; the free radical can modulate the protein activity through S-nitrosylation of cysteine thiols [337-340], and it may also release  $Zn^{2+}$  from other Zn-thiolate centres [341, 342].

The effect of NO on MMP-9 activation in rat retinal neurons was investigated by comparing wild-type with nNOS<sup>-/-</sup> animals. Increased MMP-9 activation was observed in the wild-type rats which was attributed to S-nitrosylation of the pro-enzyme [343]. Co-localization of MMP-9 activity and nNOS was also observed in the cortex. The study went on to demonstrate that transfected recombinant MMP-9 undergoes S-nitrosylation, and thus activation, following incubation with the NO donor S-nitrosocysteine [55]. Another group working with rat brain astrocytes demonstrated an increase in tyrosine nitration of the MMP-9 enzyme by co-immunoprecipitation, corresponding to an increase in enzyme activity following iNOS induction. Inhibition of iNOS using siRNA or L-NAME significantly reduced nitrate accumulation and potential MMP-9 activity as measured by gelatin zymography [344]. A biphasic regulation of MMP-9 activity has been demonstrated in ANA-1 cells and the trend replicated in purified pro-MMP-9 enzyme where lower concentrations of spermine NONOate (SPERNO) result in activation of the enzyme and higher concentrations of NO cause inhibition [345].

#### **3.1.2.2. NO indirectly activates MMP-9**

It is argued that these experiments do not provide direct evidence for NO S-nitrosylation of the prodomain or direct activation of the cysteine switch *in-vivo*. During periods of prolonged inflammation, where large amounts of NO are produced by iNOS, there is a corresponding increase in oxidative species. The reaction of NO with superoxide anion to yield peroxynitrite is key in mediating many of the pro-oxidant and toxic effects of NO



[346]. Peroxynitrite generation could be the mechanism through which NO may indirectly activate pro-MMP-9 as has been shown for other MMPs [259, 347, 348]. Inhibition of iNOS and superoxide generation resulted in an inhibition of potential MMP-9 activity as measured by zymography, however; no experiments were carried out to ascertain whether the observed activity was as a result of decreased protein synthesis or inhibition of protein activation [349]. A study on term placentas of type II diabetic patients showed that an increase in potential gelatinase B activity measured by zymography was associated with nitration of the enzyme by peroxynitrite [350]. Purified pro-MMP-9 was shown to be activated by peroxynitrite and to a much greater extent by GSNO<sub>2</sub>, a product of the reaction of glutathione and peroxynitrite. As well as increased substrate digestion, evidence of S-glutathiolation of the pro-domain was shown using radiolabelling and MALDI-TOF MS [351]. A rat model of reperfusion injury showed that a peroxynitrite decomposition catalyst reduced MMP-9 activation as shown by gelatin and in situ zymography [352]. Although cell surface activation of MMP-9 is likely to be less frequent, another proposed mechanism of the indirect action of NO on MMP-9 enzyme activation is the upregulation of urokinase plasminogen activator (uPA), which has been shown to activate pro-MMP-9 [64]. While S-nitrosocysteine caused mild activation of recombinant pro-MMP-9, incubation of DETA NONOate with HBE1 or NHBE cell resulted in increased uPA mRNA and therefore increased pro-MMP-9 activation [353].

### **3.1.2.3. NO-mediated inhibition of MMP-9**

The above studies provide evidence for NO activation of MMP-9 either directly or indirectly; however, there is substantial evidence for an inhibitory role of NO on MMP-9 activity. For example, endothelial and carcinoma co-cultures showed a marked increase in potential MMP-9 activity measured by gelatin zymography when incubated with the iNOS

inhibitor aminoguanidine. To explain the result, purified MMP-9 enzyme was incubated with NO donor spermine-NONOate and the NO/superoxide donor SIN-1 which was expected to produce peroxynitrite. Both incubations resulted in a significant decrease in enzyme activity [354]. A very interesting study in this context, suggests that NO does not directly modulate pro MMP-9 activation. A range of NO donors; S-nitroso-glutathione (GSNO), SPERNO, DETA NONOate (DETA-NO), DEA NONOate (DEA-NO) and S-nitrosocysteine (CSNO) were tested on purified pro-MMP-9 enzyme. Of these NO donors, only SNOC caused any increase in activity. At high concentrations, DETA-NO inhibited gelatinase activity measured using a fluorescent substrate. While the compounds produced different modifications to a synthetic pro domain, these alterations were deemed to be unrelated to enzyme activation. The NO donors were incubated with the active form of MMP-9 and again, DETA-NO was found to markedly inhibit enzyme activity which was unrelated to cysteine switch activation or other oxidative modifications to the enzyme [355] and presumably due to interactions at the active site.

While activation of pro-MMP-9 by NO seems plausible, it has not been conclusively proven in an *in-vitro* or *in-vivo* setting. Variation in observations may be accounted for by the use of different NO donors with differing release properties and NO flux and duration. The use of S-nitrosocysteine as a surrogate of endogenous NO has also been questioned [356]. The above studies show that direct activation of pro-MMP-9 by NO is possible. The effect on MMP-9 is concentration dependent with a trend of increased activity at low concentration and inhibition at higher concentrations. The biological relevance of this observation remains to be determined as the presence of other oxidants and known MMP-9 activators are likely to be more salient *in-vivo*. The actions of NO in regulation of MMP-9 distribution and expression are expected to provide a greater net contribution to MMP-9 activity.

### 3.1.3. Effect of NO on MMP-9 release and distribution

Following synthesis of pro-MMP-9 enzyme, activation is dependent on its release from the cell and availability of activating agents. Once activated, the effect that the enzyme will exert is dependent on its distribution at the cell surface, in the extracellular milieu or even within the cell. Its gelatinolytic activity is therefore affected by cell surface associations, internalisation or other protein interactions. As generalised proteolysis is seen as counterproductive for cell migration, interaction with receptors, adhesion sites and invasive protrusions may have developed to allow local effective concentrations of active MMP-9 and directed ECM degradation [354, 357].

Following its release, surface associated MMP-9 has been identified in a variety of biological systems under both physiological and pathological conditions including neutrophils [358], endothelial cells [359-361], myocardium [330, 362-364], keratinocytes [365], breast epithelial [359, 366], breast cancer [367], pancreatic cancer [368], ovarian cancer [369], prostate cancer [370], fibrosarcoma [371, 372], and mouse mammary carcinoma cells [373]. It has been proposed that the affinity of the gelatinases for collagen IV, specifically through the  $\alpha 2$  (IV) chain may cause the ECM to act as a reservoir for the enzymes which become activated by inflammatory cells. Other interactions with CD44, RECK and LRP proteins have been shown to cause surface localisation, inhibition and internalisation respectively. These interactions have demonstrated an additional, complex layer of MMP-9 regulation which can direct the activity of the enzyme and are the subject of other reviews [59, 374]. Here we will focus on interactions that NO is reported to influence.



Treatment of neonatal rats subjected to hyperoxia with L-NAME, an inhibitor of NOS, led to increased activity of MMP-2 and MMP-9 in lungs [329]. The latter effect could reflect the inhibitory effects of NO on the release of these gelatinases from leukocyte gelatinase granules [329, 375], as well as from human platelets [376].

In a study investigating the effect of doxycycline on neutrophil degranulation and MMP-9 release, nitro-glycerine (GTN) caused a reduction in the MMP-9 activity in the cell supernatant, even though microscopy revealed that degranulation had occurred. Most of the MMP-9 activity was found to be associated with the cell pellet and so it was hypothesised that nitrate caused increased cell surface association of the enzyme [298].

Migrating trophoblasts have been shown to express MMP-9 in a manner regulated by NO [377]. The motile cells actively redistribute iNOS to the leading migrating edge of the cell. Interestingly, MMP-9 was found to be co-localised with iNOS at the lamellopodia and to be crucial for cell invasion. This group postulate that the co-localisation is either NO-mediated S-nitrosylation and activation of the pro-MMP-9 enzyme, or else a possible effect on the release or distribution of the enzyme [378]. In either case, the directed generation of NO and thus MMP-9 activity establishes a further role of NO in the distribution of active MMP-9.

The activity of MMP-9 in colon cancer cell lines is inhibited by cGMP analogues as shown by immunoblotting and gelatin zymography. It was discovered that this inhibition is not caused by a decrease in mRNA levels but by a compartmental redistribution of the enzyme leading to a tenfold increase in intracellular MMP-9 shown by flow cytometry [379].

Caveolin-1 (Cav-1) is a scaffold protein believed to play a role in survival and invasion of certain cancer types. While its exact role is poorly understood, it seems to act as an oncogene in some cancers [380-382] while playing the role of a tumour suppressor in

others [383-386]. In a model of hepatocellular carcinoma, overexpression of cav-1 resulted in an increased expression of MMP-9 [387]. Conversely, a breast cancer model shows that MMP-9 activity is reduced in cells expressing cav-1 while cell lysates showed no alteration in endogenous expression of the enzyme. It has been suggested that cav-1 mediates an alteration in the secretion of the gelatinase [388]. Interestingly, caveolin also plays an important role in regulation of NOS [389]. In this context, Philips and Birnby studied the interactions of NO with MMP-9 and cav-1 using an endothelial and lung carcinoma cell co-culture model. Treatment with an iNOS inhibitor resulted in strong co-localisation. This localisation is believed necessary for optimum activation of MMP-9 but is abolished in the presence of an NO donor [354].

Activation of pro-MMP-9 by other MMPs such as MMP-2, MMP-7 and MMP-13 is likely to be a cell surface event as these enzymes associate with the cell surface. One activation cascade described for MMP-9 involves the activation of plasmin from plasminogen following binding of the urokinase plasminogen activator (uPA) to the urokinase plasminogen activator receptor (uPAR) which is on the plasma membrane. Activated plasmin can activate pro-MMP-3 which can in turn activate pro-MMP-9 [390]. This cascade offers the cell an opportunity to control the distribution of activated MMP-9 and directed proteolysis. There is evidence that NO can increase expression of uPAR but inhibit the expression of uPA [353, 391, 392] and so the net effect on the distribution of active MMP-9 is not clear.

Localisation of MMP-9 has been demonstrated to represent another layer of regulation on its activity and NO is implicated in this regulation. Increasing concentration of NO will increase the internalisation or cell surface association of MMP-9 which may occur through interaction with CD44 or collagen IV. NO can also regulate the expression and activation

of MMP-9 activating factors including other MMPs, cav-1 and uPA which will affect the distribution of the active enzyme.

### **3.1.4. Effect of NO on expression of MMP-9**

MMP-9 is an inducible enzyme and is transcriptionally upregulated in response to various pro-inflammatory cytokines, physical interactions with other cells or the ECM through integrins and adhesion molecules and mechanical or physical stresses as discussed previously in section 1.1.2.1. This will trigger signalling cascades such as the MAPK or NF- $\kappa$ B leading to an increase in MMP-9 gene transcription.

Although the effects of NO on MMP-9 expression have been studied by a number of investigators there is no agreement if NO promotes or reduces the expression of MMP-9. The following section reviews this conundrum by presenting the studies where NO has been reported to inhibit MMP-9 expression and those where it has been shown to promote it.

#### **3.1.4.1. NO inhibits MMP-9 Expression**

Several studies report an inhibitory effect of NO donors on MMP-9 mRNA compared with stimulated controls [393-399]. Consistent with these observations are reports that in similar cell culture models, NOS inhibitors, which reduce NO availability, increase MMP-9 expression [393, 394, 400, 401]. The change in mRNA concentration appears to be dependent on the concentration of the NOS inhibitor or NO donor used, however, a biphasic regulation has been demonstrated where the increase in MMP-9 expression



following incubation with the NOS inhibitor L-NMMA peaked at 0.5 mM (approximately 1250ng NO<sub>x</sub>/ mg protein). Further increase in concentration of the inhibitor resulted in a decrease in mRNA until it reached control levels at 5 mM (approximately 500ng NO<sub>x</sub>/mg protein) [402]. An indirect role of NO in MMP-9 expression is through its ability to inhibit platelet aggregation [403]. This inhibition will prevent platelet aggregate mediated increase in MMP-9 expression [404-406]

#### **3.1.4.2. NO promotes MMP-9 Expression**

In several studies, incubation of cells with NOS inhibitors caused an inhibition of MMP-9 expression suggesting a promoter roll for NO [353, 407-409]. In a rat model of atherosclerosis it was reported that MMP-9 was induced to a greater extent in iNOS<sup>+/+</sup> rather than iNOS<sup>-/-</sup> animals indicating that NO increases MMP-9 expression [410]. As discussed previously, the effects of NO donors on MMP-9 expression may also be concentration dependent, as seen with a biphasic response to DETA-NONOate [353]. In this study, low levels of the NO donor (10μM) resulted in increased gene expression; however, higher concentrations (100-500μM) had the opposite effect. The biphasic response may be attributed to peroxynitrite following reaction with superoxide. In an ischemic-reperfusion injury model, peroxynitrite was found to increase the expression of MMP-9, an effect that was inhibited by NOS inhibitor L-NAME [411, 412]. A study on amyloid beta degradation in Alzheimer's disease found that NO increased MMP-9 expression both *in-vitro* and *in-vivo* [413]. Further evidence of the complex indirect role of NO on MMP-9 expression was shown in a similar model where Cav-1 inhibited MMP-9 activity. L-NAME and iNOS null mice showed that NO decreased Cav-1 expression and so increased MMP-9 activity [414, 415].

### 3.1.5. Understanding the interactions of NO and MMP-9

The role of NO in the regulation of MMP-9 has been the subject of intense study over the previous two decades and the models used have spanned several cell types and disease states. The conflicting results of the studies presented represent the dual nature of NO at almost every level of MMP-9 regulation. In making sense of the apparent contradiction in the results, it is crucial to first understand the role of concentration in this biphasic nature of NO. As stated previously, NO effects are often separated into cGMP dependent, which tend to occur at lower NO flux, and cGMP independent, occurring at higher concentrations. These cGMP independent effects are often mediated by formation of peroxynitrite [262, 263, 271, 272], leading to direct reaction with proteins to alter their function through S-nitrosylation, tyrosine nitration or oxidisation [273]. The potent oxidant, peroxynitrite will often exert an opposite effect to that of NO [262, 263, 274-276]. The balance of these reactions will, in certain cases, give rise to a threshold in concentration, beyond which the role of NO may change. To further complicate this concentration-dependent role of NO, effects will also be cell- and environment-specific depending on the presence of endogenous antioxidants [277] and other genes involved in regulating a given response.

Through studies with recombinant pro-MMP-9, activation of the zymogen by NO donors has been demonstrated. Other studies have shown that this effect is dependent on the donor used and that higher concentrations of NO may in fact inhibit enzyme activity through interaction with the active site. The overall relevance of these findings in an *in-vivo* setting remains to be determined. NO also directs proteolysis by MMP-9 by affecting local activity through increased cell surface association, directed distribution, internalisation or modulation of pro-MMP-9 activating factors. Regulation of MMP-9 expression by NO is a

concentration dependent event with a trend of increased expression at low NO concentration and downregulation at higher concentrations of NO. This trend may not hold for all cell types and will depend on the stimulating factors and so, the transcription factors involved in the expression. Activity of NF- $\kappa$ B and cGMP are both increased at low NO and inhibited at high NO concentration and so follow this observed trend. Increasing levels of NO will also reduce MMP-9 expression through a decrease in mRNA stability. A summary of these studies is set out in Table 3.1.



Cell line/ Strain	Stimulating Factor	Incubation time	NO conc.	NO donor/ iNOS inhibitor	Observed effect	Ref.
nNOS <sup>-/-</sup> and wild type rats	Focal cerebral ischemia and reperfusion		NA	nNOS <sup>-/-</sup> or 3-bromo-7-nitroindazole	↓MMP-9 compared to controls	[55]
Purified MMP-9		0-25 hours	NA	S-nitrosocysteine	↑activation compared to controls	[55]
nNOS <sup>-/-</sup> and wild type rats	intravitreal injections of NMDA and glycine	0-12 hours	NA	nNOS <sup>-/-</sup> vs wild type rats	↓MMP-9 compared to controls	[343]
Rat Brain Astrocyte cells RBA-1.	Endothelin-1	16 hrs	≈50% reduction in NO, relative to ET-1 induced levels with L-NAME 100nM	L-NAME (1, 10, 100nM) and iNOS siRNA	Dose dependent reduction (up to 10 fold) in MMP 9 activity	[344]
ANA-1 macrophage	INF-γ, LPS, L-arginine	4 hrs	50nM	NO/sper	↑ at ≤50nM and ↓ at higher concs	[345]
Lewis and Brown-Norway rats	Allogenic (Brown Norway to Lewis) heterotopic cardiac transplantation	24 hrs		1400W (N-(3-(Aminomethyl) benzyl) acetamidine (selective iNOS inhibitor)	↓ MMP-9 activity	[349]
HUVEC, NCI-H157, squamous carcinoma (SQ); NCI-H125, adenosquamous (AS); and NCI-H522, adenocarcinoma (AD).	AMPA	16hrs		aminoguanidine 100μM	↑ activity following incubation with aminoguanidine	[354]
Purified recombinant MMP-9	AMPA	6hrs	5 or 10 nmol/min (for 0.5 and 1μM spermin-NONOate). 30μM NO from 100μM SIN-1	spermine-NONOate (0.5 and 1μM) or SIN-1 (20μM, 200μM, and 2mM)	Dose dependent inhibition following incubation with the NO donors.	[354]
Purified recombinant MMP-9		0-2 hrs		GSNO, SPER-NO, DETA NONOate, DEA-NONOate, SNO C	DETA NONOate or Sper-NO - ↓activity at high concentration. SNOC - ↑ activity	[355]
Rat glomerular mesangial cells	IL-1β	36hrs		SNAP (up to 1mMol/L)	Conc dependent ↓ inhibition (up to 90%)	[393]
MDA-MB-231, MCF-7	TPA	24hrs	?	DETA-NO, SNAP or Spermine-NO (500μM)	Conc dependent inhibition. (max at 500μM)	[395]
Rat primary astrocytes	LPS	48hrs	Donors of 100μM (max inhibition)	SNAP or SNP	↓ MMP 9 expression	[394]
NHBE, HBE1, CFT1, A549	IL-1β, INF-γ, TNF-α	24hrs		spermine NONOate, DETA	Dose dependent ↓ with SNAP and GSNO.	[396]

RA-SMCs of Sprague Dawley rats	IL-1 $\beta$ (2ng/ml)	24hrs	2 to six fold increase in NO.	NONOate, SIN-1, SNAP, GSNO DETA NONOate (0.1-500 $\mu$ M)	Dose dependent $\downarrow$ in MMP-9 activity and expression	[397]
NIH/3T3 cells	Thapsigargin-induced store-operated Ca <sup>2+</sup> entry			SNAP (200 $\mu$ M)	$\downarrow$ in MMP-9 activity	[398]
VSM from male Wistar rats	IL-1 $\beta$ (5ng/ml)	24hrs		DETA NONOate (500 $\mu$ M)	$\downarrow$ in MMP-9 activity and expression	[399]
Rat glomerular mesangial cells	IL-1 $\beta$ (2nmol)	48hrs		L-NMMA (0.3-5mM)	Conc dependent $\uparrow$ in expression and activity.	[393]
Rat primary astrocytes	LPS	48hrs	7 $\mu$ M of nitrite	L-NAME (100 $\mu$ M)	$\uparrow$ MMP 9 expression	[394]
Rat Aortic SMC	IL-1 $\beta$	48hrs	approximately 50ng NO <sub>x</sub> /mg protein	L-NMMA (50nM)	5 fold $\uparrow$ in pro MMP-9 mRNA	[400]
Rat aortic smooth muscle cells from Sprague Dawley rats	IL-1 $\beta$ (2ng/ml)	48hrs	$\downarrow$ to 8.2 NO <sub>x</sub> (ng/mg of protein)	aminoguanidine (0-5mM)	Conc dependent. Up to 155% $\uparrow$ in mRNA	[401]
Rat infrarenal aorta tissue	IL-1 $\beta$	72hrs	approximately 1250ng/mg protein (at max increase)	L-NMMA	$\uparrow$ at $\leq$ 0.5mM and $\downarrow$ at higher concs	[402]
NHBE, HBE1	Linear scratch in the cells	24hrs	approximately 14.1 – 389.1 $\mu$ M NO <sub>x</sub>	DETA NONOate (10-500 $\mu$ M)	$\uparrow$ expression at $\leq$ 10 $\mu$ M and $\downarrow$ at higher concs	[353]
C57BL/6 iNOS <sup>-/-</sup> . Murine neutrophils and macrophage	Hepatic I/R injury. IL-6, or INF- $\gamma$	24hrs		iNOS <sup>-/-</sup> , ONO-1714	iNOS inhibition $\downarrow$ MMP-9 activity.	[407]
Rat Aortic Vascular SMC (A7r5)	INF- $\gamma$ , LPS, PMA	12hrs		L-NAME (300 $\mu$ M)	Inhibition to near control	[408]
WiDR		8hrs		SNAP	$\uparrow$ expression	[409]

Table 3.1: Studies of the effects of NO on activation or expression of MMP-9

## 3.2. Results

### 3.2.1. Synthesis of nitrate-barbiturates

Synthesis of the nitrate-barbiturate compounds required the commercially available aminoalkylalcohols side-chains to be converted to the corresponding nitrates and is laid out in Figure 3.2.

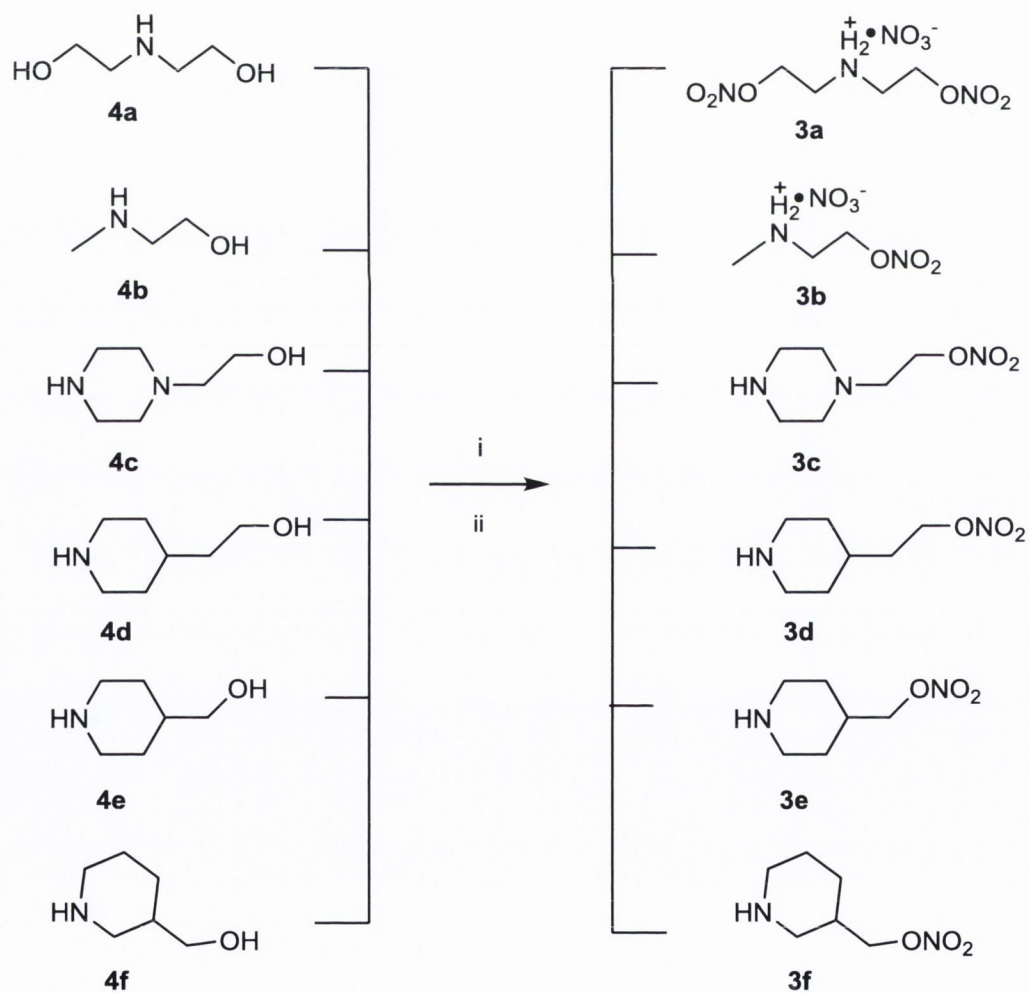


Figure 3.2: Preparation of the nitrate side-chains using the commercially available corresponding alcohols. i) DCM, fuming nitric acid, -10°C, 0.5 h. ii) acetic anhydride, 15 min.



Synthesis of the barbiturate-aminoalkylalcohols involved substitution of the bromine on the intermediate (**3**) with the commercially available aminoalkylalcohol side chains (Figure 3.3). The nitrate-barbiturates were synthesised under the same conditions with the nitrate side chains.

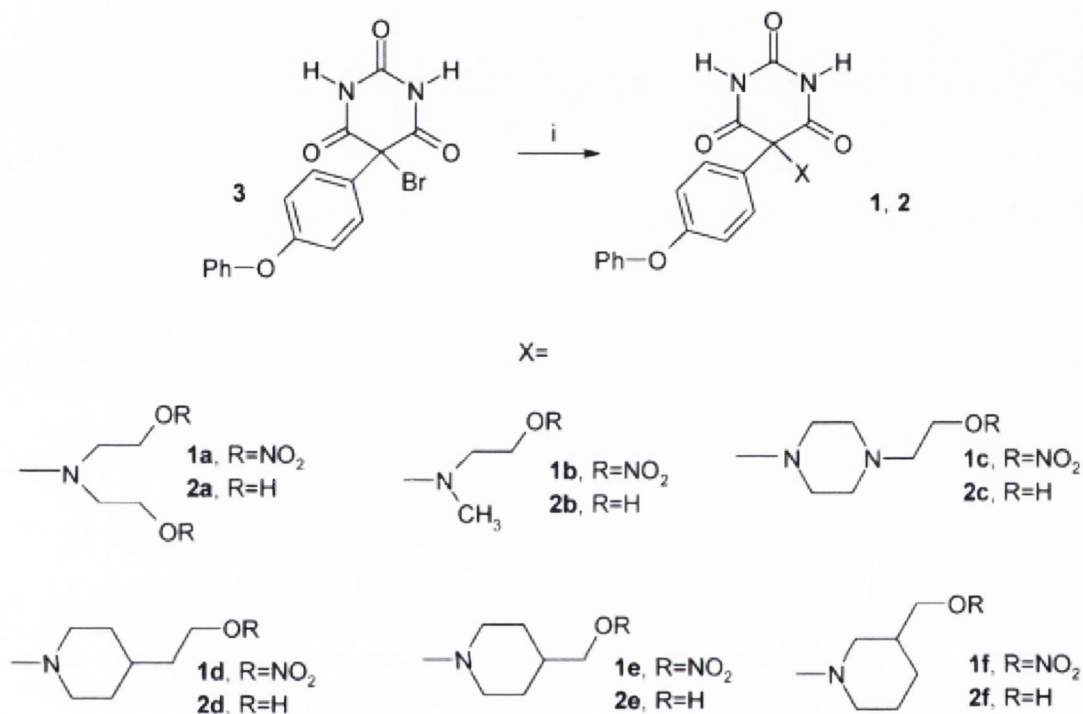


Figure 3.3: Preparation of 5-phenoxyphenyl barbiturate-5-aminoalkyl nitrates (1a-f) and aminoalkylalcohols (2a-f); i) Et<sub>3</sub>N, MeOH, RT, 24 h [315].

### 3.2.2. Effect of the nitrate-barbiturate compounds on cell viability

#### 3.2.2.1. MTT assay

In order to determine the toxicity of the compounds and a dose at which they could be effectively used, MTT assays were carried out in conjunction with Dr Jun Wang and Dr

Shona Harmon. This was performed at a range of concentrations in Caco-2 and HT1080 cell lines.

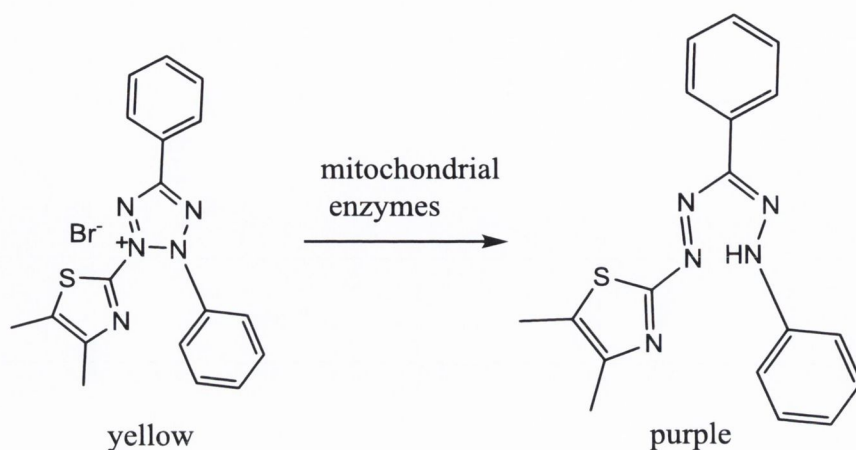


Figure 3.4: Cleavage of MTT by mitochondrial enzymes to cause the conversion from a yellow to purple colour.

This widely used cytotoxicity assay uses the ability of mitochondrial enzymes in viable cells to reduce MTT (3(4,5-dimethylthiazol-2-yl)-2,5-diphenyltetrazolium) bromide) to produce formazan crystals which can be seen as a colour change from pale yellow to purple (Figure 3.4).

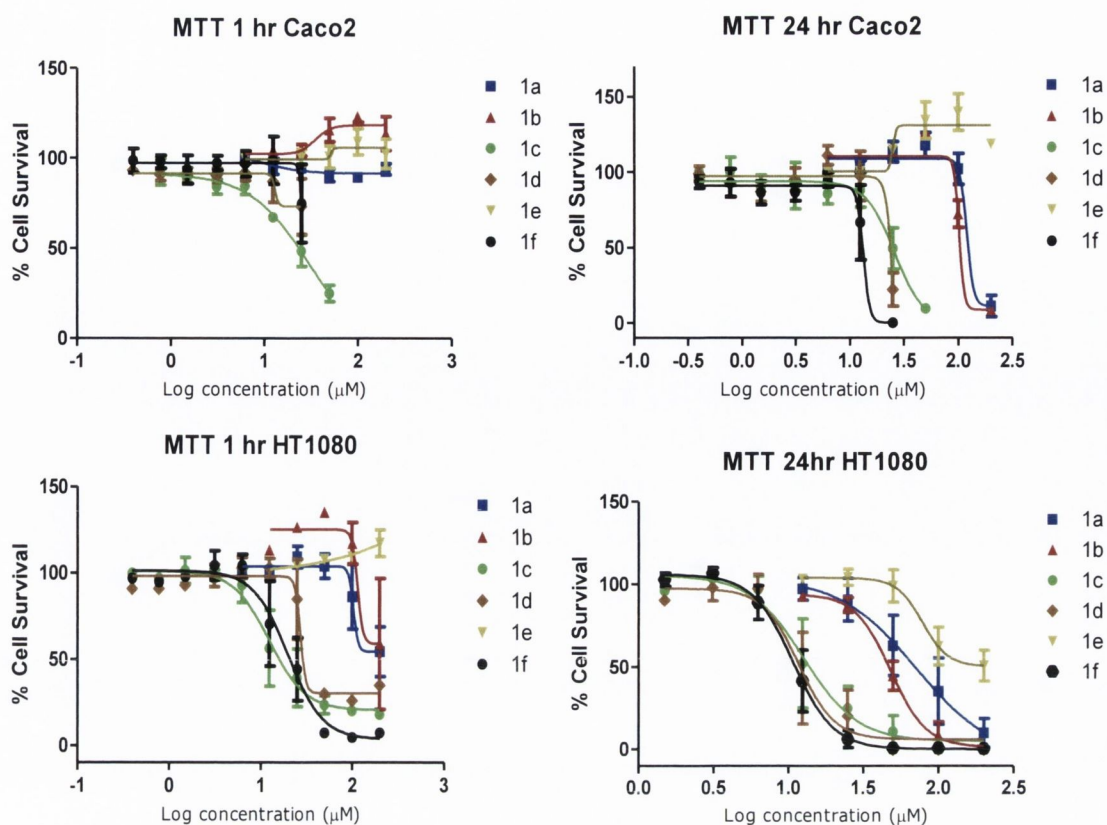


Figure 3.5: MTT assay of nitrate-barbiturate compounds (1a-f). The log concentration of the compound ( $\mu\text{M}$ ) is plotted against the % of cell survival. Compounds were tested at a range of concentrations at 1 hour and 24 hours and in Caco-2 and HT1080 cell lines.

It was observed that the Caco-2 cells were less sensitive to the cytotoxic effects of the compounds than the HT1080. As seen in Figure 3.5, Caco-2 cells showed almost complete survival at 24 hours when incubated with the nitrate barbiturate compounds at  $10\mu\text{M}$  and this was chosen as the maximum dose at which to carry out experiments with the compounds. Compounds *1c*, *1d* and *1f* were more toxic than the other nitrate-barbiturates in both cell lines and Caco-2 cell viability reduces rapidly with increasing concentration above  $10\mu\text{M}$  for these compounds.



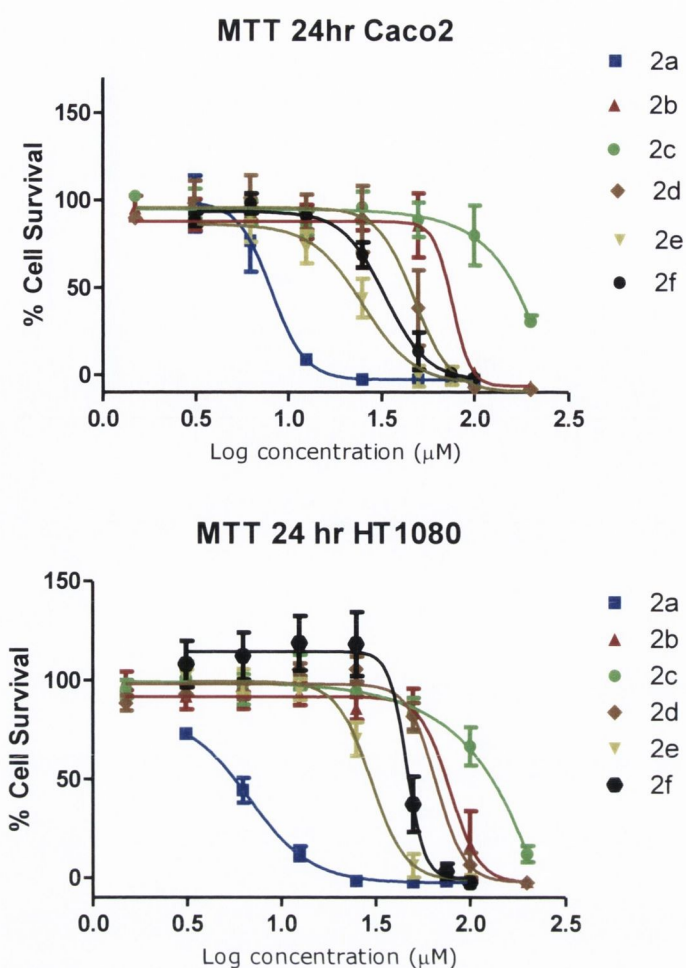


Figure 3.6: MTT assay of alcohol-barbiturate compounds (2a-f). Log concentration of the compounds ( $\mu\text{M}$ ) is plotted against % cell survival. The compounds were tested at a range of concentrations at 24 hours in Caco-2 and HT1080 cell lines.

The alcohol-barbiturate series of compounds were tested at 24 hours in Caco-2 and HT1080 cell lines (Figure 3.6). As a group, the non-nitrates were less toxic to the cells than the corresponding nitrate-barbiturates; however, **2a** caused the greatest reduction in the % cell survival in both Caco-2 and HT1080 cell lines. Cell survival was approximately 25% and 20% for Caco-2 and HT1080 at  $10\mu\text{M}$ .

### 3.2.2.2. Annexin V flow cytometry

Flow cytometry was carried out in Caco-2 and HT1080 cells in conjunction with Dr Shona Harmon to ascertain whether the nitrate compounds induced apoptosis or caused necrosis. Annexin V can bind to phosphatidylserine (PS), a phospholipid that becomes exposed on the cell surface in early apoptosis [318] to determine induction of apoptosis. PI is a nuclear stain and so positive staining indicates late apoptosis or necrosis

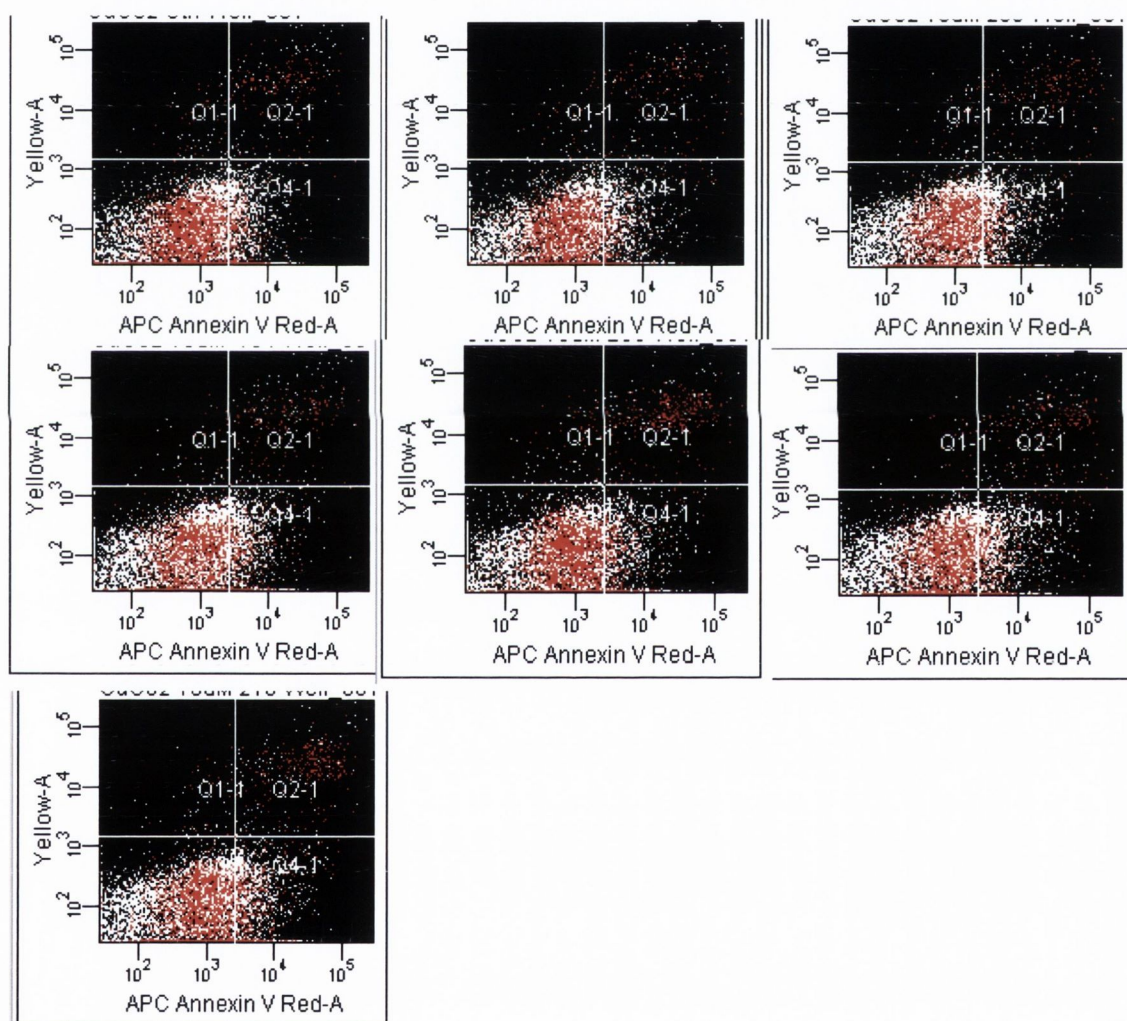


Figure 3.7: Representative traces from annexin V flow cytometry analysis with nitrate-barbiturate compounds at 10µM in Caco-2 cells after 24 hours. Propidium iodide is shown on the Y axis and annexin V on the X axis. From top left panel, untreated cells (control), 1a, 1b, 1c, 1d, 1e, 1f. Within each panel, bottom left (Q3) shows healthy cells, bottom right (Q4) shows early apoptotic cells, top right (Q2) shows necrotic cells.

The nitrate-barbiturate compounds at 10 $\mu$ M showed no effect on Caco-2 cells as measured by annexin V flow cytometry. Most of the cells stained negative for PI and annexin V and were found in the Q3 quadrant indicating healthy cells (Figure 3.7).

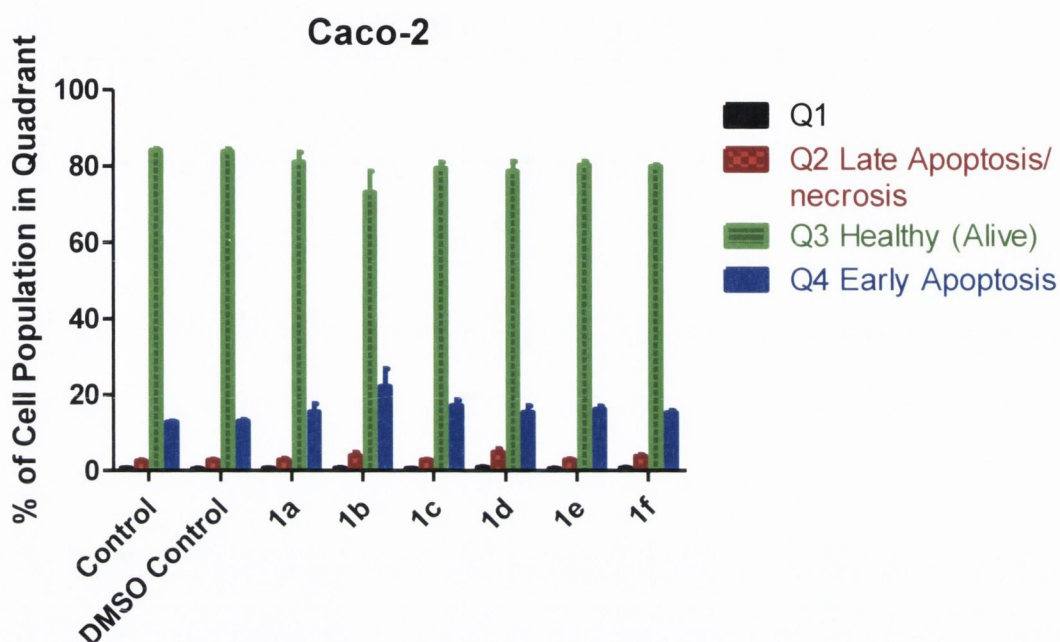


Figure 3.8: Histogram of annexin V flow cytometry in Caco-2 cells. Cells were treated with the nitrate-barbiturate compounds for 24 hours. Data are expressed as the percentage of total cells in a given quadrant following treatment with nitrate-barbiturates (1 a-f) 10 $\mu$ M, control (untreated), or DMSO (1%) where quadrant 2 (red) represents cells in late apoptosis/necrosis, quadrant 3 (green) represents healthy cells and quadrant 4 (blue) represents cells in early apoptosis.

Compound **1a** had the highest number of healthy cells with 81% compared with 83% of untreated control cells. Compound **1b** had the lowest number of healthy cell at 73%.



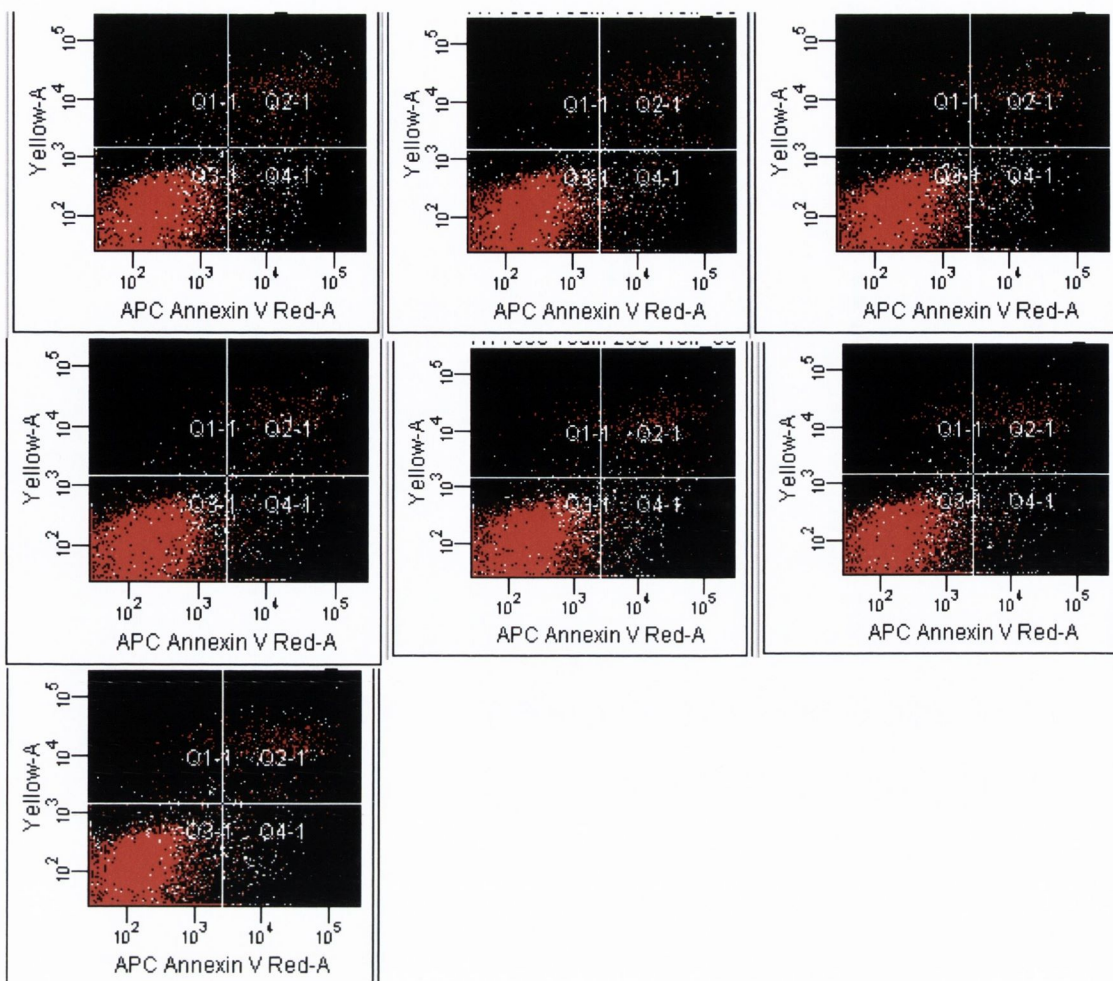


Figure 3.9: Representative traces from annexin V flow cytometry analysis with nitrate-barbiturate compounds at 10µM in HT1080 cells after 24 hours. Propidium iodide is shown on the Y axis and annexin V on the X axis. Left to right, from top left panel, untreated cells (control), Ia, Ib, Ic, Id, Ie, If. Within each panel, bottom left (Q3) shows healthy cells, bottom right (Q4) shows early apoptotic cells, top right (Q2) shows necrotic cells.

Similar results were observed following treatment of HT1080 cells with the nitrate-barbiturates at 10µM (Figure 3.9). 93-96% of control cells or cells treated with any of the compounds were detected in the healthy quadrant (Figure 3.10).

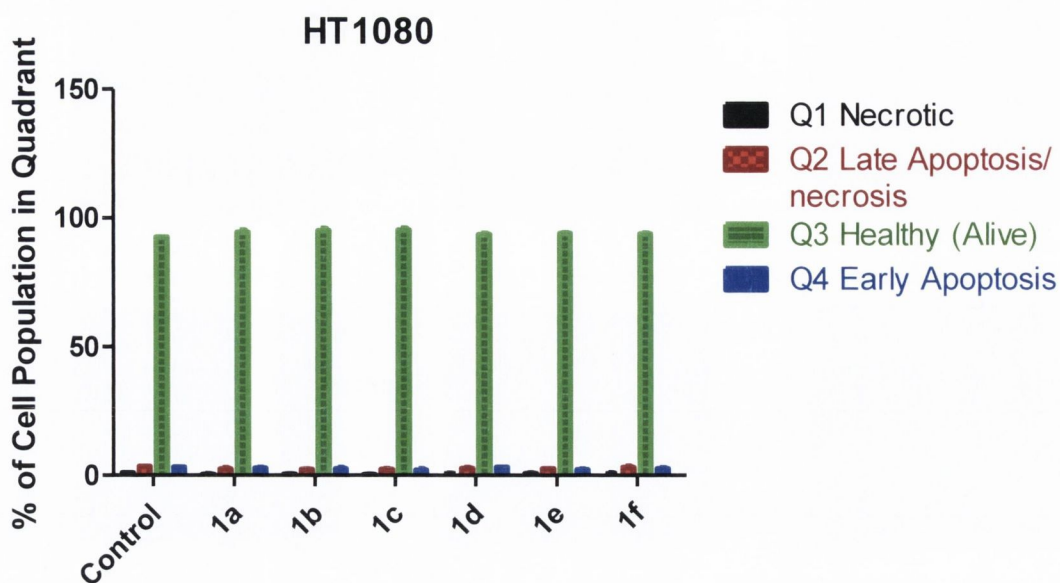


Figure 3.10: Histogram of annexin V flow cytometry in HT1080 cells. Cells were treated with the nitrate-barbiturate compounds for 24 hours. Data are expressed as the percentage of total cells in a given quadrant following treatment with nitrate-barbiturates (1 a-f) 10 $\mu$ M, control (untreated), or DMSO (1%) where quadrant 2 (red) represents cells in late apoptosis/necrosis, quadrant 3 (green) represents healthy cells and quadrant 4 (blue) represents cells in early apoptosis.

From the results of the MTT assay and the annexin V flow cytometry, we were satisfied that the compounds had little or no effect on the viability of HT1080 and Caco-2 cells after 24 hours when used at 10 $\mu$ M.

### 3.2.3. Effect of nitrate-barbiturate compounds and corresponding non-nitrates and nitrate side-chains on the expression and activity of MMP-

9

Preliminary work on the ability of the compounds to inhibit the gelatinases was carried out by Dr Jun Wang and has been previously published [315]. IC<sub>50</sub> values were calculated

following incubation of the compounds with recombinant MMP-2 and -9. Activity of the enzyme was measured by their ability to digest a fluorescently labelled substrate.

	IC <sub>50</sub> (nM)			IC <sub>50</sub> (nM)	
	MMP-2	MMP-9		MMP-2	MMP-9
<b>1a</b>	328 (273–395)	91 (63–131)	<b>2a</b>	3.8 (2.6–5.7)	26 (21–32)
<b>1b</b>	53 (43–65)	48 (38–60)	<b>2b</b>	24 (15–36)	145 (110–191)
<b>1c</b>	149 (129–171)	92 (71–118)	<b>2c</b>	7.3 (5.3–9.9)	8.1 (7–10)
<b>1d</b>	158 (125–199)	152 (120–193)	<b>2d</b>	10 (7.5–14)	12 (7.7–19)
<b>1e</b>	219 (174–274)	212 (170–266)	<b>2e</b>	66 (51–86)	97 (81–115)
<b>1f</b>	179 (155–208)	104 (77–140)	<b>2f</b>	15 (9–26)	6.2 (4–9)

Table 3.2: IC<sub>50</sub> values (nM) with 95% confidence interval for nitrate-barbiturate hybrids (1a-f) and alcohol-barbiturates (2a-f). Activated recombinant MMP-2 and -9 were incubated with the compounds for 30 minutes at 37°C. Following addition of the substrate, fluorescence was measured over time and this change was compared to the uninhibited enzyme to calculate the % inhibition. This was repeated for a range of concentrations and the IC<sub>50</sub> is given from the sigmoidal dose response curve after plotting % inhibition vs log concentration.



From the IC<sub>50</sub> values in Table 3.2, the nitrate-barbiturates have a general selectivity for MMP-9 over MMP-2 as seen by the lower values. This trend is not held for the alcohol-barbiturates where the IC<sub>50</sub> values are similar for both the gelatinases or else a preference for MMP-2 as in the case for **2a** and **2b**. When directly comparing the two groups, it is interesting to note that the alcohol-barbiturates have lower IC<sub>50</sub> values for MMP-9 with the exception of **2b**. This shows that addition of the nitrate group can reduce the ability of the compounds to bind the active site of MMP-9.

In order to test the ability of the compounds to inhibit MMP-9 in a model of intestinal inflammation, the human epithelial colon cell line, Caco-2 cells, were stimulated for 24 hours by pro-inflammatory cytokines TNF- $\alpha$  and IL-1 $\beta$  at 10ng/ml. Any compounds tested were added to the cell media 30 minutes prior to adding the cytokines. This model was chosen as these cytokines are known to be upregulated in IBD and trigger the inflammatory response represent a realistic stimulus. The time and concentration used are based on previously published results where MMP-9 was shown to be increased in response to these cytokines but not to LPS [416, 417]. This model of MMP-9 stimulation was used in all subsequent experiments.

#### **3.2.3.1. Effect of the compounds on MMP-9 activity**

Gelatin zymography was used to assess the potential activity of MMP-9 in the conditioned media following treatment of the cells with the compounds. Proteins in the media are separated on gelatin impregnated gels according to size during electrophoresis so that MMP-2 and MMP-9 are distinct bands. Washing with Triton-X 2.5% allows refolding of the proteins to their catalytic conformation. The gels are incubated in a water bath so that the gelatinase enzymes can digest the gelatin in the gels. These regions of digestion are

visible as clear bands against a dark blue background when the gels are stained with coumassie blue. Care is taken when making assumptions following densitometry results as incomplete folding of the enzyme results in the pro-form of the enzyme being visualised as a lytic band, albeit as a higher molecular weight band. Secondly, the assay takes no account of endogenous inhibitors present in the milieu as they would dissociate from the active-site [332]. Gelatin zymography remains a key technique in the study of the regulation of MMP-9 [38]. From our experiments, addition of cytokines to the cell model increased the observed activity of MMP-9; however MMP-2 remained unaltered.

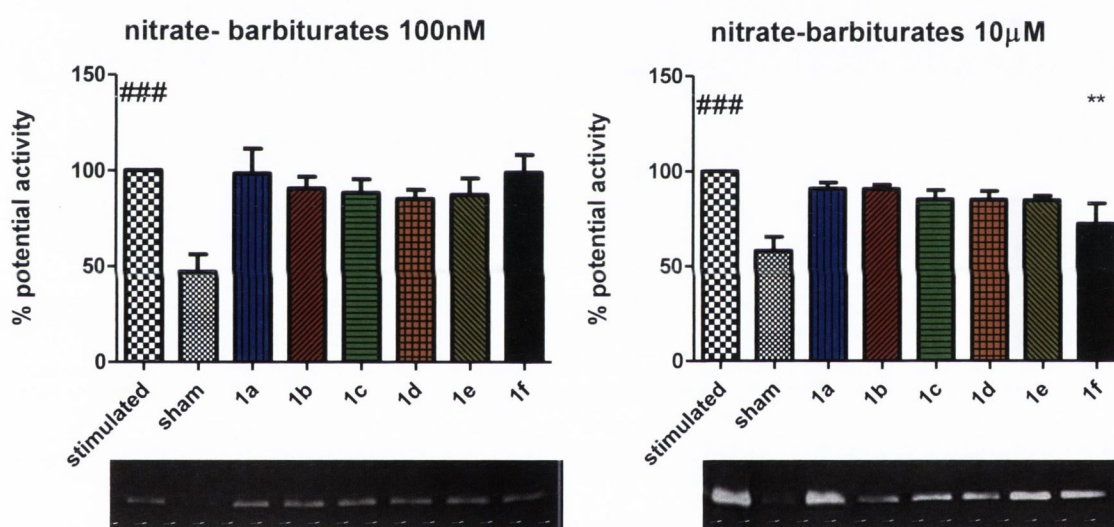


Figure 3.11: Gelatin-zymography of conditioned media from Caco-2 cells treated with the nitrate-barbiturate compounds (1 a-f) (100nM and 10µM) and cytokines (TNF- $\alpha$  and IL-1 $\beta$ , 10ng/ml) for 24 hours. Cytokine stimulated cells alone are represented as stimulated and sham group represents untreated cells. The densitometry results of trace mm x intensity are normalised to the stimulated group for each replicate.

The nitrate-barbiturate compounds had little effect at 100nM for most of the compounds (Figure 3.11). **1d** caused a 15% reduction in MMP-9 potential activity at 100nM compared to stimulated cells which was statistically significant when a paired t-test was carried out (P = 0.0279). A greater inhibition was observed overall when the compounds were used at

10 $\mu$ M (Figure 3.11). *If* gave a statistically significant result when analysed using ANOVA. If a paired, two-tailed t-test is used, many of the observed inhibitions reach statistical significance: *1a* (P = 0.0324), *1b* (P = 0.0046), *1c* (P = 0.0173), *1d* (P = 0.016), *1e* (P = 0.0005), *1f* (P = 0.0413).

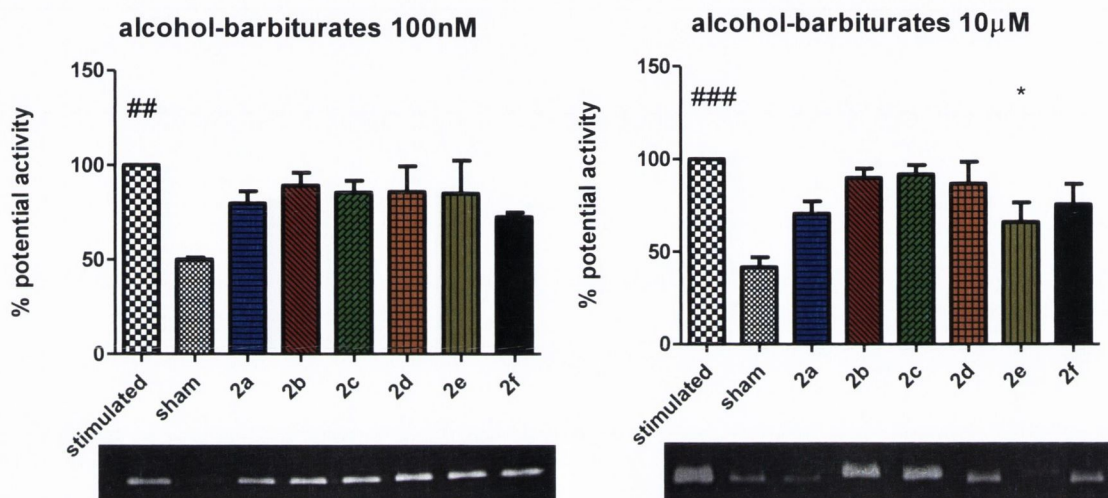


Figure 3.12: Gelatin-zymography of conditioned media from Caco-2 cells treated with the alcohol-barbiturate compounds (2 a-f) (100nM and 10 $\mu$ M) and cytokines (TNF- $\alpha$  and IL-1 $\beta$ , 10ng/ml) for 24 hours. Cytokine stimulated cells alone are represented as stimulated and sham group represents untreated cells. The densitometry results of trace mm x intensity are normalised to the stimulated group for each replicate.

The alcohol-barbiturates showed a similar inhibitory effect to the nitrate-barbiturates with a range of average potential activity compared to the stimulated group of ~ 65.9 – 91.8% (Figure 3.12). *2e* showed the greatest inhibition at 10 $\mu$ M and was statistically significant.



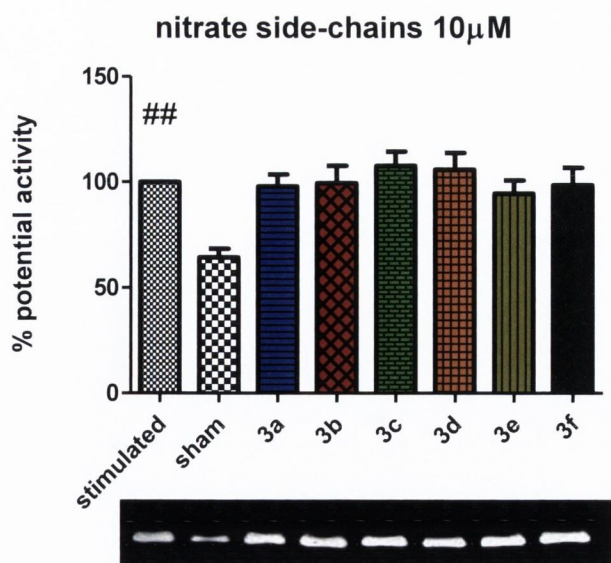


Figure 3.13: Gelatin-zymography of conditioned media from Caco-2 cells treated with the nitrate side-chains (3 a-f) (10 $\mu$ M) and cytokines (TNF- $\alpha$  and IL-1 $\beta$ , 10ng/ml) for 24 hours. Cytokine stimulated cells alone are represented as stimulated and sham group represents untreated cells. The densitometry results of trace mm x intensity are normalised to the stimulated group for each replicate.

The nitrate side-chains were tested at 10 $\mu$ M to assess if the nitrate group alone had inherent inhibitory action on MMP-9 activity when not coupled with the barbiturate scaffold (Figure 3.13). The side-chains showed limited activity when assessed by gelatin zymography with **3e** having the greatest inhibition of about 5% compared to stimulated cells. None of the side-chains were statistically significantly different from the stimulated group.

### 3.2.3.2. Effect of the compounds on MMP-9 expression

NO has been shown to influence MMP-9 gene expression in several models and so we decided to study the possible effects of our compounds on MMP-9 mRNA and the influence of the nitrate group. To examine and compare the effect that the nitrate and alcohol-barbiturates compounds were having on MMP-9 in our cell model, we used qPCR. The expression of MMP-9 is induced in an inflammatory setting by pro-inflammatory

cytokines such as TNF- $\alpha$  and IL-1 $\beta$  that are used in our model. While the barbiturate scaffold was found to inhibit the gelatinases by chelation of the zinc ion in the active site, other compounds such as the tetracyclines have been found to inhibit MMPs by blocking their transcriptional upregulation [418] and so this alternative mechanism of action was explored.

PCR was used to measure the cDNA amounts in samples where mRNA had been isolated from cells and converted to cDNA by reverse transcription. The master mix, primers and sample template are run at heat cycles to allow denaturing of the DNA (95 °C), annealing of the primers to the specific chosen region of the denatured strand and extension of the polymerase from the primers to generate a new sequence strand (60 °C). These cycles of denaturing, annealing and extension are cycled 40 times. When the probe anneals to the gene of interest, it has a reporter dye (FAM) attached to the 5' end and a quencher molecule attach to the 3' end which absorbs the excitation energy when the probe is intact. The forward primer anneals downstream of the probe and as the polymerase enzyme extends, it disrupts the reporter dye from the probe and a fluorescent signal is transmitted and picked up by the detector. During the exponential phase of the PCR, when the sequence is doubled during each cycle, the fluorescent signal released is precise and specific and can be used for relative quantitation.

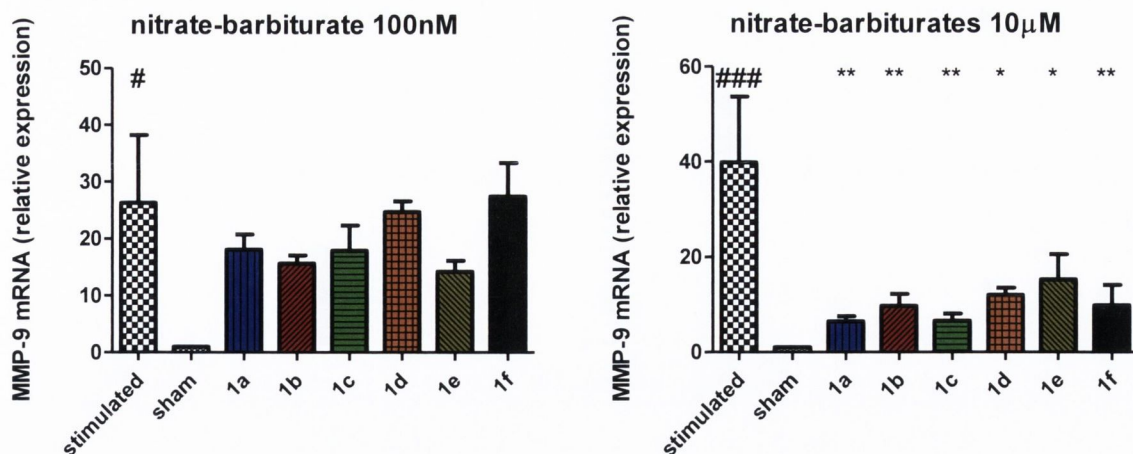


Figure 3.14: Relative quantitation of MMP-9 mRNA following treatment with nitrate-barbiturate compounds. The compounds (1a-f) were incubated in Caco-2 cells for 30 minutes prior to addition of cytokines (TNF- $\alpha$  and IL-1 $\beta$ , 10ng/ml). Cells were then incubated for 24 hours before RNA isolation. RT-qPCR was performed on cDNA from reverse transcription of the isolated RNA. Stimulated group represents cytokine stimulated cells and sham group is untreated cells. Relative expression is calculated by the  $2^{-\Delta\Delta CT}$  method with 18S as the endogenous control and the sham group used as the calibrator.

The nitrate-barbiturates caused a large and statistically significant reduction in MMP-9 mRNA relative to stimulated cells when used at 10 $\mu$ M (Figure 3.14). Compounds *1c* and *1a* caused the greatest inhibition relative to stimulated cells with 95% confidence intervals (CI) of 10.18-56.37 and 10.28-56.46 respectively, although none of the compound treated groups were statistically significantly different from each other when analysed using ANOVA and Tukey post-test. These compounds had no effect on MMP-9 expression when tested at 100nM and so any further testing was carried out at 10 $\mu$ M.



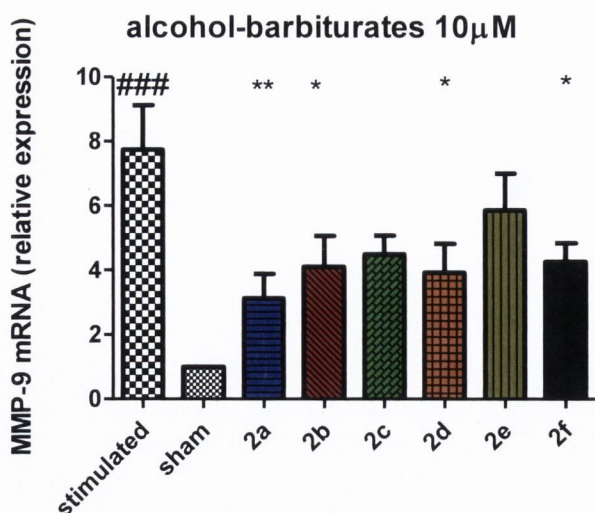


Figure 3.15: Relative quantitation of MMP-9 mRNA following treatment with alcohol-barbiturate compounds. The compounds (2a-f) were incubated in Caco-2 cells for 30 minutes prior to addition of cytokines (TNF- $\alpha$  and IL-1 $\beta$ , 10ng/ml). Cells were then incubated for 24 hours before RNA isolation. RT-qPCR was performed on cDNA from reverse transcription of the isolated RNA. Stimulated group represents cytokine stimulated cells and sham group is untreated cells. Relative expression is calculated by the  $2^{-\Delta\Delta CT}$  method with 18S as the endogenous control and the sham group used as the calibrator.

To ascertain the contribution of the nitrate group, the observed reduction in MMP-9 expression from the nitrate-barbiturates was compared to that of the alcohol-barbiturates. The alcohol-barbiturates also inhibited the expression of MMP-9 at 10 $\mu$ M but to a lesser extent (Figure 3.15). Compound **2a** showed the greatest inhibition relative to the stimulated group (95% CI: 1.066-8.163). Compounds **2b**, **2d** and **2f** also statistically significantly reduce MMP-9 relative to the stimulated control group.

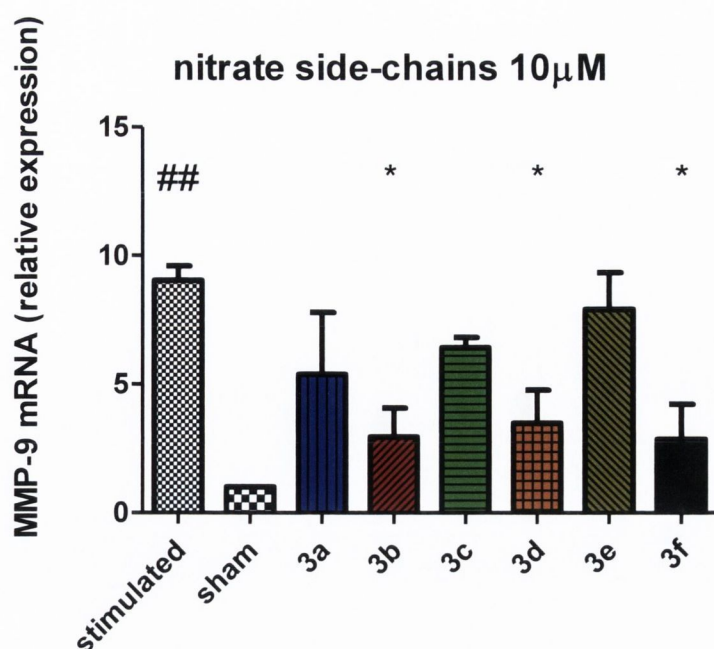


Figure 3.16: Relative quantitation of MMP-9 mRNA following treatment with nitrate side chains. The compounds (3a-f) were incubated in Caco-2 cells for 30 minutes prior to addition of cytokines (TNF- $\alpha$  and IL-1 $\beta$ , 10ng/ml). Cells were then incubated for 24 hours before RNA isolation. RT-qPCR was performed on cDNA from reverse transcription of the isolated RNA. Stimulated group represents cytokine stimulated cells and sham group is untreated cells. Relative expression is calculated by the  $2^{-(\Delta\Delta CT)}$  method with 18S as the endogenous control and the sham group used as the calibrator.

The nitrate side-chains also inhibited MMP-9 expression when tested at 10 $\mu$ M (Figure 3.16). **3f** showed the greatest inhibition relative to the stimulated group (95% CI: 0.86-11.48) which was statistically significant. Compounds **3b** and **3d** also inhibited MMP-9 gene expression to statistically significant levels relative to the stimulated group and the level of inhibition exerted by the nitrate side-chains was comparable to that of the alcohol-barbiturates.

### 3.3. Discussion

Our group have synthesised a series of nitrate-barbiturate hybrid compounds in an effort to inhibit MMP-9 at the level of gene expression as well as binding the zinc ion in the active site and inhibiting enzyme activity. Obtaining selectivity between MMP-9 and other MMPs such as MMP-2, -3 and -8 with traditional active site inhibitors has proven difficult owing to similarities in the pockets of the catalytic domain [419] and so we attached a nitrate moiety on the P2' position as a nitric oxide-mimetic. With this group, we hoped to take advantage of the properties of NO that can inhibit the upregulated MMP-9 in a disease setting. The MMPs are suitable for application of hybrid design approaches since, in these enzymes, the catalytic  $Zn^{2+}$  lies on the protein surface with shallow solvent accessible binding sites. A single deep pocket (S1') provides affinity and some selectivity towards multiple MMP-inhibitory chemo-types. In barbiturate-based (pyrimidine-3-trione) inhibitors, the S1' pocket is optimally filled with a C5-phenyloxyphenyl group. The second C-5 substituent group, which is directed towards the S2' pocket on binding, is relatively tolerant of substitution. These features present an opportunity to incorporate a nitrate group that may affect MMP upregulation through its NO-mimetic character. Nitric oxide donor groups or mimetics have been attached to numerous drug types leading, in some instances, to clinical candidates with improved risk-benefit profiles. Considering the barbiturate binding mode, there seemed a strong possibility that appropriately substituted compounds would possess intrinsic MMP-inhibitory activity, as well as NO-mimetic capability which could inhibit MMP-9 expression.

It is now apparent that in addition to inflammatory cells, the intestinal epithelium may play



an important role in IBD. It has been shown that intestinal epithelial cells produce several immunomodulatory substances such as cytokines, complement factors, immune receptors and MMP-9 [420](Figure 3.17). The release of MMP-9 may contribute to the loss of intestinal epithelium integrity facilitating interactions between the luminal antigenic stimuli and the mucosal immune system, resulting in chronic intestinal inflammation.

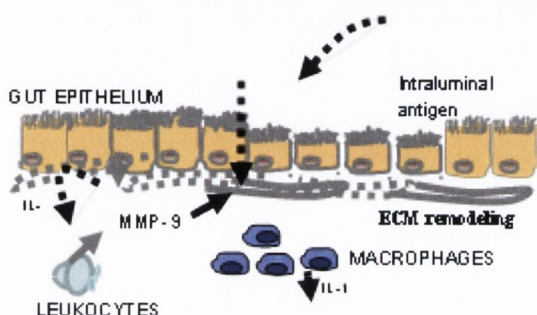


Figure 3.17: Intestinal epithelial cells play an important role in chronic inflammation. The release of MMP-9 could lead to the loss of mucosal integrity and interactions between luminal antigens and different intestinal immune cells.

We have therefore used an *in-vitro* model of intestinal inflammation using cytokine-stimulated epithelial cells which induced the expression and release of MMP-9. In the experiments carried out, Caco-2 cells released low levels of MMP-9 under basal conditions. Following incubation with cytokines, there was a significant upregulation of MMP-9 activity and expression; however MMP-2 remained unchanged. This is not surprising as the promoter region of the MMP-9 gene contains cis-acting regulatory elements with binding sites for NF- $\kappa$ B, AP-1, and PEA-3, and is therefore responsive to different cytokines, such as TNF- $\alpha$  and IL-1 $\beta$ . MMP-2, however, is considered to be a constitutive enzyme and is ubiquitously expressed in non-stimulated epithelial cells. These results are in agreement with previous work performed by Santana et al. [416]

In order to evaluate the concentration at which the compounds should be used at in the following *in-vitro* experiments, we tested the cytotoxic effects of the compounds in two different cell lines, HT1080 and Caco-2 cells. MTT assays were first carried out at a range of concentrations. With the exception of **2a**, the compounds did not affect cell viability at 10 $\mu$ M. The HT1080 cells were more sensitive to the cytotoxic effects of the compounds and **1c**, **1d**, **1f** and **2a** all affected cell viability to a greater or lesser extent at 10 $\mu$ M when incubated for 24 hours. The cells were then tested in both Caco-2 and H1080 cell lines to see whether they induced apoptotic pathways or necrosis of the cells after 24 hours. Annexin V flow cytometry showed that there was no difference between the untreated cells and the compounds after 24 hours so we were confident that we could proceed to testing the efficacy of the compounds at 10 $\mu$ M or less.

To assess the efficacy of the compounds in inhibiting MMP-9, gelatin zymography was first performed on the conditioned media. Both the nitrate-barbiturates and alcohol-barbiturate compounds showed a greater inhibition at 10 $\mu$ M compared with 100nM and so this concentration was chosen to run all further experiments. Similar inhibitions of between 10% and 35% were observed for the nitrate and alcohol-barbiturates but the nitrate side-chains on their own had no demonstrable effect. As previously discussed, during electrophoresis, any non-covalently bound elements will be separated from the enzyme, and so the observed bands on the gel represent the secreted enzyme in the absence of any inhibitors. It was interesting to observe that although it had been previously demonstrated by our group that the alcohol-barbiturates generally had much lower IC<sub>50</sub> values than their nitrate counterparts (Table 3.2) [315], the two groups showed similar levels of inhibition of MMP-9 activity as measured by zymography despite the nitrate side-chains having no effect.

We next investigated whether reduction in the transcription of MMP-9 mRNA might explain a mechanism for the observed reduction in secretion of MMP-9 with the nitrate-barbiturates. We observed a statistically significant reduction in the alcohol-barbiturate treated cells relative to the stimulated group and the reduction observed with the nitrate-barbiturates was in the region of twice that of the alcohol analogues. These results were interesting and proved firstly, that the compounds have a dual inhibitory effect on MMP-9 as being active-site inhibitors and also inhibiting its expression. Secondly, the results show that the nitrate group contributes to the inhibition of MMP-9 gene expression. The nitrate side-chains tested alone also inhibited MMP-9 in a similar order of magnitude to the alcohol-barbiturates and the effect of the nitrate-barbiturates may be seen as being a synergistic combination of these two effects.

From the results in this chapter we have established a toxicity profile for the compounds and decided that 10 $\mu$ M is the most effective and maximum dose with which the compounds should be tested at. Both the alcohol-barbiturates and the nitrate-barbiturates were able to inhibit the potential activity or secretion of MMP-9 as measured by gelatin zymography, whereas the nitrate side-chains had no demonstrable effect. qPCR results show that the compounds can all inhibit MMP-9 at the level of gene transcription with the nitrate-barbiturate compounds being in the region of twice as effective as the alcohol-barbiturates or the nitrate side-chain leading us to hypothesise that this observed inhibition from the nitrate-barbiturate involves a contribution from the component parts of the molecule in the barbiturate scaffold and the nitrate group, with the differences between the compounds within the groups being slight and not statistically significant. Direct



comparison between these groups or even between the compounds within a group is difficult as each group or compound may have varying pharmacokinetic or binding profile, or indeed varying mechanisms of action. The nitrate-barbiturate hybrid compounds may behave very differently from the alcohol-barbiturates and nitrate side-chains separately and the nitrate group may not serve the same function as part of the nitrate-barbiturate as it does as a side-chain.

**Chapter 4: NO donors and mechanism of action of nitrate-  
barbiturate compounds**

## 4. NO donors and mechanism of action of nitrate-barbiturate compounds

### 4.1. Introduction and background

MMP-9 expression is controlled by extracellular factors which trigger a network of signal transduction pathways resulting in transcriptional upregulation and a simplified summary is shown in Figure 4.3. The human MMP-9 gene lies on chromosome 20 and covers 13 exons spanning 7.7kb [421]. Expression of the gene yields a 2.5kb mRNA which is regulated by a 670bp sequence within the promoter that contains binding sites for NF- $\kappa$ B, AP-1, PEA3, and SP-1 [421, 422]. The complex transcriptional regulation of MMP-9 has been the subject of intense study [160, 162, 423-428]. NO may preferentially alter transcription factors that are sensitive to the cellular redox state including NF- $\kappa$ B, AP-1 and SP-1 [256].

#### 4.1.1. NO, MMP-9 and NF- $\kappa$ B

NF- $\kappa$ B is a transcription factor that exists in the cytoplasm as an inactive dimer, bound to inhibitory proteins of the inhibitor  $\kappa$ B (I $\kappa$ B) family [429]. This dimer is comprised of subunits of the NF- $\kappa$ B/Rel family which are c-Rel, NF- $\kappa$ B1 (p50, p105), NF- $\kappa$ B2 (p52, p100), RelA (p65) and RelB. Stimulation of the cell results in a phosphorylation cascade beginning with the liberation of IKK (I $\kappa$ B kinase). The liberated IKK causes phosphorylation of I $\kappa$ B and ubiquitylation-dependent degradation by a proteasome. NF- $\kappa$ B



is then free to migrate to the nucleus to interact with  $\kappa\text{B}$  binding sites as shown in Figure 4.1 [430]. The human MMP-9 gene contains at least two of these binding sites in its promoter region [424] and NF- $\kappa\text{B}$  has been shown to be essential for MMP-9 upregulation [431-433].

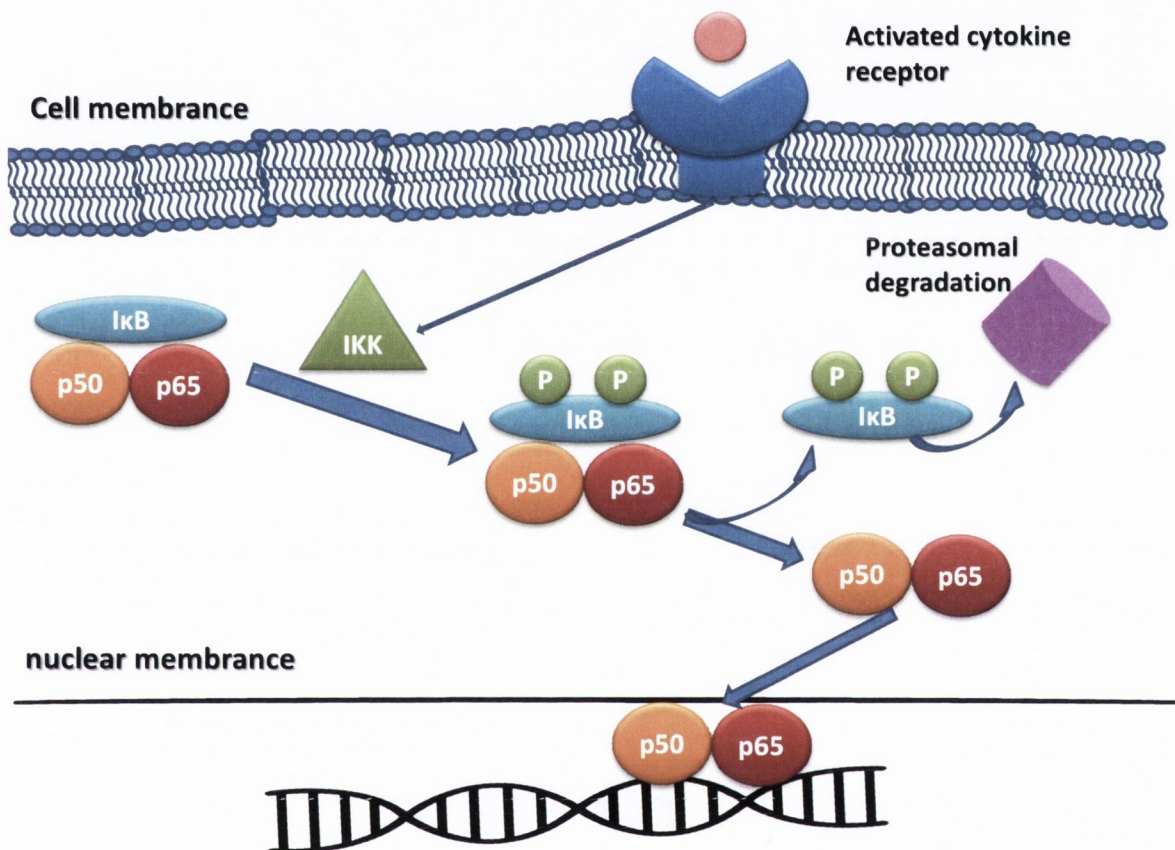


Figure 4.1: Activation of the NF- $\kappa\text{B}$  pathway. Cytokine receptors such as those for TNF- $\alpha$  and IL1- $\beta$  activate the IKK complex which can then phosphorylate I $\kappa\text{B}$  leading to its proteasomal degradation. This leaves the NF- $\kappa\text{B}$  complex free to migrate through nuclear pores to bind to its response elements on specific genes.

The interaction between NO and NF- $\kappa\text{B}$  has been widely studied and previously reviewed [434, 435]; however, the picture remains unclear. A significant complicating factor in the context of MMP-9 regulation is the NF- $\kappa\text{B}$  involvement in iNOS upregulation. Low concentrations of NO or presence of peroxynitrite will augment NF- $\kappa\text{B}$  activity, whereas at

high concentration, NO is likely to function in a negative feedback loop to reduce iNOS expression. Reductions in NF- $\kappa$ B activity following exposure to NO have been attributed to S-nitrosylation of a cysteine residue in the p50 subunit [436, 437], inhibition of NF- $\kappa$ B DNA binding [438] or stabilization of I $\kappa$ B [439]. Increased activity has been observed at low concentration of NO [440] through stimulation of IKK- $\alpha$  which likely occurs following S-nitrosylation and activation of ras, a family of GTPases [441].

Regulation of the NF- $\kappa$ B pathway by NO is likely to be the same for MMP-9 as iNOS and will depend on NO concentration and presence of superoxide. The iNOS inhibitor aminoguanidine caused an upregulation of MMP-9 through increased I $\kappa$ B degradation and NF- $\kappa$ B binding [401]. S-nitrosothiols inhibited p50 nuclear translocation and NF- $\kappa$ B DNA binding, thus reducing TNF- $\alpha$  mediated MMP-9 expression [396]. Superoxide and peroxynitrite have an opposite role to NO and increase p65 nuclear translocation and NF- $\kappa$ B binding [431, 442]. ROS generated from nicotinamide adenine dinucleotide phosphate (NADPH) oxidase also activated NF- $\kappa$ B resulting in an upregulation of MMP-9 [443]. The effects on MMP-9 expression are, however, cell specific and NF- $\kappa$ B has been reported to play no role in some cases [395, 444].

#### **4.1.2. NO, MMP-9 and AP-1**

AP-1 consists of a mixture of dimeric basic region-leucine zipper proteins (bZIP) proteins that belong to the Jun (c-Jun, JunB, JunD), Fos (c-Fos, FosB, Fra-1 and Fra2), Maf (c-Maf, MafB, MafA, MafG/F/K and Nrl), and ATF (ATF2, LRF1/ATF3, B-ATF, JDP1, JDP2)

sub families. c-Jun is the most potent transcriptional activator whereas Fos proteins cannot homodimerise but form heterodimers with Jun proteins [445]. The AP-1 motif in the MMP-9 gene is considered by some to be the most important for its expression [424, 432]. Indeed, a single mutation in the AP-1 binding site abolishes TNF- $\alpha$  or IL-1 $\beta$  induced MMP-9 expression [431, 446]. NO can modulate AP-1 activity through modifications of a redox sensitive cysteine residue in c-Jun or c-Fos [447] and oxidation or nitrosylation reduces DNA binding [448].

DETA-NO is reported to inhibit the MMP-9 transcriptional upregulation in response to 12-*O*-Tetradecanoylphorbol-13-acetate (TPA) in breast cancer cells. This effect was attributed to inhibition of c-Jun using electrophoretic mobility shift assay (EMSA), an electrophoresis based technique used to measure binding of a transcription factor to DNA and an AP-1 ELISA (TransAM) assay [395]. NOS inhibitors increase AP-1 binding by approximately 200% compared with IL-1 $\beta$  stimulated cells [401]. Where NO caused the upregulation of MMP-9, AP-1 was shown to be critical by using AP-1 deletion mutants of MMP-9 luciferase promoter constructs [409]. Superoxide has been shown to increase AP-1 binding in MMP-9 upregulation [431].

#### **4.1.3. NO, MMP-9 and cGMP/ PKG**

Many of NO's diverse physiological actions are attributed to its ability to activate sGC through binding of its heme group. Activation of sGC triggers formation of cyclic GMP, an important signalling molecule [256]. cGMP exerts its effects through cyclic nucleotide-gated channels, phosphodiesterases, PKA and PKG [449], where change is effected through transcription factor phosphorylation and/or transcription. Interestingly,



transcription factors, including AP-1, that are activated by cGMP are also regulated by NO through protein modification [450]. Several conflicting studies have used inhibitors or analogues of sGC, cGMP or PKG to determine whether observed effects of NO on MMP-9 expression are mediated through this pathway as shown in Figure 4.2.

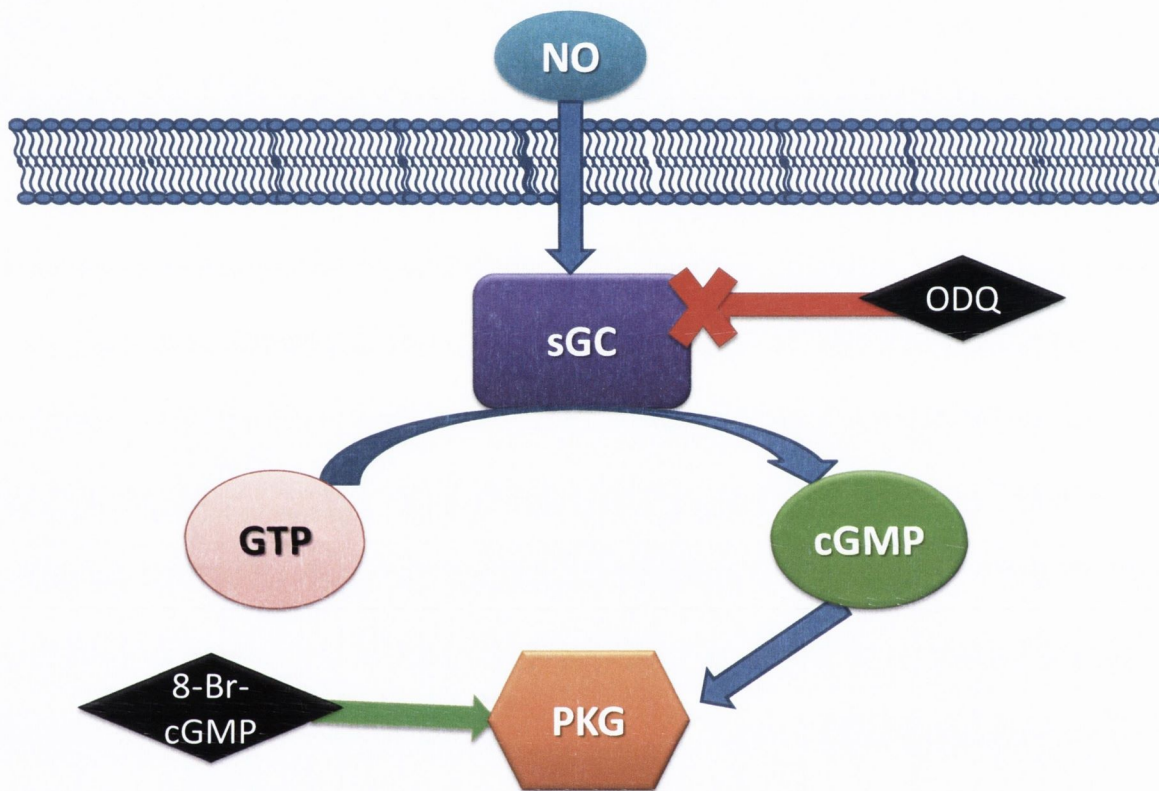


Figure 4.2: NO and the activation of the cGMP pathway. NO activates sGC which converts GTP to cGMP which can in turn activate PKG among other signalling molecules. Pharmacological research tools are shown in the black diamonds where ODQ can inhibit sGC and so block any downstream effects. 8-Br-cGMP is a cGMP analogue which can activate PKG.

cGMP analogues can mimic the NO donor mediated downregulation of MMP-9 in MCF-7 cells. This downregulation was blocked following co-incubation with a PKG inhibitor, implicating the cGMP/PKG pathway [395]. Similar results were reported in smooth muscle

cells where inhibition of MMP-9 activity by eNOS gene transfer was mimicked by DETA-NONOate or the cGMP analogue 8-bromo-cGMP [451].

Where MMP-9 expression was potentiated by NO, the addition of a sGC inhibitor returned MMP-9 mRNA to basal levels [409]. Similar results were reported when NO-donor mediated upregulation of MMP-9 was inhibited following co-incubation with sGC or PKG inhibitors. The role of the pathway was confirmed when the addition of a cGMP analogue reversed the effect [408].

Where a biphasic regulation of MMP-9 was observed, the stimulation observed at low NO level were attributed to cGMP, whereas the inhibition observed at higher concentrations was independent of sGC/cGMP [345]. In another study where MMP-9 was upregulated by NO, activation of a sGC/PKA pathway resulted in phosphorylation of Wilms tumor 1 (WT1). Phosphorylation caused a shuttling of WT1, a transcriptional repressor, from the nucleus to the cytosol causing upregulation of MMP-9 [452]. The NO sensitive cGMP/PKG pathway also negatively regulates store-operated calcium entry (SOC) in fibroblasts. This inhibition has been reported to indirectly inhibit MMP-9 synthesis and release, where increased SOC increases MMP-9 release [398].

The influence of cGMP is likely cell specific, as NO-donor mediated inhibition of MMP-9 was found to be independent of cGMP in endothelial cells [444] and cGMP analogues were unable to replicate the effects of NO in IL-1 $\beta$  stimulated rat mesangial cells [393]. It is reported elsewhere that where sGC was found to be essential, inhibition of PKG had no effect on basal or NO modulated MMP-9 expression [353]. This suggests cGMP mediated pathway independent of PKG.

#### 4.1.4. NO, MMP-9 and MAP Kinases/ PKC

The MAPKs and PKC are two families of kinase signalling cascades involved in the activation of MMP-9 transcription factors. MAPK are differentially activated by growth factors, mitogens and hormones. Activation is triggered by phosphorylation of tyrosine and threonine residues by MAPK kinases (MKK) which are first activated by MKK kinases (MKKK) [453]. Three pathways characterised are the extracellular signal regulated kinase (ERK1/ERK2), cJun-N-terminal kinase (JNK)/stress activated protein kinase (SAPK), and p38 [424]. AP-1 and NF- $\kappa$ B are both regulated by MAP kinases which can in turn be activated by PKC- $\zeta$ , so interactions between the molecules in MMP-9 regulation seem likely [423].

Protein Kinase C is a family of isoenzymes with differential distribution, substrate specificities and activation responsiveness. They are split into conventional ( $\alpha$ ,  $\beta$ I,  $\beta$ II,  $\gamma$ ), novel ( $\delta$ ,  $\epsilon$ ,  $\eta$ /L,  $\theta$ ) and atypical ( $\zeta$ ,  $\lambda$ /L) [423]. Few studies have examined the specific isoenzyme involved in MMP-9 expression but PKC- $\alpha$ ,  $\beta$ , and in particular  $\zeta$  have been implicated [423, 424]. NO donors have been shown to inhibit JNK through S-nitrosylation in several cell models [454-457]. Inhibitors of p38 and ERK MAP kinases showed an additive reduction though not complete inhibition of IL-1 $\beta$  or superoxide stimulated MMP-9 mRNA. Superoxide worked with IL-1 $\beta$  to increase phosphorylation of ERK, p38 and JNK to increase MMP-9 expression [431].

In one study where AP-1 was inhibited by an NO donor, the upstream MAPK, JNK was unaffected. The donor caused an inhibition of PKC-  $\delta$  resulting in reduced MMP-9 expression [395]. ERK 1/2 stimulated by LPS was also shown to be inhibited by an NO donor. Interestingly, the inhibition was reversed with a cGMP analogue [394]. DETA-



NONOate was found to attenuate superoxide mediated ERK activation and MMP-9 upregulation in vascular smooth muscle cells [399].

In a colon cancer cell line, NO caused the upregulation of MMP-9. The upregulation was abolished in the presence of inhibitors of sGC, PKG or ERK. The study showed that NO caused the upregulation in a cGMP/PKG/ERK dependent manner and can increase ERK 1/2 phosphorylation by 12 fold [409].

#### **4.1.5. NO and its effects on MMP-9 mRNA stability**

Post-transcriptional regulation is increasingly recognised as being critical for gene expression. Microarray studies have shown that over half of stress-response genes are regulated by changes in mRNA stability [458, 459]. Regulation of the fate of mRNA is through its 3' UTR (untranslated region) which contain cis-regulatory elements. The adenylate and uridylate-rich elements (AREs) constitute one class of these elements that regulate cytoplasmic mRNA [460] and target labile mRNA for degradation [461]. Several families of ARE-binding proteins (ARE-BP) regulate the fate of the mRNA. HuR is a ubiquitously expressed ARE-BP belonging to the ELAV family which stabilizes ARE containing mRNAs [462, 463]. NO has been shown to regulate the expression of several genes including heme oxygenase 1 [464], transforming growth factor- $\beta$ 3 [465], endothelin-converting-enzyme-1 [466], IL-8, TNF- $\alpha$  and p21/Waf1 [467] by influencing the mRNA stability. Interestingly, binding of HuR is found to be essential for the stability of iNOS mRNA [468]. There is known cross-talk between the cGMP and cAMP pathways [469]. In

one study it was demonstrated that inhibition of sGC induced by cAMP results from inhibition of HuR expression [470]. It has also been shown elsewhere that cGMP-elevating agents decrease the expression and RNA binding of HuR [471].

MMP-9 mRNA contains numerous AUUA motifs in its 3'UTR and the stabilizing effects of HuR have been reported [472, 473]. The stability of existing mRNA can be measured using actinomycin to block *de novo* synthesis of mRNA. Nitric oxide donors were shown to inhibit the expression of HuR and thus reduce its binding to the 3'UTR through a sGC-cGMP pathway [474]. The half-life of MMP-9 mRNA from rat mesangial cells was reduced from 8 hours to 4 hours following co-incubation with NO-donors [475]. This finding was consistent with the discovery that the stability of the MMP-9 mRNA is dependent on HuR binding to the ARE.

Where DETA-NONOate reduced the stability of MMP-9 mRNA in cultured astrocytes, AUF-1, and not HuR, was found to play a mediating role. Protein levels of the mRNA destabilising factor and its binding to the MMP-9 3' UTR were found to be increased following addition of the NO donor [476]. Addition of AUF-1 small interfering RNA (siRNA) was found to partially reverse the NO mediated inhibition of MMP-9 and thus confirming a further mechanism of NO mediated MMP-9 mRNA destabilisation.

Based on these studies, we conclude that increased concentrations of NO reduce the stability of MMP-9 mRNA, most likely, through downregulation of HuR and increased expression of AUF-1.

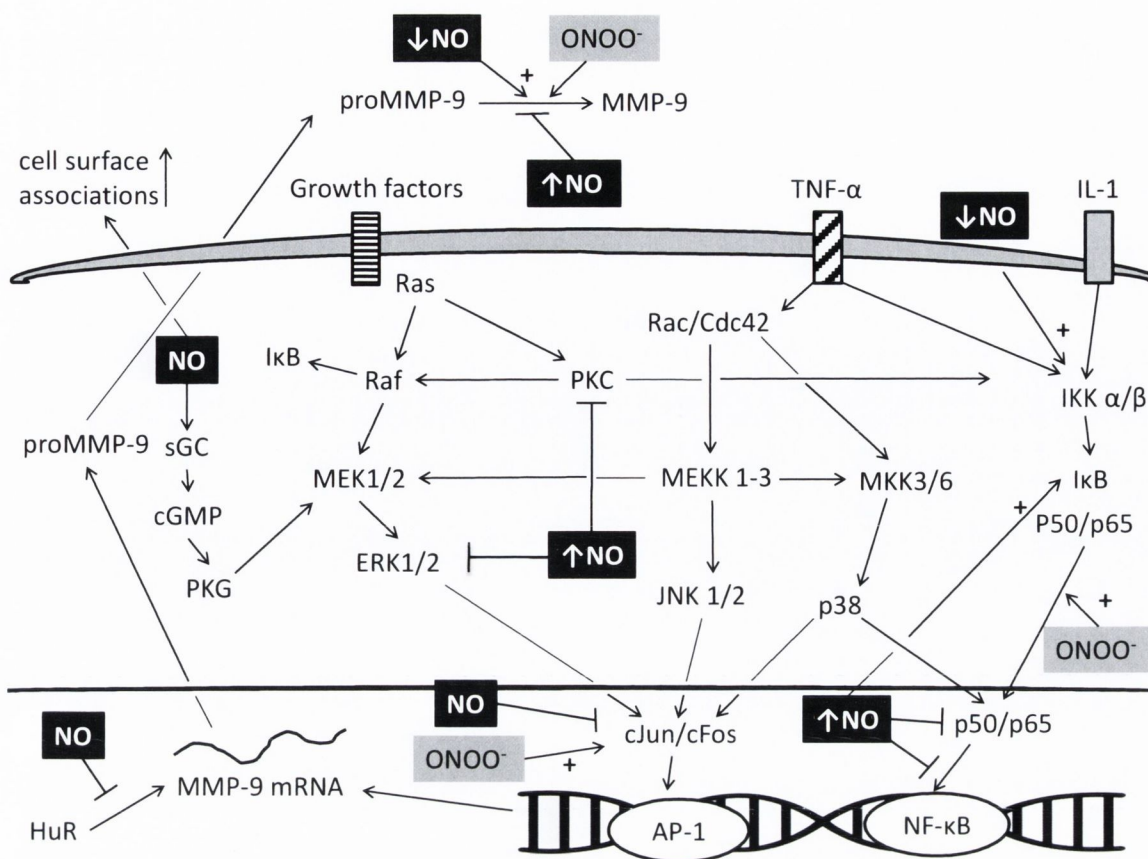


Figure 4.3: Representation of some of the pathways involved in the transcriptional upregulation of MMP-9 and the possible impacts of NO and peroxynitrite (ONOO<sup>-</sup>). ↑ indicates high concentration and ↓ indicates low concentration. + indicates a promoter role and - indicates an inhibitory role. The effect exerted by NO will depend on concentration and presence of peroxynitrite. Possible pathways that NO may influence include cGMP, the MAPKs and AP-1, and NF-κB [313].

It is difficult to tease out the relative importance of the reported effects that NO has on the various aspects of MMP-9 regulation but the evidence points towards its effects on gene transcription being more relevant in an in-vivo setting. Various regulatory elements control the expression of MMP-9 (Figure 1.3) however, NF-κB [431-433] and AP-1 [424, 432] have been described as essential for the upregulation of MMP-9. NO is known to interact with elements of both these signal transduction pathways as described previously and it is likely that many of these interactions will have downstream effects on NF-κB or AP-1 to alter the transcription of MMP-9. The most relevant or important signalling molecules



involved or the importance of NO's regulation of mRNA stability will likely be cell and setting dependent.

#### 4.1.6. NO-donors

Using NO in an experimental setting is extremely difficult owing to its reactivity and extremely short half-life. These issues severely limit the ability to maintain a constant concentration of NO for *in-vivo* or *in-vitro* experiments and for this reason, NO-donors have become extremely useful tools for studying the effects of NO.

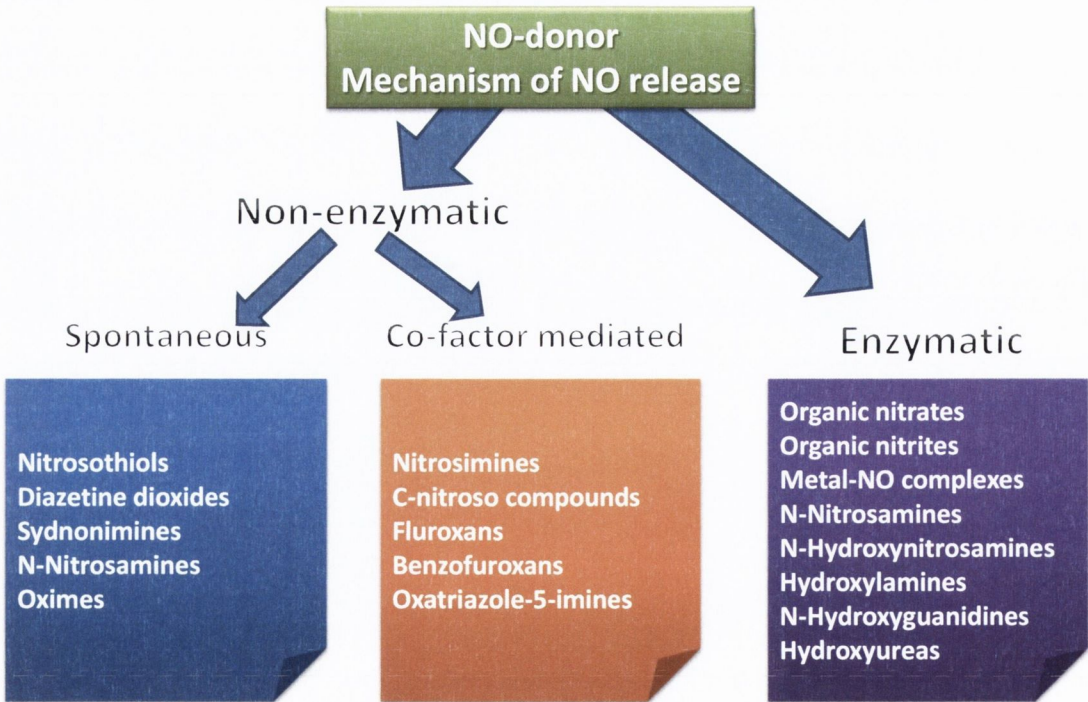


Figure 4.4: Crude classification of NO-donors according to pathway of NO generation. Many of the NO-donors where NO is formed enzymatically will also be formed by other means [328].

The NO-donors used can differ in the half-life of the compound, the release profile of NO, the generation of by-products and the mechanism by which NO is generated. For a large number of the compounds, NO release can be induced by thiols as a co-factor through reduction or transnitrosation. Other heat, light or pH sensitive compounds will spontaneously generate NO under certain conditions, whereas enzymatic release by cytochrome P<sub>450</sub> enzymes, peroxidases, a glutathione S-transferase (GST) [477] or mitochondrial aldehyde dehydrogenase (ALDH-2) may be required for the more stable compounds. The mechanisms for release for various classes of NO donor compounds are set out in Figure 4.4.

The organic nitrates represent the most clinically used NO donors. GTN is used sublingually for acute relief from pain associated with angina and as a transdermal patch for heart failure or chronic angina. Isosorbide mononitrate (ISMN), a slower releasing NO-donor is taken orally for chronic angina. While the mechanism of NO release from organic nitrates is generally agreed to be enzymatic, it is interesting to note that it is not yet fully understood how GTN activates sGC. The current understanding is that ALDH-2 enzyme, which is mostly located in the cytoplasm and not the mitochondria of vascular smooth muscle cells, can release NO from GTN [478]. This theory is disputed by some groups who have shown that the potent vasodilatory effect of GTN is not related to its weak NO donating ability but may be able to activate sGC through another intermediate [479, 480]. Several enzymes including the GSTs, cytochrome P<sub>450</sub> enzymes and ALDH-2 can release NO<sub>2</sub><sup>-</sup> from organic nitrates which is believed to be an intermediate but it is also of interest to note that nitrite is now believed to be a key endogenous storage pool for NO and mimic its effects under certain conditions [481].

A commonly used group of NO-donors for biological research are the S-nitrosothiols with members that include S-nitrosoglutathione (GSNO) and S-Nitroso-N-acetylpenicillamine

(SNAP). This group encompasses a vast array of compounds, all with a single bond between the thiol (R-SH) and NO groups. The mechanisms of NO release are extremely complex and dependent on the structure of the individual compound but can include light, heat, metals, thiols, superoxides [482], xanthine oxidase [483], superoxide dismutase [484], protein disulphide isomerases [485], and dehydrogenases [486]. Owing to all these factors and the variation of the R group in the compounds, the half-life can vary from milliseconds to several hours. The half-life of SNAP in aqueous media is about 4 hours and NO formation is high, where 100 $\mu$ M yields about 1.4 $\mu$ M NO/minute at 37°C and is linear over a wide concentration range [487].

The diazeniumdiolates or NONOates are another group commonly used to study the effects of NO in biological systems. They consist of a diolate group attached to a nucleophile adduct (usually an amine) via a nitrogen atom. These compounds are attractive for research purposes as they decompose spontaneously in solution and the rate is strongly dependent on the nucleophile adduct, the pH and the temperature but the breakdown is not catalysed by biological components [327]. This is seen where DEA-NONOate (diethylamine NONOate) has a half-life of 2 minutes at a pH of 7.4 and 37°C where the half-life of DETA-NONOate (diethylene triamine NONOate) is 20 hours under the same conditions [482]. This decomposition follows simple, first order kinetics to generate two molar equivalents of NO and so the biological yields can be predicted.



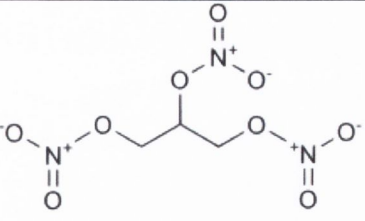
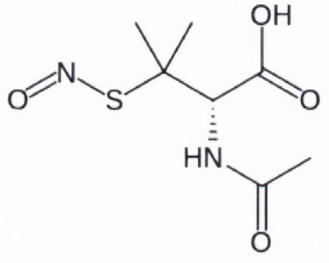
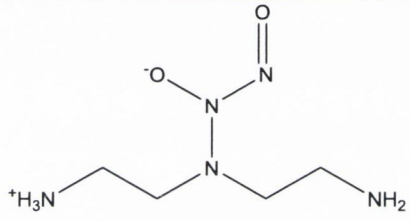
Structure	Compound name and group	Half-life	Ref.
	GTN (organic nitrates)	1-4 seconds	[328]
	<i>S</i> -Nitroso- <i>N</i> -acetylpenicillamine ( <i>S</i> -nitrosothiols)	~4 hours	[487]
	DETA-NONOate (diazoniumdiolates)	~20 hours	[482]

Table 4.1: Representations of commonly used NO-donor compounds and their expected half-lives.

It is clear from the variation in half-lives amongst the NO-donor compounds (Table 4.1) and expected production of NO that the local NO flux and duration will be very different for the same concentration of donor used. This must be taken into account when interpreting the results of NO-donor experiments in biological systems where the local concentration of NO may determine the effect observed.

## 4.2. Results

### 4.2.1. The effect of NO-donors on MMP-9 in Caco-2 cells

In order to establish whether the effects that the nitrate-barbiturates had on MMP-9 synthesis in cytokine stimulated Caco-2 cells were NO mediated, we tested the effects of the NO-donors SNAP and DETA-NONOate at a range of concentrations for 24 hours. The time-point chosen is the same as that used for assessment of the effect of the compounds and concentrations of NO-donors used were based on previously published literature [393-396, 465].

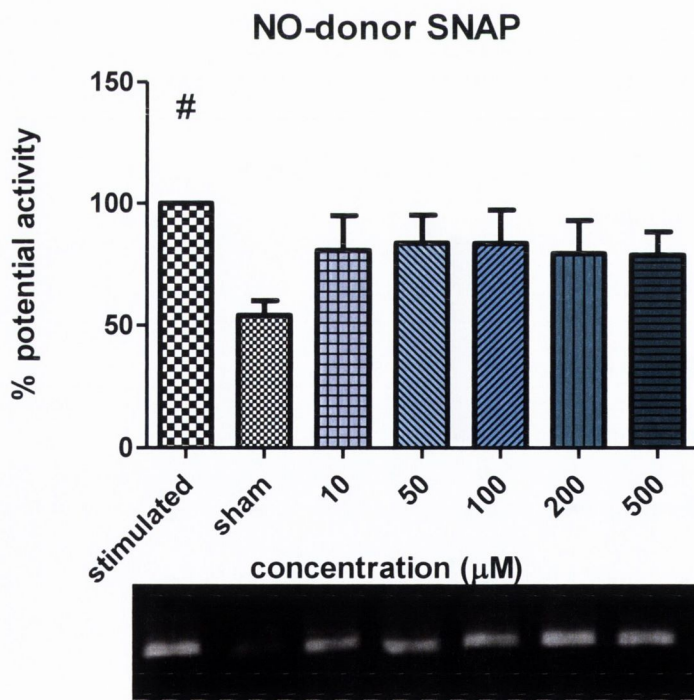


Figure 4.5: The effects of SNAP on MMP-9 potential activity from Caco-2 cells. SNAP (10-500 $\mu\text{M}$ ) was added to the culture media 30 minutes prior to adding cytokines (TNF- $\alpha$  and IL-1 $\beta$ , 10ng/ml). The cultured media was then collected after 24 hours. Stimulated group represents cytokine stimulated cells and sham group represents untreated cells. The densitometry results of trace mm x intensity are normalised to the stimulated group for each replicate and expressed as a percentage.

SNAP caused a reduction of MMP-9 secretion or potential activity of 16-21% compared to stimulated cells but this trend did not reach statistical significance (Figure 4.5). The greatest inhibition of ~21% was seen when SNAP was used at 500µM but there was limited difference between the groups and no obvious concentration dependent trend.

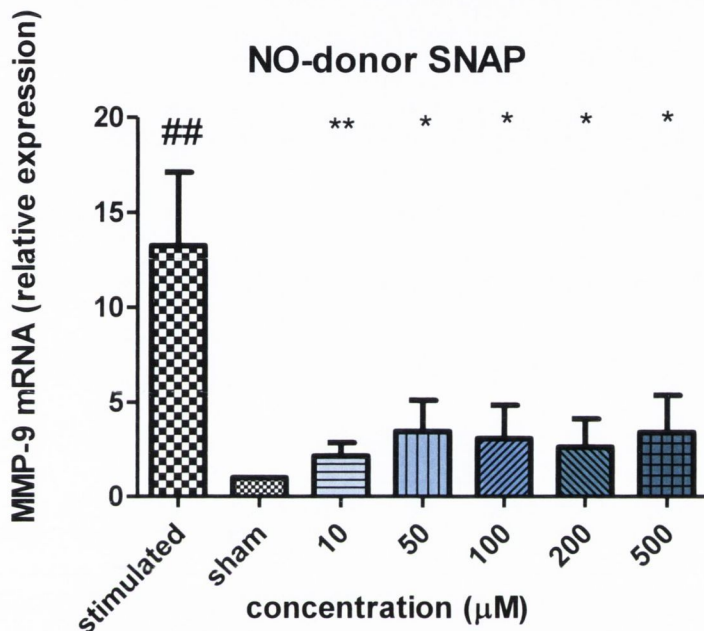


Figure 4.6: Relative quantitation of MMP-9 mRNA following treatment with SNAP. Varying concentrations of SNAP (10-500µM) were incubated in Caco-2 cells for 30 minutes prior to addition of cytokines (TNF-α and IL-1β, 10ng/ml). Cells were then incubated for 24 hours before RNA isolation. RT-qPCR was performed on cDNA from reverse transcription of the isolated RNA. Stimulated group represents cytokine stimulated cells and sham group is untreated cells. Relative expression is calculated by the  $2^{-(\Delta\Delta CT)}$  method with 18S as the endogenous control and the sham group used as the calibrator.

When the effect of SNAP on MMP-9 mRNA was measured, a large reduction was observed (Figure 4.6). All concentrations of SNAP that were tested resulted in a statistically significant reduction in MMP-9 gene expression compared with the stimulated group. The greatest inhibition relative to the stimulated group was observed with the 10µM SNAP treatment, although there were no statistically significant differences between any of the SNAP treatment groups.



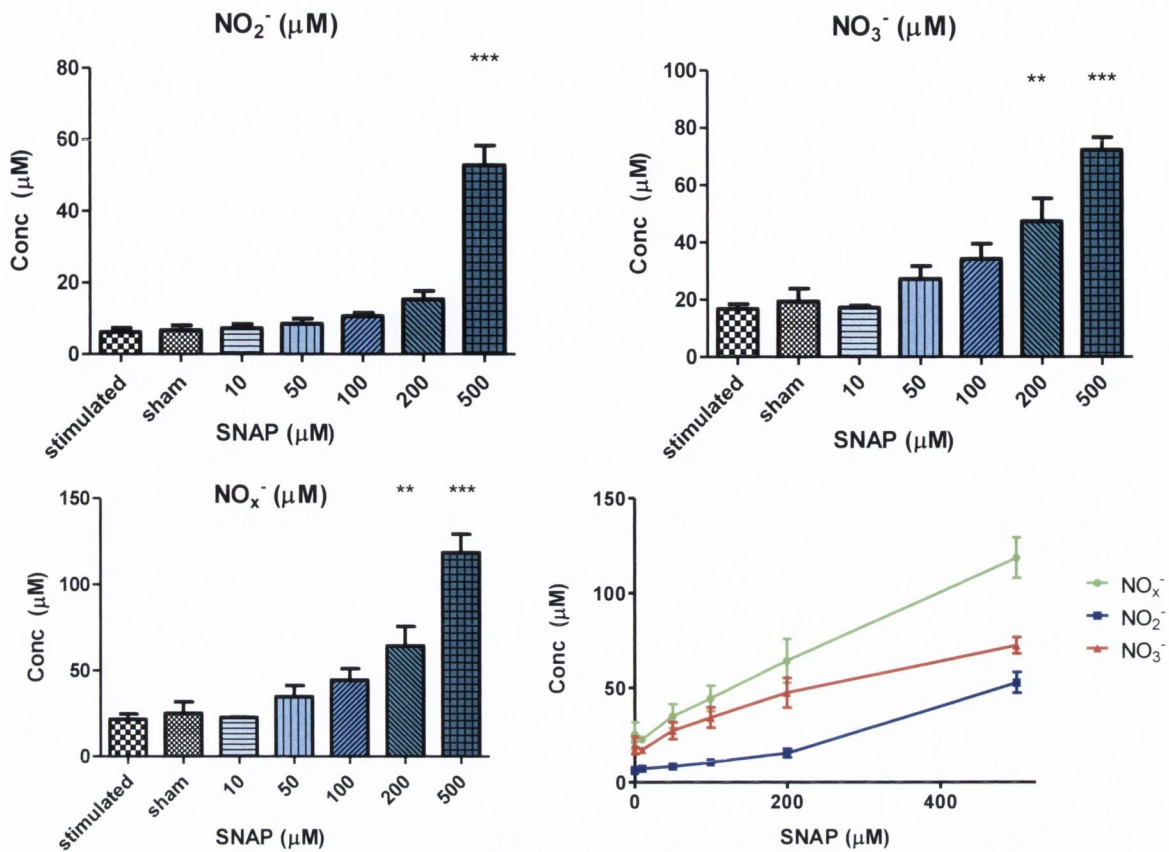


Figure 4.7: Measurements of nitrate and nitrite concentrations as breakdown products of NO by the Griess assay on the conditioned media of Caco-2 cells after 24 hours with SNAP and proinflammatory cytokines (TNF- $\alpha$  and IL-1 $\beta$ , 10ng/ml). Top left pane shows the nitrite concentration, top right pane shows the nitrate concentration, bottom left pane shows the combined reduced NO groups and bottom right shows the linear correlations of SNAP concentrations versus the concentration of measured NO<sub>x</sub><sup>-</sup> species.

Incubations with SNAP showed a linear correlation between the concentration used and the resultant nitrate and nitrite concentrations that were present in the conditioned media after 24 hours (Figure 4.7). The results of correlation analysis of NO<sub>x</sub><sup>-</sup> ( $P < 0.0001$ ,  $R^2 = 0.9964$ ), NO<sub>2</sub><sup>-</sup> ( $P < 0.0001$ ,  $R^2 = 0.9696$ ) and NO<sub>3</sub><sup>-</sup> ( $P = 0.0002$ ,  $R^2 = 0.9525$ ) are to be expected considering that SNAP is expected to spontaneously yield NO which will be broken down to nitrite and nitrate. At 500μM of SNAP, the difference in nitrite concentrations reached statistical significance for all groups when analysed by ANOVA and Tukey post-test. Similar results were observed for nitrate and NO<sub>x</sub><sup>-</sup> concentrations where 500μM SNAP resulted in statistically significant differences with all other groups and 200μM was also

statistically different from the controls and 10 $\mu$ M SNAP. There is no obvious correlation between these results and the effect on MMP-9 activity or expression.

We next investigated if another NO-donor, with a different release mechanism and profile which will likely yield a different NO flux over the 24 hours, would have a different effect on MMP-9.

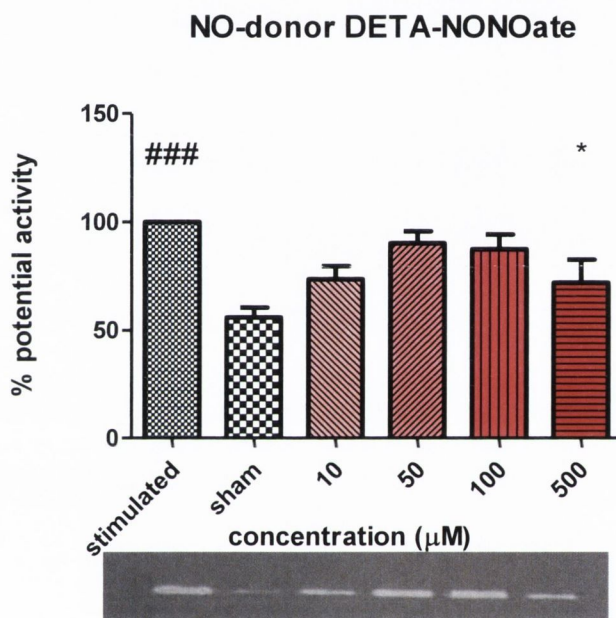


Figure 4.8: The effects of DETA-NONOate on MMP-9 potential activity from Caco-2 cells. DETA-NONOate (10-500 $\mu$ M) was added to the culture media 30 minutes prior to adding cytokines (TNF- $\alpha$  and IL-1 $\beta$ , 10ng/ml). The cultured media was then collected after 24 hours. Stimulated group represents cytokine stimulated cells and sham group represents untreated cells. The densitometry results of trace mm x intensity are normalised to the stimulated group for each replicate and expressed as a percentage.

We observed a reduction in mean MMP-9 potential activity following incubation with DETA-NONOate (Figure 4.8). The reduction was concentration dependent and ranged from ~10-28% with the greatest inhibition observed at 500 $\mu$ M which reached statistical significance. While there appeared to be a trend towards a biphasic regulation of MMP-9 with the greatest reductions being observed at 500 $\mu$ M and 10 $\mu$ M, there was no statistically

significant difference between the groups when analysed with a Tukey's multiple comparison post-test.

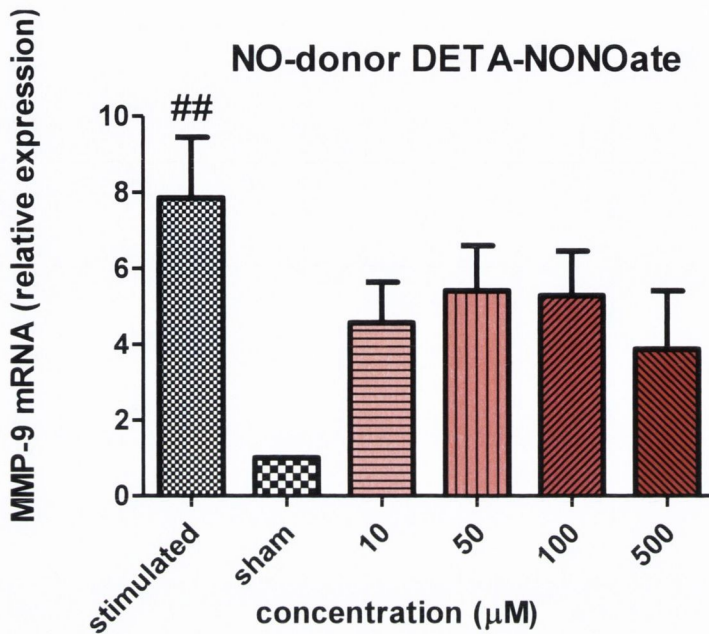


Figure 4.9: Relative quantitation of MMP-9 mRNA following treatment with DETA-NONOate. Varying concentrations of DETA-NONOate (10-500µM) were incubated in Caco-2 cells for 30 minutes prior to addition of cytokines (TNF- $\alpha$  and IL-1 $\beta$ , 10ng/ml). Cells were then incubated for 24 hours before RNA isolation. RT-qPCR was performed on cDNA from reverse transcription of the isolated RNA. Stimulated group represents cytokine stimulated cells and sham group is untreated cells. Relative expression is calculated by the  $2^{-\Delta\Delta CT}$  method with 18S as the endogenous control and the sham group used as the calibrator.

PCR was carried out on the cells following treatment with DETA-NONOate at various concentrations (Figure 4.9). The trend observed was similar to that seen following gelatin zymography with the greatest inhibition being at the highest concentration of 500µM and 10µM showing the second greatest inhibition. Neither of these reductions reached statistical significance following ANOVA with a Dunnet's post hoc-test compared to the stimulated group and no significant differences were seen between the groups.



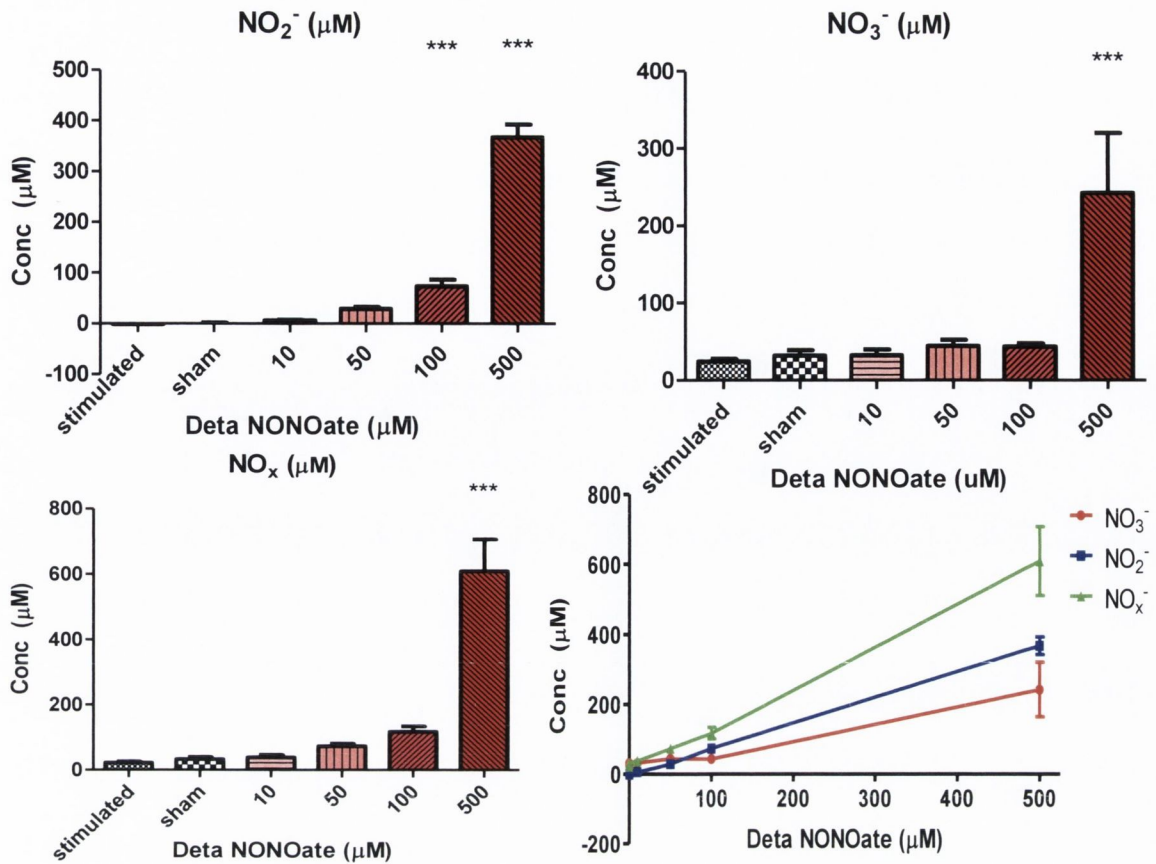


Figure 4.10: Measurements of nitrate and nitrite concentrations as breakdown products of NO by the Griess assay on the conditioned media of Caco-2 cells after 24 hours with DETA-NONOate and pro-inflammatory cytokines (TNF- $\alpha$  and IL-1 $\beta$ , 10ng/ml). Top left pane shows the nitrite concentration, top right pane shows the nitrate concentration, bottom left pane shows the combined reduced NO groups and bottom right shows the linear correlations of DETA-NONOate concentrations versus the concentration of measured NO<sub>x</sub><sup>-</sup> species.

As expected from a NONOate NO-donor, there was a linear relationship between the concentration used and the NO released with correlation analysis results for NO<sub>x</sub><sup>-</sup> ( $P < 0.0001$ ,  $R^2 = 0.9975$ ), NO<sub>2</sub><sup>-</sup> ( $P < 0.0001$ ,  $R^2 = 0.9996$ ) and NO<sub>3</sub><sup>-</sup> ( $P < 0.0001$ ,  $R^2 = 0.9828$ ) being statistically significant (Figure 4.10). There is little to no difference in NO yielded from the lower concentrations of DETA-NONOate used which may reflect the limited sensitivity of the Griess assay. At a concentration of 500 $\mu$ M, the NO-donor yielded statistically significantly more of all NO<sup>-</sup> species than the stimulated control following ANOVA with Tukey's post-test. 100 $\mu$ M also reached statistical significance when nitrite

was measured. For nitrite measurement, statistically significant differences were observed when comparing 10 $\mu$ M with 100 $\mu$ M and 500 $\mu$ M, 50 $\mu$ M with 500 $\mu$ M, and 100 $\mu$ M with 500 $\mu$ M. For nitrate measurement, statistically significant differences were observed between the stimulated group and 500 $\mu$ M, 10 $\mu$ M and 500 $\mu$ M, 50 $\mu$ M and 500 $\mu$ M, and 100 $\mu$ M and 500 $\mu$ M. Statistical significance was reached between the pairs stimulated and 500 $\mu$ M, 10 $\mu$ M and 500 $\mu$ M, 50 $\mu$ M and 500 $\mu$ M, and 100 $\mu$ M and 500 $\mu$ M for NO $_x^-$ . The highest concentrations of nitrate and nitrite were produced from the highest concentration of DETA-NONOate which also produced the highest inhibition of MMP-9 potential activity and gene expression.

It is interesting to note that there is no difference between the stimulated and sham groups in Figure 4.7 and Figure 4.10. It was expected that the addition of the cytokines would induce iNOS, leading to an increase to NO $_x^-$  production but from these figures and Figure 4.11 we can see that the cytokine mix that we used did not induce iNOS in Caco-2 cells. It is likely that the concentration and/or combination used was not sufficient to induce the enzyme in this cell line which was demonstrated previously [488].

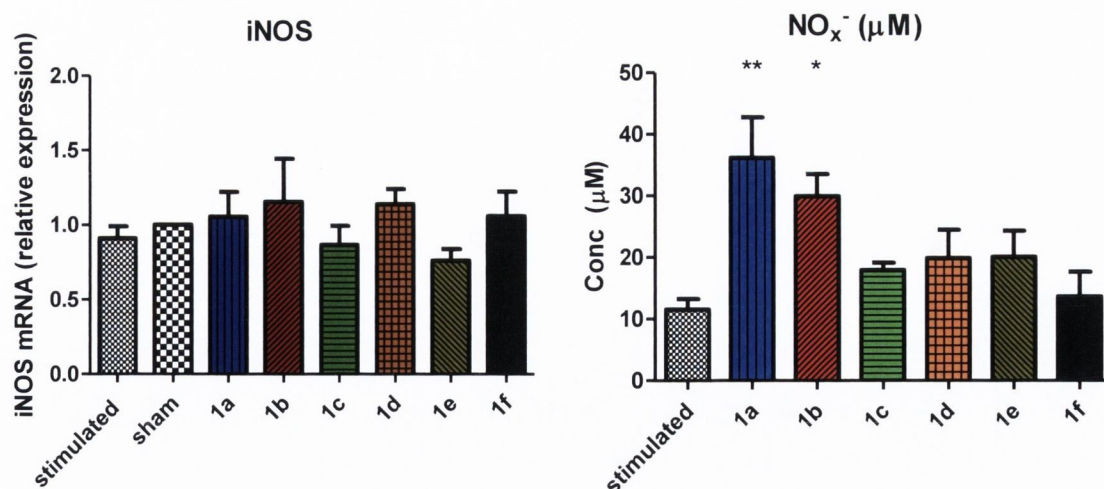


Figure 4.11: Expression of iNOS and NO<sub>x</sub><sup>-</sup> production following treatment of Caco-2 cells with the nitrate-barbiturates (1a-f) at 10 μM for 30 minutes prior to 24 hour incubation with cytokines (TNF-α and IL-1β, 10ng/ml). Left pane shows quantitation of iNOS relative to the stimulated cells with 18S used as the endogenous control with the sham group as the calibrator. The right pane shows the results of the Griess assay for the conditioned media taken after 24 hours.

Despite the cytokines or compounds having no effect on iNOS expression, we can see from the Griess assay results in Figure 4.11 that the compounds increased NO<sub>x</sub><sup>-</sup> levels in the conditioned media. This result represents the NO donor capacity of the compounds and was statistically significant for compounds **1a** and **1b**. It is interesting to note that the two amino-alkyl side-chains resulted in the biggest increase in NO<sub>x</sub><sup>-</sup> and probably less surprising is that the greatest increase was from compound **1a** which has two nitrate groups in its side-chain.



#### 4.2.2. The role of the NF- $\kappa$ B pathway in the downregulation of MMP-9 by the nitrate-barbiturate compounds

The NF- $\kappa$ B pathway is activated by pro-inflammatory cytokines such as those used in our *in-vitro* model and this pathway is known to be involved in the transcriptional upregulation of MMP-9. As laid out in 4.1.1, NO may also negatively regulate this pathway and so we decided to examine whether the MMP-9 inhibition caused by our nitrate-barbiturate compounds was mediated through this pathway.

To assess the impact of the compounds, we used an ELISA kit to assess the relative amount of p65/RelA in the nucleus of Caco-2 cells. After 24 hour incubation of the nitrate-barbiturates with cytokines, the nuclear fraction of the cells was isolated and was added to the ELISA 96-well plate. Any p65 in that had migrated to the nucleus of the sample would bind to a specific NF- $\kappa$ B response element coated to the bottom of the plate. This was measurable and gave a reading of the degree of activation of NF- $\kappa$ B.

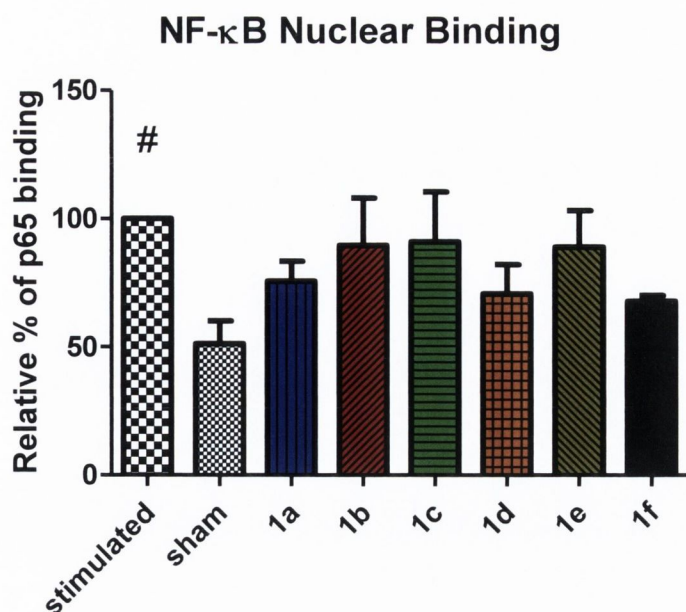


Figure 4.12: p65 nuclear binding. The nuclear fraction of Caco-2 cells was isolated following 24 hour incubation with the nitrate-barbiturates (1a-f) (10 $\mu$ M) and cytokines (TNF- $\alpha$  and IL-1 $\beta$ , 10ng/ml). A p65 transcription factor assay (ELISA) was used to detect the presence of p65 in the nucleus. Data were normalised to the stimulated group for each replicate and are presented as a percentage

A trend towards inhibition was observed for the nitrate-barbiturates that did not reach statistical significance (Figure 4.12). The greatest inhibition was observed for *1f* and *1d* with 32% and 30% inhibition of p65 nuclear translocation respectively. A 25% mean reduction was observed for *1a* and the other compounds *1b*, *1c* and *1e* had approximately 10% mean reduction. When paired t-tests were carried out, *1a* and *1f* were statistically significant with P values of 0.0267 and 0.043 respectively. *1d* had a P value of 0.0623. It was decided to examine the effect of the compounds on the transcription of some of the elements of the NF- $\kappa$ B pathway.

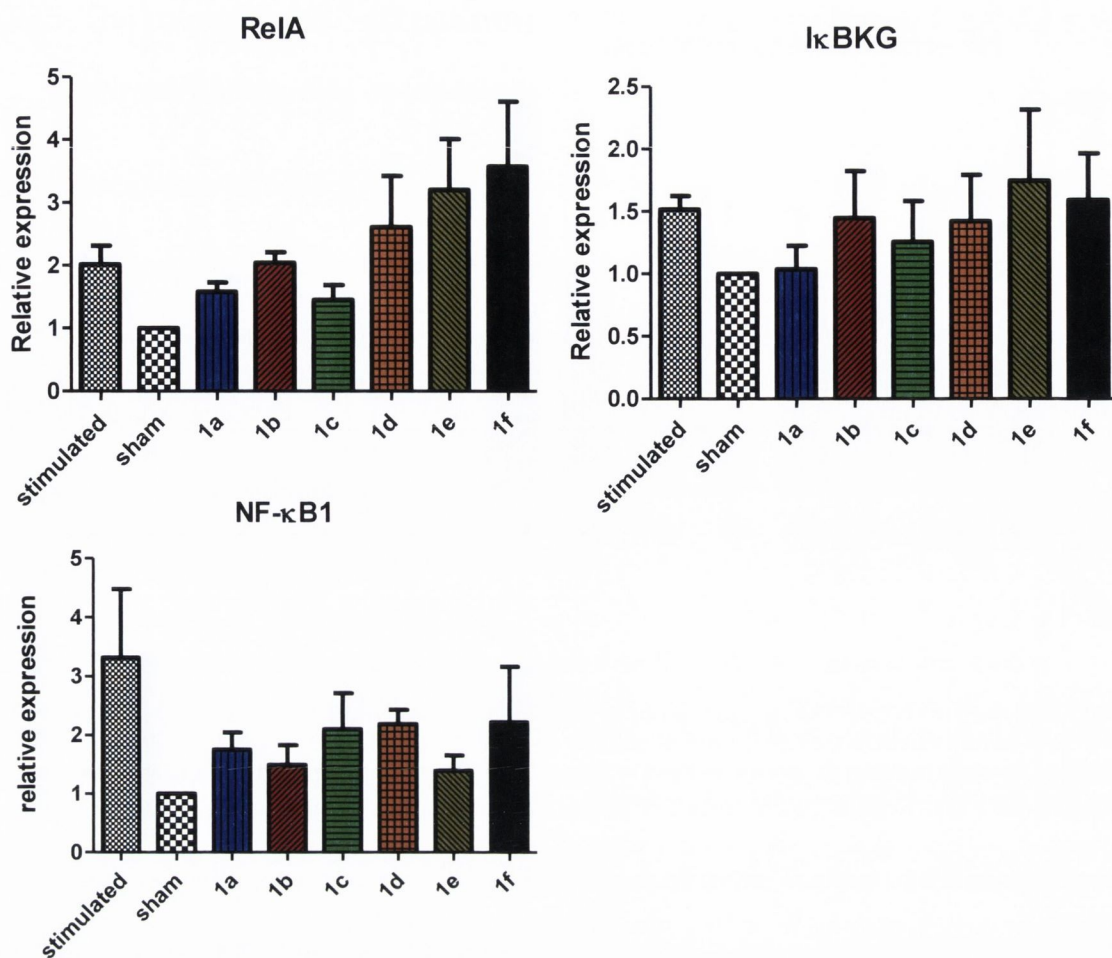


Figure 4.13: Relative quantitation of mRNA of RelA, IκBKG and NF-κB1 following treatment with nitrate-barbiturate compounds. The compounds (1a-f)(10μM) were incubated in Caco-2 cells for 30 minutes prior to addition of cytokines (TNF-α and IL-1β, 10ng/ml). Cells were then incubated for 24 hours before RNA isolation. RT-qPCR was performed on cDNA from reverse transcription of the isolated RNA. Stimulated group represents cytokine stimulated cells and sham group is untreated cells. Relative expression is calculated by the  $2^{-\Delta\Delta CT}$  method with 18S as the endogenous control and the sham group used as the calibrator.

The expression of RelA/p65, NF-κB1/p105 and IκBKG/NEMO which forms part of the IKK complex, were assessed by qPCR and the results are shown in Figure 4.13.

RelA and NF-κB1 are common components of the NF-κB complex, a protein dimer that will bind to its response element on certain genes. Although the primary mechanism of regulation is its liberation from IκB, it is still under transcriptional control and these two components are both upregulated by pro-inflammatory cytokines in Caco-2 cells. For RelA, ANOVA with a Dunnet's post-test showed no statistically significant differences



between the stimulated cells and any other group comparisons between the stimulated cell group and the sham group, *1a*, *1b* and *1c* respectively. Similarly, there were no statistically significant differences between the groups for NF- $\kappa$ B1 where the greatest inhibition was seen for *1a* and *1e* (95% CI: -0.66-4.5 and -1-4.1 respectively).

I $\kappa$ BKG is part of the IKK complex, shown in Figure 4.1, which can phosphorylate I $\kappa$ B leaving the NF- $\kappa$ B complex free to migrate to the nucleus. The difference between the stimulated and sham controls is small, which reflects the fact that transcriptional control is not the primary mechanism of regulation. None of compounds reached statistically significant inhibition compared with the stimulated group when analysed by ANOVA but paired t-test with the stimulated group found statistical significance between it and the sham group and *1a* with P values of 0.04 and 0.026 respectively.

#### **4.2.3. The role of the cGMP pathway in the downregulation of MMP-9 by the nitrate-barbiturate compounds**

The cGMP pathway is one of the most well defined ways that NO exerts many of its effects such as vasodilation and inhibition of platelet aggregation. NO can react with the heme centre of sGC leading to its activation and once active, it can convert GTP to cGMP. Following the limited effect of the compounds in altering NF- $\kappa$ B nuclear binding or expression of components of the pathway, it was decided to test the role of the cGMP pathway in mediating the inhibition of MMP-9 by the nitrate-barbiturates. This was first achieved using the pharmacological inhibitor 1H-[1,2,4]oxadiazolo[4,3-a]quinoxalin-1-one

(ODQ) at 10 $\mu$ M based on published literature [345, 353], which is a highly selective and irreversible heme site inhibitor of sGC and is competitive with NO [489, 490](Figure 4.2).

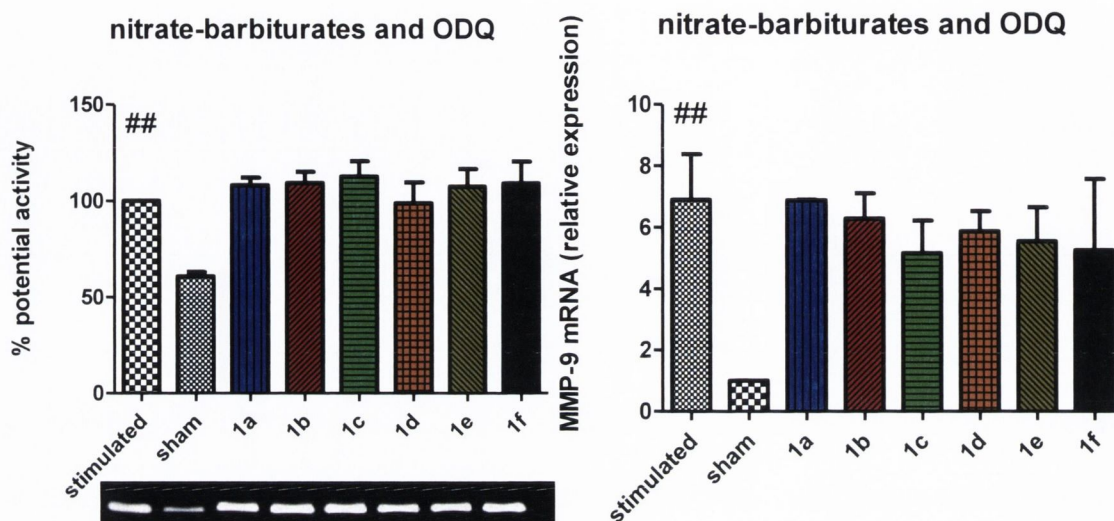


Figure 4.14: MMP-9 gelatin zymography (left) and qPCR (right) following co-incubation of stimulated Caco-2 cells with nitrate-barbiturates and ODQ. The compounds (1a-f)(10 $\mu$ M) and ODQ (10 $\mu$ M) were incubated with Caco-2 cells for 30 minutes prior to addition of cytokines (TNF- $\alpha$  and IL-1 $\beta$ , 10ng/ml). Cells were then incubated for 24 hours before RNA isolation or removal of conditioned media. RT-qPCR was performed on cDNA from reverse transcription of the isolated RNA. Stimulated group represents cytokine stimulated cells and sham group is untreated cells. Relative expression is calculated by the  $2^{-\Delta\Delta CT}$  method with 18S as the endogenous control and the sham group used as the calibrator. For gelatin zymography, densitometry results of trace mm x intensity are normalised to the stimulated group for each replicate and presented as a percentage.

Co-incubation of the nitrate-barbiturates with ODQ abolished any reduction in MMP-9 expression or secretion (Figure 4.14) that had been seen previously when the compounds alone were able to reduce the expression of MMP-9 in cytokine stimulated cells (Figure 3.14). There was no difference between any of the compound treated groups and the stimulated group.

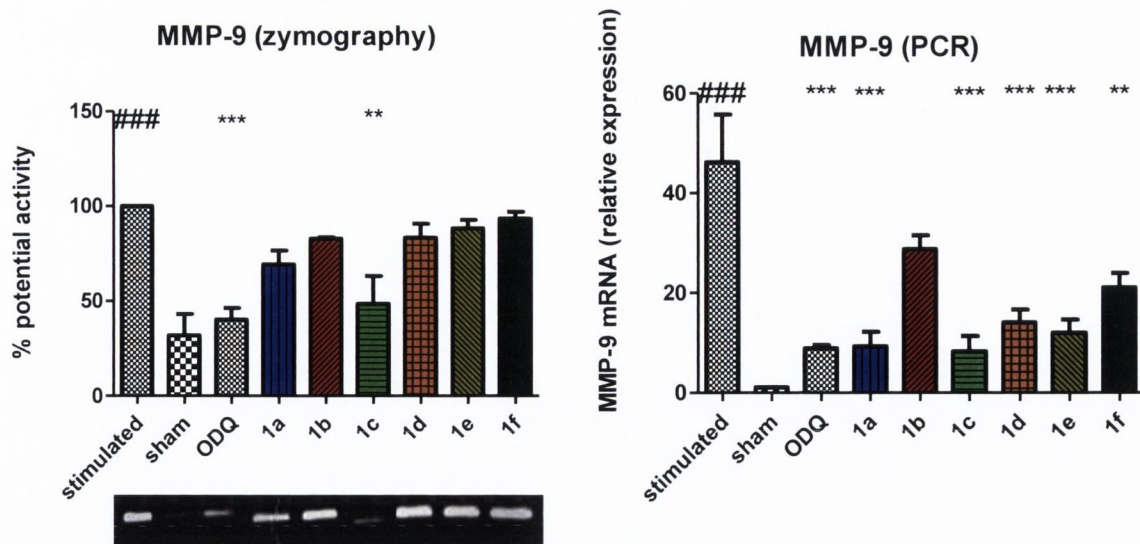


Figure 4.15: MMP-9 gelatin zymography (left) and qPCR (right) following co-incubation of stimulated Caco-2 cells with nitrate-barbiturates, ODQ and 8-Br-cGMP. The compounds (1a-f)(10 $\mu$ M), ODQ (10 $\mu$ M) and 8-Br-cGMP (10 $\mu$ M) were incubated with Caco-2 cells for 30 minutes prior to addition of cytokines (TNF- $\alpha$  and IL-1 $\beta$ , 10ng/ml). Cells were then incubated for 24 hours before RNA isolation or removal of conditioned media. RT-qPCR was performed on cDNA from reverse transcription of the isolated RNA. Stimulated group represents cytokine stimulated cells, sham group is untreated cells and ODQ group is unstimulated cells with ODQ. Relative expression is calculated by the  $2^{-(\Delta\Delta CT)}$  method with 18S as the endogenous control and the sham group used as the calibrator. For gelatin zymography, densitometry results of trace mm x intensity are normalised to the stimulated group for each replicate and presented as a percentage.

Having seen the abolition of the compounds efficacy following co-incubation with ODQ, we added 8-Br-cGMP, the cGMP analogue (Figure 4.2) to the cells at 10 $\mu$ M based on previously published literature [345, 353], along with ODQ and the nitrate-barbiturate compounds. The results were interesting and show a restoration of MMP-9 inhibition following addition of the 8-Br-cGMP (Figure 4.15) to levels comparable to the effect of the compounds alone with cytokine stimulated cells (Figure 3.14). The gelatin zymography results show that **1c** is statistically significantly lower than the stimulated group with a 51% inhibition. All the other compounds had mean inhibitions ranging from 7% for **1f** to 31% for **1a**. Paired t-tests of the compounds and the stimulated control gave P values of 0.053, 0.0018, 0.0728, 0.1497, 0.119 and 0.2 respectively for **1a-f**.



qPCR results showed statistically significant reductions relative to the stimulated group for all the compound treated groups with the exception of **1b**. Incubation with ODQ alone showed no difference between it and the sham group when measured by zymography or qPCR which shows that it has no effect on the unstimulated cells alone. Addition of the 8-Br-cGMP to the cells with the ODQ and compounds gives results that are similar to the compounds alone.

### 4.3. Discussion

Having discovered that the series of nitrate-barbiturate compounds were potent inhibitors of MMP-9 transcription and were more effective than either the alcohol-barbiturates or the nitrate side-chains alone, we decide to further investigate this mechanism of action and the role of the nitrate group. NO effects are often separated into cGMP dependent, which tend to occur at lower NO flux, and cGMP independent, occurring at higher concentrations. These cGMP independent effects are often mediated by formation of peroxynitrite [262, 263, 271, 272], leading to direct reaction with proteins to alter their function through S-nitrosylation, tyrosine nitration or oxidisation [273]. Peroxynitrite formation tends to occur in a pro-inflammatory environment where it is generated from high levels of NO and superoxide and often opposes the biological effects of NO [262, 263, 274-276]. The presence of superoxide alters the balance of protein alterations made by NO and will often give rise to a threshold in concentration, beyond which the role of NO may change. To further complicate this concentration-dependent role of NO, effects will also be cell- and environment-specific depending on the presence of endogenous antioxidants [277] and other genes involved in regulating a given response.

With the effects of NO seeming to be concentration dependent and in an attempt to ascribe some of the MMP-9 inhibitory action of the compounds to the nitrate moiety, we tested the effects of NO-donors on MMP-9 in our model of intestinal epithelial inflammation. It was previously found that endogenous or exogenously provided NO decreased MMP-9 gene expression in rat mesangial cells [393]. NO can reduce the half-life of MMP-9 mRNA [475], as well as S-nitrosylate nuclear factor- $\kappa$ B [436], two mechanisms by which NO may modulate MMP-9 expression. In our experiments, SNAP and DETA-NONOate were

chosen as NO-donors to represent varying NO release profiles. There was a linear relationship between the concentration of the compound used and the concentration of nitrate and nitrite, which represent the breakdown products of NO, that were in the media after 24 hours (Figure 4.7 and Figure 4.10). The variations in these breakdown products over the 24 hours for the two compounds were not measured. Cytokine stimulated cells that were incubated with SNAP showed a slight reduction at the level of enzyme activity (Figure 4.5) and a large inhibition of MMP-9 gene expression which was statistically significant at all concentrations (Figure 4.6). There was no difference in the effects observed at the different concentrations of SNAP. DETA-NONOate was used in the same range of concentrations (10–500 $\mu$ M) as SNAP but did not result in the same effect on MMP-9. A statistically significant reduction in potential activity was observed with 500 $\mu$ M treatment and a reduction also observed at 10 $\mu$ M (Figure 4.8). A similar trend was found following qPCR but these results were not statistically significant (Figure 4.9). It is interesting to note that while there was a direct correlation between the concentration of donor used and the  $\text{NO}_x^-$  species measured, this did not correlate with the effect on MMP-9 despite both NO-donors having some effect. The mean maximum  $\text{NO}_x^-$  measured was approximately 600 $\mu$ M for DETA-NONOate and approximately 120 $\mu$ M for SNAP. The range of concentrations of  $\text{NO}_x^-$  from SNAP that yielded the several fold reduction in MMP-9 transcription was approximately 23-120 $\mu$ M. DETA-NONOate used in the range of 10-100 $\mu$ M yielded similar quantities of  $\text{NO}_x^-$  but did not produce the same level of inhibition. This perhaps highlights the importance of the release profile of the NO-donor. The half-life of NO in a biological setting is in the range of seconds and so the measurement of its breakdown products after 24 hours may not necessarily be relevant. SNAP is expected to breakdown spontaneously and has a shorter half-life than DETA-NONOate (Table 4.1) and will likely produce a higher concentration of NO that may be



sustained for a shorter period of time and it may be this property that resulted in the inhibition of MMP-9 expression. The nitrate-barbiturate compounds had no effect on iNOS expression and there was a statistically significant increase in  $\text{NO}_x^-$  with ***1a*** and ***1b***, both of which have amino-alkyl side-chains (Figure 4.11). The dinitrate compound (***1a***) had the highest  $\text{NO}_x^-$  concentrations but it was difficult to relate these differences with any of the inhibitory effects of the nitrate-barbiturates that were observed in the chapter 3. In summary, both NO donors were able to exert some inhibitory effect on MMP-9 but this effect was independent of the  $\text{NO}_x^-$  concentration after 24 hours. The concentration and mix of cytokines used did not induce iNOS in Caco-2 cells and the nitrate-barbiturates had no effect on its basal expression. Compounds ***1a*** and ***1b*** were able to increase the  $\text{NO}_x^-$  concentration after 24 hours which is a feature of the side-chain structure and not obviously linked with its ability to inhibit MMP-9.

With the difficulties in finding selective and clinically useful active-site inhibitors, searching for alternative targets such as blocking upstream pathways of activation [491, 492] or indeed targeting the transcriptional upregulation of the enzyme is of utmost importance. Xanthine-derivatives, NSAIDs and 3-hydroxy-3-methylglutaryl coenzyme A (HMG-CoA) reductase inhibitors have all been studied as inhibitors of MMP-9 expression [39]. The tetracyclines are another group of compounds that are widely studied as for their ability to inhibit gelatinase synthesis [1, 493, 494]. Blocking of extracellular factors that can upregulate MMP-9 expression is another avenue of research that has been pursued where monoclonal antibodies against TNF [158], or blocking of IL-1, EGF [159] or TGF- $\beta$  receptors [495] has been shown to reduce MMP synthesis. Similarly, inhibition of signal transduction pathways that are involved in the upregulation of MMP-9 such as the MAPKs may be a strategy for inhibition of transcription [160, 161]. Finally, blocking of nuclear

factors such as AP-1 and NF- $\kappa$ B may provide a means of selectively blocking certain MMPs which they upregulate.

Knowing that the nitrate-barbiturates can inhibit MMP-9 transcription, that NF- $\kappa$ B is involved in the upregulation of MMP-9 and that NF- $\kappa$ B is sensitive to NO, we decided to assess the effect of the compounds on the NF- $\kappa$ B pathway. An ELISA of the p65 subunit was used to measure the nuclear binding of the NF- $\kappa$ B complex. There was a trend of inhibition for all the compounds with a maximum mean reduction of 32% but the observed reductions were not statistically significant following ANOVA (Figure 4.12). To further investigate the approximate 20% inhibition of p65 nuclear binding, we measured the effect of the compounds on the expression of some of the components of the NF- $\kappa$ B pathway. The compounds showed a limited effect on RelA/p65, NF- $\kappa$ B1/p105 and I $\kappa$ BKG/NEMO with *1a*, *1b* and *1c* causing the greatest reduction in transcription of these elements (Figure 4.13).

It was decided that following the limited effect of the compounds on the NF- $\kappa$ B pathway, it would be worth examining an alternative mechanism by which the compounds were inhibiting MMP-9 gene expression. We decided to investigate cGMP which is the most noted mediator of NO effects. sGC can mediate the transcriptional upregulation of COX-2, TNF, plasminogen activator inhibitor-1 (PAI-1), vascular endothelial growth factor receptor-1 (VEGFR1), mitogen activated protein kinase phosphatase-1 (MKP-1) and MMP-9. The exact mechanism by which cGMP exerts its transcription regulatory functions has not been fully elucidated but can alter the function of cGMP-regulated ion channels, cGMP-regulated phosphodiesterases and cGMP-dependent protein kinases (PKG). Several lines of evidence appear to involve PKG as the mediator of soluble guanylate cyclase action on MMP-9 gene transcription [496-498]. In our current studies, co-incubation of the compounds with the sGC inhibitor conclusively abolished their MMP-

9 inhibitory effects and no differences were observed between the compound treated cells and the stimulated control at the level of gene transcription or enzyme activity (Figure 4.14). We could therefore deduce that the nitrate-barbiturates inhibited MMP-9 transcription in a sGC dependent manner. To confirm this result and further elucidate the pathway, the cGMP analogue, 8-Br-cGMP was added with the compounds and ODQ and it was found that the inhibitory properties of the compounds were restored to what they were with the compounds alone (Figure 4.15). We can therefore conclude from this chapter that nitrate-barbiturates can exert their inhibitory action on MMP-9 transcription through a sGC-cGMP pathway; however, more experiments are required to elucidate the role of PKG as the mediator of cGMP action on the MMP-9 expression.



**Chapter 5: In-vivo assessment of dinitrate-barbiturate and  
corresponding alcohol-barbiturate and side chain**

## **5. In-vivo assessment of dinitrate-barbiturate and corresponding alcohol-barbiturate and side chain**

### **5.1. Introduction and background**

#### **5.1.1. Impact of IBD**

It is widely estimated that the number of patients suffering from IBD, in Europe alone, is approximately 2.2 million. The estimated mean prevalence of IBD in western countries is 1 in 1,000 [499, 500] and although data are less available for the developing world, incidence of the disease are rising globally [501, 502]. Moreover, rates of UC and CD in northern European countries (including Ireland) are 40% and 80% higher respectively than those in the rest of Europe [503]. Therefore, IBD is becoming a serious health-related problem in Ireland, with significant quality of life impact and financial burden, particularly because the incidence of this disease is increasing.

IBD is a chronic relapsing condition whose aetiology is still unknown. In addition, there is currently no ultimate cure for IBD patients. Existing therapies may alleviate inflammatory symptoms, however, IBD patients are likely to suffer many relapses over the course of the disease. Indeed, surgery has to be performed in many cases to control the disease, particularly in CD patients with stenosing behaviour. In addition, IBD is frequently aggravated by digestive and extradigestive complications. Therefore, the well-being and health-related quality of life of patients suffering from IBD can be seriously affected. Moreover, these disorders typically affect people during their economically productive lives and as stated before, they may require extensive medical and surgical treatments over

decades. The potential economic impact in our society of managing IBD is therefore considerable. According to the Economic and Social Research Institute (ESRI), approximately 3000 IBD patients are admitted to different Irish Hospitals every year for the treatment of this condition or its complications. Current mainline therapies, such as the salicylates like sulphasalazine or mesalazine and corticosteroids are largely generic. As a consequence, the global market, estimated at more than €3 billion, is probably undervalued. Exceptions are the anti-TNF $\alpha$  therapies, monoclonal antibodies directed against TNF-alpha such as infliximab. There are, however, a number of limitations with these therapies: they are not orally active, and while the response rate is about 80% in CD, it may be less than 50% for UC. It may give rise to opportunistic infections such as tuberculosis and patients may become refractory as a consequence of formation of antibodies against infliximab. Hence, the research to discover new molecules involved in IBD and new therapeutic approaches including efficient drug delivery systems is of utmost importance. With the involvement of MMP-9 in IBD confirmed, it remains a viable target for potential MMP-9 inhibitors.

### **5.1.2. In-vivo models of IBD**

Animal models of disease are used to investigate the effect of treatments or to study certain aspects of a disease, of which, all the complexities cannot be mimicked in cell culture. UC and CD are complex diseases whose aetiology is still not fully understood involving the gut epithelium, innate and adaptive immune systems and rat or murine models are invaluable in assessing the progression of the disease and the potential success of interventions. The first animal model of IBD was described 57 years ago [504] and since



then with a greater understanding of the disease, the advent of genetic manipulation and human genome-wide IBD association studies have left us with a wide-array of models with specific pathologies and features. These models seek to mimic the clinical and morphological features of UC or CD. For CD, phenotypic similarity is through the presence of discontinuous transmural inflammation of the intestinal wall, small bowel involvement, stricture development, granuloma formation and perianal disease with fistulae. For UC, this is inflammation with rectal involvement, crypt abscess formation and superficial involvement of the bowel wall [505].

Animal models of IBD are broadly grouped into 1) chemically induced, 2) congenic, 3) cell transfer models and 4) genetically engineered which include various knock out (KO) and transgenic (Tg) models.

#### **5.1.2.1. Chemically induced colitis**

Colitis that is chemically induced by an administered agent were the first established and are still the most common animal models for studying IBD. These models are easy to use, flexible, reliable and relatively inexpensive [505]. On the other hand, they fall short in the likeness to human IBD in that many models produce an acute, self-limiting colitis that develops quickly (days) and lasts weeks, as opposed to a chronic colitis which develops and persists over weeks to months. The pathogenesis is artificially induced by chemicals which damage the epithelium which is not a feature of the human disease. Some commonly used models of chemically induced colitis are summarised in Table 5.1.

<b>Model</b>	<b>Pathogenesis</b>	<b>Phenotype</b>	<b>Immunological features</b>	<b>Ref.</b>
<b>DSS</b>	Chelation of divalent cations required for IEC tight junctions	UC-like acute or chronic self-limiting colitis	Innate immunity, M1 macrophage, initially Th1, but later Th1/2	[208, 506]
<b>TNBS</b>	Haptenization of colonic proteins	CD-like acute self-limiting colitis	DTH-like response; Th1 (and possibly Th2)	[507]
<b>Oxazolone</b>	Haptenization of colonic proteins	UC-like acute self-limited leftsided colitis	Th2 and NK T cells	[508]

Table 5.1: Models of chemically induced colitis with features. IEC (intestinal epithelial cell), DTH (delayed-type hypersensitivity). Adapted from [509].

DSS is commonly used to induce colitis in rats and mice where it is dissolved in water at 3-5% and administered for 5-7 days to induce an acute or chronic colitis with epithelial injury and crypt loss [510]. Clinical features include weight loss, loose stools/diarrhoea, and rectal bleeding and histopathological analysis typically reveals crypt loss, epithelial cell damage, significant infiltration of granulocytes and mononuclear immune cells, and tissue oedema, often accompanied with severe ulceration [510]. Initial, acute colitis is mediated by pro-inflammatory cytokines released by macrophages [208], however chronic colitis induced by DSS has been shown to be mediated by CD4<sup>+</sup> T cells [511]. These CD4<sup>+</sup> T cells can increase local concentrations of IFN- $\gamma$  and IL-4 which suggests that the chronic inflammation caused by DSS can be mediated by Th1 and Th2 cells [506]. As in human IBD, bacteria will play a role in the pathogenesis of DSS induced colitis and it has been shown that antibiotics can prevent against or even treat this colitis in mice and rats [512]. A study using temporal genomewide expression profiling compared distal colon samples from DSS induced colitic mice to corresponding human UC results. The group found 1,609 genes that were significantly altered in DSS induced colitis and of these, 152 genes were

similarly upregulated when compared with the human UC results and 52 were similarly downregulated [513]. A rat model of DSS induced colitis is what we used to assess the effects of compound **1a** and the corresponding alcohol-barbiturate and nitrate side-chain. Over the course of 5 days, the rats develop an acute colitis that begins in the distal colon. This model was chosen for its ease of use and the fact that epithelial integrity becomes compromised and MMP-9 is known to be upregulated.

TNBS is a hapten that is delivered intrarectally in ethanol solution to rats or mice to produce a model of colitis with many of the features of human CD. Ethanol is required to disrupt the epithelium and expose the lamina propria to the lumen [514]. This produces a transmural inflammation with granulomas and infiltration of inflammatory cells through all layers of the intestine which results in diarrhoea, rectal prolapse and weight loss. Isolated macrophages produce large amounts of IL-12 and lymphocytes produced IFN- $\gamma$  and IL-2 which is characteristic of a Th1 response that is seen in CD [507].

Oxazolone is another hapten that is used to induce colitis in animals with a Th2 polarized response. Like TNBS, oxazolone is administered rectally in an ethanol enema solution and induces colitis that is limited to the distal colon with superficial ulceration which resembles UC. The TGF- $\beta$  mediated Th2 response is characterised by high levels of IL-4 [508].

Other chemicals that have been or continue to be used to induce colitis in animal models include acetic acid [515], indomethacin [516] and iodoacetamide [517], each with differing methods of administration and resulting in varying forms of colitis.



### 5.1.2.2. *Congenetic or transgenic models of colitis*

Congenetic animals are produced from crossbreeding two inbred strains of known genome that differ at a certain chromosome. Any difference in phenotype of the congenic animal from the inbred parents can be attributed to the area of difference in the genomes. An example of a congenic mouse model is a specific substrain of C3H/HeJ obtained through selective breeding known as C3H/HeJBir. This substrain lacks TLR-4 and is unresponsive to LPS and spontaneously develops colitis in the third to fourth week of life. The colitis is characterised by ulcer and crypt abscess and increased levels of IL-2 and IFN- $\gamma$  from lamina lymphocytes has been observed which is indicative of a Th1 type response (Table 5.2) [518].

SAMP1/Yit mice are another example of a congenic model of colitis where spontaneous terminal ileitis develops after approximately 10 weeks [519]. Interestingly, another group discovered that numerous phenotypic features of the colitis changed from those originally described after more than 20 generations of brother-sister mating [520]. These changes included accelerated onset of disease features including high IFN- $\gamma$  production after 4 weeks which preceded the onset of ileitis, chronic ileitis with prominent muscular hypertrophy and focal collagen deposition in inflamed segments and mesenteric lymph node lymphocyte activation. Perhaps most interestingly, approximately 5% developed perianal disease with ulceration and fistulae which had not been seen in an animal model before and the strain was redefined as SAMP1/YitFc.

A transgenic animal is produced from injecting genetic material into a single stem cell of the embryo which will then randomly integrate into the animal genome. IL-7 is a key cytokine in the proliferation and regulation of epithelial cells and lymphocytes in UC patients [521]. Transgenic mice that overexpress IL-7 develop colitis within 1 to 3 weeks with infiltration of neutrophils and CD4<sup>+</sup> T cells. In the acute phase, high levels of IL-7 are

found in inflamed regions and after 8 to 12 weeks, proctoposis with rectal bleeding, infiltration of monocytes, decrease in goblet cells and crypt abscesses were observed in the lamina. Although this model produces UC like phenotype, a Th1 type response is dominant with increases in IL-2 and IFN- $\gamma$ . STAT4 transgenic animals overexpress STAT4 leading to an increase in IL-12 synthesis in the animal. A Th1 type response is elicited and a transmural inflammation of the intestine with similarities to human CD results [522].

<b>Model</b>	<b>Pathogenesis</b>	<b>Phenotype</b>	<b>Immunological features</b>	<b>Ref.</b>
<b>C3H/HeJBir</b>	A substrain of TLR-4 lacking, C3H/HeJ mice unresponsive to LPS	CD-like chronic colitis of the caecum and proximal colon, antibodies against microflora	Th1	[518, 523]
<b>SAMP1/Yit</b>	Sublines of SAM mice from the AKR/J background	CD like, chronic segmental ileitis and typhlitis with granulomas	Early Th1 later mixed Th1/Th2; Increased epithelial permeability	[519, 520, 524]
<b>IL-7 tg</b>	Enhanced IL-7 production by mucosal T cells	UC-like chronic pancolitis	Sustained survival of colitogenic IL-7R $\alpha$ -expressing memory CD4 <sup>+</sup> T cells, Th1	[525]
<b>STAT4 tg</b>	STAT4 overexpression in CD4 <sup>+</sup> T cells	CD-like chronic transmural ileitis/colitis	Loss of STAT4 transcriptional regulation of IL-12/IL-23 receptor signalling results in enhanced Th1	[522]

Table 5.2: Models of congenic or transgenic colitis with features. Tg (transgenic). Adapted from [509].

### **5.1.2.3. Gene KO models of colitis**

A KO model is created by modifying embryonic stem cells with a DNA construct containing DNA of a target gene and then injecting them into the blastocyte. With this method, a single gene can be modified or knocked out. The ability to KO one single gene is a hugely valuable research tool in assessing the effects of that gene and can also provide a wide range of models of disease to study the progression and possible interventions. Despite this, care must be taken when evaluating the results of interventions from KO animal models as signalling pathways that may affect the performance of the therapeutic may not be present. Indeed, while the specific KO might provide a phenotype seen in CD or UC, the human disease is polygenic and may not have loss of the gene that is knocked out such as IL-10 or STAT3. Some commonly used KO models of UC and CD are summarised in Table 5.3.



Model	Pathogenesis	Phenotype	Immunological features	Ref.
<b>IL-2<sup>-/-</sup> / IL-2 receptor <math>\alpha</math><sup>-/-</sup></b>	Disruption of the IL-2 or IL-2 receptor $\alpha$ gene	Multiorgan inflammation, transmural chronic colitis, lymphoproliferation	deficient Tregs; Deficient activation-induced T cell apoptosis; Enhanced antigen-presentation by epithelial cells, Th1	[526]
<b>IL-10<sup>-/-</sup>/IL-10 receptor</b>	Disruption of the IL-10 or IL-10 receptor gene	Chronic transmural colitis accelerated by helicobacter hepaticus	IL-12/23-dependent Th1/Th17; Th2 in late phase	[527]
<b>Macrophage-PMN STAT3<sup>-/-</sup></b>	Disruption of the signal transducer and activator of transcription 3 (STAT3) gene in neutrophils and macrophages	Chronic transmural colitis with malignant transformation	Absence of the IL-10 counterregulatory effect on neutrophils and colonic macrophages; TLR-dependent enhanced IL-12p40, Th1	[528]
<b>TNF<math>\alpha</math><sup><math>\Delta</math>ARE<sup>-/-</sup></sup></b>	Deletion of a segment in the 3' UTR region increases TNF- $\alpha$ mRNA stability and protein production	CD-like chronic transmural ileitis/proximal colitis with granulomata, arthritis, alopecia	Th1 driven CD8 <sup>+</sup> effector T cell inflammation	[529]

Table 5.3: Models of gene KO colitis with features. Adapted from [509]

IL-2 is considered to be a key regulatory cytokine in the immune system with functions including the activation of T cells, macrophages, natural killer cells and differentiation of B cells. In models of IL-2 or IL-2 receptor KO, colitis develops between 6 and 15 weeks [530]. While the small intestine is unaffected, the entire colon becomes ulcerated with wall thickening. Infiltration of activated T and B cells has been observed with an increase in antibody production and major histocompatibility complex (MHC) class II expression.

Increased levels of IL-12 and IFN- $\gamma$  indicate that this is a Th1 type response [514]. IL-2 also mediates activation-induced cell death and it is believed that incomplete depletion of activated T-cells may mediate the colitis observed in this model [531].

IL-10 is considered to be an anti-inflammatory cytokine and crucial to maintaining homeostasis of the gut immune system. It is secreted by T cells, B cells, macrophages, thymic cells, and keratinocytes. It inhibits the function of Th1 cells, NK cells, and macrophages. IL-10<sup>-/-</sup> animals are by far the most widely used gene-target model of colitis and first develop inflammation in the proximal colon at 3 weeks old with increased severity and distribution over time and pancolitis and caecal inflammation at 2 to 4 months old [532]. Goblet cell depletion, degeneration of the epithelium, infiltration of IgA-producing plasma cells, and an increase in MHC class II expression have been detected in the colon [533]. Activation of CD4<sup>+</sup> Th1 cells and depletion of Tregs is believed to mediate the colitis in this model but there may be two distinct phases where IL-12 mediates early colitis but IL-4 and IL-13, but not IL-12, mediate chronic colitis [527].

STAT3 is the downstream molecule for IL-10 and so it was discovered that knocking out this gene in macrophages and neutrophils resulted in the development of spontaneous colitis similar to that seen in the IL-10<sup>-/-</sup> model [528].

Another commonly used rodent model of colitis involves TNF $\alpha^{\Delta ARE/-}$  where deletion of ARE in the 3' UTR results in more stable TNF- $\alpha$  mRNA. Increasing the synthesis of this well-known pro-inflammatory cytokine unsurprisingly results in colitis. The KO models discussed here all involved altering cytokine signalling to alter immune functions in the gut but it should be noted that several other KO models, not listed in Table 5.3, exist, whose genetic modification alters the physiological working of the epithelial barrier such as



mucin (MUC) 1/2<sup>-/-</sup> results in a loss of mucin production or Mdr1a<sup>-/-</sup> where colitis results from a loss of the intestinal transporter P-glycoprotein.

#### 5.1.2.4. Cell transfer models

These models involve disruption of T cell homeostasis to induce colitis in an animal. The most common of these models involves adoptive transfer of CD4<sup>+</sup>, CD45RB<sup>high</sup> T cells from healthy wild type animals into syngeneic recipients that lack T and B cells where pancolitis and small bowel inflammation results after 5 to 8 weeks [534, 535]. The colitis is characterised by a predominant involvement of the distal colon with transmural inflammation, epithelial cell hyperplasia, leukocyte infiltration, crypt abscesses and epithelial cell erosions.

#### 5.1.3. Experimental design

Our *in-vivo* experiments sought to examine the ability of compound **1a** to inhibit MMP-9 in the distal colon and thus reduce DSS induced colitis and compare its effects to that of compounds **2a** and **3a**. We also wished to discover if the ability to inhibit MMP-9 in the colon would result in reduced inflammation and severity of the disease. **1a** was chosen as a representative compound as it has two nitrate moieties on its side chain and produced the greatest increase in NO<sub>x</sub><sup>-</sup> after 24 hours and so would be best suited for discerning any contribution from the nitrate in an *in-vivo* model. **2a** and **3a** are the corresponding alcohol-barbiturate and nitrate-side chain respectively and so could be used compare the effects of the component parts of the molecule. Owing to an undetermined pharmacokinetic profile,



it was decided that local administration of the compounds, intrarectally by enema, would best allow us to determine efficacy. Male Wistar rats are commonly used in DSS induced colitis experiments and were chosen over mice for ease of enema administration and to enable greater accuracy of dosing. Five weight controlled groups were assessed in total with between 10 and 20 animals in each group, where the sham group received tap water but all the other groups received 5% DSS in lieu of this. Rectal enemas were administered twice daily which contained vehicle only for the DSS and sham groups and one of three compounds for the other groups as showed in Figure 5.1. Drug administration began on Day 0 at the same time as the commencement of the DSS.

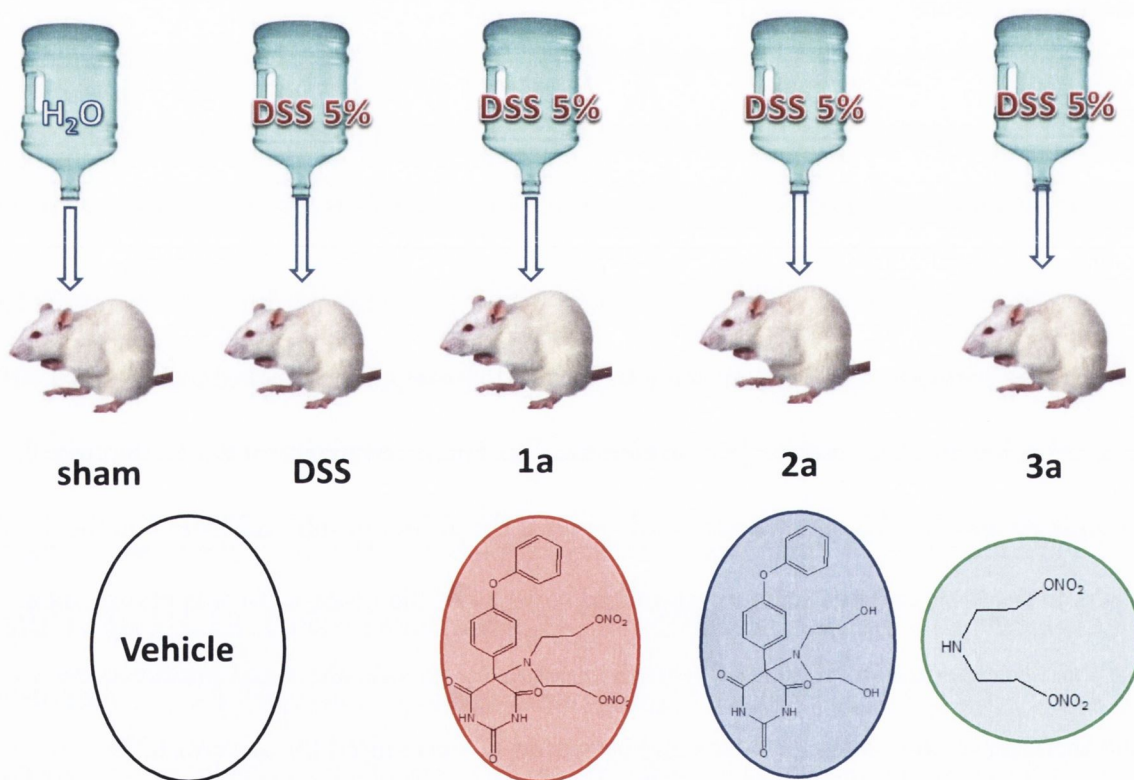


Figure 5.1: Experimental design. Five groups in total were used, four of which received DSS 5% in their drinking water, whereas the sham group received drinking water alone. Rectal enemas were administered twice daily to each animal. Sham and DSS groups received vehicle (1% cremophor, 5% ethanol in ddH<sub>2</sub>O) where the other three groups received compounds dissolved in the same vehicle.

This layout allowed us to assess induction of colitis by comparing the two control groups and any improvement following administration of the compounds, by comparing those treatment groups to the DSS group, while using as few animals as possible.

## 5.2. Results

### 5.2.1. Clinical and histological assessment

To follow on from the establishment of efficacy and mechanism of action of the nitrate-barbiturate compounds in our cell culture model, we tested compound *1a* in our rat model of colitis induced by DSS. The progression of the disease was monitored each day with a clinical score given by the DAI.

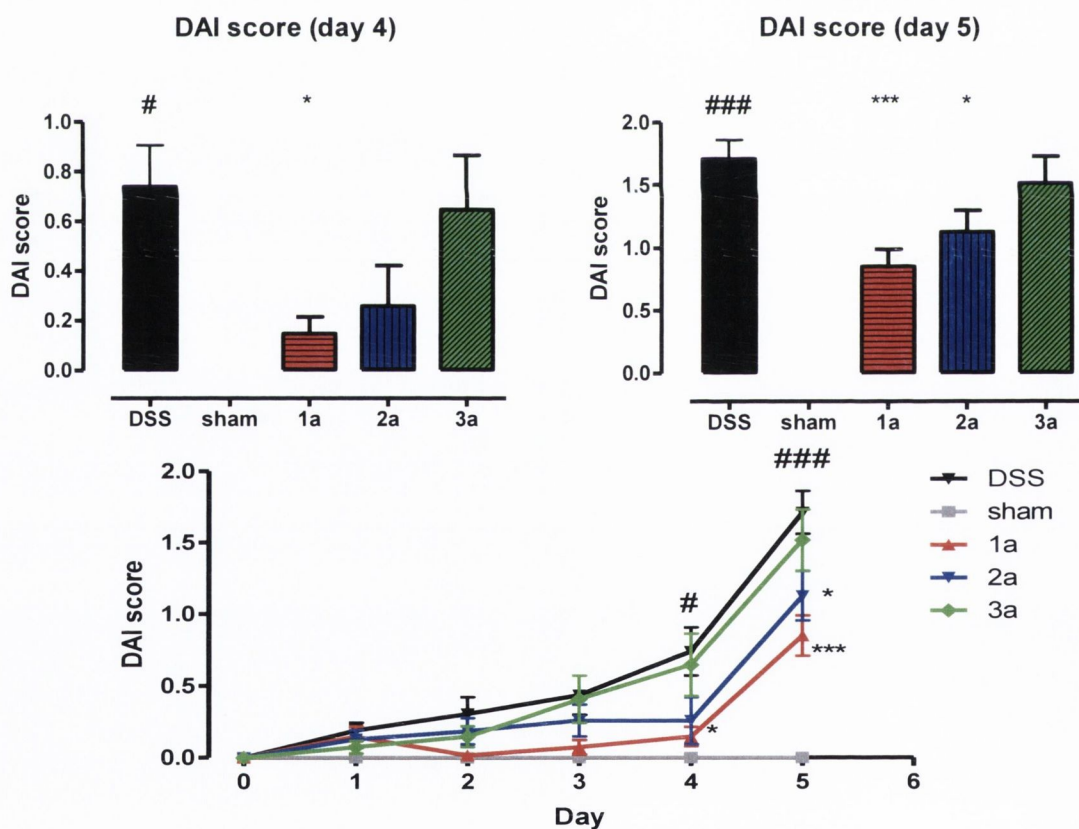


Figure 5.2: Progression of disease activity over the course of the experiment as measured by the DAI. Top pane shows histograms of the DAI scores for the rats on day 4 (left) and day 5 (right) when statistically significant differences were observed following treatment with 1a, 2a or 3a. Bottom pane shows the DAI scores for each day for all groups. Results are pooled from three experiments (n=87) with a minimum of 10 animals in each group.



The mean DAI score for sham group animals never changed from zero as can be seen in Figure 5.2. Statistically significant differences were observed between the DSS and sham groups and **1a** and the DSS group by day 4. It was at this point that several of the DSS group animals started to develop diarrhoea and rectal bleeding. By day 5, most of the DSS group had diarrhoea and bloody stools or rectal bleeding. An obvious trend emerged among the compound treated groups where the animals that were administered **1a** developed fewer and less severe colitic features which was highly statistically significant. **2a** also protected the animals from the severity of disease activity but to a lesser extent than the nitrate equivalent and the nitrate side-chain had a slight protective effect that was not statistically significant.

From these results, we can conclude that **1a** can protect against DSS induced colitis and is more effective than the non-nitrate equivalent and so the reduction in the severity of the colitis is partly mediated through the nitrate group. It is tempting to speculate that the observed effect of the nitrate-barbiturate results from the additive or synergistic combination of the component parts but this theory was not tested experimentally and **1a** may have a mechanism of action and pharmacokinetic profile that is distinct from either **2a** or **3a**.

To follow on from the success of the nitrate-barbiturate in treating the clinical manifestations of the colitis, four representative distal colon samples from each of the DSS and sham groups and **1a** treated group were processed for histological assessment with the help of Dr Noreen Boyle and Dr Neil Docherty. The results were very clear upon visualisation as seen in Figure 5.3.



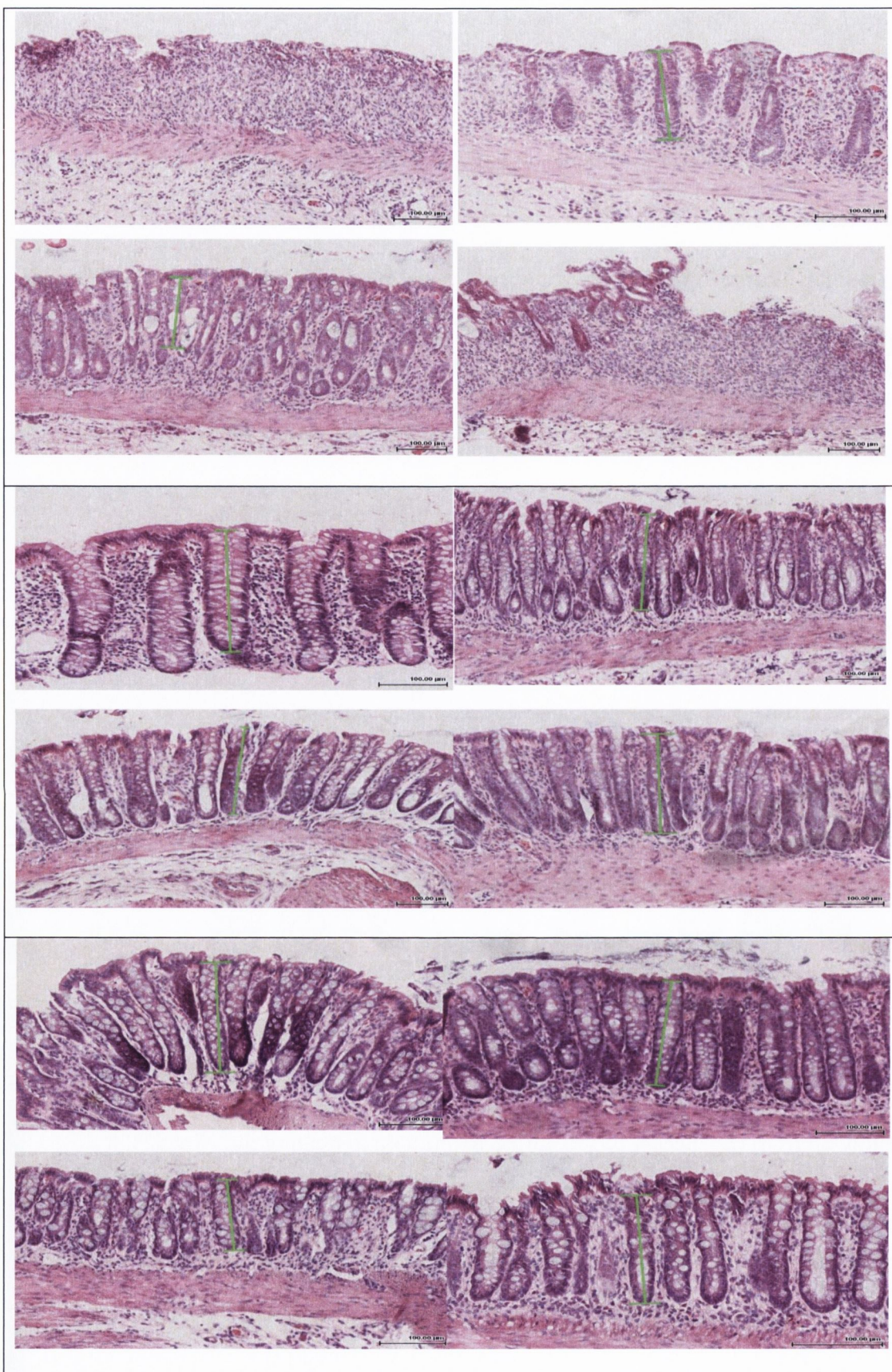


Figure 5.3: Representative images of H&E stained distal colon samples from four different animals from each group. The top row shows representative images from the DSS group with epithelial stripping and near complete crypt loss with increased infiltration of inflammatory cells. The second row shows representative images from the sham group with an intact epithelium and crypts that extend almost as far as the muscularis. The third row shows representative images from the *1a* group with features similar to the sham group.



The images in Figure 5.3 show conclusively that *1a* protects the epithelium from the damaging effects of DSS induced colitis and samples from this group look histologically comparable to those from the sham group. Notable features from the DSS group include a stripping of the surface epithelium, shortening of crypt depth, increased distance between crypts and in some cases complete crypt loss. None of these features were present in the sham group or the *1a* group.

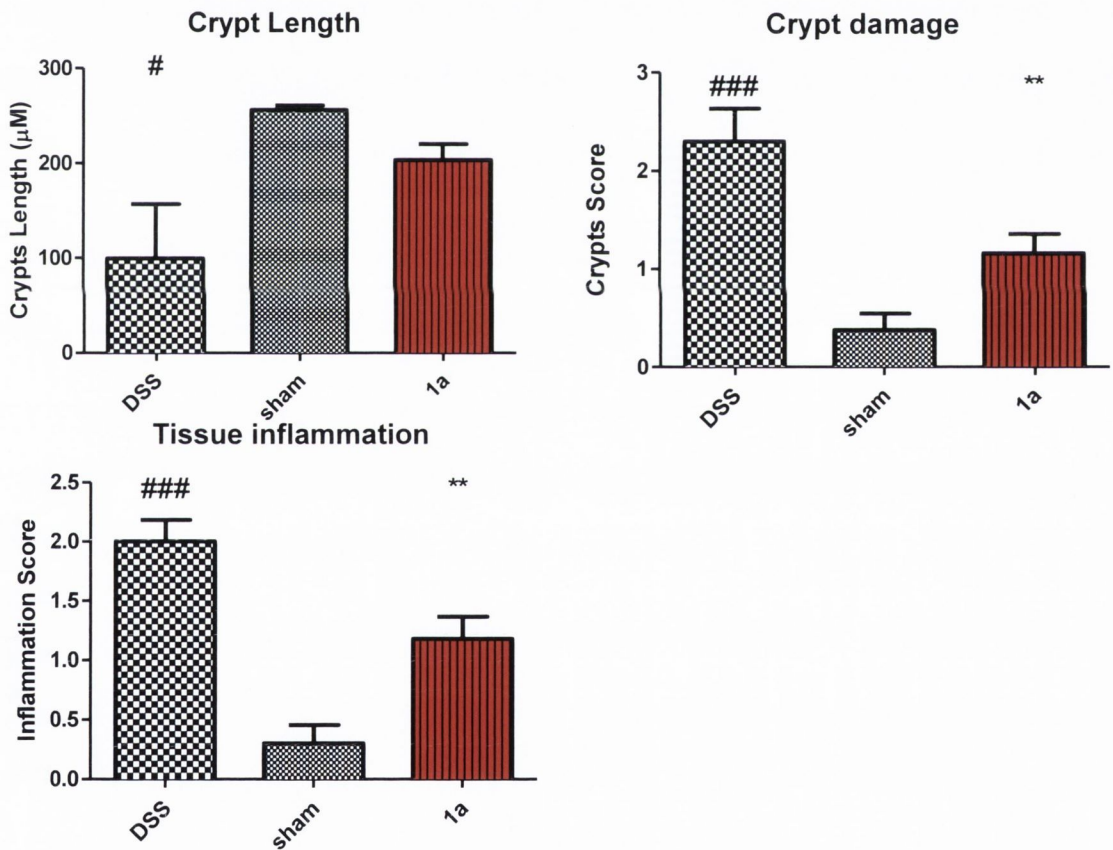


Figure 5.4: Histological measures of inflammation. All measures were based on average scores for 5 areas of distal colon sample for 10 animals for each group. Crypt length (top left) was measured using the annotation function on Digital Slidebox software following digital scan. Crypt damage (top right) was assigned a subjective score, following blinding, based on crypt shortening and surface erosions. Tissue inflammation (bottom left) was assigned a subjective score, following blinding, based on enlargement of the lamina and infiltration of nuclei. Results are presented as averaged absolute values or scores.



Each colon sample was analysed and assigned a score for tissue inflammation and crypt damage across 5 areas of each sample which were averaged. Crypt length was also measured across 5 areas of each sample using the Digital Slidebox software as described in materials and methods. While there was a notable difference between the crypt lengths for the DSS and the *Ia* groups, this did not reach statistical significance. The other histological scores of crypt damage and tissue inflammation did reach statistically significant differences between the DSS group and *Ia*, which is in agreement with the DAI scores (Figure 5.2) and the images of the colon samples in Figure 5.3 which is shown in the correlations in Figure 5.5. The results of this regression analysis show that the DAI and crypt damage score ( $P < 0.0001$ ,  $R^2 = 0.602$ ) and the DAI and tissue inflammation score ( $P < 0.0001$ ,  $R^2 = 0.5906$ ) both represent the same trend of results. All the results confirm that *Ia* can reduce the level of intestinal inflammation in the distal colon of rats with DSS induced colitis.

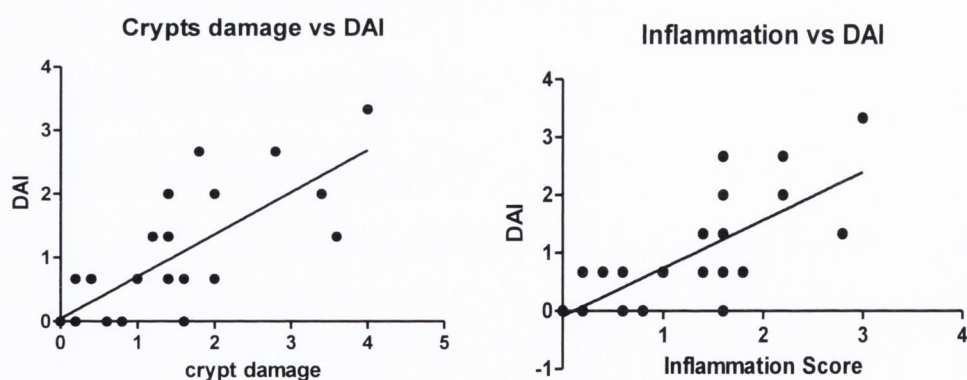


Figure 5.5: Correlations of histological measures of inflammation and the DAI scores. The scores for crypt damage were correlated with the corresponding scores for DAI for the same animal (left). The score for tissue inflammation were correlated with the corresponding scores for DAI for the same animal (right)

## 5.2.2. The effect of compound *1a* on MMP-9 and a gene expression analysis in the distal colon

Having seen the ability of *1a* to protect against DSS induce colitis, we wished to ascertain the effect it was having on MMP transcription and activity in the distal colon. The lysed distal colon tissue was not analysed for cell types but likely contained a variety of including epithelial cells, smooth muscle cells, dendritic cells and macrophage etc. It is worth noting that following an acute course of DSS, the cellular make up of tissue may change with fewer epithelial cells present and a greater number of infiltrating inflammatory cells which may produce and release different inflammatory mediators [316].

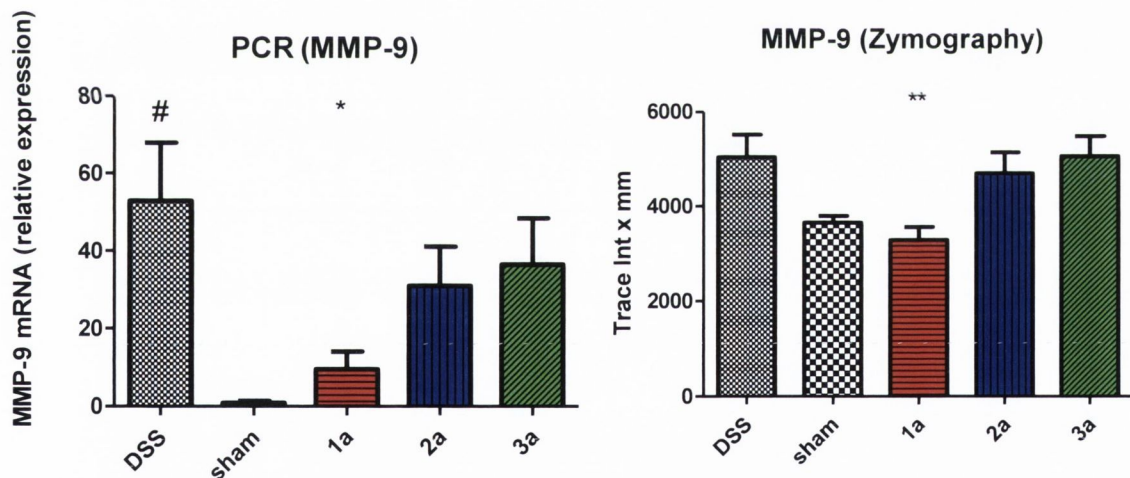


Figure 5.6: Gene expression and activity of MMP-9 in the distal colon. Data represent three pooled experiments with a total of  $n = 77$ . Following sacrifice, RNA was isolated from the distal colon of the rats or distal colon samples were lysed for gelatin zymography. RT-qPCR was performed on cDNA from reverse transcription of the isolated RNA. DSS group represents animals that were given DSS and treated with vehicle and sham group represents rats that received drinking water and treated with vehicle. The 1a, 2a and 3a groups received DSS and were treated with the respective compounds. Relative expression is calculated by the  $2^{-\Delta\Delta CT}$  method with 18S as the endogenous control and a median animal of the sham group used as the calibrator. For gelatin zymography, the data are expressed as the average of the densitometry results; trace mm x intensity.

In Figure 5.6, we can see that *1a* statistically significantly reduces both MMP-9 expression and activity in this model of colitis. *2a* and *3a* appeared to have some effect in reducing MMP-9 mRNA but the result was not statistically different from the DSS group. These results show a similar trend to the DAI scores.

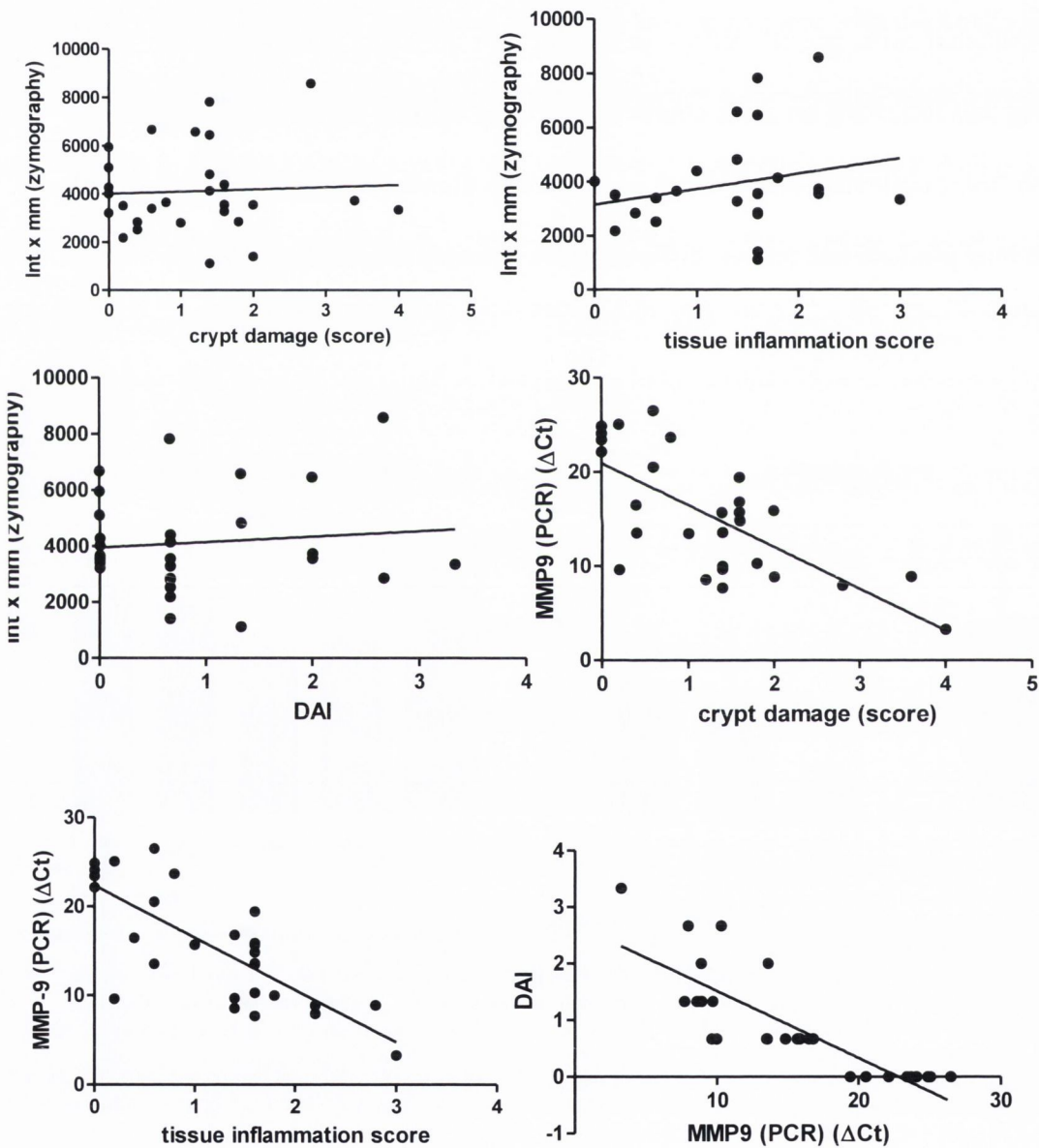


Figure 5.7: Correlation of MMP-9 activity and expression and DAI score and histological scores of inflammation. All graphs represent animals from different groups (n=30) following linear regression analysis. PCR results are expressed as  $\Delta$ Ct values, zymography as intensity x mm, and DAI, tissue inflammation and crypt damage as absolute scores on day 5. From left to right and top to bottom: zymography vs crypt damage, zymography vs tissue inflammation, zymography vs DAI, PCR vs crypt damage, PCR vs tissue inflammation and DAI vs PCR.



Having observed a similar trend between MMP-9 inhibition and a reduction in inflammation, Figure 5.7 shows the correlations between the measures of MMP-9 activity and expression and the measures of inflammation used. The first three graphs from left to right and top to bottom show the densitometry results following zymography and the other measures of inflammation. These correlations were poor; zymography and crypt damage ( $P = 0.78$ ,  $R^2 = 0.03$ ), zymography and tissue inflammation score ( $P = 0.27$ ,  $R^2 = 0.0537$ ), zymography and DAI score ( $P = 0.59$ ,  $R^2 = 0.012$ ) and can only be explained by poor sensitivity of the zymography analysis. To correlate the qPCR results with the inflammation scores,  $\Delta C_T$  was used which is unique to each sample and not relative to any other group and where a high  $\Delta C_T$  is indicative of low MMP-9 mRNA levels. The expression MMP-9 correlated well with the other measures of inflammation and were statistically significant; PCR  $\Delta C_T$  and crypt damage ( $P < 0.0001$ ,  $R^2 = 0.5$ ), PCR  $\Delta C_T$  and tissue inflammation score ( $P < 0.0001$ ,  $R^2 = 0.058$ ) and PCR  $\Delta C_T$  and DAI score ( $P < 0.0001$ ,  $R^2 = 0.682$ ).

The expression of pro-inflammatory cytokines in the distal colon and any influence of the compounds on this expression was then analysed.

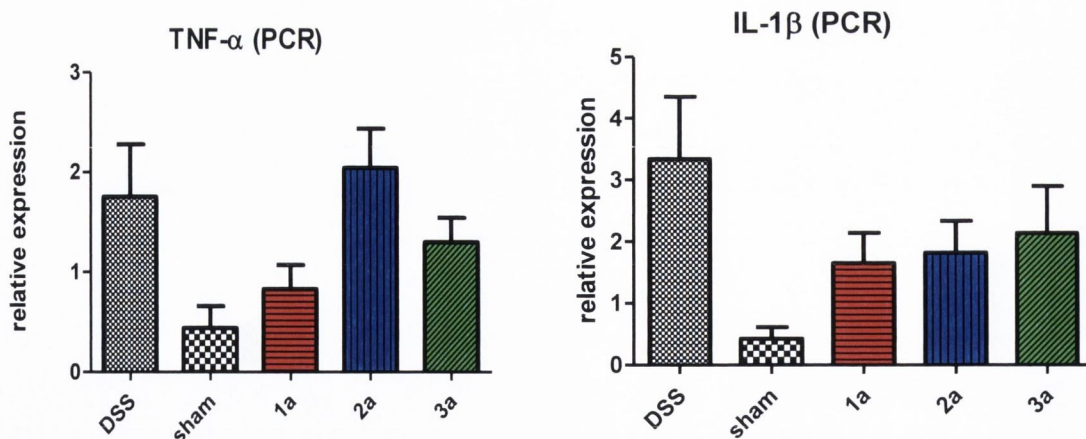


Figure 5.8: Gene expression and activity of TNF- $\alpha$  and IL-1 $\beta$  in the distal colon. Data represent three pooled experiments with a total of  $n = 77$ . Following sacrifice, RNA was isolated from the distal colon of the rats. RT-qPCR was performed on cDNA from reverse transcription of the isolated RNA. DSS group represents animals that were given DSS and treated with vehicle and sham group represents rats that received drinking water and treated with vehicle. The 1a, 2a and 3a groups received DSS and were treated with the respective compounds. Relative expression is calculated by the  $2^{-\Delta\Delta CT}$  method with 18S as the endogenous control and a median animal from the sham group used as the calibrator

The expression of the cytokines follows a similar trend to that of MMP-9 but no statistically significant differences between the treatment groups and the DSS group were observed (Figure 5.8). The 95% confidence interval for the DSS group versus **1a** was -0.4 – 2.25 for TNF- $\alpha$  and -0.9 – 4.3 for IL-1 $\beta$  and so very close to statistical significance. A notable difference to a trend with all the *in-vivo* results so far is the absence of any effect exerted by **2a** on TNF- $\alpha$  expression.

To further explore the effect that MMP-9 inhibition had on the expression of inflammatory regulating proteins, representative animals from each of the DSS, sham and **1a** groups were chosen and RNA samples from the distal colon were analysed using TaqMan inflammatory array cards. Relative quantitation was carried out as described previously and a correlation matrix (Figure 5.9) was generated using the dChip software to assess the correlation of gene expression profiles of animals within and between experimental group. This clusters samples together based on the gene expression profile. The degree of correlation is given a colour to allow visualization with positive correlations relating to the

brightness of the red colour and negative correlations given by the brightness of the green colour. Following clustering, the samples are presented in a square where the colour of the box at the intersection of two samples indicates the degree of correlation. From the correlation matrix, we can see that all but one of the DSS group animals clustered together and had strong correlation. Similarly, the sham group and 1a treated group clustered together.

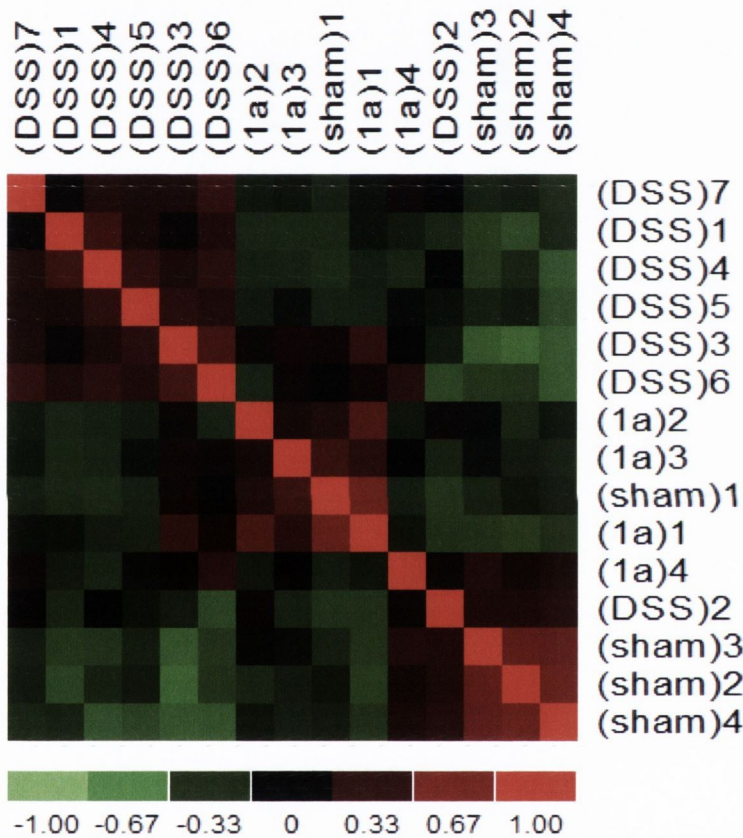


Figure 5.9: Correlation matrix of samples used in gene profiling experiment. Samples are clustered and correlated according to gene expression profile calculated from relative expression results from TaqMan rat inflammatory array cards and are shown grouped on the x and y axis. The colour at the point of intersection of two samples on the matrix indicates the level of correlation as shown in the legend where bright green indicates -1 and bright red indicates 1.

The heatmap in Figure 5.10 shows the same information where all but one of the DSS samples clustered to one side of the map and the sham and *1a* treated samples clustered to the other side with the one outlying DSS group sample. From the branching at the top of



the map, we could see that the expression profile of the inflammatory genes for the *Ia* treated animals was comparable to the sham group and separate from the DSS group.

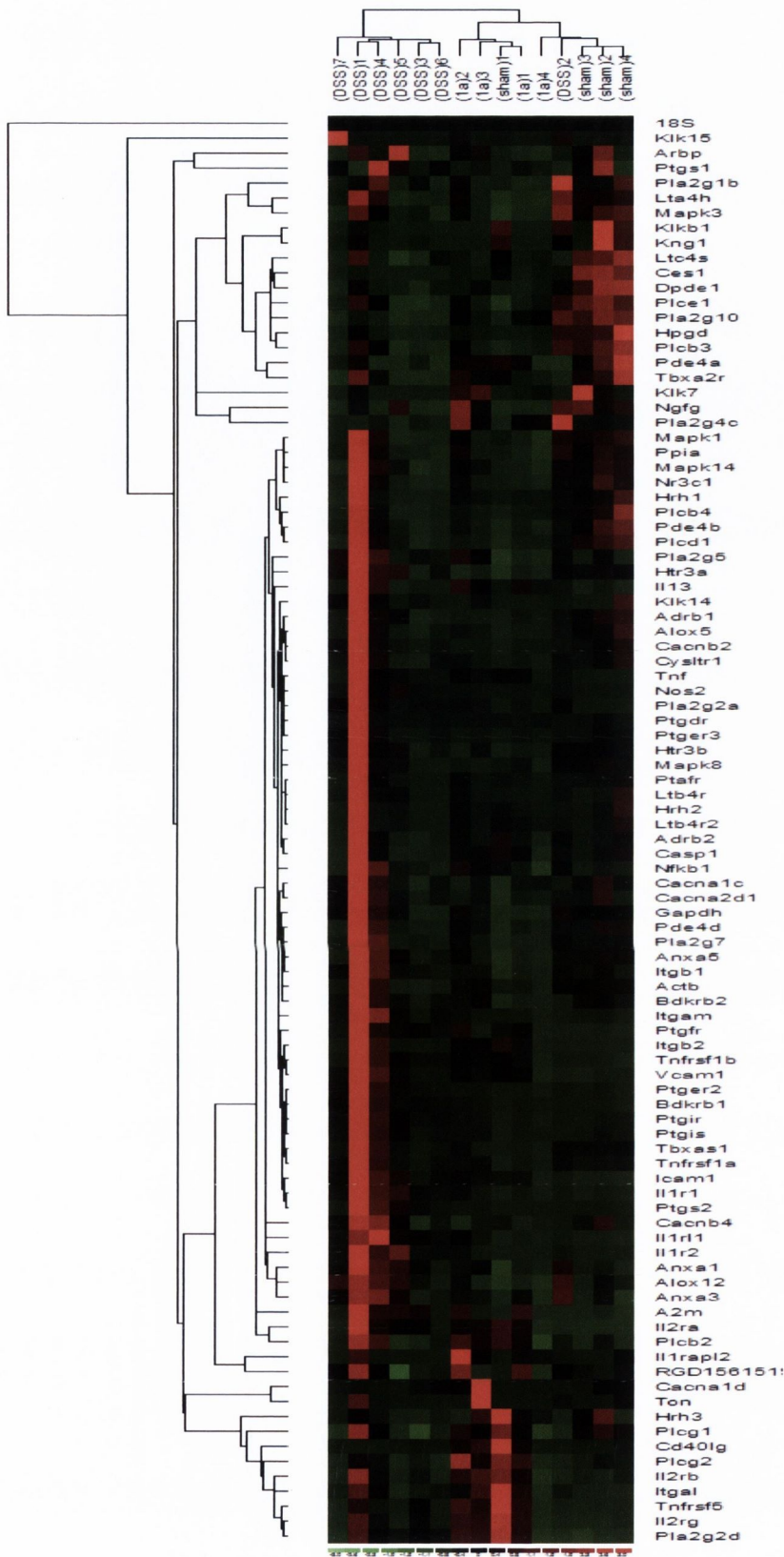


Figure 5.10: Heatmap of expression profiles of distal colon samples with clustering of samples and genes. The top of the heatmap shows the samples used in the inflammatory array and their clustering based on the gene expression profile. The side of the heatmap shows the clustering of the genes themselves and the intersection of a gene and sample on the map is given a colour to represent level of expression where the relative quantitation results are standardised for each row by subtracting the mean and dividing by the standard deviation.

Following relative quantitation, genes from the sham group and *Ia* treated groups that were up or downregulated more than two-fold relative to the representative DSS animal were assessed for common elements. This was carried out using the web-based Venn diagram software, Venny. The lists of the genes that met these criteria for each sample were added to the software which generates an oval or circle for each list. From the four animal samples analysed from the sham group, we can see that a total of 40 genes are commonly downregulated by two-fold or more in three or more of the samples. This is seen from areas of overlap of the ovals in Figure 5.11. This process was repeated for the *Ia* treated group and 46 genes were identified. These two lists were then cross-checked and 30 genes were identified as being commonly downregulated in both the sham group and *Ia* treated groups (Figure 5.11).



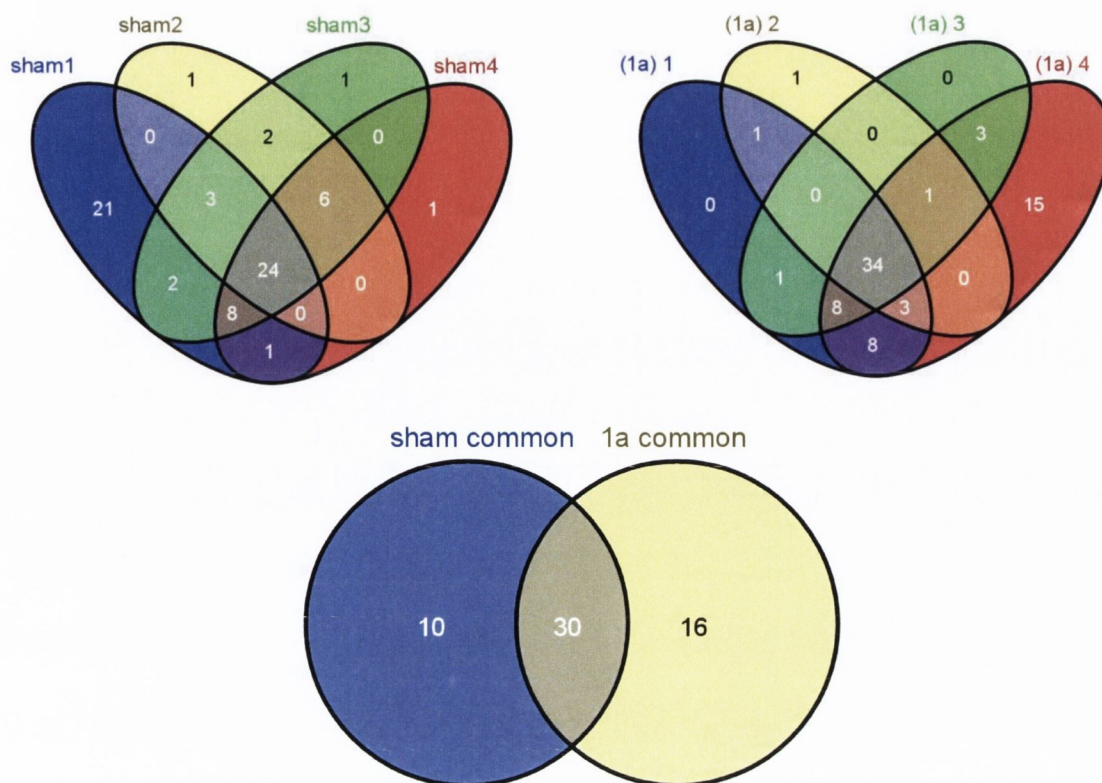


Figure 5.11: Venn diagrams of commonly downregulated genes. The number of genes that are greater than two fold downregulated relative to the DSS group are shown. Top left shows the number genes that meet this criterion for the four sham group animals, top right, the genes that meet the criterion for the four 1a treated animals and bottom shows the elements common to both groups. Sham(1-4) and 1a(1-4) represent animal samples that were tested in the inflammatory array. Areas of overlap indicate number of genes that are common to those animals/groups.

The process was repeated for commonly upregulated genes in the sham group and *1a* treated groups relative to the DSS group (Figure 5.12).

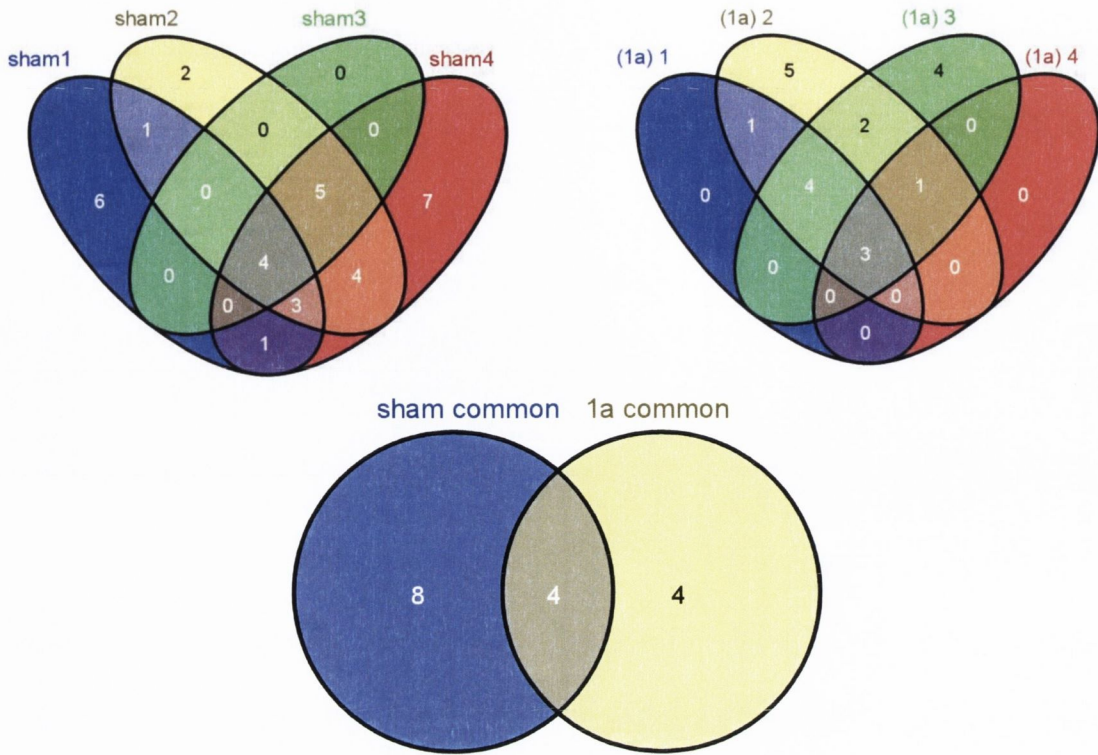


Figure 5.12: Venn diagrams of commonly upregulated genes. The number of genes that are greater than two fold upregulated relative to the DSS group are shown. Top left shows the number genes that meet this criterion for the four sham group animals, top right, the genes that meet the criterion for the four 1a treated animals and bottom shows the elements common to both groups. Sham(1-4) and 1a(1-4) represent animal samples that were tested in the inflammatory array. Areas of overlap indicate number of genes that are common to those animals/groups.

12 genes were found to be commonly upregulated in three or more of the sham group relative to the DSS group and 8 were found in the *1a* treated group. Of these, four genes were commonly upregulated in both groups as seen in the bottom Venn diagram of Figure 5.12.

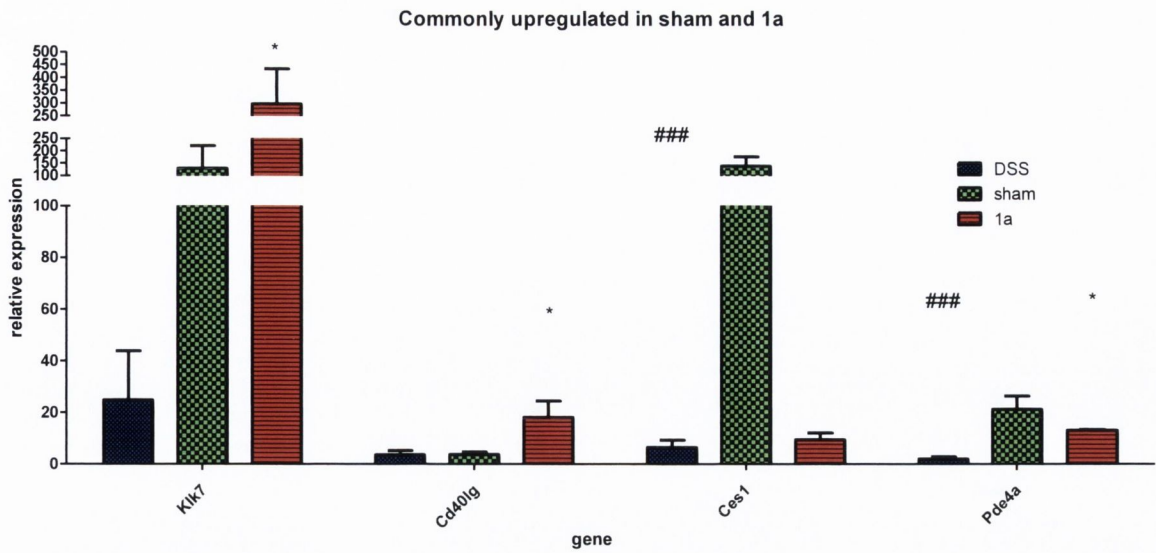


Figure 5.13: Relative quantitation of mRNA of genes commonly upregulated in the sham and *1a* treated group compared to the DSS group. RNA was isolated from distal colon samples of rats following sacrifice on day 5 of the experiment. RT-qPCR was performed on cDNA from reverse transcription of the isolated RNA. Relative expression is calculated by the  $2^{-(\Delta\Delta CT)}$  method with 18S as the endogenous control and a representative animal of the DSS group used as the calibrator.

Of the four genes that were commonly upregulated, KLK (kalikrein related peptidase) 7, CD40 ligand (CD40Lg) and PDE4a had statistically significant differences between the *1a* group and the DSS group whereas the *1a* group of carboxylesterase 1 (Ces1) was not statistically different from the DSS group.



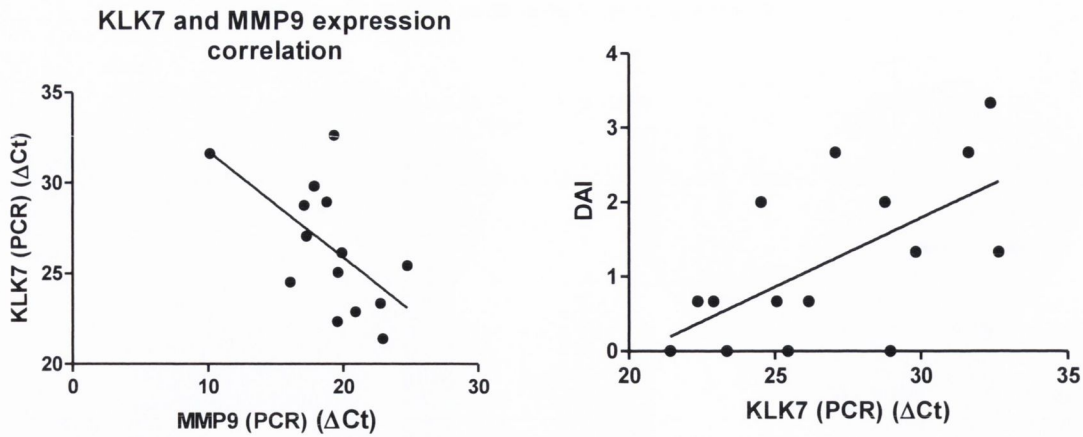


Figure 5.14: Correlation of  $\Delta C_T$  values of MMP-9 and KLK7 and KLK7  $\Delta C_T$  values with DAI score. Graphs show linear regression of  $\Delta C_T$  values of KLK7 and MMP-9 (left) and the DAI scores and KLK7  $\Delta C_T$  values. Correlations are based on 14 different animals where scores or  $\Delta C_T$  values are matched for the same animal.

Of the three genes that were significantly upregulated following *1a* treatment relative to the DSS group, KLK7 was the only one that statistically significantly correlated with MMP-9 expression across all groups ( $P = 0.025$ ,  $R^2 = 0.35$ ). This was a negative correlation where the lower the levels of MMP-9 mRNA, the higher the levels of KLK7 mRNA (Figure 5.14). KLK7  $\Delta C_T$  also correlated with the DAI score where increasing  $\Delta C_T$  values (lower levels of KLK7) correlated with higher DAI score ( $P = 0.01$ ,  $R^2 = 0.387$ ).

Commonly downregulated in sham and 1a

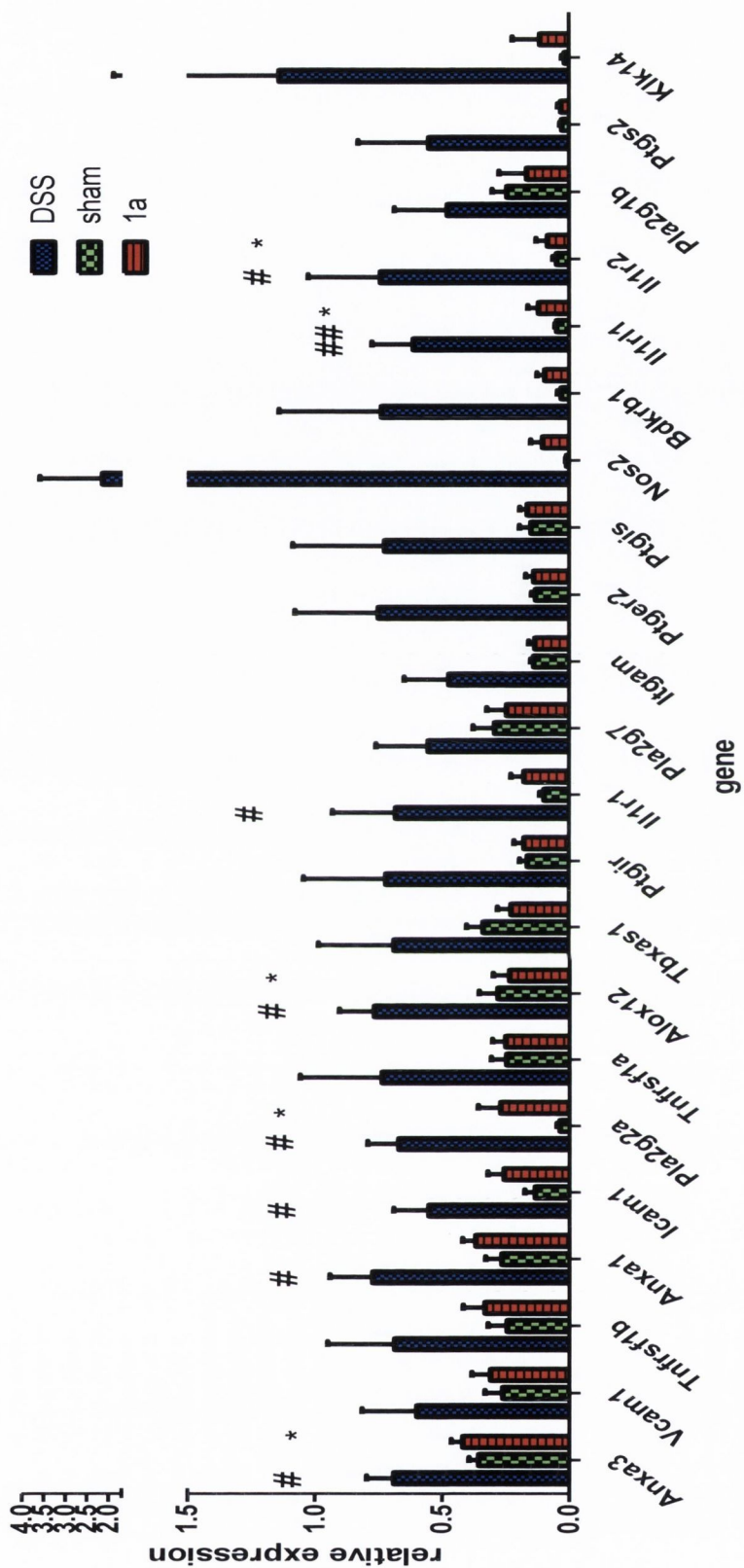


Figure 5.15: Relative quantitation of mRNA of genes commonly downregulated in the sham and 1a treated group compared to the DSS group. RNA was isolated from distal colon samples of rats following sacrifice on day 5 of the experiment. RT-qPCR was performed on cDNA from reverse transcription of the isolated RNA. Relative expression is calculated by the  $2^{-(\Delta\Delta CT)}$  method with 18S as the endogenous control and a representative animal of the DSS group used as the calibrator.

Of the 30 genes that were found to be commonly downregulated (Figure 5.11), the 22 with the greatest difference between the DSS group and the other groups are shown in Figure 5.15.

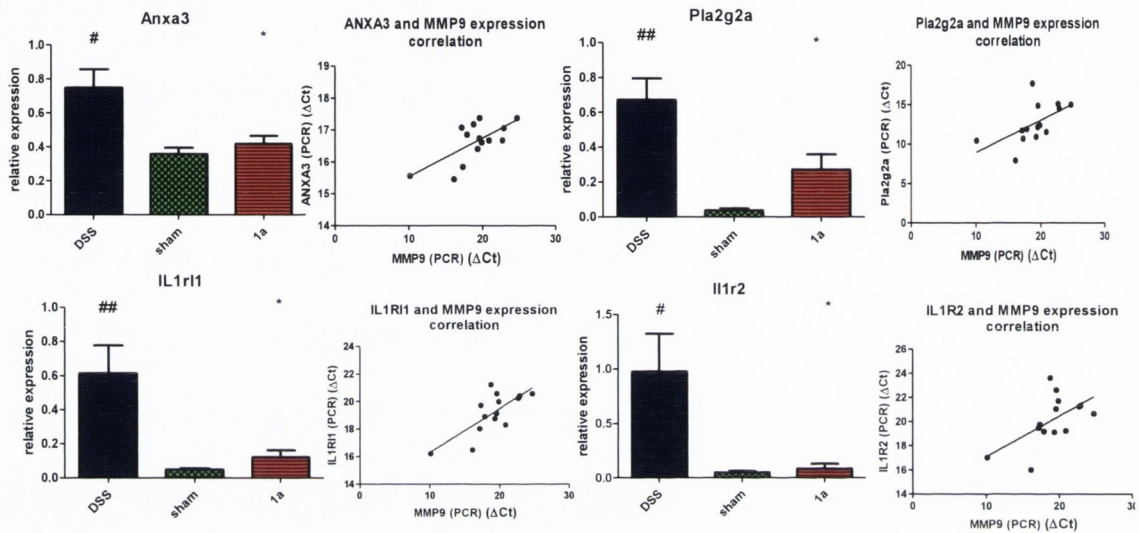


Figure 5.16: Graphs of genes where the 1a group is statistically significantly downregulated compared with the DSS group and correlation with MMP-9  $\Delta C_T$  value. Histograms and linear regression is shown for four genes; Anxa3 (top left), Pla2g2a (top right), IL1r1 (bottom left) and IL1r2 (bottom right). Histograms show relative expression calculated by the  $2^{-\Delta\Delta C_T}$  method following RNA isolation from the distal colon of rats sacrificed after 5 days of the experiment. Inflammatory array cards were performed on DNA converted from RNA by reverse transcription. Linear regression of  $\Delta C_T$  values for the four genes and MMP-9. Correlations are based on 14 different animals where  $\Delta C_T$  values are matched for the same animal

Of the 22 genes shown in Figure 5.15, 4 had statistically significant differences between the DSS and the 1a treated groups. All of these four genes positively correlated with MMP-9 expression; annexin A3 ( $P = 0.0067$ ,  $R^2 = 0.47$ ), phospholipase A2 group IIA ( $P = 0.032$ ,  $R^2 = 0.33$ ), interleukin 1 receptor-like 1 ( $P = 0.0025$ ,  $R^2 = 0.55$ ) and interleukin 1 receptor 2 ( $P = 0.0285$ ,  $R^2 = 0.34$ ). We have demonstrated that 1a can inhibit the expression of these inflammatory regulators and that the expression profiles correlate with that of MMP-9 but it has yet to be determined whether this is due to specific inhibition of



the transcription by the compounds, elements of signal transduction pathways that are responsible for the upregulation of these mediators are blocked, or whether blocking MMP-9 synthesis reduces overall inflammation in the gut and thus reducing the transcription of the other elements.

### 5.3. Discussion

IBD is a disease with significant quality of life and morbidity implications for patients. While aetiology has yet to be fully elucidated, significant progress has been made through the development of tens of different animal models where colitis is induced to mimic the features of UC and CD. This can be achieved quickly and easily in chemically induced models where a physical injury to the colon epithelium elicits an inflammatory response and with gene KO models where targeted deletion of certain genes can trigger an IBD phenotype. The type and range of KO models used is testament to the progress that has been made in the field where defects in innate and adaptive immune response or disruption of epithelial barrier integrity can all result in a colitic phenotype is in and of itself a significant discovery. Animal models have also shown us that genetic susceptibility on its own is not enough to trigger IBD and that environmental factors and gut bacteria play a crucial role in this complex disease. This has been demonstrated where antibiotics have been shown to be of some value in treating symptoms [191], that susceptible animals that are maintained germ free only develop colitis if commensal bacteria are reintroduced [192, 193] and that most models of IBD are likely to be driven by bacterial flora [536]. Animal models of colitis are commonly used in drug discovery and the DSS model of induced colitis in rats was chosen to study the effects of compound **1a**. It has previously been demonstrated that the zinc-chelator, phenanthroline, which inhibits MMPs, can reduce epithelial injury in this model [211] and the deficiency in MMP-9 can attenuate DSS induced colitis in mice [416]. This evidence for the crucial role of MMP-9 in the development of colitis in the DSS model made it ideal for studying the effects of our MMP-9 inhibitor compound.

It was clear from the DAI scoring that **1a** reduced the severity of the clinical features of the DSS induced colitis including diarrhoea and rectal bleed which developed in the DSS group. The alcohol-barbiturate equivalent **2a** also had a protective role and statistically significantly reduced the DAI score by day 5. The nitrate-side chain **3a** showed no statistically significant difference from the DSS group although the group had a lower mean DAI score. It is interesting that replacement of the alcohol with the nitrate group improves the efficacy of the compound and a similar trend was observed in the reduction of MMP-9 activity and expression in our *in-vitro* model. Clear visual evidence for the protective effect of **1a** is shown in Figure 5.3 which is converted to scores and graphed in Figure 5.4. This shows the ability of the compound to reduce crypt shortening and surface epithelial stripping as well as enlargement of the lamina and infiltration of inflammatory cells.

Inhibition of MMP-9 expression and activity in the distal colon follow similar trends to that of the DAI score (Figure 5.6). **1a** statistically significantly reduced both MMP-9 expression and activity in the distal colon where the other treatments did not. While both **2a** and **3a** showed trends towards reduction, they could not inhibit to the same extent and the nitrate-barbiturates effect on MMP-9 transcription does appear to be mediated by contributions from both component parts. MMP-9 expression levels also correlated well with both the DAI score and the histological measures of inflammation which is further evidence for the pivotal role of the protease in mediating DSS induced colitis and the benefits of its inhibition.

Initial analysis of the TaqMan inflammatory array results in Figure 5.9 and Figure 5.10 show that the expression profiles of all but one of the DSS group cluster together whereas the sham and **1a** treated group are clustered together which is evidence in and of itself of the ability of the inhibitor to attenuate the induced colitis. Relative quantitation and



analysis of the commonly up or downregulated genes in the sham and *Ia* groups yielded some interesting results. Some of these results are difficult to interpret as the genes upregulated in the sham and *Ia* treated group are considered pro-inflammatory. KLK 7 is a serine protease whose main function is understood to be in skin homeostasis. Although limited study has been carried out on its role in the gut, it has been shown to be associated with poor prognosis in colon cancer [537, 538]. CD40Lg is associated with IBD where it is transcriptionally upregulated in activated platelets and T-cells and can trigger a proinflammatory response through binding to CD40 [539]. PDE4a inhibition is believed to be anti-inflammatory and is being investigated as a possible treatment for respiratory disorders and other inflammatory conditions [540, 541]. This phosphodiesterase is specific for cAMP which it regulates through hydrolysis and thus preventing its activation of downstream mediators such as PKA. It is interesting to note that although targeted inhibition of PDE4 would seem to be anti-inflammatory, PKA has been implicated in the upregulation of MMP-9 [452]. This array of genes is extremely interesting and their upregulation seems, on the surface, paradoxical and certainly warrants further exploration. It is also interesting to note that neither PDE4a nor CD40Lg expression levels correlate with MMP-9 expression, but MMP-9 expression does correlate negatively with KLK7 expression. Decreasing synthesis of MMP-9 is associated with reduced severity of colitis (Figure 5.7) and this reduced severity is also associated with increasing expression of KLK7 (Figure 5.14).

The selection of genes commonly downregulated in the sham and *Ia* groups are shown in Figure 5.15. Annexin A1 has been shown to be upregulated in IBD and is known for its anti-inflammatory effects and promotes mucosal homeostasis [542]. Its downregulation in the *Ia* group is a result of decreased overall inflammation and thus prevention of its upregulation. The figure features a range of other pro-inflammatory mediators, including

adhesion molecules, cytokine receptors, mediators of the arachidonic acid pathway and prostaglandin receptors. Of those, annexin A3, phospholipase A2 (PLA2) group IIA, interleukin 1 receptor-like 1 and interleukin 1 receptor 2 had a statistically significant inhibition by *Ia*. Phospholipase A2 is involved in the production of prostaglandins, leukotriens and thromboxanes by hydrolysing phospholipids to release arachidonic acid. This family of enzymes, including group IIA are known to be upregulated in IBD and correlate with the severity of the disease [543-545]. A group has shown that a specific inhibitor of PLA2 group IIA can protect rats from DSS induced colitis [546] and similar results are seen in the TNBS model [547, 548], confirming the pro-inflammatory role of the gene. Annexin A3 is a known inhibitor of phospholipase A2 [549] and is upregulated in an inflammatory setting without itself mediating the inflammation. Prostaglandin endoperoxide synthase 2 (PTGS2)/cyclooxygenase (COX) 2, PLA2G7, arachidonate 12 lipoxygenase (ALOX12), and thromboxane A synthase 1 (TBXAS1) are all involved in the production of proinflammatory mediators from the arachidonic acid pathway and these as well as the prostaglandin receptors prostaglandin I2 receptor (Ptgir) and prostaglandin E receptor 2 (Ptger2), which mediate the response, were all commonly regulated in the *Ia* and sham groups but the difference between *Ia* and the DSS control did not reach statistical significance with the samples used.

The other two genes that were statistically significantly different in the *Ia* group were both cytokine receptors. IL1RL1, which is also known as ST-2, is expressed on macrophages, mast cells, Th2 cells and colonic epithelial cells and when stimulated, can activate MAPKs but inhibit NF- $\kappa$ B signalling, resulting in a dominant Th2 and not Th1 type response through inhibition of IL1R1 response [550]. The ligand for ST-2 is IL-33 and several lines of evidence point to this pathway being a desirable drug target in IBD [551]. Both IL-33 and ST-2 are upregulated in IBD patients [552, 553] as was seen in our animal model. A



recent study on the blocking of this pathway in animal models using gene knock outs or an anti-ST-2 antibody found that blocking of IL-33/ST-2 signalling attenuates colitis in animals including the DSS model [554]. Inhibition of the transcriptional upregulation of this receptor could represent a novel mechanism of action of **Ia**. IL1R2 (interleukin-1 receptor type II) is a receptor for IL-1 $\alpha$  and  $\beta$  and acts as a dummy receptor to prevent these ligands binding to IL1R1 and triggering an inflammatory response. Polymorphisms in the IL1R2 gene is associated with UC [555] and the expression profile of the receptor is independently and accurately associated with mucosal healing in UC with potential as a biomarker [556]. The transcriptional upregulation of this receptor is believed to be the mechanism of action of the anti-inflammatory cytokine IL4 but despite its association with UC, a functional analysis in animal models of IBD could not be found.

The gene expression profiling identified a number of interesting genes that the dinitrate-barbiturate compound **Ia** inhibits in DSS induced colitis. Perhaps of particular interest are PLA2G2 and IL1RL1 which are known to contribute to inflammation in IBD but without an exact mechanism. It is also interesting that the serine protease KLK7 expression negatively correlates with DAI score and may play a protective role during colitis. Despite the 4 genes that are downregulated by **Ia** correlating with MMP-9 expression, it is unknown whether this is a cause of the targeted inhibition of all targets separately, together, or whether an inhibition of MMP-9 reduces the signals leading to upregulation of the other genes. Further studies to elucidate the time points of upregulation of these mediators and the exact role **Ia** plays needs to be carried out.

We can conclude from the *in-vivo* experiments carried out, that the dinitrate-barbiturate compound **Ia** is effective in preventing DSS-induced colitis in rats as it can inhibit both MMP-9 activity and gene expression. This effect correlates well with a reduction of the



DAI score and histological measures of inflammation. In addition, MMP-9 inhibition was also correlated with the inhibition of other inflammatory mediators in the distal colon.

## **Chapter 6: Future directions**

## 6. Future directions

There are several areas of the project where I envisage work being done in the future.

The effect of the compounds in inhibiting MMP-9 has been demonstrated but I feel that it would be worthwhile to explore the selectivity of the compounds for this enzyme over the other MMPs. Our group has previously demonstrated that some of the nitrate compounds are selective for MMP-9 over MMP-2 which was measured using recombinant enzymes [315]. We have already begun preliminary investigations into the effect of our compounds on the protein levels of MMP-1, -2, -3, -9 and -10 using Multiplex ELISA kits from MSD. These results will provide accurate information on the levels of these MMPs released from Caco-2 cells in response to the pro-inflammatory cytokines and the effect of the compounds. Protein levels from the ELISA can be combined with qPCR to discover if the effect that the compounds demonstrate at gene level is specific to MMP-9, or more general pro-inflammatory signalling inhibition.

We have demonstrated the involvement of the sGC/cGMP pathway in the inhibition of MMP-9 gene transcription but it would be interesting to further develop the mechanism through which the compounds exert their effect. PKG is the primary downstream signalling molecule of cGMP and a co-incubation experiment with the compounds and an inhibitor of PKG such as DT-2 would reveal its involvement. The involvement of other signalling molecules such as the MAPKs would also be interesting to ascertain, or indeed, the effects of the compounds on MMP-9 mRNA stability and HuR or AUF-1 levels would prove a novel mechanism of action. The specific role of the nitrate in the nitrate-barbiturate mediated inhibition can be further clarified through comparing the results of the experiments described to the alcohol-barbiturates. Having speculated that the effect of the



nitrate-barbiturates is a sum of the alcohol-barbiturate and the nitrate side-chain effects, it would be interesting to test if the combination of the two component parts of the molecule would be as effective as the hybrid molecule, and if not, it may reveal properties that are specific to the hybrid.

The *in-vivo* studies demonstrated the efficacy of the dinitrate-barbiturate in the DSS-induced colitis model when administered by rectal enema. Earlier pilot studies showed that compound *Ic* at 10mg/kg was toxic to mice when administered by oral gavage in the DSS model and resulted in the fatal hepatotoxicity in some cases. In the same model, compound *Ie* given twice daily at 1mg/kg had no effect. In the interest of drug development, it would be important to determine a safe and effective oral dose for *Ia* and to develop a full pharmacokinetic profile for the drug. While DSS induced colitis was an effective model for studying MMP-9 inhibition, studying the effects of the compounds in other *in-vivo* models would be essential in assessing their potential efficacy in treating human IBD.

The results of the TLDA experiment showed us other inflammatory mediators that were affected by the addition of the compound. It will be extremely interesting to evaluate whether the changes in these mediators are as a consequence of MMP-9 inhibition or if the compounds directly affect them causing a reduction in inflammation and thus a reduction in MMP-9. These questions can first be addressed in a cell culture model with extraction of mRNA and conditioned media at various time points over the experiment to discover proteins whose gene expression are first altered.

## Chapter 7: References

## 7. References

- [1] M. Egeblad, Z. Werb, New functions for the matrix metalloproteinases in cancer progression, *Nat Rev Cancer*, 2 (2002) 161-174.
- [2] Z.S. Galis, J.J. Khatri, Matrix metalloproteinases in vascular remodeling and atherogenesis: the good, the bad, and the ugly, *Circ Res*, 90 (2002) 251-262.
- [3] I. Stamenkovic, Matrix metalloproteinases in tumor invasion and metastasis, *Semin Cancer Biol*, 10 (2000) 415-433.
- [4] F.G. Spinale, Matrix metalloproteinases: regulation and dysregulation in the failing heart, *Circ Res*, 90 (2002) 520-530.
- [5] M. Bjorklund, E. Koivunen, Gelatinase-mediated migration and invasion of cancer cells, *Biochim Biophys Acta*, 1755 (2005) 37-69.
- [6] W.C. Parks, S.D. Shapiro, Matrix metalloproteinases in lung biology, *Respir Res*, 2 (2001) 10-19.
- [7] J. Gross, C.M. Lapiere, Collagenolytic activity in amphibian tissues: a tissue culture assay, *Proc Natl Acad Sci U S A*, 48 (1962) 1014-1022.
- [8] C.M. Overall, C. Lopez-Otin, Strategies for MMP inhibition in cancer: innovations for the post-trial era, *Nat Rev Cancer*, 2 (2002) 657-672.
- [9] C. Andreini, L. Banci, I. Bertini, C. Luchinat, A. Rosato, Bioinformatic comparison of structures and homology-models of matrix metalloproteinases, *J Proteome Res*, 3 (2004) 21-31.
- [10] K.A. Szabo, R.J. Ablin, G. Singh, Matrix metalloproteinases and the immune response, *Clinical and Applied Immunology Reviews*, 4 (2004) 295-319.
- [11] M.D. Sternlicht, Z. Werb, How matrix metalloproteinases regulate cell behavior, *Annu Rev Cell Dev Biol*, 17 (2001) 463-516.
- [12] M.M. Handsley, D.R. Edwards, Metalloproteinases and their inhibitors in tumor angiogenesis, *Int J Cancer*, 115 (2005) 849-860.
- [13] G. Murphy, V. Knauper, Relating matrix metalloproteinase structure to function: why the "hemopexin" domain?, *Matrix Biol*, 15 (1997) 511-518.
- [14] H. Sato, T. Takino, Y. Okada, J. Cao, A. Shinagawa, E. Yamamoto, M. Seiki, A matrix metalloproteinase expressed on the surface of invasive tumour cells, *Nature*, 370 (1994) 61-65.
- [15] Y. Itoh, M. Kajita, H. Kinoh, H. Mori, A. Okada, M. Seiki, Membrane type 4 matrix metalloproteinase (MT4-MMP, MMP-17) is a glycosylphosphatidylinositol-anchored proteinase, *J Biol Chem*, 274 (1999) 34260-34266.
- [16] S. Kojima, Y. Itoh, S. Matsumoto, Y. Masuho, M. Seiki, Membrane-type 6 matrix metalloproteinase (MT6-MMP, MMP-25) is the second glycosyl-phosphatidyl inositol (GPI)-anchored MMP, *FEBS Lett*, 480 (2000) 142-146.
- [17] E.B. Springman, E.L. Angleton, H. Birkedal-Hansen, H.E. Van Wart, Multiple modes of activation of latent human fibroblast collagenase: evidence for the role of a Cys73 active-site zinc complex in latency and a "cysteine switch" mechanism for activation, *Proc Natl Acad Sci U S A*, 87 (1990) 364-368.
- [18] H.E. Van Wart, H. Birkedal-Hansen, The cysteine switch: a principle of regulation of metalloproteinase activity with potential applicability to the entire matrix metalloproteinase gene family, *Proc Natl Acad Sci U S A*, 87 (1990) 5578-5582.



- [19] H. Nagase, J.F. Woessner, Jr., Matrix metalloproteinases, *J Biol Chem*, 274 (1999) 21491-21494.
- [20] W. Bode, F.X. Gomis-Ruth, W. Stockler, Astacins, serralysins, snake venom and matrix metalloproteinases exhibit identical zinc-binding environments (HEXXHXXGXXH and Met-turn) and topologies and should be grouped into a common family, the 'metzincins', *FEBS Lett*, 331 (1993) 134-140.
- [21] G.S. Butler, E.M. Tam, C.M. Overall, The canonical methionine 392 of matrix metalloproteinase 2 (gelatinase A) is not required for catalytic efficiency or structural integrity: probing the role of the methionine-turn in the metzincin metalloprotease superfamily, *J Biol Chem*, 279 (2004) 15615-15620.
- [22] W. Stocker, F. Grams, U. Baumann, P. Reinemer, F.X. Gomis-Ruth, D.B. McKay, W. Bode, The metzincins--topological and sequential relations between the astacins, adamalysins, serralysins, and matrixins (collagenases) define a superfamily of zinc-peptidases, *Protein Sci*, 4 (1995) 823-840.
- [23] V. Dhanaraj, Q.Z. Ye, L.L. Johnson, D.J. Hupe, D.F. Ortwine, J.B. Dunbar, Jr., J.R. Rubin, A. Pavlovsky, C. Humblet, T.L. Blundell, X-ray structure of a hydroxamate inhibitor complex of stromelysin catalytic domain and its comparison with members of the zinc metalloproteinase superfamily, *Structure*, 4 (1996) 375-386.
- [24] C.H. Bu, T. Pourmotabbed, Mechanism of Ca<sup>2+</sup>-dependent activity of human neutrophil gelatinase B, *J Biol Chem*, 271 (1996) 14308-14315.
- [25] L. Aureli, M. Gioia, I. Cerbara, S. Monaco, G.F. Fasciglione, S. Marini, P. Ascenzi, A. Topai, M. Coletta, Structural bases for substrate and inhibitor recognition by matrix metalloproteinases, *Curr Med Chem*, 15 (2008) 2192-2222.
- [26] M.F. Browner, W.W. Smith, A.L. Castelhana, Matrilysin-inhibitor complexes: common themes among metalloproteases, *Biochemistry*, 34 (1995) 6602-6610.
- [27] C.M. Overall, Matrix metalloproteinase substrate binding domains, modules and exosites. Overview and experimental strategies, *Methods Mol Biol*, 151 (2001) 79-120.
- [28] S.J. De Souza, H.M. Pereira, S. Jacchieri, R.R. Brentani, Collagen/collagenase interaction: does the enzyme mimic the conformation of its own substrate?, *FASEB J*, 10 (1996) 927-930.
- [29] V. Knäuper, A.J.P. Docherty, B. Smith, H. Tschesche, G. Murphy, Analysis of the contribution of the hinge region of human neutrophil collagenase (HNC, MMP-8) to stability and collagenolytic activity by alanine scanning mutagenesis, *FEBS Letters*, 405 (1997) 60-64.
- [30] P. Osenkowski, S.O. Meroueh, D. Pavel, S. Mobashery, R. Fridman, Mutational and structural analyses of the hinge region of membrane type 1-matrix metalloproteinase and enzyme processing, *J Biol Chem*, 280 (2005) 26160-26168.
- [31] E. Roeb, K. Schleinkofer, T. Kernebeck, S. Potsch, B. Jansen, I. Behrmann, S. Matern, J. Grotzinger, The matrix metalloproteinase 9 (mmp-9) hemopexin domain is a novel gelatin binding domain and acts as an antagonist, *J Biol Chem*, 277 (2002) 50326-50332.
- [32] R. Sanchez-Lopez, C.M. Alexander, O. Behrendtsen, R. Breathnach, Z. Werb, Role of zinc-binding- and hemopexin domain-encoded sequences in the substrate specificity of collagenase and stromelysin-2 as revealed by chimeric proteins, *J Biol Chem*, 268 (1993) 7238-7247.
- [33] G. Murphy, J.A. Allan, F. Willenbrock, M.I. Cockett, J.P. O'Connell, A.J. Docherty, The role of the C-terminal domain in collagenase and stromelysin specificity, *J Biol Chem*, 267 (1992) 9612-9618.
- [34] K.B. Taylor, L.J. Windsor, N.C. Caterina, M.K. Bodden, J.A. Engler, The mechanism of inhibition of collagenase by TIMP-1, *J Biol Chem*, 271 (1996) 23938-23945.



- [35] J. Redondo-Munoz, E. Ugarte-Berzal, M.J. Terol, P.E. Van den Steen, M. Hernandez del Cerro, M. Roderfeld, E. Roeb, G. Opdenakker, J.A. Garcia-Marco, A. Garcia-Pardo, Matrix metalloproteinase-9 promotes chronic lymphocytic leukemia b cell survival through its hemopexin domain, *Cancer Cell*, 17 (2010) 160-172.
- [36] J. Vandooren, P.E. Van den Steen, G. Opdenakker, Biochemistry and molecular biology of gelatinase B or matrix metalloproteinase-9 (MMP-9): the next decade, *Crit Rev Biochem Mol Biol*, 48 (2013) 222-272.
- [37] J. Hu, P.E. Van den Steen, Q.X. Sang, G. Opdenakker, Matrix metalloproteinase inhibitors as therapy for inflammatory and vascular diseases, *Nat Rev Drug Discov*, 6 (2007) 480-498.
- [38] P.E. Van den Steen, B. Dubois, I. Nelissen, P.M. Rudd, R.A. Dwek, G. Opdenakker, Biochemistry and molecular biology of gelatinase B or matrix metalloproteinase-9 (MMP-9), *Crit Rev Biochem Mol Biol*, 37 (2002) 375-536.
- [39] G. Opdenakker, P.E. Van den Steen, J. Van Damme, Gelatinase B: a tuner and amplifier of immune functions, *Trends Immunol*, 22 (2001) 571-579.
- [40] M. Chabaud, J.M. Durand, N. Buchs, F. Fossiez, G. Page, L. Frappart, P. Miossec, Human interleukin-17: A T cell-derived proinflammatory cytokine produced by the rheumatoid synovium, *Arthritis Rheum*, 42 (1999) 963-970.
- [41] R.N. Johnatty, D.D. Taub, S.P. Reeder, S.M. Turcovski-Corrales, D.W. Cottam, T.J. Stephenson, R.C. Rees, Cytokine and chemokine regulation of proMMP-9 and TIMP-1 production by human peripheral blood lymphocytes, *J Immunol*, 158 (1997) 2327-2333.
- [42] S. Caudroy, M. Polette, B. Nawrocki-Raby, J. Cao, B.P. Toole, S. Zucker, P. Birembaut, EMMPRIN-mediated MMP regulation in tumor and endothelial cells, *Clin Exp Metastasis*, 19 (2002) 697-702.
- [43] D.L. Crowe, C.F. Shuler, Regulation of tumor cell invasion by extracellular matrix, *Histol Histopathol*, 14 (1999) 665-671.
- [44] F. Aoudjit, E.F. Potworowski, Y. St-Pierre, Bi-directional induction of matrix metalloproteinase-9 and tissue inhibitor of matrix metalloproteinase-1 during T lymphoma/endothelial cell contact: implication of ICAM-1, *J Immunol*, 160 (1998) 2967-2973.
- [45] A.M. Romanic, J.A. Madri, The induction of 72-kD gelatinase in T cells upon adhesion to endothelial cells is VCAM-1 dependent, *J Cell Biol*, 125 (1994) 1165-1178.
- [46] N. Malik, B.W. Greenfield, A.F. Wahl, P.A. Kiener, Activation of human monocytes through CD40 induces matrix metalloproteinases, *J Immunol*, 156 (1996) 3952-3960.
- [47] M.P. Vincenti, C.E. Brinckerhoff, Signal transduction and cell-type specific regulation of matrix metalloproteinase gene expression: can MMPs be good for you?, *J Cell Physiol*, 213 (2007) 355-364.
- [48] L.G. Hudson, N.M. Moss, M.S. Stack, EGF-receptor regulation of matrix metalloproteinases in epithelial ovarian carcinoma, *Future Oncol*, 5 (2009) 323-338.
- [49] S. Masure, P. Proost, J. Van Damme, G. Opdenakker, Purification and identification of 91-kDa neutrophil gelatinase. Release by the activating peptide interleukin-8, *Eur J Biochem*, 198 (1991) 391-398.
- [50] S.L. Raza, L.C. Nehring, S.D. Shapiro, L.A. Cornelius, Proteinase-activated receptor-1 regulation of macrophage elastase (MMP-12) secretion by serine proteinases, *J Biol Chem*, 275 (2000) 41243-41250.
- [51] J.W. Becker, A.I. Marcy, L.L. Rokosz, M.G. Axel, J.J. Burbaum, P.M. Fitzgerald, P.M. Cameron, C.K. Esser, W.K. Hagmann, J.D. Hermes, et al., Stromelysin-1: three-dimensional structure of the inhibited catalytic domain and of the C-truncated proenzyme, *Protein Sci*, 4 (1995) 1966-1976.



- [52] V. Ellis, Plasminogen activation at the cell surface, *Curr Top Dev Biol*, 54 (2003) 263-312.
- [53] G.A. Bannikov, T.V. Karelina, I.E. Collier, B.L. Marmer, G.I. Goldberg, Substrate binding of gelatinase B induces its enzymatic activity in the presence of intact propeptide, *J Biol Chem*, 277 (2002) 16022-16027.
- [54] G.J. Peppin, S.J. Weiss, Activation of the endogenous metalloproteinase, gelatinase, by triggered human neutrophils, *Proc Natl Acad Sci U S A*, 83 (1986) 4322-4326.
- [55] Z. Gu, M. Kaul, B. Yan, S.J. Kridel, J. Cui, A. Strongin, J.W. Smith, R.C. Liddington, S.A. Lipton, S-nitrosylation of matrix metalloproteinases: signaling pathway to neuronal cell death, *Science*, 297 (2002) 1186-1190.
- [56] B. Paquette, M. Bisson, H. Therriault, R. Lemay, M. Paré, P. Banville, A.M. Cantin, Activation of matrix metalloproteinase-2 and -9 by 2- and 4-hydroxyestradiol, *The Journal of Steroid Biochemistry and Molecular Biology*, 87 (2003) 65-73.
- [57] H. Sato, T. Kinoshita, T. Takino, K. Nakayama, M. Seiki, Activation of a recombinant membrane type 1-matrix metalloproteinase (MT1-MMP) by furin and its interaction with tissue inhibitor of metalloproteinases (TIMP)-2, *FEBS Lett*, 393 (1996) 101-104.
- [58] I. Yana, S.J. Weiss, Regulation of membrane type-1 matrix metalloproteinase activation by proprotein convertases, *Mol Biol Cell*, 11 (2000) 2387-2401.
- [59] R. Fridman, M. Toth, I. Chvyrkova, S.O. Meroueh, S. Mobashery, Cell surface association of matrix metalloproteinase-9 (gelatinase B), *Cancer Metastasis Rev*, 22 (2003) 153-166.
- [60] A.Y. Strongin, I. Collier, G. Bannikov, B.L. Marmer, G.A. Grant, G.I. Goldberg, Mechanism of cell surface activation of 72-kDa type IV collagenase. Isolation of the activated form of the membrane metalloprotease, *J Biol Chem*, 270 (1995) 5331-5338.
- [61] E. Morgunova, A. Tuuttila, U. Bergmann, M. Isupov, Y. Lindqvist, G. Schneider, K. Tryggvason, Structure of human pro-matrix metalloproteinase-2: activation mechanism revealed, *Science*, 284 (1999) 1667-1670.
- [62] G. Murphy, T. Crabbe, Gelatinases A and B, *Methods Enzymol*, 248 (1995) 470-484.
- [63] Y. He, X.D. Liu, Z.Y. Chen, J. Zhu, Y. Xiong, K. Li, J.H. Dong, X. Li, Interaction between cancer cells and stromal fibroblasts is required for activation of the uPAR-uPA-MMP-2 cascade in pancreatic cancer metastasis, *Clin Cancer Res*, 13 (2007) 3115-3124.
- [64] C. Legrand, M. Polette, J.M. Tournier, S. de Bentzmann, E. Huet, M. Monteau, P. Birembaut, uPA/plasmin system-mediated MMP-9 activation is implicated in bronchial epithelial cell migration, *Exp Cell Res*, 264 (2001) 326-336.
- [65] H. Gotoh, H. Yamada, Y. Yoshihara, T. Kikuchi, K. Obata, M. Shinmei, [Levels of matrix metalloproteinase-3 and urokinase-type plasminogen activator in knee synovial fluids from patients with rheumatoid arthritis and osteoarthritis], *Ryumachi*, 37 (1997) 3-8.
- [66] K.S. Kim, Y.A. Lee, H.M. Choi, M.C. Yoo, H.I. Yang, Implication of MMP-9 and urokinase plasminogen activator (uPA) in the activation of pro-matrix metalloproteinase (MMP)-13, *Rheumatol Int*, 32 (2012) 3069-3075.
- [67] E. Hahn-Dantona, N. Ramos-DeSimone, J. Siple, H. Nagase, D.L. French, J.P. Quigley, Activation of proMMP-9 by a plasmin/MMP-3 cascade in a tumor cell model. Regulation by tissue inhibitors of metalloproteinases, *Ann N Y Acad Sci*, 878 (1999) 372-387.
- [68] A.R. Radjabi, K. Sawada, S. Jagadeeswaran, A. Eichbichler, H.A. Kenny, A. Montag, K. Bruno, E. Lengyel, Thrombin induces tumor invasion through the induction and association of matrix metalloproteinase-9 and beta1-integrin on the cell surface, *J Biol Chem*, 283 (2008) 2822-2834.



- [69] L. Sottrup-Jensen, H. Birkedal-Hansen, Human fibroblast collagenase-alpha-macroglobulin interactions. Localization of cleavage sites in the bait regions of five mammalian alpha-macroglobulins, *J Biol Chem*, 264 (1989) 393-401.
- [70] G.S. Salvesen, C.A. Sayers, A.J. Barrett, Further characterization of the covalent linking reaction of alpha 2-macroglobulin, *Biochem J*, 195 (1981) 453-461.
- [71] S.K. Moestrup, T.L. Holtet, M. Etzerodt, H.C. Thogersen, A. Nykjaer, P.A. Andreasen, H.H. Rasmussen, L. Sottrup-Jensen, J. Gliemann, Alpha 2-macroglobulin-proteinase complexes, plasminogen activator inhibitor type-1-plasminogen activator complexes, and receptor-associated protein bind to a region of the alpha 2-macroglobulin receptor containing a cluster of eight complement-type repeats, *J Biol Chem*, 268 (1993) 13691-13696.
- [72] R.A. Williamson, F.A. Marston, S. Angal, P. Koklitis, M. Panico, H.R. Morris, A.F. Carne, B.J. Smith, T.J. Harris, R.B. Freedman, Disulphide bond assignment in human tissue inhibitor of metalloproteinases (TIMP), *Biochem J*, 268 (1990) 267-274.
- [73] D.E. Gomez, D.F. Alonso, H. Yoshiji, U.P. Thorgeirsson, Tissue inhibitors of metalloproteinases: structure, regulation and biological functions, *Eur J Cell Biol*, 74 (1997) 111-122.
- [74] G. Murphy, A. Houbrechts, M.I. Cockett, R.A. Williamson, M. O'Shea, A.J. Docherty, The N-terminal domain of tissue inhibitor of metalloproteinases retains metalloproteinase inhibitory activity, *Biochemistry*, 30 (1991) 8097-8102.
- [75] F. Willenbrock, G. Murphy, Structure-function relationships in the tissue inhibitors of metalloproteinases, *Am J Respir Crit Care Med*, 150 (1994) S165-170.
- [76] J.P. O'Connell, F. Willenbrock, A.J. Docherty, D. Eaton, G. Murphy, Analysis of the role of the COOH-terminal domain in the activation, proteolytic activity, and tissue inhibitor of metalloproteinase interactions of gelatinase B, *J Biol Chem*, 269 (1994) 14967-14973.
- [77] M.W. Olson, D.C. Gervasi, S. Mobashery, R. Fridman, Kinetic analysis of the binding of human matrix metalloproteinase-2 and -9 to tissue inhibitor of metalloproteinase (TIMP)-1 and TIMP-2, *J Biol Chem*, 272 (1997) 29975-29983.
- [78] Z. Wang, R. Juttermann, P.D. Soloway, TIMP-2 is required for efficient activation of proMMP-2 in vivo, *J Biol Chem*, 275 (2000) 26411-26415.
- [79] Y. Jiang, M. Wang, M.Y. Celiker, Y.E. Liu, Q.X. Sang, I.D. Goldberg, Y.E. Shi, Stimulation of mammary tumorigenesis by systemic tissue inhibitor of matrix metalloproteinase 4 gene delivery, *Cancer Res*, 61 (2001) 2365-2370.
- [80] D.W. Seo, H. Li, L. Guedez, P.T. Wingfield, T. Diaz, R. Salloum, B.Y. Wei, W.G. Stetler-Stevenson, TIMP-2 mediated inhibition of angiogenesis: an MMP-independent mechanism, *Cell*, 114 (2003) 171-180.
- [81] J.H. Qi, Q. Ebrahim, N. Moore, G. Murphy, L. Claesson-Welsh, M. Bond, A. Baker, B. Anand-Apte, A novel function for tissue inhibitor of metalloproteinases-3 (TIMP3): inhibition of angiogenesis by blockage of VEGF binding to VEGF receptor-2, *Nat Med*, 9 (2003) 407-415.
- [82] N. Boujrad, S.O. Ogwuegbu, M. Garnier, C.H. Lee, B.M. Martin, V. Papadopoulos, Identification of a stimulator of steroid hormone synthesis isolated from testis, *Science*, 268 (1995) 1609-1612.
- [83] A. Amour, P.M. Slocombe, A. Webster, M. Butler, C.G. Knight, B.J. Smith, P.E. Stephens, C. Shelley, M. Hutton, V. Knauper, A.J. Docherty, G. Murphy, TNF-alpha converting enzyme (TACE) is inhibited by TIMP-3, *FEBS Lett*, 435 (1998) 39-44.
- [84] P.G. Hargreaves, F. Wang, J. Antcliff, G. Murphy, J. Lawry, R.G. Russell, P.I. Croucher, Human myeloma cells shed the interleukin-6 receptor: inhibition by tissue



- inhibitor of metalloproteinase-3 and a hydroxamate-based metalloproteinase inhibitor, *Br J Haematol*, 101 (1998) 694-702.
- [85] I.M. Clark, L.K. Powell, T.E. Cawston, Tissue inhibitor of metalloproteinases (TIMP-1) stimulates the secretion of collagenase from human skin fibroblasts, *Biochem Biophys Res Commun*, 203 (1994) 874-880.
- [86] J.D. Mott, C.L. Thomas, M.T. Rosenbach, K. Takahara, D.S. Greenspan, M.J. Banda, Post-translational proteolytic processing of procollagen C-terminal proteinase enhancer releases a metalloproteinase inhibitor, *J Biol Chem*, 275 (2000) 1384-1390.
- [87] K.O. Netzer, K. Suzuki, Y. Itoh, B.G. Hudson, R.G. Khalifah, Comparative analysis of the noncollagenous NC1 domain of type IV collagen: identification of structural features important for assembly, function, and pathogenesis, *Protein Sci*, 7 (1998) 1340-1351.
- [88] M.P. Herman, G.K. Sukhova, W. Kisiel, D. Foster, M.R. Kehry, P. Libby, U. Schonbeck, Tissue factor pathway inhibitor-2 is a novel inhibitor of matrix metalloproteinases with implications for atherosclerosis, *J Clin Invest*, 107 (2001) 1117-1126.
- [89] Y.M. Kim, J.W. Jang, O.H. Lee, J. Yeon, E.Y. Choi, K.W. Kim, S.T. Lee, Y.G. Kwon, Endostatin inhibits endothelial and tumor cellular invasion by blocking the activation and catalytic activity of matrix metalloproteinase, *Cancer Res*, 60 (2000) 5410-5413.
- [90] P. Nyberg, P. Heikkila, T. Sorsa, J. Luostarinen, R. Heljasvaara, U.H. Stenman, T. Pihlajaniemi, T. Salo, Endostatin inhibits human tongue carcinoma cell invasion and intravasation and blocks the activation of matrix metalloprotease-2, -9, and -13, *J Biol Chem*, 278 (2003) 22404-22411.
- [91] K. Bein, M. Simons, Thrombospondin type 1 repeats interact with matrix metalloproteinase 2. Regulation of metalloproteinase activity, *J Biol Chem*, 275 (2000) 32167-32173.
- [92] J.C. Rodriguez-Manzaneque, T.F. Lane, M.A. Ortega, R.O. Hynes, J. Lawler, M.L. Iruela-Arispe, Thrombospondin-1 suppresses spontaneous tumor growth and inhibits activation of matrix metalloproteinase-9 and mobilization of vascular endothelial growth factor, *Proc Natl Acad Sci U S A*, 98 (2001) 12485-12490.
- [93] Z. Yang, D.K. Strickland, P. Bornstein, Extracellular matrix metalloproteinase 2 levels are regulated by the low density lipoprotein-related scavenger receptor and thrombospondin 2, *J Biol Chem*, 276 (2001) 8403-8408.
- [94] C. Takahashi, Z. Sheng, T.P. Horan, H. Kitayama, M. Maki, K. Hitomi, Y. Kitaura, S. Takai, R.M. Sasahara, A. Horimoto, Y. Ikawa, B.J. Ratzkin, T. Arakawa, M. Noda, Regulation of matrix metalloproteinase-9 and inhibition of tumor invasion by the membrane-anchored glycoprotein RECK, *Proc Natl Acad Sci U S A*, 95 (1998) 13221-13226.
- [95] J. Oh, R. Takahashi, S. Kondo, A. Mizoguchi, E. Adachi, R.M. Sasahara, S. Nishimura, Y. Imamura, H. Kitayama, D.B. Alexander, C. Ide, T.P. Horan, T. Arakawa, H. Yoshida, S. Nishikawa, Y. Itoh, M. Seiki, S. Itohara, C. Takahashi, M. Noda, The membrane-anchored MMP inhibitor RECK is a key regulator of extracellular matrix integrity and angiogenesis, *Cell*, 107 (2001) 789-800.
- [96] A. Berton, V. Rigot, E. Huet, M. Decarme, Y. Eeckhout, L. Patthy, G. Godeau, W. Hornebeck, G. Bellon, H. Emonard, Involvement of fibronectin type II repeats in the efficient inhibition of gelatinases A and B by long-chain unsaturated fatty acids, *J Biol Chem*, 276 (2001) 20458-20465.
- [97] B.G. Rao, Recent developments in the design of specific Matrix Metalloproteinase inhibitors aided by structural and computational studies, *Curr Pharm Des*, 11 (2005) 295-322.



- [98] C.M. Overall, O. Kleifeld, Towards third generation matrix metalloproteinase inhibitors for cancer therapy, *Br J Cancer*, 94 (2006) 941-946.
- [99] I. Botos, L. Scapozza, D. Zhang, L.A. Liotta, E.F. Meyer, Batimastat, a potent matrix metalloproteinase inhibitor, exhibits an unexpected mode of binding, *Proc Natl Acad Sci U S A*, 93 (1996) 2749-2754.
- [100] F.E. Jacobsen, M.W. Buczynski, E.A. Dennis, S.M. Cohen, A macrophage cell model for selective metalloproteinase inhibitor design, *Chembiochem*, 9 (2008) 2087-2095.
- [101] L.M. Coussens, B. Fingleton, L.M. Matrisian, Matrix metalloproteinase inhibitors and cancer: trials and tribulations, *Science*, 295 (2002) 2387-2392.
- [102] B. Fingleton, MMPs as therapeutic targets--still a viable option?, *Semin Cell Dev Biol*, 19 (2008) 61-68.
- [103] R. Renkiewicz, L. Qiu, C. Lesch, X. Sun, R. Devalaraja, T. Cody, E. Kaldjian, H. Welgus, V. Baragi, Broad-spectrum matrix metalloproteinase inhibitor marimastat-induced musculoskeletal side effects in rats, *Arthritis Rheum*, 48 (2003) 1742-1749.
- [104] M. Whittaker, C.D. Floyd, P. Brown, A.J.H. Gearing, Design and Therapeutic Application of Matrix Metalloproteinase Inhibitors, *Chemical Reviews*, 99 (1999) 2735-2776.
- [105] S.M. Wojtowicz-Praga, R.B. Dickson, M.J. Hawkins, Matrix metalloproteinase inhibitors, *Invest New Drugs*, 15 (1997) 61-75.
- [106] M. Whittaker, C.D. Floyd, P. Brown, A.J. Gearing, Design and therapeutic application of matrix metalloproteinase inhibitors. (*Chem. Rev.* 1999, 99, 2735-2776. Published on the web september 8, 1999), *Chem Rev*, 101 (2001) 2205-2206.
- [107] D.R. Shalinsky, J. Brekken, H. Zou, C.D. McDermott, P. Forsyth, D. Edwards, S. Margosiak, S. Bender, G. Truitt, A. Wood, N.M. Varki, K. Appelt, Broad antitumor and antiangiogenic activities of AG3340, a potent and selective MMP inhibitor undergoing advanced oncology clinical trials, *Ann N Y Acad Sci*, 878 (1999) 236-270.
- [108] A. Rossello, E. Nuti, P. Carelli, E. Orlandini, M. Macchia, S. Nencetti, M. Zandomenighi, F. Balzano, G. Uccello Barretta, A. Albini, R. Benelli, G. Cercignani, G. Murphy, A. Balsamo, N-i-Propoxy-N-biphenylsulfonaminobutylhydroxamic acids as potent and selective inhibitors of MMP-2 and MT1-MMP, *Bioorg Med Chem Lett*, 15 (2005) 1321-1326.
- [109] G.A. Whitlock, K.N. Dack, R.P. Dickinson, M.L. Lewis, A novel series of highly selective inhibitors of MMP-3, *Bioorg Med Chem Lett*, 17 (2007) 6750-6753.
- [110] L.J. MacPherson, E.K. Bayburt, M.P. Capparelli, B.J. Carroll, R. Goldstein, M.R. Justice, L. Zhu, S. Hu, R.A. Melton, L. Fryer, R.L. Goldberg, J.R. Doughty, S. Spirito, V. Blancuzzi, D. Wilson, E.M. O'Byrne, V. Ganu, D.T. Parker, Discovery of CGS 27023A, a non-peptidic, potent, and orally active stromelysin inhibitor that blocks cartilage degradation in rabbits, *J Med Chem*, 40 (1997) 2525-2532.
- [111] L.A. Reiter, R.P. Robinson, K.F. McClure, C.S. Jones, M.R. Reese, P.G. Mitchell, I.G. Otterness, M.L. Bliven, J. Liras, S.R. Cortina, K.M. Donahue, J.D. Eskra, R.J. Griffiths, M.E. Lame, A. Lopez-Anaya, G.J. Martinelli, S.M. McGahee, S.A. Yocum, L.L. Lopresti-Morrow, L.M. Tobiassen, M.L. Vaughn-Bowser, Pyran-containing sulfonamide hydroxamic acids: potent MMP inhibitors that spare MMP-1, *Bioorg Med Chem Lett*, 14 (2004) 3389-3395.
- [112] M. Arlt, C. Kopitz, C. Pennington, K.L. Watson, H.W. Krell, W. Bode, B. Gansbacher, R. Khokha, D.R. Edwards, A. Kruger, Increase in gelatinase-specificity of matrix metalloproteinase inhibitors correlates with antimetastatic efficacy in a T-cell lymphoma model, *Cancer Res*, 62 (2002) 5543-5550.



- [113] M. Whittaker, C.D. Floyd, P. Brown, A.J. Gearing, Design and therapeutic application of matrix metalloproteinase inhibitors, *Chem Rev*, 99 (1999) 2735-2776.
- [114] L.G. Monovich, R.A. Tommasi, R.A. Fujimoto, V. Blancuzzi, K. Clark, W.D. Cornell, R. Doti, J. Doughty, J. Fang, D. Farley, J. Fitt, V. Ganu, R. Goldberg, R. Goldstein, S. Lavoie, R. Kulathila, W. Macchia, D.T. Parker, R. Melton, E. O'Byrne, G. Pastor, T. Pellas, E. Quadros, N. Reel, D.M. Roland, Y. Sakane, H. Singh, J. Skiles, J. Somers, K. Toscano, A. Wigg, S. Zhou, L. Zhu, W.C. Shieh, S. Xue, L.W. McQuire, Discovery of potent, selective, and orally active carboxylic acid based inhibitors of matrix metalloproteinase-13, *J Med Chem*, 52 (2009) 3523-3538.
- [115] Y. Tamura, F. Watanabe, T. Nakatani, K. Yasui, M. Fuji, T. Komurasaki, H. Tsuzuki, R. Maekawa, T. Yoshioka, K. Kawada, K. Sugita, M. Ohtani, Highly selective and orally active inhibitors of type IV collagenase (MMP-9 and MMP-2): N-sulfonylamino acid derivatives, *J Med Chem*, 41 (1998) 640-649.
- [116] P.M. O'Brien, D.F. Ortwine, A.G. Pavlovsky, J.A. Picard, D.R. Sliskovic, B.D. Roth, R.D. Dyer, L.L. Johnson, C.F. Man, H. Hallak, Structure-activity relationships and pharmacokinetic analysis for a series of potent, systemically available biphenylsulfonamide matrix metalloproteinase inhibitors, *J Med Chem*, 43 (2000) 156-166.
- [117] M.H. Parker, D.F. Ortwine, P.M. O'Brien, E.A. Lunney, C.A. Banotai, W.T. Mueller, P. McConnell, C.G. Brouillette, Stereoselective binding of an enantiomeric pair of stromelysin-1 inhibitors caused by conformational entropy factors, *Bioorg Med Chem Lett*, 10 (2000) 2427-2430.
- [118] S. Pikul, N.E. Ohler, G. Ciszewski, M.C. Laufersweiler, N.G. Almstead, B. De, M.G. Natchus, L.C. Hsieh, M.J. Janusz, S.X. Peng, T.M. Branch, S.L. King, Y.O. Taiwo, G.E. Mieling, Potent and selective carboxylic acid-based inhibitors of matrix metalloproteinases, *J Med Chem*, 44 (2001) 2499-2502.
- [119] Y.M. Zhang, X. Fan, B. Xiang, D. Chakravarty, R. Scannevin, S. Burke, P. Karnachi, K. Rhodes, P. Jackson, Synthesis and SAR of alpha-sulfonylcarboxylic acids as potent matrix metalloproteinase inhibitors, *Bioorg Med Chem Lett*, 16 (2006) 3096-3100.
- [120] Y. Hu, J.S. Xiang, M.J. DiGrandi, X. Du, M. Ipek, L.M. Laakso, J. Li, W. Li, T.S. Rush, J. Schmid, J.S. Skotnicki, S. Tam, J.R. Thomason, Q. Wang, J.I. Levin, Potent, selective, and orally bioavailable matrix metalloproteinase-13 inhibitors for the treatment of osteoarthritis, *Bioorg Med Chem*, 13 (2005) 6629-6644.
- [121] D. Ma, Y. Jiang, F. Chen, L.K. Gong, K. Ding, Y. Xu, R. Wang, A. Ge, J. Ren, J. Li, Q. Ye, Selective inhibition of matrix metalloproteinase isozymes and in vivo protection against emphysema by substituted gamma-keto carboxylic acids, *J Med Chem*, 49 (2006) 456-458.
- [122] F. Grams, P. Reinemer, J.C. Powers, T. Kleine, M. Pieper, H. Tschesche, R. Huber, W. Bode, X-ray structures of human neutrophil collagenase complexed with peptide hydroxamate and peptide thiol inhibitors. Implications for substrate binding and rational drug design, *Eur J Biochem*, 228 (1995) 830-841.
- [123] S. Foley, M. Enescu, A Raman spectroscopy and theoretical study of zinc-cysteine complexation, *Vibrational Spectroscopy*, 44 (2007) 256-265.
- [124] J.G. Naglich, M. Jure-Kunkel, E. Gupta, J. Fagnoli, A.J. Henderson, A.C. Lewin, R. Talbott, A. Baxter, J. Bird, R. Savopoulos, R. Wills, R.A. Kramer, P.A. Trail, Inhibition of angiogenesis and metastasis in two murine models by the matrix metalloproteinase inhibitor, BMS-275291, *Cancer Res*, 61 (2001) 8480-8485.
- [125] J.W. Skiles, N.C. Gonnella, A.Y. Jeng, The design, structure, and clinical update of small molecular weight matrix metalloproteinase inhibitors, *Curr Med Chem*, 11 (2004) 2911-2977.



- [126] Q.X. Sang, M.C. Jia, M.A. Schwartz, M.C. Jaye, H.K. Kleinman, M.A. Ghaffari, Y.L. Luo, New thiol and sulfodiimine metalloproteinase inhibitors and their effect on human microvascular endothelial cell growth, *Biochem Biophys Res Commun*, 274 (2000) 780-786.
- [127] D.R. Hurst, M.A. Schwartz, Y. Jin, M.A. Ghaffari, P. Kozarekar, J. Cao, Q.X. Sang, Inhibition of enzyme activity of and cell-mediated substrate cleavage by membrane type 1 matrix metalloproteinase by newly developed mercaptosulphide inhibitors, *Biochem J*, 392 (2005) 527-536.
- [128] C. Gatto, M. Rieppi, P. Borsotti, S. Innocenti, R. Ceruti, T. Drudis, E. Scanziani, A.M. Casazza, G. Taraboletti, R. Giavazzi, BAY 12-9566, a novel inhibitor of matrix metalloproteinases with antiangiogenic activity, *Clin Cancer Res*, 5 (1999) 3603-3607.
- [129] L.A. Reiter, P.G. Mitchell, G.J. Martinelli, L.L. Lopresti-Morrow, S.A. Yocum, J.D. Eskra, Phosphinic acid-based MMP-13 inhibitors that spare MMP-1 and MMP-3, *Bioorg Med Chem Lett*, 13 (2003) 2331-2336.
- [130] C. Bankhead, Bisphosphonates spearhead new approach to treating bone metastases, *J Natl Cancer Inst*, 89 (1997) 115-116.
- [131] O. Teronen, Y.T. Konttinen, C. Lindqvist, T. Salo, T. Ingman, A. Lauhio, Y. Ding, S. Santavirta, H. Valleala, T. Sorsa, Inhibition of matrix metalloproteinase-1 by dichloromethylene bisphosphonate (clodronate), *Calcif Tissue Int*, 61 (1997) 59-61.
- [132] E. Giraud, M. Inoue, D. Hanahan, An amino-bisphosphonate targets MMP-9-expressing macrophages and angiogenesis to impair cervical carcinogenesis, *J Clin Invest*, 114 (2004) 623-633.
- [133] P. Clezardin, Anti-tumour activity of zoledronic acid, *Cancer Treat Rev*, 31 Suppl 3 (2005) 1-8.
- [134] J. Bird, R.C. De Mello, G.P. Harper, D.J. Hunter, E.H. Karran, R.E. Markwell, A.J. Miles-Williams, S.S. Rahman, R.W. Ward, Synthesis of novel N-phosphonoalkyl dipeptide inhibitors of human collagenase, *J Med Chem*, 37 (1994) 158-169.
- [135] G. Pochetti, E. Gavuzzo, C. Campestre, M. Agamennone, P. Tortorella, V. Consalvi, C. Gallina, O. Hiller, H. Tschesche, P.A. Tucker, F. Mazza, Structural insight into the stereoselective inhibition of MMP-8 by enantiomeric sulfonamide phosphonates, *J Med Chem*, 49 (2006) 923-931.
- [136] R.A. Garcia, D.P. Pantazatos, C.R. Gessner, K.V. Go, V.L. Woods, Jr., F.J. Villarreal, Molecular interactions between matrilysin and the matrix metalloproteinase inhibitor doxycycline investigated by deuterium exchange mass spectrometry, *Mol Pharmacol*, 67 (2005) 1128-1136.
- [137] M.R. Acharya, J. Venitz, W.D. Figg, A. Sparreboom, Chemically modified tetracyclines as inhibitors of matrix metalloproteinases, *Drug Resist Updat*, 7 (2004) 195-208.
- [138] T.Y. Huang, H.C. Chu, Y.L. Lin, C.K. Lin, T.Y. Hsieh, W.K. Chang, Y.C. Chao, C.L. Liao, Minocycline attenuates experimental colitis in mice by blocking expression of inducible nitric oxide synthase and matrix metalloproteinases, *Toxicol Appl Pharmacol*, 237 (2009) 69-82.
- [139] G. Dorman, K. Kocsis-Szommer, C. Spadoni, P. Ferdinandy, MMP inhibitors in cardiac diseases: an update, *Recent Pat Cardiovasc Drug Discov*, 2 (2007) 186-194.
- [140] Z. Yu, M.K. Leung, N.S. Ramamurthy, T.F. McNamara, L.M. Golub, HPLC determination of a chemically modified nonantimicrobial tetracycline: biological implications, *Biochem Med Metab Biol*, 47 (1992) 10-20.
- [141] J.F. Fisher, S. Mobashery, Recent advances in MMP inhibitor design, *Cancer Metastasis Rev*, 25 (2006) 115-136.



- [142] M.O. Griffin, E. Fricovsky, G. Ceballos, F. Villarreal, Tetracyclines: a pleiotropic family of compounds with promising therapeutic properties. Review of the literature, *Am J Physiol Cell Physiol*, 299 (2010) C539-548.
- [143] S. Gilbertson-Beadling, E.A. Powers, M. Stamp-Cole, P.S. Scott, T.L. Wallace, J. Copeland, G. Petzold, M. Mitchell, S. Ledbetter, R. Poorman, The tetracycline analogs minocycline and doxycycline inhibit angiogenesis in vitro by a non-metalloproteinase-dependent mechanism, *Cancer Chemother Pharmacol*, 36 (1995) 418-424.
- [144] F. Grams, H. Brandstetter, S. D'Alo, D. Geppert, H.W. Krell, H. Leinert, V. Livi, E. Menta, A. Oliva, G. Zimmermann, F. Gram, V.E. Livi, Pyrimidine-2,4,6-Triones: a new effective and selective class of matrix metalloproteinase inhibitors, *Biol Chem*, 382 (2001) 1277-1285.
- [145] H.J. Breyholz, M. Schafers, S. Wagner, C. Holtke, A. Faust, H. Rabeneck, B. Levkau, O. Schober, K. Kopka, C-5-disubstituted barbiturates as potential molecular probes for noninvasive matrix metalloproteinase imaging, *J Med Chem*, 48 (2005) 3400-3409.
- [146] L.H. Foley, R. Palermo, P. Dunten, P. Wang, Novel 5,5-disubstitutedpyrimidine-2,4,6-triones as selective MMP inhibitors, *Bioorg Med Chem Lett*, 11 (2001) 969-972.
- [147] J.A. Blagg, M.C. Noe, L.A. Wolf-Gouveia, L.A. Reiter, E.R. Laird, S.P. Chang, D.E. Danley, J.T. Downs, N.C. Elliott, J.D. Eskra, R.J. Griffiths, J.R. Hardink, A.I. Haugeto, C.S. Jones, J.L. Liras, L.L. Lopresti-Morrow, P.G. Mitchell, J. Pandit, R.P. Robinson, C. Subramanyam, M.L. Vaughn-Bowser, S.A. Yocum, Potent pyrimidinetrione-based inhibitors of MMP-13 with enhanced selectivity over MMP-14, *Bioorg Med Chem Lett*, 15 (2005) 1807-1810.
- [148] A.R. Johnson, A.G. Pavlovsky, D.F. Ortwine, F. Prior, C.F. Man, D.A. Bornemeier, C.A. Banotai, W.T. Mueller, P. McConnell, C. Yan, V. Baragi, C. Lesch, W.H. Roark, M. Wilson, K. Datta, R. Guzman, H.K. Han, R.D. Dyer, Discovery and characterization of a novel inhibitor of matrix metalloprotease-13 that reduces cartilage damage in vivo without joint fibroplasia side effects, *J Biol Chem*, 282 (2007) 27781-27791.
- [149] C.K. Engel, B. Pirard, S. Schimanski, R. Kirsch, J. Habermann, O. Klingler, V. Schlotte, K.U. Weithmann, K.U. Wendt, Structural basis for the highly selective inhibition of MMP-13, *Chem Biol*, 12 (2005) 181-189.
- [150] A.C. Dublanchet, P. Ducrot, C. Andrianjara, M. O'Gara, R. Morales, D. Compere, A. Denis, S. Blais, P. Cluzeau, K. Courte, J. Hamon, F. Moreau, M.L. Prunet, A. Tertre, Structure-based design and synthesis of novel non-zinc chelating MMP-12 inhibitors, *Bioorg Med Chem Lett*, 15 (2005) 3787-3790.
- [151] L.T. Gooljarsingh, A. Lakdawala, F. Coppo, L. Luo, G.B. Fields, P.J. Tummino, R.R. Gontarek, Characterization of an exosite binding inhibitor of matrix metalloproteinase 13, *Protein Sci*, 17 (2008) 66-71.
- [152] M. Ikejiri, M.M. Bernardo, R.D. Bonfil, M. Toth, M. Chang, R. Fridman, S. Mobashery, Potent mechanism-based inhibitors for matrix metalloproteinases, *J Biol Chem*, 280 (2005) 33992-34002.
- [153] S. Brown, M.M. Bernardo, Z.-H. Li, L.P. Kotra, Y. Tanaka, R. Fridman, S. Mobashery, Potent and Selective Mechanism-Based Inhibition of Gelatinases, *J Am Chem Soc*, 122 (2000) 6799-6800.
- [154] M. Lee, M.M. Bernardo, S.O. Meroueh, S. Brown, R. Fridman, S. Mobashery, Synthesis of chiral 2-(4-phenoxyphenylsulfonylmethyl)thiiranes as selective gelatinase inhibitors, *Org Lett*, 7 (2005) 4463-4465.
- [155] R. Ala-aho, N. Johansson, R. Grenman, N.E. Fusenig, C. Lopez-Otin, V.M. Kahari, Inhibition of collagenase-3 (MMP-13) expression in transformed human keratinocytes by



interferon-gamma is associated with activation of extracellular signal-regulated kinase-1,2 and STAT1, *Oncogene*, 19 (2000) 248-257.

[156] Z. Ma, H. Qin, E.N. Benveniste, Transcriptional suppression of matrix metalloproteinase-9 gene expression by IFN-gamma and IFN-beta: critical role of STAT-1alpha, *J Immunol*, 167 (2001) 5150-5159.

[157] J.W. Slaton, T. Karashima, P. Perrotte, K. Inoue, S.J. Kim, J. Izawa, D. Kedar, D.J. McConkey, R. Millikan, P. Sweeney, C. Yoshikawa, T. Shuin, C.P. Dinney, Treatment with low-dose interferon-alpha restores the balance between matrix metalloproteinase-9 and E-cadherin expression in human transitional cell carcinoma of the bladder, *Clin Cancer Res*, 7 (2001) 2840-2853.

[158] J.A. Mengshol, K.S. Mix, C.E. Brinckerhoff, Matrix metalloproteinases as therapeutic targets in arthritic diseases: bull's-eye or missing the mark?, *Arthritis Rheum*, 46 (2002) 13-20.

[159] A. Lal, C.A. Glazer, H.M. Martinson, H.S. Friedman, G.E. Archer, J.H. Sampson, G.J. Riggins, Mutant epidermal growth factor receptor up-regulates molecular effectors of tumor invasion, *Cancer Res*, 62 (2002) 3335-3339.

[160] C. Simon, H. Goepfert, D. Boyd, Inhibition of the p38 mitogen-activated protein kinase by SB 203580 blocks PMA-induced Mr 92,000 type IV collagenase secretion and in vitro invasion, *Cancer Res*, 58 (1998) 1135-1139.

[161] N. Johansson, R. Ala-aho, V. Uitto, R. Grenman, N.E. Fusenig, C. Lopez-Otin, V.M. Kahari, Expression of collagenase-3 (MMP-13) and collagenase-1 (MMP-1) by transformed keratinocytes is dependent on the activity of p38 mitogen-activated protein kinase, *J Cell Sci*, 113 Pt 2 (2000) 227-235.

[162] M. Shin, C. Yan, D. Boyd, An inhibitor of c-jun aminoterminal kinase (SP600125) represses c-Jun activation, DNA-binding and PMA-inducible 92-kDa type IV collagenase expression, *Biochim Biophys Acta*, 1589 (2002) 311-316.

[163] J. Adams, V.J. Palombella, E.A. Sausville, J. Johnson, A. Destree, D.D. Lazarus, J. Maas, C.S. Pien, S. Prakash, P.J. Elliott, Proteasome inhibitors: a novel class of potent and effective antitumor agents, *Cancer Res*, 59 (1999) 2615-2622.

[164] M. Karin, L. Chang, AP-1--glucocorticoid receptor crosstalk taken to a higher level, *J Endocrinol*, 169 (2001) 447-451.

[165] C. Medina, M.W. Radomski, Role of matrix metalloproteinases in intestinal inflammation, *J Pharmacol Exp Ther*, 318 (2006) 933-938.

[166] M. Orholm, P. Munkholm, E. Langholz, O.H. Nielsen, T.I. Sorensen, V. Binder, Familial occurrence of inflammatory bowel disease, *N Engl J Med*, 324 (1991) 84-88.

[167] V. Binder, M. Orholm, Familial occurrence and inheritance studies in inflammatory bowel disease, *Neth J Med*, 48 (1996) 53-56.

[168] J.B. Park, S.K. Yang, J.S. Byeon, E.R. Park, G. Moon, S.J. Myung, W.K. Park, S.G. Yoon, H.S. Kim, J.G. Lee, J.H. Kim, Y. Il Min, K.Y. Kim, Familial occurrence of inflammatory bowel disease in Korea, *Inflamm Bowel Dis*, 12 (2006) 1146-1151.

[169] R.J. Xavier, D.K. Podolsky, Unravelling the pathogenesis of inflammatory bowel disease, *Nature*, 448 (2007) 427-434.

[170] J.P. Hugot, M. Chamaillard, H. Zouali, S. Lesage, J.P. Cezard, J. Belaiche, S. Almer, C. Tysk, C.A. O'Morain, M. Gassull, V. Binder, Y. Finkel, A. Cortot, R. Modigliani, P. Laurent-Puig, C. Gower-Rousseau, J. Macry, J.F. Colombel, M. Sahbatou, G. Thomas, Association of NOD2 leucine-rich repeat variants with susceptibility to Crohn's disease, *Nature*, 411 (2001) 599-603.

[171] J.H. Cho, The Nod2 gene in Crohn's disease: implications for future research into the genetics and immunology of Crohn's disease, *Inflamm Bowel Dis*, 7 (2001) 271-275.



- [172] Y. Ogura, D.K. Bonen, N. Inohara, D.L. Nicolae, F.F. Chen, R. Ramos, H. Britton, T. Moran, R. Karaliuskas, R.H. Duerr, J.P. Achkar, S.R. Brant, T.M. Bayless, B.S. Kirschner, S.B. Hanauer, G. Nunez, J.H. Cho, A frameshift mutation in NOD2 associated with susceptibility to Crohn's disease, *Nature*, 411 (2001) 603-606.
- [173] E. Bairead, D.L. Harmon, A.M. Curtis, Y. Kelly, C. O'Leary, M. Gardner, D.T. Leahy, P. Vaughan, D. Keegan, C. O'Morain, D. O'Donoghue, F. Shanahan, N.A. Parfrey, K.A. Quane, Association of NOD2 with Crohn's disease in a homogenous Irish population, *Eur J Hum Genet*, 11 (2003) 237-244.
- [174] B. Hall, Holleran, G., O'Sullivan, S., Smith, S., Medina, C., McNamara, D., Poster 659: Crohn's Disease in an Irish population - a pilot genotype-phenotype analysis, in: 9th Congress of ECCO, Copenhagen, 2014.
- [175] J.P. Hugot, P. Laurent-Puig, C. Gower-Rousseau, J.M. Olson, J.C. Lee, L. Beaugerie, I. Naom, J.L. Dupas, A. Van Gossum, M. Orholm, C. Bonaiti-Pellie, J. Weissenbach, C.G. Mathew, J.E. Lennard-Jones, A. Cortot, J.F. Colombel, G. Thomas, Mapping of a susceptibility locus for Crohn's disease on chromosome 16, *Nature*, 379 (1996) 821-823.
- [176] Y. Ma, J.D. Ohmen, Z. Li, L.G. Bentley, C. McElree, S. Pressman, S.R. Targan, N. Fischel-Ghodsian, J.I. Rotter, H. Yang, A genome-wide search identifies potential new susceptibility loci for Crohn's disease, *Inflamm Bowel Dis*, 5 (1999) 271-278.
- [177] J.D. Rioux, M.S. Silverberg, M.J. Daly, A.H. Steinhart, R.S. McLeod, A.M. Griffiths, T. Green, T.S. Brettin, V. Stone, S.B. Bull, A. Bitton, C.N. Williams, G.R. Greenberg, Z. Cohen, E.S. Lander, T.J. Hudson, K.A. Siminovitch, Genomewide search in Canadian families with inflammatory bowel disease reveals two novel susceptibility loci, *Am J Hum Genet*, 66 (2000) 1863-1870.
- [178] J. Satsangi, M. Parkes, E. Louis, L. Hashimoto, N. Kato, K. Welsh, J.D. Terwilliger, G.M. Lathrop, J.I. Bell, D.P. Jewell, Two stage genome-wide search in inflammatory bowel disease provides evidence for susceptibility loci on chromosomes 3, 7 and 12, *Nat Genet*, 14 (1996) 199-202.
- [179] S. Vermeire, J. Satsangi, M. Peeters, M. Parkes, D.P. Jewell, R. Vlietinck, P. Rutgeerts, Evidence for inflammatory bowel disease of a susceptibility locus on the X chromosome, *Gastroenterology*, 120 (2001) 834-840.
- [180] H. Yang, S.E. Plevy, K. Taylor, D. Tyan, N. Fischel-Ghodsian, C. McElree, S.R. Targan, J.I. Rotter, Linkage of Crohn's disease to the major histocompatibility complex region is detected by multiple non-parametric analyses, *Gut*, 44 (1999) 519-526.
- [181] R.H. Duerr, K.D. Taylor, S.R. Brant, J.D. Rioux, M.S. Silverberg, M.J. Daly, A.H. Steinhart, C. Abraham, M. Regueiro, A. Griffiths, T. Dassopoulos, A. Bitton, H. Yang, S. Targan, L.W. Datta, E.O. Kistner, L.P. Schumm, A.T. Lee, P.K. Gregersen, M.M. Barmada, J.I. Rotter, D.L. Nicolae, J.H. Cho, A genome-wide association study identifies IL23R as an inflammatory bowel disease gene, *Science*, 314 (2006) 1461-1463.
- [182] J. Hampe, A. Franke, P. Rosenstiel, A. Till, M. Teuber, K. Huse, M. Albrecht, G. Mayr, F.M. De La Vega, J. Briggs, S. Gunther, N.J. Prescott, C.M. Onnie, R. Hasler, B. Sipos, U.R. Folsch, T. Lengauer, M. Platzer, C.G. Mathew, M. Krawczak, S. Schreiber, A genome-wide association scan of nonsynonymous SNPs identifies a susceptibility variant for Crohn disease in ATG16L1, *Nat Genet*, 39 (2007) 207-211.
- [183] M.S. Silverberg, R.H. Duerr, S.R. Brant, G. Bromfield, L.W. Datta, N. Jani, S.V. Kane, J.I. Rotter, L. Philip Schumm, A. Hillary Steinhart, K.D. Taylor, H. Yang, J.H. Cho, J.D. Rioux, M.J. Daly, Refined genomic localization and ethnic differences observed for the IBD5 association with Crohn's disease, *Eur J Hum Genet*, 15 (2007) 328-335.
- [184] K. Wiencke, A.S. Louka, A. Spurkland, M. Vatn, E. Schrumpf, K.M. Boberg, Association of matrix metalloproteinase-1 and -3 promoter polymorphisms with clinical



subsets of Norwegian primary sclerosing cholangitis patients, *J Hepatol*, 41 (2004) 209-214.

[185] J. Satsangi, R.W. Chapman, N. Haldar, P. Donaldson, S. Mitchell, J. Simmons, S. Norris, S.E. Marshall, J.I. Bell, D.P. Jewell, K.I. Welsh, A functional polymorphism of the stromelysin gene (MMP-3) influences susceptibility to primary sclerosing cholangitis, *Gastroenterology*, 121 (2001) 124-130.

[186] B.D. Juran, E.J. Atkinson, E.M. Schlicht, J.J. Larson, D. Ellinghaus, A. Franke, K.N. Lazaridis, Genetic polymorphisms of matrix metalloproteinase 3 in primary sclerosing cholangitis, *Liver Int*, 31 (2011) 785-791.

[187] A. Madisch, S. Hellmig, S. Schreiber, B. Bethke, M. Stolte, S. Miehke, Allelic variation of the matrix metalloproteinase-9 gene is associated with collagenous colitis, *Inflamm Bowel Dis*, 17 (2011) 2295-2298.

[188] M.J. Meijer, M.A. Mieremet-Ooms, R.A. van Hogezaand, C.B. Lamers, D.W. Hommes, H.W. Verspaget, Role of matrix metalloproteinase, tissue inhibitor of metalloproteinase and tumor necrosis factor-alpha single nucleotide gene polymorphisms in inflammatory bowel disease, *World J Gastroenterol*, 13 (2007) 2960-2966.

[189] A.R. Morgan, D.Y. Han, W.J. Lam, C.M. Triggs, A.G. Fraser, M. Barclay, R.B. Gearry, S. Meisner, P. Stokkers, G.E. Boeckxstaens, L.R. Ferguson, Genetic variations in matrix metalloproteinases may be associated with increased risk of ulcerative colitis, *Hum Immunol*, 72 (2011) 1117-1127.

[190] P. Gionchetti, F. Rizzello, U. Helwig, A. Venturi, K.M. Lammers, P. Brigidi, B. Vitali, G. Poggioli, M. Miglioli, M. Campieri, Prophylaxis of pouchitis onset with probiotic therapy: a double-blind, placebo-controlled trial, *Gastroenterology*, 124 (2003) 1202-1209.

[191] L. Sutherland, J. Singleton, J. Sessions, S. Hanauer, E. Krawitt, G. Rankin, R. Summers, H. Mekhjian, N. Greenberger, M. Kelly, et al., Double blind, placebo controlled trial of metronidazole in Crohn's disease, *Gut*, 32 (1991) 1071-1075.

[192] C.O. Elson, Y. Cong, V.J. McCracken, R.A. Dimmitt, R.G. Lorenz, C.T. Weaver, Experimental models of inflammatory bowel disease reveal innate, adaptive, and regulatory mechanisms of host dialogue with the microbiota, *Immunol Rev*, 206 (2005) 260-276.

[193] A.B. Onderdonk, J.A. Hermos, J.G. Bartlett, The role of the intestinal microflora in experimental colitis, *Am J Clin Nutr*, 30 (1977) 1819-1825.

[194] N. Gassler, C. Rohr, A. Schneider, J. Kartenbeck, A. Bach, N. Obermuller, H.F. Otto, F. Autschbach, Inflammatory bowel disease is associated with changes of enterocytic junctions, *Am J Physiol Gastrointest Liver Physiol*, 281 (2001) G216-228.

[195] C. Fiocchi, Intestinal inflammation: a complex interplay of immune and nonimmune cell interactions, *Am J Physiol*, 273 (1997) G769-775.

[196] D.K. Podolsky, The current future understanding of inflammatory bowel disease, *Best Pract Res Clin Gastroenterol*, 16 (2002) 933-943.

[197] R.P. McCabe, H. Secrist, M. Botney, M. Egan, M.G. Peters, Cytokine mRNA expression in intestine from normal and inflammatory bowel disease patients, *Clin Immunol Immunopathol*, 66 (1993) 52-58.

[198] M.J. Meijer, M.A. Mieremet-Ooms, A.M. van der Zon, W. van Duijn, R.A. van Hogezaand, C.F. Sier, D.W. Hommes, C.B. Lamers, H.W. Verspaget, Increased mucosal matrix metalloproteinase-1, -2, -3 and -9 activity in patients with inflammatory bowel disease and the relation with Crohn's disease phenotype, *Dig Liver Dis*, 39 (2007) 733-739.

[199] M.D. Baugh, M.J. Perry, A.P. Hollander, D.R. Davies, S.S. Cross, A.J. Lobo, C.J. Taylor, G.S. Evans, Matrix metalloproteinase levels are elevated in inflammatory bowel disease, *Gastroenterology*, 117 (1999) 814-822.



- [200] T. Kirkegaard, A. Hansen, E. Bruun, J. Brynskov, Expression and localisation of matrix metalloproteinases and their natural inhibitors in fistulae of patients with Crohn's disease, *Gut*, 53 (2004) 701-709.
- [201] B. von Lampe, B. Barthel, S.E. Coupland, E.O. Riecken, S. Rosewicz, Differential expression of matrix metalloproteinases and their tissue inhibitors in colon mucosa of patients with inflammatory bowel disease, *Gut*, 47 (2000) 63-73.
- [202] R.B. Heuschkel, T.T. MacDonald, G. Monteleone, M. Bajaj-Elliott, J.A. Smith, S.L. Pender, Imbalance of stromelysin-1 and TIMP-1 in the mucosal lesions of children with inflammatory bowel disease, *Gut*, 47 (2000) 57-62.
- [203] R.E. Vandenbroucke, E. Dejonckheere, F. Van Hauwermeiren, S. Lodens, R. De Rycke, E. Van Wouterghem, A. Staes, K. Gevaert, C. Lopez-Otin, C. Libert, Matrix metalloproteinase 13 modulates intestinal epithelial barrier integrity in inflammatory diseases by activating TNF, *EMBO Mol Med*, 5 (2013) 932-948.
- [204] C.J. Bailey, R.M. Hembry, A. Alexander, M.H. Irving, M.E. Grant, C.A. Shuttleworth, Distribution of the matrix metalloproteinases stromelysin, gelatinases A and B, and collagenase in Crohn's disease and normal intestine, *J Clin Pathol*, 47 (1994) 113-116.
- [205] S.L. Pender, S.P. Tickle, A.J. Docherty, D. Howie, N.C. Wathen, T.T. MacDonald, A major role for matrix metalloproteinases in T cell injury in the gut, *J Immunol*, 158 (1997) 1582-1590.
- [206] M.T. Salmela, T.T. MacDonald, D. Black, B. Irvine, T. Zhuma, U. Saarialho-Kere, S.L. Pender, Upregulation of matrix metalloproteinases in a model of T cell mediated tissue injury in the gut: analysis by gene array and in situ hybridisation, *Gut*, 51 (2002) 540-547.
- [207] G.P. Morris, P.L. Beck, M.S. Herridge, W.T. Depew, M.R. Szewczuk, J.L. Wallace, Hapten-induced model of chronic inflammation and ulceration in the rat colon, *Gastroenterology*, 96 (1989) 795-803.
- [208] I. Okayasu, S. Hatakeyama, M. Yamada, T. Ohkusa, Y. Inagaki, R. Nakaya, A novel method in the induction of reliable experimental acute and chronic ulcerative colitis in mice, *Gastroenterology*, 98 (1990) 694-702.
- [209] C. Medina, S. Videla, A. Radomski, M.W. Radomski, M. Antolin, F. Guarner, J. Vilaseca, A. Salas, J.R. Malagelada, Increased activity and expression of matrix metalloproteinase-9 in a rat model of distal colitis, *Am J Physiol Gastrointest Liver Physiol*, 284 (2003) G116-122.
- [210] C. Medina, A. Santana, M.C. Paz, F. Diaz-Gonzalez, E. Farre, A. Salas, M.W. Radomski, E. Quintero, Matrix metalloproteinase-9 modulates intestinal injury in rats with transmural colitis, *J Leukoc Biol*, 79 (2006) 954-962.
- [211] C. Medina, S. Videla, A. Radomski, M. Radomski, M. Antolin, F. Guarner, J. Vilaseca, A. Salas, J.R. Malagelada, Therapeutic effect of phenantroline in two rat models of inflammatory bowel disease, *Scand J Gastroenterol*, 36 (2001) 1314-1319.
- [212] A.P. Sykes, R. Bhogal, C. Brampton, C. Chander, C. Whelan, M.E. Parsons, J. Bird, The effect of an inhibitor of matrix metalloproteinases on colonic inflammation in a trinitrobenzenesulphonic acid rat model of inflammatory bowel disease, *Aliment Pharmacol Ther*, 13 (1999) 1535-1542.
- [213] P. Di Sebastiano, F.F. di Mola, L. Artese, C. Rossi, G. Mascetta, H. Pernthaler, P. Innocenti, Beneficial effects of Batimastat (BB-94), a matrix metalloproteinase inhibitor, in rat experimental colitis, *Digestion*, 63 (2001) 234-239.
- [214] Y. Naito, T. Takagi, M. Kuroda, K. Katada, H. Ichikawa, S. Kokura, N. Yoshida, T. Okanoue, T. Yoshikawa, An orally active matrix metalloproteinase inhibitor, ONO-4817, reduces dextran sulfate sodium-induced colitis in mice, *Inflamm Res*, 53 (2004) 462-468.



- [215] M.D. Baugh, G.S. Evans, A.P. Hollander, D.R. Davies, M.J. Perry, A.J. Lobo, C.J. Taylor, Expression of matrix metalloproteases in inflammatory bowel disease, *Ann N Y Acad Sci*, 859 (1998) 249-253.
- [216] F.E. Castaneda, B. Walia, M. Vijay-Kumar, N.R. Patel, S. Roser, V.L. Kolachala, M. Rojas, L. Wang, G. Oprea, P. Garg, A.T. Gewirtz, J. Roman, D. Merlin, S.V. Sitaraman, Targeted deletion of metalloproteinase 9 attenuates experimental colitis in mice: central role of epithelial-derived MMP, *Gastroenterology*, 129 (2005) 1991-2008.
- [217] M.E. Fini, W.C. Parks, W.B. Rinehart, M.T. Girard, M. Matsubara, J.R. Cook, J.A. West-Mays, P.M. Sadow, R.E. Burgeson, J.J. Jeffrey, M.B. Raizman, R.R. Krueger, J.D. Zieske, Role of matrix metalloproteinases in failure to re-epithelialize after corneal injury, *Am J Pathol*, 149 (1996) 1287-1302.
- [218] R. Mohan, S.K. Chintala, J.C. Jung, W.V. Villar, F. McCabe, L.A. Russo, Y. Lee, B.E. McCarthy, K.R. Wollenberg, J.V. Jester, M. Wang, H.G. Welgus, J.M. Shipley, R.M. Senior, M.E. Fini, Matrix metalloproteinase gelatinase B (MMP-9) coordinates and effects epithelial regeneration, *J Biol Chem*, 277 (2002) 2065-2072.
- [219] J.S. Alexander, J.W. Elrod, Extracellular matrix, junctional integrity and matrix metalloproteinase interactions in endothelial permeability regulation, *J Anat*, 200 (2002) 561-574.
- [220] J.J. Atkinson, Matrix Metalloproteinase-9 in Lung Remodeling, *American Journal of Respiratory Cell and Molecular Biology*, 28 (2003) 12-24.
- [221] F. Kuwahara, H. Kai, K. Tokuda, M. Takeya, A. Takeshita, K. Egashira, T. Imaizumi, Hypertensive myocardial fibrosis and diastolic dysfunction: another model of inflammation?, *Hypertension*, 43 (2004) 739-745.
- [222] P. Collier, C.J. Watson, V. Voon, D. Phelan, A. Jan, G. Mak, R. Martos, J.A. Baugh, M.T. Ledwidge, K.M. McDonald, Can emerging biomarkers of myocardial remodelling identify asymptomatic hypertensive patients at risk for diastolic dysfunction and diastolic heart failure?, *Eur J Heart Fail*, 13 (2011) 1087-1095.
- [223] D.M. Basalyga, D.T. Simionescu, W. Xiong, B.T. Baxter, B.C. Starcher, N.R. Vyavahare, Elastin degradation and calcification in an abdominal aorta injury model: role of matrix metalloproteinases, *Circulation*, 110 (2004) 3480-3487.
- [224] S. Heymans, F. Lupu, S. Terclavers, B. Vanwetswinkel, J.-M. Herbert, A. Baker, D. Collen, P. Carmeliet, L. Moons, Loss or Inhibition of uPA or MMP-9 Attenuates LV Remodeling and Dysfunction after Acute Pressure Overload in Mice, *Am J Pathol*, 166 (2005) 15-25.
- [225] R. Mukherjee, G.P. Colbath, C.D. Justus, J.A. Bruce, C.M. Allen, K.W. Hewett, J.P. Saul, R.G. Gourdie, F.G. Spinale, Spatiotemporal induction of matrix metalloproteinase-9 transcription after discrete myocardial injury, *FASEB J*, 24 (2010) 3819-3828.
- [226] R. Mukherjee, J.M. Snipes, S.M. Saunders, J.A. Zavadzkas, F.G. Spinale, Discordant activation of gene promoters for matrix metalloproteinases and tissue inhibitors of the metalloproteinases following myocardial infarction, *J Surg Res*, 172 (2012) 59-67.
- [227] R. Mukherjee, J.T. Mingoia, J.A. Bruce, J.S. Austin, R.E. Stroud, G.P. Escobar, D.M. McClister, Jr., C.M. Allen, M.A. Alfonso-Jaume, M.E. Fini, D.H. Lovett, F.G. Spinale, Selective spatiotemporal induction of matrix metalloproteinase-2 and matrix metalloproteinase-9 transcription after myocardial infarction, *Am J Physiol Heart Circ Physiol*, 291 (2006) H2216-2228.
- [228] R. Martos, J. Baugh, M. Ledwidge, C. O'Loughlin, C. Conlon, A. Patle, S.C. Donnelly, K. McDonald, Diastolic heart failure: evidence of increased myocardial collagen turnover linked to diastolic dysfunction, *Circulation*, 115 (2007) 888-895.
- [229] R. Martos, J. Baugh, M. Ledwidge, C. O'Loughlin, N.F. Murphy, C. Conlon, A. Patle, S.C. Donnelly, K. McDonald, Diagnosis of heart failure with preserved ejection



fraction: improved accuracy with the use of markers of collagen turnover, *Eur J Heart Fail*, 11 (2009) 191-197.

[230] M.R. Zile, S.M. Desantis, C.F. Baicu, R.E. Stroud, S.B. Thompson, C.D. McClure, S.M. Mehurg, F.G. Spinale, Plasma biomarkers that reflect determinants of matrix composition identify the presence of left ventricular hypertrophy and diastolic heart failure, *Circ Heart Fail*, 4 (2011) 246-256.

[231] W. Kuliczowski, J. Urbaniak, J. Hallen, M. Wozniak, L. Polonski, A. Mysiak, D. Atar, M. Zembala, V. Serebruany, Matrix metalloproteinases and the activity of their tissue inhibitors in patients with ST-elevation myocardial infarction treated with primary angioplasty, *Kardiol Pol*, 71 (2013) 453-463.

[232] R.A. Kowluru, G. Mohammad, J.M. dos Santos, Q. Zhong, Abrogation of MMP-9 gene protects against the development of retinopathy in diabetic mice by preventing mitochondrial damage, *Diabetes*, 60 (2011) 3023-3033.

[233] K.M. Thrailkill, C.S. Moreau, G.E. Cockrell, C.H. Jo, R.C. Bunn, A.E. Morales-Pozzo, C.K. Lumpkin, J.L. Fowlkes, Disease and gender-specific dysregulation of NGAL and MMP-9 in type 1 diabetes mellitus, *Endocrine*, 37 (2010) 336-343.

[234] T. Ishibashi, M. Kawaguchi, K. Sugimoto, H. Uekita, N. Sakamoto, K. Yokoyama, Y. Maruyama, Y. Takeishi, Advanced glycation end product-mediated matrix metalloproteinase-9 and apoptosis via renin-angiotensin system in type 2 diabetes, *J Atheroscler Thromb*, 17 (2010) 578-589.

[235] A.W. Chung, H.H. Yang, M.K. Sigrist, G. Brin, E. Chum, W.A. Gourlay, A. Levin, Matrix metalloproteinase-2 and -9 exacerbate arterial stiffening and angiogenesis in diabetes and chronic kidney disease, *Cardiovasc Res*, 84 (2009) 494-504.

[236] Y. Wang, Y. Su, Y. Xu, S.H. Pan, G.D. Liu, Genetic polymorphism c.1562C>T of the MMP-9 is associated with macroangiopathy in type 2 diabetes mellitus, *Biochem Biophys Res Commun*, 391 (2010) 113-117.

[237] R. Roy, J. Yang, M.A. Moses, Matrix metalloproteinases as novel biomarkers and potential therapeutic targets in human cancer, *J Clin Oncol*, 27 (2009) 5287-5297.

[238] G. Bergers, R. Brekken, G. McMahon, T.H. Vu, T. Itoh, K. Tamaki, K. Tanzawa, P. Thorpe, S. Itohara, Z. Werb, D. Hanahan, Matrix metalloproteinase-9 triggers the angiogenic switch during carcinogenesis, *Nat Cell Biol*, 2 (2000) 737-744.

[239] A. Noel, M. Jost, E. Maquoi, Matrix metalloproteinases at cancer tumor-host interface, *Semin Cell Dev Biol*, 19 (2008) 52-60.

[240] R. Kalluri, R.A. Weinberg, The basics of epithelial-mesenchymal transition, *J Clin Invest*, 119 (2009) 1420-1428.

[241] I. Stamenkovic, Extracellular matrix remodelling: the role of matrix metalloproteinases, *J Pathol*, 200 (2003) 448-464.

[242] L.M. Coussens, Z. Werb, Matrix metalloproteinases and the development of cancer, *Chem Biol*, 3 (1996) 895-904.

[243] S. Vosseler, W. Lederle, K. Airola, E. Obermueller, N.E. Fusenig, M.M. Mueller, Distinct progression-associated expression of tumor and stromal MMPs in HaCaT skin SCCs correlates with onset of invasion, *Int J Cancer*, 125 (2009) 2296-2306.

[244] A. Kruger, M.J. Arlt, M. Gerg, C. Kopitz, M.M. Bernardo, M. Chang, S. Mobashery, R. Fridman, Antimetastatic activity of a novel mechanism-based gelatinase inhibitor, *Cancer Res*, 65 (2005) 3523-3526.

[245] G. Batist, F. Patenaude, P. Champagne, D. Croteau, C. Levinton, C. Hariton, B. Escudier, E. Dupont, Neovastat (AE-941) in refractory renal cell carcinoma patients: report of a phase II trial with two dose levels, *Ann Oncol*, 13 (2002) 1259-1263.

[246] X. Li, J.F. Wu, Recent developments in patent anti-cancer agents targeting the matrix metalloproteinases (MMPs), *Recent Pat Anticancer Drug Discov*, 5 (2010) 109-141.



- [247] V.L. Gadd, M. Melino, S. Roy, L. Horsfall, P. O'Rourke, M.R. Williams, K.M. Irvine, M.J. Sweet, J.R. Jonsson, A.D. Clouston, E.E. Powell, Portal, but not lobular, macrophages express matrix metalloproteinase-9: association with the ductular reaction and fibrosis in chronic hepatitis C, *Liver Int*, 33 (2013) 569-579.
- [248] T. Hori, S. Uemoto, L.B. Walden, F. Chen, A.M. Baine, T. Hata, T. Kogure, J.H. Nguyen, Matrix metalloproteinase-9 as a therapeutic target for the progression of fulminant liver failure with hepatic encephalopathy: A pilot study in mice, *Hepatol Res*, (2013).
- [249] J.P. Tsai, J.H. Liou, W.T. Kao, S.C. Wang, J.D. Lian, H.R. Chang, Increased expression of intranuclear matrix metalloproteinase 9 in atrophic renal tubules is associated with renal fibrosis, *PLoS One*, 7 (2012) e48164.
- [250] K.A. Czech, M. Bennett, P. Devarajan, Distinct metalloproteinase excretion patterns in focal segmental glomerulosclerosis, *Pediatr Nephrol*, 26 (2011) 2179-2184.
- [251] J.S. Beckman, W.H. Koppenol, Nitric oxide, superoxide, and peroxynitrite: the good, the bad, and ugly, *Am J Physiol*, 271 (1996) C1424-1437.
- [252] S.R. Vincent, Nitric oxide neurons and neurotransmission, *Prog Neurobiol*, 90 (2010) 246-255.
- [253] D. Chakravorty, M. Hensel, Inducible nitric oxide synthase and control of intracellular bacterial pathogens, *Microbes Infect*, 5 (2003) 621-627.
- [254] J.R. Kanwar, R.K. Kanwar, H. Burrow, S. Baratchi, Recent advances on the roles of NO in cancer and chronic inflammatory disorders, *Curr Med Chem*, 16 (2009) 2373-2394.
- [255] H. Rubbo, V. Darley-Usmar, B.A. Freeman, Nitric oxide regulation of tissue free radical injury, *Chem Res Toxicol*, 9 (1996) 809-820.
- [256] J. Pfeilschifter, W. Eberhardt, K.F. Beck, Regulation of gene expression by nitric oxide, *Pflugers Arch*, 442 (2001) 479-486.
- [257] R.J. Gryglewski, R.M. Palmer, S. Moncada, Superoxide anion is involved in the breakdown of endothelium-derived vascular relaxing factor, *Nature*, 320 (1986) 454-456.
- [258] L. Castro, M. Rodriguez, R. Radi, Aconitase is readily inactivated by peroxynitrite, but not by its precursor, nitric oxide, *J Biol Chem*, 269 (1994) 29409-29415.
- [259] T. Okamoto, T. Akaike, T. Nagano, S. Miyajima, M. Suga, M. Ando, K. Ichimori, H. Maeda, Activation of human neutrophil procollagenase by nitrogen dioxide and peroxynitrite: a novel mechanism for procollagenase activation involving nitric oxide, *Arch Biochem Biophys*, 342 (1997) 261-274.
- [260] J.B. Hibbs, Jr., R.R. Taintor, Z. Vavrin, Macrophage cytotoxicity: role for L-arginine deiminase and imino nitrogen oxidation to nitrite, *Science*, 235 (1987) 473-476.
- [261] R. Radi, M. Rodriguez, L. Castro, R. Telleri, Inhibition of mitochondrial electron transport by peroxynitrite, *Arch Biochem Biophys*, 308 (1994) 89-95.
- [262] M.A. Moro, V.M. Darley-Usmar, D.A. Goodwin, N.G. Read, R. Zamora-Pino, M. Feelisch, M.W. Radomski, S. Moncada, Paradoxical fate and biological action of peroxynitrite on human platelets, *Proc Natl Acad Sci U S A*, 91 (1994) 6702-6706.
- [263] L.M. Villa, E. Salas, V.M. Darley-Usmar, M.W. Radomski, S. Moncada, Peroxynitrite induces both vasodilatation and impaired vascular relaxation in the isolated perfused rat heart, *Proc Natl Acad Sci U S A*, 91 (1994) 12383-12387.
- [264] R. Radi, J.S. Beckman, K.M. Bush, B.A. Freeman, Peroxynitrite oxidation of sulfhydryls. The cytotoxic potential of superoxide and nitric oxide, *J Biol Chem*, 266 (1991) 4244-4250.
- [265] H. Rubbo, A. Denicola, R. Radi, Peroxynitrite inactivates thiol-containing enzymes of *Trypanosoma cruzi* energetic metabolism and inhibits cell respiration, *Arch Biochem Biophys*, 308 (1994) 96-102.



- [266] J.P. Crow, J.S. Beckman, J.M. McCord, Sensitivity of the essential zinc-thiolate moiety of yeast alcohol dehydrogenase to hypochlorite and peroxynitrite, *Biochemistry*, 34 (1995) 3544-3552.
- [267] H. Ischiropoulos, L. Zhu, J. Chen, M. Tsai, J.C. Martin, C.D. Smith, J.S. Beckman, Peroxynitrite-mediated tyrosine nitration catalyzed by superoxide dismutase, *Arch Biochem Biophys*, 298 (1992) 431-437.
- [268] B. Alvarez, R. Radi, Peroxynitrite reactivity with amino acids and proteins, *Amino Acids*, 25 (2003) 295-311.
- [269] O. Augusto, M.G. Bonini, A.M. Amanso, E. Linares, C.C. Santos, S.L. De Menezes, Nitrogen dioxide and carbonate radical anion: two emerging radicals in biology, *Free Radic Biol Med*, 32 (2002) 841-859.
- [270] R. Radi, Peroxynitrite reactions and diffusion in biology, *Chem Res Toxicol*, 11 (1998) 720-721.
- [271] H.T. Chung, H.O. Pae, B.M. Choi, T.R. Billiar, Y.M. Kim, Nitric oxide as a bioregulator of apoptosis, *Biochem Biophys Res Commun*, 282 (2001) 1075-1079.
- [272] J.S. Beckman, T.W. Beckman, J. Chen, P.A. Marshall, B.A. Freeman, Apparent hydroxyl radical production by peroxynitrite: implications for endothelial injury from nitric oxide and superoxide, *Proc Natl Acad Sci U S A*, 87 (1990) 1620-1624.
- [273] J.B. Mannick, C.M. Schonhoff, Nitrosylation: the next phosphorylation?, *Arch Biochem Biophys*, 408 (2002) 1-6.
- [274] B.J. Whittle, Nitric oxide and the gut injury induced by non-steroidal anti-inflammatory drugs, *Inflammopharmacology*, 11 (2003) 415-422.
- [275] T.L. Wellman, J. Jenkins, P.L. Penar, B. Tranmer, R. Zahr, K.M. Lounsbury, Nitric oxide and reactive oxygen species exert opposing effects on the stability of hypoxia-inducible factor-1alpha (HIF-1alpha) in explants of human pial arteries, *FASEB J*, 18 (2004) 379-381.
- [276] S.B. Abramson, Nitric oxide in inflammation and pain associated with osteoarthritis, *Arthritis Res Ther*, 10 Suppl 2 (2008) S2.
- [277] M.A. Moro, V.M. Darley-Usmar, I. Lizasoain, Y. Su, R.G. Knowles, M.W. Radomski, S. Moncada, The formation of nitric oxide donors from peroxynitrite, *Br J Pharmacol*, 116 (1995) 1999-2004.
- [278] E. Darra, A. Rungatscher, A. Carcereri de Prati, B.K. Podesser, G. Faggian, T. Scarabelli, A. Mazzucco, S. Hallstrom, H. Suzuki, Dual modulation of nitric oxide production in the heart during ischaemia/reperfusion injury and inflammation, *Thromb Haemost*, 104 (2010) 200-206.
- [279] G.A. Blaise, D. Gauvin, M. Gangal, S. Authier, Nitric oxide, cell signaling and cell death, *Toxicology*, 208 (2005) 177-192.
- [280] S. Moochhala, V.J. Chhatwal, S.T. Chan, S.S. Ngoi, Y.W. Chia, A. Rauff, Nitric oxide synthase activity and expression in human colorectal cancer, *Carcinogenesis*, 17 (1996) 1171-1174.
- [281] J.C. Toledo, Jr., O. Augusto, Connecting the chemical and biological properties of nitric oxide, *Chem Res Toxicol*, 25 (2012) 975-989.
- [282] A. Perner, J. Rask-Madsen, Review article: the potential role of nitric oxide in chronic inflammatory bowel disorders, *Aliment Pharmacol Ther*, 13 (1999) 135-144.
- [283] K. Palatka, Z. Serfozo, Z. Vereb, Z. Hargitay, B. Lontay, F. Erdodi, G. Banfalvi, Z. Nemes, M. Udvardy, I. Altorjay, Changes in the expression and distribution of the inducible and endothelial nitric oxide synthase in mucosal biopsy specimens of inflammatory bowel disease, *Scand J Gastroenterol*, 40 (2005) 670-680.



- [284] C.M. Hogaboam, K. Jacobson, S.M. Collins, M.G. Blennerhassett, The selective beneficial effects of nitric oxide inhibition in experimental colitis, *Am J Physiol*, 268 (1995) G673-684.
- [285] J. Kiss, D. Lamarque, J.C. Delchier, B.J. Whittle, Time-dependent actions of nitric oxide synthase inhibition on colonic inflammation induced by trinitrobenzene sulphonic acid in rats, *Eur J Pharmacol*, 336 (1997) 219-224.
- [286] H. Nakamura, H. Tsukada, M. Oya, M. Onomura, T. Saito, K. Fukuda, M. Kodama, T. Taniguchi, M. Tominaga, M. Hosokawa, Y. Seino, Aminoguanidine has both an anti-inflammatory effect on experimental colitis and a proliferative effect on colonic mucosal cells, *Scand J Gastroenterol*, 34 (1999) 1117-1122.
- [287] N. Dikopoulos, A.K. Nussler, S. Liptay, M. Bachem, M. Reinshagen, M. Stiegler, R.M. Schmid, G. Adler, H. Weidenbach, Inhibition of nitric oxide synthesis by aminoguanidine increases intestinal damage in the acute phase of rat TNB-colitis, *Eur J Clin Invest*, 31 (2001) 234-239.
- [288] T. Yamaguchi, N. Yoshida, E. Ichiishi, N. Sugimoto, Y. Naito, T. Yoshikawa, Differing effects of two nitric oxide synthase inhibitors on experimental colitis, *Hepatology*, 48 (2001) 118-122.
- [289] R. Hokari, S. Kato, K. Matsuzaki, M. Kuroki, A. Iwai, A. Kawaguchi, S. Nagao, T. Miyahara, K. Itoh, E. Sekizuka, H. Nagata, H. Ishii, S. Miura, Reduced sensitivity of inducible nitric oxide synthase-deficient mice to chronic colitis, *Free Radic Biol Med*, 31 (2001) 153-163.
- [290] C.F. Krieglstein, W.H. Cerwinka, F.S. Laroux, J.W. Salter, J.M. Russell, G. Schuermann, M.B. Grisham, C.R. Ross, D.N. Granger, Regulation of murine intestinal inflammation by reactive metabolites of oxygen and nitrogen: divergent roles of superoxide and nitric oxide, *J Exp Med*, 194 (2001) 1207-1218.
- [291] B. Zingarelli, C. Szabo, A.L. Salzman, Reduced oxidative and nitrosative damage in murine experimental colitis in the absence of inducible nitric oxide synthase, *Gut*, 45 (1999) 199-209.
- [292] D. Rachmilewitz, J.S. Stampler, F. Karmeli, M.E. Mullins, D.J. Singel, J. Loscalzo, R.J. Xavier, D.K. Podolsky, Peroxynitrite-induced rat colitis--a new model of colonic inflammation, *Gastroenterology*, 105 (1993) 1681-1688.
- [293] S. Cuzzocrea, E. Mazzon, L. Dugo, A.P. Caputi, D.P. Riley, D. Salvemini, Protective effects of M40403, a superoxide dismutase mimetic, in a rodent model of colitis, *Eur J Pharmacol*, 432 (2001) 79-89.
- [294] B. Zingarelli, S. Cuzzocrea, C. Szabo, A.L. Salzman, Mercaptoethylguanidine, a combined inhibitor of nitric oxide synthase and peroxynitrite scavenger, reduces trinitrobenzene sulfonic acid-induced colonic damage in rats, *J Pharmacol Exp Ther*, 287 (1998) 1048-1055.
- [295] A. Kruger, R.E. Kates, D.R. Edwards, Avoiding spam in the proteolytic internet: future strategies for anti-metastatic MMP inhibition, *Biochim Biophys Acta*, 1803 (2010) 95-102.
- [296] A. Tochowicz, K. Maskos, R. Huber, R. Oltenfreiter, V. Dive, A. Yiotakis, M. Zanda, T. Pourmotabbed, W. Bode, P. Goettig, Crystal structures of MMP-9 complexes with five inhibitors: contribution of the flexible Arg424 side-chain to selectivity, *J Mol Biol*, 371 (2007) 989-1006.
- [297] N. Marsh, A. Marsh, A short history of nitroglycerine and nitric oxide in pharmacology and physiology, *Clin Exp Pharmacol Physiol*, 27 (2000) 313-319.
- [298] N. Fiotti, N. Altamura, M. Moretti, S. Wassermann, S. Zacchigna, R. Farra, B. Dapas, L. Consoloni, M. Giacca, G. Grassi, C. Giansante, Short term effects of



- doxycycline on matrix metalloproteinases 2 and 9, *Cardiovasc Drugs Ther*, 23 (2009) 153-159.
- [299] A.S. Krishnatry, T. Kamei, H. Wang, J. Qu, H.L. Fung, Identification of nitroglycerin-induced cysteine modifications of pro-matrix metalloproteinase-9, *Rapid Commun Mass Spectrom*, 25 (2011) 2291-2298.
- [300] A.S. Krishnatry, S.M. Fung, D.A. Brazeau, D. Soda, H.L. Fung, Nitroglycerin alters matrix remodeling proteins in THP-1 human macrophages and plasma metalloproteinase activity in rats, *Nitric Oxide*, 24 (2011) 66-76.
- [301] A.K. Death, S. Nakhla, K.C. McGrath, S. Martell, D.K. Yue, W. Jessup, D.S. Celermajer, Nitroglycerin upregulates matrix metalloproteinase expression by human macrophages, *J Am Coll Cardiol*, 39 (2002) 1943-1950.
- [302] B. Rigas, K. Kashfi, Nitric-oxide-donating NSAIDs as agents for cancer prevention, *Trends Mol Med*, 10 (2004) 324-330.
- [303] R.K. Yeh, J. Chen, J.L. Williams, M. Baluch, T.R. Hundley, R.E. Rosenbaum, S. Kalala, F. Traganos, F. Benardini, P. del Soldato, K. Kashfi, B. Rigas, NO-donating nonsteroidal antiinflammatory drugs (NSAIDs) inhibit colon cancer cell growth more potently than traditional NSAIDs: a general pharmacological property?, *Biochem Pharmacol*, 67 (2004) 2197-2205.
- [304] J.L. Williams, K. Kashfi, N. Ouyang, P. del Soldato, L. Kopelovich, B. Rigas, NO-donating aspirin inhibits intestinal carcinogenesis in Min (APC(Min/+)) mice, *Biochem Biophys Res Commun*, 313 (2004) 784-788.
- [305] G.R. Thatcher, A.C. Nicolescu, B.M. Bennett, V. Toader, Nitrates and NO release: contemporary aspects in biological and medicinal chemistry, *Free Radic Biol Med*, 37 (2004) 1122-1143.
- [306] J.E. Keeble, P.K. Moore, Pharmacology and potential therapeutic applications of nitric oxide-releasing non-steroidal anti-inflammatory and related nitric oxide-donating drugs, *Br J Pharmacol*, 137 (2002) 295-310.
- [307] S. Fiorucci, E. Antonelli, E. Distrutti, P. Del Soldato, R.J. Flower, M.J. Clark, A. Morelli, M. Perretti, L.J. Ignarro, NCX-1015, a nitric-oxide derivative of prednisolone, enhances regulatory T cells in the lamina propria and protects against 2,4,6-trinitrobenzene sulfonic acid-induced colitis in mice, *Proc Natl Acad Sci U S A*, 99 (2002) 15770-15775.
- [308] M.J. Paul-Clark, L. Mancini, P. Del Soldato, R.J. Flower, M. Perretti, Potent antiarthritic properties of a glucocorticoid derivative, NCX-1015, in an experimental model of arthritis, *Proc Natl Acad Sci U S A*, 99 (2002) 1677-1682.
- [309] F. Turesin, P. del Soldato, J.L. Wallace, Enhanced anti-inflammatory potency of a nitric oxide-releasing prednisolone derivative in the rat, *Br J Pharmacol*, 139 (2003) 966-972.
- [310] V. Lagente, C. Advenier, New nitric oxide-donating drugs for the treatment of airway diseases, *Curr Opin Investig Drugs*, 5 (2004) 537-541.
- [311] V. Lagente, E. Naline, I. Guenon, M. Corbel, E. Boichot, J.L. Burgaud, P. Del Soldato, C. Advenier, A nitric oxide-releasing salbutamol elicits potent relaxant and anti-inflammatory activities, *J Pharmacol Exp Ther*, 310 (2004) 367-375.
- [312] D.L. Turner, N. Ferrari, W.R. Ford, E.J. Kidd, L. Paquet, P. Renzi, K.J. Broadley, TPI 1020, a novel anti-inflammatory, nitric oxide donating compound, potentiates the bronchodilator effects of salbutamol in conscious guinea-pigs, *Eur J Pharmacol*, 641 (2010) 213-219.
- [313] S. O'Sullivan, C. Medina, M. Ledwidge, M.W. Radomski, J.F. Gilmer, Nitric oxide-matrix metalloproteinase-9 interactions: Biological and pharmacological significance: NO and MMP-9 interactions, *Biochim Biophys Acta*, 1843 (2013) 603-617.



- [314] J. Wang, C. Medina, M.W. Radomski, J.F. Gilmer, N-substituted homopiperazine barbiturates as gelatinase inhibitors, *Bioorg Med Chem*, 19 (2011) 4985-4999.
- [315] J. Wang, S. O'Sullivan, S. Harmon, R. Keaveny, M.W. Radomski, C. Medina, J.F. Gilmer, Design of barbiturate-nitrate hybrids that inhibit MMP-9 activity and secretion, *J Med Chem*, 55 (2012) 2154-2162.
- [316] M. Perse, A. Cerar, Dextran sodium sulphate colitis mouse model: traps and tricks, *J Biomed Biotechnol*, 2012 (2012) 718617.
- [317] H.S. Cooper, S.N. Murthy, R.S. Shah, D.J. Sedergran, Clinicopathologic study of dextran sulfate sodium experimental murine colitis, *Lab Invest*, 69 (1993) 238-249.
- [318] M. Suzanne, H. Steller, Shaping organisms with apoptosis, *Cell Death Differ*, 20 (2013) 669-675.
- [319] G.A. Whitlock, K.N. Dack, D.R. Dickinson, M.L. Lewis, A novel series of highly selective inhibitors of MMP-3, *Bioorg Med Chem Lett*, 17 (2007) 6750-6753.
- [320] H.J. Breyholz, M. Schäfers, S. Wagner, C. Höltke, A. Faust, H. Rabeneck, B. Levkau, e. al., C-5-disubstituted barbiturates as potential molecular probes for noninvasive matrix metalloproteinase imaging, *J Med Chem*, 48 (2005) 3400-3409.
- [321] J.C. Oliveros, Venny. An interactive tool for comparing lists with Venn Diagrams, in, 2007.
- [322] C. Li, W.H. Wong, Model-based analysis of oligonucleotide arrays: expression index computation and outlier detection, *Proc Natl Acad Sci U S A*, 98 (2001) 31-36.
- [323] K.M. Miranda, M.G. Espey, D.A. Wink, A rapid, simple spectrophotometric method for simultaneous detection of nitrate and nitrite, *Nitric Oxide*, 5 (2001) 62-71.
- [324] S.I. Gutman, C.A. Hollywood, Simple, rapid method for determining nitrates and nitrites in biological fluids, *Clin Chem*, 38 (1992) 2152.
- [325] M. Marzinzig, A.K. Nussler, J.S. Stadler, e. al., Improved methods to measure end products of nitric oxide in biological fluids: nitrite, nitrate, and S-Nitrosothiols., *Nitric Oxide*, 1 (1997) 177-189.
- [326] M.D. Martin, L.M. Matrisian, The other side of MMPs: protective roles in tumor progression, *Cancer Metastasis Rev*, 26 (2007) 717-724.
- [327] M.R. Miller, I.L. Megson, Recent developments in nitric oxide donor drugs, *Br J Pharmacol*, 151 (2007) 305-321.
- [328] S. Huerta, S. Chilka, B. Bonavida, Nitric oxide donors: novel cancer therapeutics (review), *Int J Oncol*, 33 (2008) 909-927.
- [329] A. Radomski, G. Sawicki, D.M. Olson, M.W. Radomski, The role of nitric oxide and metalloproteinases in the pathogenesis of hyperoxia-induced lung injury in newborn rats, *Br J Pharmacol*, 125 (1998) 1455-1462.
- [330] I. Mayers, T. Hurst, L. Puttagunta, A. Radomski, T. Mycyk, G. Sawicki, D. Johnson, M.W. Radomski, Cardiac surgery increases the activity of matrix metalloproteinases and nitric oxide synthase in human hearts, *J Thorac Cardiovasc Surg*, 122 (2001) 746-752.
- [331] I. Mayers, T. Hurst, A. Radomski, D. Johnson, S. Fricker, G. Bridger, B. Cameron, M. Darkes, M.W. Radomski, Increased matrix metalloproteinase activity after canine cardiopulmonary bypass is suppressed by a nitric oxide scavenger, *J Thorac Cardiovasc Surg*, 125 (2003) 661-668.
- [332] J. Vandooren, N. Geurts, E. Martens, P.E. Van den Steen, G. Opdenakker, Zymography methods for visualizing hydrolytic enzymes, *Nat Methods*, 10 (2013) 211-220.
- [333] Z. Zhang, J.K. Kolls, P. Oliver, D. Good, P.O. Schwarzenberger, M.S. Joshi, J.L. Ponthier, J.R. Lancaster, Jr., Activation of tumor necrosis factor-alpha-converting enzyme-mediated ectodomain shedding by nitric oxide, *J Biol Chem*, 275 (2000) 15839-15844.



- [334] S. Viappiani, A.C. Nicolescu, A. Holt, G. Sawicki, B.D. Crawford, H. Leon, T. van Mulligen, R. Schulz, Activation and modulation of 72kDa matrix metalloproteinase-2 by peroxynitrite and glutathione, *Biochem Pharmacol*, 77 (2009) 826-834.
- [335] K. Migita, Y. Maeda, S. Abiru, A. Komori, T. Yokoyama, Y. Takii, M. Nakamura, H. Yatsushashi, K. Eguchi, H. Ishibashi, Peroxynitrite-mediated matrix metalloproteinase-2 activation in human hepatic stellate cells, *FEBS Lett*, 579 (2005) 3119-3125.
- [336] H. Saari, K. Suomalainen, O. Lindy, Y.T. Konttinen, T. Sorsa, Activation of latent human neutrophil collagenase by reactive oxygen species and serine proteases, *Biochem Biophys Res Commun*, 171 (1990) 979-987.
- [337] L. Jia, C. Bonaventura, J. Bonaventura, J.S. Stamler, S-nitrosohaemoglobin: a dynamic activity of blood involved in vascular control, *Nature*, 380 (1996) 221-226.
- [338] Y.B. Choi, L. Tanneti, D.A. Le, J. Ortiz, G. Bai, H.S. Chen, S.A. Lipton, Molecular basis of NMDA receptor-coupled ion channel modulation by S-nitrosylation, *Nat Neurosci*, 3 (2000) 15-21.
- [339] S.R. Jaffrey, H. Erdjument-Bromage, C.D. Ferris, P. Tempst, S.H. Snyder, Protein S-nitrosylation: a physiological signal for neuronal nitric oxide, *Nat Cell Biol*, 3 (2001) 193-197.
- [340] J.R. Matthews, C.H. Botting, M. Panico, H.R. Morris, R.T. Hay, Inhibition of NF-kappaB DNA binding by nitric oxide, *Nucleic Acids Res*, 24 (1996) 2236-2242.
- [341] D. Berendji, V. Kolb-Bachofen, K.L. Meyer, O. Grapenthin, H. Weber, V. Wahn, K.D. Kroncke, Nitric oxide mediates intracytoplasmic and intranuclear zinc release, *FEBS Lett*, 405 (1997) 37-41.
- [342] C.M. St Croix, K.J. Wasserloos, K.E. Dineley, I.J. Reynolds, E.S. Levitan, B.R. Pitt, Nitric oxide-induced changes in intracellular zinc homeostasis are mediated by metallothionein/thionein, *Am J Physiol Lung Cell Mol Physiol*, 282 (2002) L185-192.
- [343] S. Manabe, Z. Gu, S.A. Lipton, Activation of matrix metalloproteinase-9 via neuronal nitric oxide synthase contributes to NMDA-induced retinal ganglion cell death, *Invest Ophthalmol Vis Sci*, 46 (2005) 4747-4753.
- [344] H.H. Wang, H.L. Hsieh, C.M. Yang, Nitric oxide production by endothelin-1 enhances astrocytic migration via the tyrosine nitration of matrix metalloproteinase-9, *J Cell Physiol*, 226 (2011) 2244-2256.
- [345] L.A. Ridnour, A.N. Windhausen, J.S. Isenberg, N. Yeung, D.D. Thomas, M.P. Vitek, D.D. Roberts, D.A. Wink, Nitric oxide regulates matrix metalloproteinase-9 activity by guanylyl-cyclase-dependent and -independent pathways, *Proc Natl Acad Sci U S A*, 104 (2007) 16898-16903.
- [346] P. Pacher, J.S. Beckman, L. Liaudet, Nitric oxide and peroxynitrite in health and disease, *Physiol Rev*, 87 (2007) 315-424.
- [347] S. Rajagopalan, X.P. Meng, S. Ramasamy, D.G. Harrison, Z.S. Galis, Reactive oxygen species produced by macrophage-derived foam cells regulate the activity of vascular matrix metalloproteinases in vitro. Implications for atherosclerotic plaque stability, *J Clin Invest*, 98 (1996) 2572-2579.
- [348] M.W. Owens, S.A. Milligan, D. Jourdeuil, M.B. Grisham, Effects of reactive metabolites of oxygen and nitrogen on gelatinase A activity, *Am J Physiol*, 273 (1997) L445-450.
- [349] K. Egi, N.E. Conrad, J. Kwan, C. Schulze, R. Schulz, S.M. Wildhirt, Inhibition of inducible nitric oxide synthase and superoxide production reduces matrix metalloproteinase-9 activity and restores coronary vasomotor function in rat cardiac allografts, *Eur J Cardiothorac Surg*, 26 (2004) 262-269.



- [350] E. Capobianco, V. White, M. Sosa, I. Di Marco, M.N. Basualdo, M.C. Faingold, A. Jawerbaum, Regulation of matrix metalloproteinases 2 and 9 activities by peroxynitrites in term placentas from type 2 diabetic patients, *Reprod Sci*, 19 (2012) 814-822.
- [351] T. Okamoto, T. Akaike, T. Sawa, Y. Miyamoto, A. van der Vliet, H. Maeda, Activation of matrix metalloproteinases by peroxynitrite-induced protein S-glutathiolation via disulfide S-oxide formation, *J Biol Chem*, 276 (2001) 29596-29602.
- [352] Y. Suofu, J. Clark, J. Broderick, K.R. Wagner, T. Tomsick, Y. Sa, A. Lu, Peroxynitrite decomposition catalyst prevents matrix metalloproteinase activation and neurovascular injury after prolonged cerebral ischemia in rats, *J Neurochem*, 115 (2010) 1266-1276.
- [353] P.F. Bove, U.V. Wesley, A.K. Greul, M. Hristova, W.R. Dostmann, A. van der Vliet, Nitric oxide promotes airway epithelial wound repair through enhanced activation of MMP-9, *Am J Respir Cell Mol Biol*, 36 (2007) 138-146.
- [354] P.G. Phillips, L.M. Birnby, Nitric oxide modulates caveolin-1 and matrix metalloproteinase-9 expression and distribution at the endothelial cell/tumor cell interface, *Am J Physiol Lung Cell Mol Physiol*, 286 (2004) L1055-1065.
- [355] S.M. McCarthy, P.F. Bove, D.E. Matthews, T. Akaike, A. van der Vliet, Nitric oxide regulation of MMP-9 activation and its relationship to modifications of the cysteine switch, *Biochemistry*, 47 (2008) 5832-5840.
- [356] J.R. Hickok, D. Vasudevan, G.R. Thatcher, D.D. Thomas, Is S-nitrosocysteine a true surrogate for nitric oxide?, *Antioxid Redox Signal*, 17 (2012) 962-968.
- [357] Z. Werb, ECM and cell surface proteolysis: regulating cellular ecology, *Cell*, 91 (1997) 439-442.
- [358] P. Gaudin, S. Berthier, C. Barro, P. Zaoui, F. Morel, Proteolytic potential of human neutrophil membranes, *Eur J Cell Biol*, 72 (1997) 345-351.
- [359] M.W. Olson, M. Toth, D.C. Gervasi, Y. Sado, Y. Ninomiya, R. Fridman, High affinity binding of latent matrix metalloproteinase-9 to the alpha2(IV) chain of collagen IV, *J Biol Chem*, 273 (1998) 10672-10681.
- [360] M. Nguyen, J. Arkell, C.J. Jackson, Active and tissue inhibitor of matrix metalloproteinase-free gelatinase B accumulates within human microvascular endothelial vesicles, *J Biol Chem*, 273 (1998) 5400-5404.
- [361] G. Taraboletti, S. D'Ascenzo, P. Borsotti, R. Giavazzi, A. Pavan, V. Dolo, Shedding of the matrix metalloproteinases MMP-2, MMP-9, and MT1-MMP as membrane vesicle-associated components by endothelial cells, *Am J Pathol*, 160 (2002) 673-680.
- [362] P. Rouet-Benzineb, J.M. Buhler, P. Dreyfus, A. Delcourt, R. Dorent, J. Perennec, B. Crozatier, A. Harf, C. Lafuma, Altered balance between matrix gelatinases (MMP-2 and MMP-9) and their tissue inhibitors in human dilated cardiomyopathy: potential role of MMP-9 in myosin-heavy chain degradation, *Eur J Heart Fail*, 1 (1999) 337-352.
- [363] M.M. Lalu, C.Q. Gao, R. Schulz, Matrix metalloproteinase inhibitors attenuate endotoxemia induced cardiac dysfunction: a potential role for MMP-9, *Mol Cell Biochem*, 251 (2003) 61-66.
- [364] N.L. Bautista-Lopez, C.A. Morillo, P. Lopez-Jaramillo, R. Quiroz, C. Luengas, S.Y. Silva, J. Galipeau, M.M. Lalu, R. Schulz, Matrix metalloproteinases 2 and 9 as diagnostic markers in the progression to Chagas cardiomyopathy, *Am Heart J*, 165 (2013) 558-566.
- [365] M. Makela, T. Salo, H. Larjava, MMP-9 from TNF alpha-stimulated keratinocytes binds to cell membranes and type I collagen: a cause for extended matrix degradation in inflammation?, *Biochem Biophys Res Commun*, 253 (1998) 325-335.
- [366] M. Toth, D.C. Gervasi, R. Fridman, Phorbol ester-induced cell surface association of matrix metalloproteinase-9 in human MCF10A breast epithelial cells, *Cancer Res*, 57 (1997) 3159-3167.



- [367] E. Mira, S. Manes, R.A. Lacalle, G. Marquez, A.C. Martinez, Insulin-like growth factor I-triggered cell migration and invasion are mediated by matrix metalloproteinase-9, *Endocrinology*, 140 (1999) 1657-1664.
- [368] S. Zucker, U.M. Moll, R.M. Lysik, E.I. DiMassimo, J.W. Schwedes, L.A. Liotta, Extraction of type IV collagenase/gelatinase from plasma membranes of human pancreatic cancer cells, *Matrix Suppl*, 1 (1992) 411.
- [369] S.M. Ellerbroek, J.M. Halbleib, M. Benavidez, J.K. Warmka, E.V. Wattenberg, M.S. Stack, L.G. Hudson, Phosphatidylinositol 3-kinase activity in epidermal growth factor-stimulated matrix metalloproteinase-9 production and cell surface association, *Cancer Res*, 61 (2001) 1855-1861.
- [370] C. Festuccia, A. Angelucci, G.L. Gravina, I. Villanova, A. Teti, A. Albini, M. Bologna, Osteoblast-derived TGF-beta1 modulates matrix degrading protease expression and activity in prostate cancer cells, *Int J Cancer*, 85 (2000) 407-415.
- [371] A. Ginestra, S. Monea, G. Seghezzi, V. Dolo, H. Nagase, P. Mignatti, M.L. Vittorelli, Urokinase plasminogen activator and gelatinases are associated with membrane vesicles shed by human HT1080 fibrosarcoma cells, *J Biol Chem*, 272 (1997) 17216-17222.
- [372] R. Mazzieri, L. Masiero, L. Zanetta, S. Monea, M. Onisto, S. Garbisa, P. Mignatti, Control of type IV collagenase activity by components of the urokinase-plasmin system: a regulatory mechanism with cell-bound reactants, *EMBO J*, 16 (1997) 2319-2332.
- [373] Q. Yu, I. Stamenkovic, Localization of matrix metalloproteinase 9 to the cell surface provides a mechanism for CD44-mediated tumor invasion, *Genes Dev*, 13 (1999) 35-48.
- [374] G. Murphy, H. Nagase, Localizing matrix metalloproteinase activities in the pericellular environment, *FEBS J*, 278 (2011) 2-15.
- [375] L. Kjeldsen, J.B. Cowland, N. Borregaard, Human neutrophil gelatinase-associated lipocalin and homologous proteins in rat and mouse, *Biochim Biophys Acta*, 1482 (2000) 272-283.
- [376] G. Sawicki, E. Salas, J. Murat, H. Miszta-Lane, M.W. Radomski, Release of gelatinase A during platelet activation mediates aggregation, *Nature*, 386 (1997) 616-619.
- [377] V. Novaro, A. Colman-Lerner, F.V. Ortega, A. Jawerbaum, D. Paz, F. Lo Nostro, C. Pustovrh, M.F. Gimeno, E. Gonzalez, Regulation of metalloproteinases by nitric oxide in human trophoblast cells in culture, *Reprod Fertil Dev*, 13 (2001) 411-420.
- [378] L.K. Harris, J. McCormick, J.E. Cartwright, G.S. Whitley, P.R. Dash, S-nitrosylation of proteins at the leading edge of migrating trophoblasts by inducible nitric oxide synthase promotes trophoblast invasion, *Exp Cell Res*, 314 (2008) 1765-1776.
- [379] W.J. Lubbe, D.S. Zuzga, Z. Zhou, W. Fu, J. Pelta-Heller, R.J. Muschel, S.A. Waldman, G.M. Pitari, Guanylyl cyclase C prevents colon cancer metastasis by regulating tumor epithelial cell matrix metalloproteinase-9, *Cancer Res*, 69 (2009) 3529-3536.
- [380] A.K. Witkiewicz, A. Dasgupta, F. Sotgia, I. Mercier, R.G. Pestell, M. Sabel, C.G. Kleer, J.R. Brody, M.P. Lisanti, An absence of stromal caveolin-1 expression predicts early tumor recurrence and poor clinical outcome in human breast cancers, *Am J Pathol*, 174 (2009) 2023-2034.
- [381] K. Wiechen, C. Sers, A. Agoulnik, K. Arlt, M. Dietel, P.M. Schlag, U. Schneider, Down-regulation of caveolin-1, a candidate tumor suppressor gene, in sarcomas, *Am J Pathol*, 158 (2001) 833-839.
- [382] H. Wikman, E. Kettunen, J.K. Seppanen, A. Karjalainen, J. Hollmen, S. Anttila, S. Knuutila, Identification of differentially expressed genes in pulmonary adenocarcinoma by using cDNA array, *Oncogene*, 21 (2002) 5804-5813.



- [383] H.J. Joo, D.K. Oh, Y.S. Kim, K.B. Lee, S.J. Kim, Increased expression of caveolin-1 and microvessel density correlates with metastasis and poor prognosis in clear cell renal cell carcinoma, *BJU Int*, 93 (2004) 291-296.
- [384] V. Barresi, S. Cerasoli, G. Tuccari, Correlative evidence that tumor cell-derived caveolin-1 mediates angiogenesis in meningiomas, *Neuropathology*, 28 (2008) 472-478.
- [385] K.C. Moon, G.K. Lee, S.H. Yoo, Y.K. Jeon, J.H. Chung, J. Han, D.H. Chung, Expression of caveolin-1 in pleomorphic carcinoma of the lung is correlated with a poor prognosis, *Anticancer Res*, 25 (2005) 4631-4637.
- [386] H.N. Choi, K.R. Kim, H.S. Park, K.Y. Jang, M.J. Kang, D.G. Lee, Y.K. Kim, B.H. Cho, E.J. Cha, W.S. Moon, [Expression of caveolin in hepatocellular carcinoma: association with unpaired artery formation and radiologic findings], *Korean J Hepatol*, 13 (2007) 396-408.
- [387] Y. Tang, X. Zeng, F. He, Y. Liao, N. Qian, M. Toi, Caveolin-1 is related to invasion, survival, and poor prognosis in hepatocellular cancer, *Med Oncol*, 29 (2012) 977-984.
- [388] T.M. Williams, F. Medina, I. Badano, R.B. Hazan, J. Hutchinson, W.J. Muller, N.G. Chopra, P.E. Scherer, R.G. Pestell, M.P. Lisanti, Caveolin-1 gene disruption promotes mammary tumorigenesis and dramatically enhances lung metastasis in vivo. Role of Cav-1 in cell invasiveness and matrix metalloproteinase (MMP-2/9) secretion, *J Biol Chem*, 279 (2004) 51630-51646.
- [389] J.H. Chidlow, Jr., W.C. Sessa, Caveolae, caveolins, and cavins: complex control of cellular signalling and inflammation, *Cardiovasc Res*, 86 (2010) 219-225.
- [390] N. Ramos-DeSimone, E. Hahn-Dantona, J. Siple, H. Nagase, D.L. French, J.P. Quigley, Activation of matrix metalloproteinase-9 (MMP-9) via a converging plasmin/stromelysin-1 cascade enhances tumor cell invasion, *J Biol Chem*, 274 (1999) 13066-13076.
- [391] S.Y. Yoon, Y.J. Lee, J.H. Seo, H.J. Sung, K.H. Park, I.K. Choi, S.J. Kim, S.C. Oh, C.W. Choi, B.S. Kim, S.W. Shin, Y.H. Kim, J.S. Kim, uPAR expression under hypoxic conditions depends on iNOS modulated ERK phosphorylation in the MDA-MB-231 breast carcinoma cell line, *Cell Res*, 16 (2006) 75-81.
- [392] S.A. ter Horst, F.J. Walther, B.J. Poorthuis, P.S. Hiemstra, G.T. Wagenaar, Inhaled nitric oxide attenuates pulmonary inflammation and fibrin deposition and prolongs survival in neonatal hyperoxic lung injury, *Am J Physiol Lung Cell Mol Physiol*, 293 (2007) L35-44.
- [393] W. Eberhardt, T. Beeg, K.F. Beck, S. Walpen, S. Gauer, H. Bohles, J. Pfeilschifter, Nitric oxide modulates expression of matrix metalloproteinase-9 in rat mesangial cells, *Kidney Int*, 57 (2000) 59-69.
- [394] C.Y. Shin, W.J. Lee, J.W. Choi, M.S. Choi, J.R. Ryu, S.J. Oh, J.H. Cheong, E.Y. Choi, K.H. Ko, Down-regulation of matrix metalloproteinase-9 expression by nitric oxide in lipopolysaccharide-stimulated rat primary astrocytes, *Nitric Oxide*, 16 (2007) 425-432.
- [395] C. Jespersen, A. Doller, S. Akool el, M. Bachmann, R. Muller, P. Gutwein, H. Muhl, J. Pfeilschifter, W. Eberhardt, Molecular mechanisms of nitric oxide-dependent inhibition of TPA-induced matrix metalloproteinase-9 (MMP-9) in MCF-7 cells, *J Cell Physiol*, 219 (2009) 276-287.
- [396] T. Okamoto, G. Valacchi, K. Gohil, T. Akaike, A. van der Vliet, S-nitrosothiols inhibit cytokine-mediated induction of matrix metalloproteinase-9 in airway epithelial cells, *Am J Respir Cell Mol Biol*, 27 (2002) 463-473.
- [397] I. Sinha, K.K. Hannawa, G. Ailawadi, D.T. Woodrum, J.W. Ford, P.K. Henke, J.C. Stanley, M.J. Eagleton, G.R. Upchurch, Jr., The nitric oxide donor DETA-NONOate decreases matrix metalloproteinase-9 expression and activity in rat aortic smooth muscle and abdominal aortic explants, *Ann Vasc Surg*, 20 (2006) 92-98.



- [398] Y. Huang, M.Q. Lu, H. Li, C. Xu, S.H. Yi, G.H. Chen, Occurrence of cGMP/nitric oxide-sensitive store-operated calcium entry in fibroblasts and its effect on matrix metalloproteinase secretion, *World J Gastroenterol*, 12 (2006) 5483-5489.
- [399] M.V. Gurjar, J. DeLeon, R.V. Sharma, R.C. Bhalla, Mechanism of inhibition of matrix metalloproteinase-9 induction by NO in vascular smooth muscle cells, *J Appl Physiol*, 91 (2001) 1380-1386.
- [400] G.R. Upchurch, Jr., J.W. Ford, S.J. Weiss, B.S. Knipp, D.A. Peterson, R.W. Thompson, M.J. Eagleton, A.J. Broady, M.C. Proctor, J.C. Stanley, Nitric oxide inhibition increases matrix metalloproteinase-9 expression by rat aortic smooth muscle cells in vitro, *J Vasc Surg*, 34 (2001) 76-83.
- [401] B.S. Knipp, G. Ailawadi, J.W. Ford, D.A. Peterson, M.J. Eagleton, K.J. Roelofs, K.K. Hannawa, M.P. Deogracias, B. Ji, C. Logsdon, K.D. Graziano, D.M. Simeone, R.W. Thompson, P.K. Henke, J.C. Stanley, G.R. Upchurch, Jr., Increased MMP-9 expression and activity by aortic smooth muscle cells after nitric oxide synthase inhibition is associated with increased nuclear factor-kappaB and activator protein-1 activity, *J Surg Res*, 116 (2004) 70-80.
- [402] M.J. Eagleton, D.A. Peterson, V.V. Sullivan, K.J. Roelofs, J.A. Ford, J.C. Stanley, G.R. Upchurch, Jr., Nitric oxide inhibition increases aortic wall matrix metalloproteinase-9 expression, *J Surg Res*, 104 (2002) 15-21.
- [403] M.W. Radomski, S. Moncada, The biological and pharmacological role of nitric oxide in platelet function, *Adv Exp Med Biol*, 344 (1993) 251-264.
- [404] C. Fernandez-Patron, M.A. Martinez-Cuesta, E. Salas, G. Sawicki, M. Wozniak, M.W. Radomski, S.T. Davidge, Differential regulation of platelet aggregation by matrix metalloproteinases-9 and -2, *Thromb Haemost*, 82 (1999) 1730-1735.
- [405] F. Lindenmeyer, Y. Legrand, S. Menashi, Upregulation of MMP-9 expression in MDA-MB231 tumor cells by platelet granular membrane, *FEBS Lett*, 418 (1997) 19-22.
- [406] C. Belloc, H. Lu, C. Soria, R. Fridman, Y. Legrand, S. Menashi, The effect of platelets on invasiveness and protease production of human mammary tumor cells, *Int J Cancer*, 60 (1995) 413-417.
- [407] T. Hamada, S. Duarte, S. Tsuchihashi, R.W. Busuttil, A.J. Coito, Inducible nitric oxide synthase deficiency impairs matrix metalloproteinase-9 activity and disrupts leukocyte migration in hepatic ischemia/reperfusion injury, *Am J Pathol*, 174 (2009) 2265-2277.
- [408] M. Marcet-Palacios, K. Graham, C. Cass, A.D. Befus, I. Mayers, M.W. Radomski, Nitric oxide and cyclic GMP increase the expression of matrix metalloproteinase-9 in vascular smooth muscle, *J Pharmacol Exp Ther*, 307 (2003) 429-436.
- [409] S. Babykutty, P. Suboj, P. Srinivas, A.S. Nair, K. Chandramohan, S. Gopala, Insidious role of nitric oxide in migration/invasion of colon cancer cells by upregulating MMP-2/9 via activation of cGMP-PKG-ERK signaling pathways, *Clin Exp Metastasis*, 29 (2012) 471-492.
- [410] Y. Chen, Y. Aratani, T. Osawa, N. Fukuyama, C. Tsuji, H. Nakazawa, Activation of inducible nitric oxide synthase increases MMP-2 and MMP-9 levels in ApoE-knockout mice, *Tokai J Exp Clin Med*, 33 (2008) 28-34.
- [411] Y. Gursoy-Ozdemir, A. Can, T. Dalkara, Reperfusion-induced oxidative/nitrative injury to neurovascular unit after focal cerebral ischemia, *Stroke*, 35 (2004) 1449-1453.
- [412] Y. Gursoy-Ozdemir, H. Bolay, O. Saribas, T. Dalkara, Role of endothelial nitric oxide generation and peroxynitrite formation in reperfusion injury after focal cerebral ischemia, *Stroke*, 31 (2000) 1974-1980; discussion 1981.
- [413] L.A. Ridnour, S. Dhanapal, M. Hoos, J. Wilson, J. Lee, R.Y. Cheng, E.E. Brueggemann, H.B. Hines, D.M. Wilcock, M.P. Vitek, D.A. Wink, C.A. Colton, Nitric



- oxide-mediated regulation of beta-amyloid clearance via alterations of MMP-9/TIMP-1, *J Neurochem*, 123 (2012) 736-749.
- [414] F. Han, H.G. Zhu, Caveolin-1 regulating the invasion and expression of matrix metalloproteinase (MMPs) in pancreatic carcinoma cells, *J Surg Res*, 159 (2010) 443-450.
- [415] Y. Gu, G. Zheng, M. Xu, Y. Li, X. Chen, W. Zhu, Y. Tong, S.K. Chung, K.J. Liu, J. Shen, Caveolin-1 regulates nitric oxide-mediated matrix metalloproteinases activity and blood-brain barrier permeability in focal cerebral ischemia and reperfusion injury, *J Neurochem*, 120 (2012) 147-156.
- [416] A. Santana, C. Medina, M.C. Paz-Cabrera, F. Diaz-Gonzalez, E. Farre, A. Salas, M.W. Radomski, E. Quintero, Attenuation of dextran sodium sulphate induced colitis in matrix metalloproteinase-9 deficient mice, *World J Gastroenterol*, 12 (2006) 6464-6472.
- [417] X. Gan, B. Wong, S.D. Wright, T.Q. Cai, Production of matrix metalloproteinase-9 in CaCO-2 cells in response to inflammatory stimuli, *J Interferon Cytokine Res*, 21 (2001) 93-98.
- [418] L.M. Wu, L. Fan, L.L. Chen, [Precondition with doxycycline administration abates ischemia/reperfusion injury and reduces the expression of matrix metalloproteinase-1/9 in myocardium in rat in vivo], *Zhongguo Wei Zhong Bing Ji Jiu Yi Xue*, 19 (2007) 679-682.
- [419] V. Lukacova, Y. Zhang, M. Mackov, P. Baricic, S. Raha, J.A. Calvo, S. Balaz, Similarity of binding sites of human matrix metalloproteinases, *J Biol Chem*, 279 (2004) 14194-14200.
- [420] H. Liu, N.R. Patel, L. Walter, S. Ingersoll, S.V. Sitaraman, P. Garg, Constitutive expression of MMP9 in intestinal epithelium worsens murine acute colitis and is associated with increased levels of proinflammatory cytokine Kc, *Am J Physiol Gastrointest Liver Physiol*, 304 (2013) G793-803.
- [421] P. Huhtala, A. Tuuttila, L.T. Chow, J. Lohi, J. Keski-Oja, K. Tryggvason, Complete structure of the human gene for 92-kDa type IV collagenase. Divergent regulation of expression for the 92- and 72-kilodalton enzyme genes in HT-1080 cells, *J Biol Chem*, 266 (1991) 16485-16490.
- [422] R. Gum, E. Lengyel, J. Juarez, J.H. Chen, H. Sato, M. Seiki, D. Boyd, Stimulation of 92-kDa gelatinase B promoter activity by ras is mitogen-activated protein kinase kinase 1-independent and requires multiple transcription factor binding sites including closely spaced PEA3/ets and AP-1 sequences, *J Biol Chem*, 271 (1996) 10672-10680.
- [423] Y. St-Pierre, C. Van Themsche, P.O. Esteve, Emerging features in the regulation of MMP-9 gene expression for the development of novel molecular targets and therapeutic strategies, *Curr Drug Targets Inflamm Allergy*, 2 (2003) 206-215.
- [424] Y. St-Pierre, J. Couillard, C. Van Themsche, Regulation of MMP-9 gene expression for the development of novel molecular targets against cancer and inflammatory diseases, *Expert Opin Ther Targets*, 8 (2004) 473-489.
- [425] S. Muhlen, A. Behren, T. Iftner, P.K. Plinkert, C. Simon, AP-1 and ERK1 but not p38 nor JNK is required for CRPV early protein 2-dependent MMP-9 promoter activation in rabbit epithelial cells, *Virus Res*, 139 (2009) 100-105.
- [426] C. Simon, M. Simon, G. Vucelic, M.J. Hicks, P.K. Plinkert, A. Koitschev, H.P. Zenner, The p38 SAPK pathway regulates the expression of the MMP-9 collagenase via AP-1-dependent promoter activation, *Exp Cell Res*, 271 (2001) 344-355.
- [427] X. Zhao, E.N. Benveniste, Transcriptional activation of human matrix metalloproteinase-9 gene expression by multiple co-activators, *J Mol Biol*, 383 (2008) 945-956.
- [428] R. Gum, H. Wang, E. Lengyel, J. Juarez, D. Boyd, Regulation of 92 kDa type IV collagenase expression by the jun aminoterminal kinase- and the extracellular signal-regulated kinase-dependent signaling cascades, *Oncogene*, 14 (1997) 1481-1493.



- [429] A.S. Baldwin, Jr., The NF-kappa B and I kappa B proteins: new discoveries and insights, *Annu Rev Immunol*, 14 (1996) 649-683.
- [430] E.B. Traenckner, H.L. Pahl, T. Henkel, K.N. Schmidt, S. Wilk, P.A. Baeuerle, Phosphorylation of human I kappa B-alpha on serines 32 and 36 controls I kappa B-alpha proteolysis and NF-kappa B activation in response to diverse stimuli, *EMBO J*, 14 (1995) 2876-2883.
- [431] W. Eberhardt, A. Huwiler, K.F. Beck, S. Walpen, J. Pfeilschifter, Amplification of IL-1 beta-induced matrix metalloproteinase-9 expression by superoxide in rat glomerular mesangial cells is mediated by increased activities of NF-kappa B and activating protein-1 and involves activation of the mitogen-activated protein kinase pathways, *J Immunol*, 165 (2000) 5788-5797.
- [432] M. Bond, R.P. Fabunmi, A.H. Baker, A.C. Newby, Synergistic upregulation of metalloproteinase-9 by growth factors and inflammatory cytokines: an absolute requirement for transcription factor NF-kappa B, *FEBS Lett*, 435 (1998) 29-34.
- [433] M. Bond, A.J. Chase, A.H. Baker, A.C. Newby, Inhibition of transcription factor NF-kappaB reduces matrix metalloproteinase-1, -3 and -9 production by vascular smooth muscle cells, *Cardiovasc Res*, 50 (2001) 556-565.
- [434] Y.M. Janssen-Heininger, M.E. Poynter, P.A. Baeuerle, Recent advances towards understanding redox mechanisms in the activation of nuclear factor kappaB, *Free Radic Biol Med*, 28 (2000) 1317-1327.
- [435] G. Dijkstra, H. Moshage, P.L. Jansen, Blockade of NF-kappaB activation and donation of nitric oxide: new treatment options in inflammatory bowel disease?, *Scand J Gastroenterol Suppl*, (2002) 37-41.
- [436] H.E. Marshall, J.S. Stamler, Inhibition of NF-kappa B by S-nitrosylation, *Biochemistry*, 40 (2001) 1688-1693.
- [437] A. delaTorre, R.A. Schroeder, C. Punzalan, P.C. Kuo, Endotoxin-mediated S-nitrosylation of p50 alters NF-kappa B-dependent gene transcription in ANA-1 murine macrophages, *J Immunol*, 162 (1999) 4101-4108.
- [438] S.K. Park, H.L. Lin, S. Murphy, Nitric oxide regulates nitric oxide synthase-2 gene expression by inhibiting NF-kappaB binding to DNA, *Biochem J*, 322 ( Pt 2) (1997) 609-613.
- [439] K. Katsuyama, M. Shichiri, F. Marumo, Y. Hirata, NO inhibits cytokine-induced iNOS expression and NF-kappaB activation by interfering with phosphorylation and degradation of IkappaB-alpha, *Arterioscler Thromb Vasc Biol*, 18 (1998) 1796-1802.
- [440] V. Umansky, S.P. Hehner, A. Dumont, T.G. Hofmann, V. Schirmacher, W. Droge, M.L. Schmitz, Co-stimulatory effect of nitric oxide on endothelial NF-kappaB implies a physiological self-amplifying mechanism, *Eur J Immunol*, 28 (1998) 2276-2282.
- [441] H.M. Lander, D.P. Hajjar, B.L. Hempstead, U.A. Mirza, B.T. Chait, S. Campbell, L.A. Quilliam, A molecular redox switch on p21(ras). Structural basis for the nitric oxide-p21(ras) interaction, *J Biol Chem*, 272 (1997) 4323-4326.
- [442] H. Sugiura, H. Kawabata, T. Ichikawa, A. Koarai, S. Yanagisawa, T. Kikuchi, Y. Minakata, K. Matsunaga, M. Nakanishi, T. Hirano, K. Akamatsu, K. Furukawa, M. Ichinose, Inhibitory effects of theophylline on the peroxynitrite-augmented release of matrix metalloproteinases by lung fibroblasts, *Am J Physiol Lung Cell Mol Physiol*, 302 (2012) L764-774.
- [443] N. Tobar, V. Villar, J.F. Santibanez, ROS-NFkappaB mediates TGF-beta1-induced expression of urokinase-type plasminogen activator, matrix metalloproteinase-9 and cell invasion, *Mol Cell Biochem*, 340 (2010) 195-202.



- [444] C.A. Meschiari, T. Izidoro-Toledo, R.F. Gerlach, J.E. Tanus-Santos, Nitric oxide attenuates matrix metalloproteinase-9 production by endothelial cells independent of cGMP- or NFkappaB-mediated mechanisms, *Mol Cell Biochem*, 378 (2013) 127-135.
- [445] E. Shaulian, M. Karin, AP-1 as a regulator of cell life and death, *Nat Cell Biol*, 4 (2002) E131-136.
- [446] H. Sato, M. Seiki, Regulatory mechanism of 92 kDa type IV collagenase gene expression which is associated with invasiveness of tumor cells, *Oncogene*, 8 (1993) 395-405.
- [447] C. Abate, L. Patel, F.J. Rauscher, 3rd, T. Curran, Redox regulation of fos and jun DNA-binding activity in vitro, *Science*, 249 (1990) 1157-1161.
- [448] D. Nikitovic, A. Holmgren, G. Spyrou, Inhibition of AP-1 DNA binding by nitric oxide involving conserved cysteine residues in Jun and Fos, *Biochem Biophys Res Commun*, 242 (1998) 109-112.
- [449] G.P. Ahern, V.A. Klyachko, M.B. Jackson, cGMP and S-nitrosylation: two routes for modulation of neuronal excitability by NO, *Trends Neurosci*, 25 (2002) 510-517.
- [450] H.E. Marshall, K. Merchant, J.S. Stamler, Nitrosation and oxidation in the regulation of gene expression, *FASEB J*, 14 (2000) 1889-1900.
- [451] M.V. Gurjar, R.V. Sharma, R.C. Bhalla, eNOS gene transfer inhibits smooth muscle cell migration and MMP-2 and MMP-9 activity, *Arterioscler Thromb Vasc Biol*, 19 (1999) 2871-2877.
- [452] M. Marcet-Palacios, M. Ulanova, F. Duta, L. Puttagunta, S. Munoz, D. Gibbings, M. Radomski, L. Cameron, I. Mayers, A.D. Befus, The transcription factor Wilms tumor 1 regulates matrix metalloproteinase-9 through a nitric oxide-mediated pathway, *J Immunol*, 179 (2007) 256-265.
- [453] T.P. Garrington, G.L. Johnson, Organization and regulation of mitogen-activated protein kinase signaling pathways, *Curr Opin Cell Biol*, 11 (1999) 211-218.
- [454] H.S. Park, S.H. Huh, M.S. Kim, S.H. Lee, E.J. Choi, Nitric oxide negatively regulates c-Jun N-terminal kinase/stress-activated protein kinase by means of S-nitrosylation, *Proc Natl Acad Sci U S A*, 97 (2000) 14382-14387.
- [455] D.S. Pei, Y.J. Song, H.M. Yu, W.W. Hu, Y. Du, G.Y. Zhang, Exogenous nitric oxide negatively regulates c-Jun N-terminal kinase activation via inhibiting endogenous NO-induced S-nitrosylation during cerebral ischemia and reperfusion in rat hippocampus, *J Neurochem*, 106 (2008) 1952-1963.
- [456] H.S. Park, S.H. Huh, M.S. Kim, D.Y. Kim, B.J. Gwag, S.G. Cho, E.J. Choi, Neuronal nitric oxide synthase (nNOS) modulates the JNK1 activity through redox mechanism: a cGMP independent pathway, *Biochem Biophys Res Commun*, 346 (2006) 408-414.
- [457] H.S. Park, J.S. Mo, E.J. Choi, Nitric oxide inhibits an interaction between JNK1 and c-Jun through nitrosylation, *Biochem Biophys Res Commun*, 351 (2006) 281-286.
- [458] J. Fan, X. Yang, W. Wang, W.H. Wood, 3rd, K.G. Becker, M. Gorospe, Global analysis of stress-regulated mRNA turnover by using cDNA arrays, *Proc Natl Acad Sci U S A*, 99 (2002) 10611-10616.
- [459] T. Kawai, J. Fan, K. Mazan-Mamczarz, M. Gorospe, Global mRNA stabilization preferentially linked to translational repression during the endoplasmic reticulum stress response, *Mol Cell Biol*, 24 (2004) 6773-6787.
- [460] C.J. Wilusz, M. Wormington, S.W. Peltz, The cap-to-tail guide to mRNA turnover, *Nat Rev Mol Cell Biol*, 2 (2001) 237-246.
- [461] C.Y. Chen, A.B. Shyu, AU-rich elements: characterization and importance in mRNA degradation, *Trends Biochem Sci*, 20 (1995) 465-470.



- [462] X.C. Fan, J.A. Steitz, Overexpression of HuR, a nuclear-cytoplasmic shuttling protein, increases the in vivo stability of ARE-containing mRNAs, *EMBO J*, 17 (1998) 3448-3460.
- [463] S.S. Peng, C.Y. Chen, N. Xu, A.B. Shyu, RNA stabilization by the AU-rich element binding protein, HuR, an ELAV protein, *EMBO J*, 17 (1998) 3461-3470.
- [464] Y. Kuwano, A. Rabinovic, S. Srikantan, M. Gorospe, B. Dimple, Analysis of nitric oxide-stabilized mRNAs in human fibroblasts reveals HuR-dependent heme oxygenase 1 upregulation, *Mol Cell Biol*, 29 (2009) 2622-2635.
- [465] N. Abdelaziz, F. Colombo, I. Mercier, A. Calderone, Nitric oxide attenuates the expression of transforming growth factor-beta(3) mRNA in rat cardiac fibroblasts via destabilization, *Hypertension*, 38 (2001) 261-266.
- [466] V. Raoch, F. Rodriguez-Pascual, V. Lopez-Martinez, D. Medrano-Andres, M. Rodriguez-Puyol, S. Lamas, D. Rodriguez-Puyol, S. Lopez-Ongil, Nitric oxide decreases the expression of endothelin-converting enzyme-1 through mRNA destabilization, *Arterioscler Thromb Vasc Biol*, 31 (2011) 2577-2585.
- [467] S. Wang, J. Zhang, Y. Zhang, S. Kern, R.L. Danner, Nitric oxide-p38 MAPK signaling stabilizes mRNA through AU-rich element-dependent and -independent mechanisms, *J Leukoc Biol*, 83 (2008) 982-990.
- [468] F. Rodriguez-Pascual, M. Hausding, I. Ihrig-Biedert, H. Furneaux, A.P. Levy, U. Forstermann, H. Kleinert, Complex contribution of the 3'-untranslated region to the expressional regulation of the human inducible nitric-oxide synthase gene. Involvement of the RNA-binding protein HuR, *J Biol Chem*, 275 (2000) 26040-26049.
- [469] M. Zaccolo, M.A. Movsesian, cAMP and cGMP signaling cross-talk: role of phosphodiesterases and implications for cardiac pathophysiology, *Circ Res*, 100 (2007) 1569-1578.
- [470] S. Kloss, R. Srivastava, A. Mulsch, Down-regulation of soluble guanylyl cyclase expression by cyclic AMP is mediated by mRNA-stabilizing protein HuR, *Mol Pharmacol*, 65 (2004) 1440-1451.
- [471] S. Kloss, H. Furneaux, A. Mulsch, Post-transcriptional regulation of soluble guanylyl cyclase expression in rat aorta, *J Biol Chem*, 278 (2003) 2377-2383.
- [472] Y.S. Hwang, K.K. Park, W.Y. Chung, Kalopanaxsaponin A inhibits the invasion of human oral squamous cell carcinoma by reducing metalloproteinase-9 mRNA stability and protein trafficking, *Biol Pharm Bull*, 35 (2012) 289-300.
- [473] A. Huwiler, S. Akool el, A. Aschrafi, F.M. Hamada, J. Pfeilschifter, W. Eberhardt, ATP potentiates interleukin-1 beta-induced MMP-9 expression in mesangial cells via recruitment of the ELAV protein HuR, *J Biol Chem*, 278 (2003) 51758-51769.
- [474] S. Akool el, H. Kleinert, F.M. Hamada, M.H. Abdelwahab, U. Forstermann, J. Pfeilschifter, W. Eberhardt, Nitric oxide increases the decay of matrix metalloproteinase 9 mRNA by inhibiting the expression of mRNA-stabilizing factor HuR, *Mol Cell Biol*, 23 (2003) 4901-4916.
- [475] W. Eberhardt, S. Akool el, J. Rebhan, S. Frank, K.F. Beck, R. Franzen, F.M. Hamada, J. Pfeilschifter, Inhibition of cytokine-induced matrix metalloproteinase 9 expression by peroxisome proliferator-activated receptor alpha agonists is indirect and due to a NO-mediated reduction of mRNA stability, *J Biol Chem*, 277 (2002) 33518-33528.
- [476] W. Liu, G.A. Rosenberg, K.J. Liu, AUF-1 mediates inhibition by nitric oxide of lipopolysaccharide-induced matrix metalloproteinase-9 expression in cultured astrocytes, *J Neurosci Res*, 84 (2006) 360-369.
- [477] P.G. Wang, M. Xian, X. Tang, X. Wu, Z. Wen, T. Cai, A.J. Janczuk, Nitric oxide donors: chemical activities and biological applications, *Chem Rev*, 102 (2002) 1091-1134.



- [478] T. Munzel, A. Daiber, T. Gori, More answers to the still unresolved question of nitrate tolerance, *Eur Heart J*, 34 (2013) 2666-2673.
- [479] A.L. Kleschyov, M. Oelze, A. Daiber, Y. Huang, H. Mollnau, E. Schulz, K. Sydow, B. Fichtlscherer, A. Mulsch, T. Munzel, Does nitric oxide mediate the vasodilator activity of nitroglycerin?, *Circ Res*, 93 (2003) e104-112.
- [480] J. DiFabio, Y. Ji, V. Vasiliou, G.R. Thatcher, B.M. Bennett, Role of mitochondrial aldehyde dehydrogenase in nitrate tolerance, *Mol Pharmacol*, 64 (2003) 1109-1116.
- [481] N.S. Bryan, B.O. Fernandez, S.M. Bauer, M.F. Garcia-Saura, A.B. Milsom, T. Rassaf, R.E. Maloney, A. Bharti, J. Rodriguez, M. Feelisch, Nitrite is a signaling molecule and regulator of gene expression in mammalian tissues, *Nat Chem Biol*, 1 (2005) 290-297.
- [482] I.L. Megson, D.J. Webb, Nitric oxide donor drugs: current status and future trends, *Expert Opin Investig Drugs*, 11 (2002) 587-601.
- [483] M. Trujillo, M.N. Alvarez, G. Peluffo, B.A. Freeman, R. Radi, Xanthine oxidase-mediated decomposition of S-nitrosothiols, *J Biol Chem*, 273 (1998) 7828-7834.
- [484] D. Jourdeheuil, F.S. Laroux, A.M. Miles, D.A. Wink, M.B. Grisham, Effect of superoxide dismutase on the stability of S-nitrosothiols, *Arch Biochem Biophys*, 361 (1999) 323-330.
- [485] N. Ramachandran, P. Root, X.M. Jiang, P.J. Hogg, B. Mutus, Mechanism of transfer of NO from extracellular S-nitrosothiols into the cytosol by cell-surface protein disulfide isomerase, *Proc Natl Acad Sci U S A*, 98 (2001) 9539-9544.
- [486] L. Liu, A. Hausladen, M. Zeng, L. Que, J. Heitman, J.S. Stamler, A metabolic enzyme for S-nitrosothiol conserved from bacteria to humans, *Nature*, 410 (2001) 490-494.
- [487] G.R. De Meyer, H. Bult, L. Ustunes, M.M. Kockx, M. Feelisch, A.G. Herman, Effect of nitric oxide donors on neointima formation and vascular reactivity in the collared carotid artery of rabbits, *J Cardiovasc Pharmacol*, 26 (1995) 272-279.
- [488] M. Cavicchi, B.J. Whittle, Regulation of induction of nitric oxide synthase and the inhibitory actions of dexamethasone in the human intestinal epithelial cell line, Caco-2: influence of cell differentiation, *Br J Pharmacol*, 128 (1999) 705-715.
- [489] A. Schrammel, S. Behrends, K. Schmidt, D. Koesling, B. Mayer, Characterization of 1H-[1,2,4]oxadiazolo[4,3-a]quinoxalin-1-one as a heme-site inhibitor of nitric oxide-sensitive guanylyl cyclase, *Mol Pharmacol*, 50 (1996) 1-5.
- [490] J. Garthwaite, E. Southam, C.L. Boulton, E.B. Nielsen, K. Schmidt, B. Mayer, Potent and selective inhibition of nitric oxide-sensitive guanylyl cyclase by 1H-[1,2,4]oxadiazolo[4,3-a]quinoxalin-1-one, *Mol Pharmacol*, 48 (1995) 184-188.
- [491] Y. Gong, E. Hart, A. Shchurin, J. Hoover-Plow, Inflammatory macrophage migration requires MMP-9 activation by plasminogen in mice, *J Clin Invest*, 118 (2008) 3012-3024.
- [492] B. Fayard, F. Bianchi, J. Dey, E. Moreno, S. Djaffer, N.E. Hynes, D. Monard, The serine protease inhibitor protease nexin-1 controls mammary cancer metastasis through LRP-1-mediated MMP-9 expression, *Cancer Res*, 69 (2009) 5690-5698.
- [493] N.S. Ramamurthy, B.R. Rifkin, R.A. Greenwald, J.W. Xu, Y. Liu, G. Turner, L.M. Golub, A.T. Vernillo, Inhibition of matrix metalloproteinase-mediated periodontal bone loss in rats: a comparison of 6 chemically modified tetracyclines, *J Periodontol*, 73 (2002) 726-734.
- [494] L. Paemen, E. Martens, K. Norga, S. Masure, E. Roets, J. Hoogmartens, G. Opdenakker, The gelatinase inhibitory activity of tetracyclines and chemically modified tetracycline analogues as measured by a novel microtiter assay for inhibitors, *Biochem Pharmacol*, 52 (1996) 105-111.
- [495] R.S. Muraoka, N. Dumont, C.A. Ritter, T.C. Dugger, D.M. Brantley, J. Chen, E. Easterly, L.R. Roebuck, S. Ryan, P.J. Gotwals, V. Koteliansky, C.L. Arteaga, Blockade of



- TGF-beta inhibits mammary tumor cell viability, migration, and metastases, *J Clin Invest*, 109 (2002) 1551-1559.
- [496] T. Gudi, G.K. Hong, A.B. Vaandrager, S.M. Lohmann, R.B. Pilz, Nitric oxide and cGMP regulate gene expression in neuronal and glial cells by activating type II cGMP-dependent protein kinase, *FASEB J*, 13 (1999) 2143-2152.
- [497] T. Gudi, I. Huvar, M. Meinecke, S.M. Lohmann, G.R. Boss, R.B. Pilz, Regulation of gene expression by cGMP-dependent protein kinase. Transactivation of the c-fos promoter, *J Biol Chem*, 271 (1996) 4597-4600.
- [498] T. Gudi, S.M. Lohmann, R.B. Pilz, Regulation of gene expression by cyclic GMP-dependent protein kinase requires nuclear translocation of the kinase: identification of a nuclear localization signal, *Mol Cell Biol*, 17 (1997) 5244-5254.
- [499] D.C. Baumgart, C.N. Bernstein, Z. Abbas, J.F. Colombel, A.S. Day, G. D'Haens, I. Dotan, K.L. Goh, T. Hibi, R.A. Kozarek, E.M. Quigley, W. Reinisch, B.E. Sands, J.D. Sollano, A.H. Steinhart, F. Steinwurz, M.H. Vatn, J.K. Yamamoto-Furusho, IBD Around the world: comparing the epidemiology, diagnosis, and treatment: proceedings of the World Digestive Health Day 2010--Inflammatory Bowel Disease Task Force meeting, *Inflamm Bowel Dis*, 17 (2011) 639-644.
- [500] J. Cosnes, S. Cattan, A. Blain, L. Beaugerie, F. Carbonnel, R. Parc, J.P. Gendre, Long-term evolution of disease behavior of Crohn's disease, *Inflamm Bowel Dis*, 8 (2002) 244-250.
- [501] N.A. Molodecky, I.S. Soon, D.M. Rabi, W.A. Ghali, M. Ferris, G. Chernoff, E.I. Benchimol, R. Panaccione, S. Ghosh, H.W. Barkema, G.G. Kaplan, Increasing incidence and prevalence of the inflammatory bowel diseases with time, based on systematic review, *Gastroenterology*, 142 (2012) 46-54 e42; quiz e30.
- [502] M. Ravikumara, B.K. Sandhu, Epidemiology of inflammatory bowel diseases in childhood, *Indian J Pediatr*, 73 (2006) 717-721.
- [503] P.L. Lakatos, Recent trends in the epidemiology of inflammatory bowel diseases: up or down?, *World J Gastroenterol*, 12 (2006) 6102-6108.
- [504] J.B. Kirsner, J. Elchlepp, The production of an experimental ulcerative colitis in rabbits, *Trans Assoc Am Physicians*, 70 (1957) 102-119.
- [505] J.R. Maxwell, J.L. Viney, Overview of mouse models of inflammatory bowel disease and their use in drug discovery, *Curr Protoc Pharmacol*, Chapter 5 (2009) Unit5 57.
- [506] L.A. Dieleman, M.J. Palmén, H. Akol, E. Bloemena, A.S. Pena, S.G. Meuwissen, E.P. Van Rees, Chronic experimental colitis induced by dextran sulphate sodium (DSS) is characterized by Th1 and Th2 cytokines, *Clin Exp Immunol*, 114 (1998) 385-391.
- [507] M.F. Neurath, I. Fuss, B.L. Kelsall, E. Stuber, W. Strober, Antibodies to interleukin 12 abrogate established experimental colitis in mice, *J Exp Med*, 182 (1995) 1281-1290.
- [508] M. Boirivant, I.J. Fuss, A. Chu, W. Strober, Oxazolone colitis: A murine model of T helper cell type 2 colitis treatable with antibodies to interleukin 4, *J Exp Med*, 188 (1998) 1929-1939.
- [509] V. Valatas, M. Vakas, G. Kolios, The value of experimental models of colitis in predicting efficacy of biological therapies for inflammatory bowel diseases, *Am J Physiol Gastrointest Liver Physiol*, 305 (2013) G763-785.
- [510] M. Kawada, A. Arihiro, E. Mizoguchi, Insights from advances in research of chemically induced experimental models of human inflammatory bowel disease, *World J Gastroenterol*, 13 (2007) 5581-5593.
- [511] N. Shintani, T. Nakajima, T. Okamoto, T. Kondo, N. Nakamura, T. Mayumi, Involvement of CD4+ T cells in the development of dextran sulfate sodium-induced experimental colitis and suppressive effect of IgG on their action, *Gen Pharmacol*, 31 (1998) 477-481.



- [512] H.C. Rath, M. Schultz, R. Freitag, L.A. Dieleman, F. Li, H.J. Linde, J. Scholmerich, R.B. Sartor, Different subsets of enteric bacteria induce and perpetuate experimental colitis in rats and mice, *Infect Immun*, 69 (2001) 2277-2285.
- [513] K. Fang, M. Bruce, C.B. Pattillo, S. Zhang, R. Stone, 2nd, J. Clifford, C.G. Kevil, Temporal genomewide expression profiling of DSS colitis reveals novel inflammatory and angiogenesis genes similar to ulcerative colitis, *Physiol Genomics*, 43 (2011) 43-56.
- [514] T. Hibi, H. Ogata, A. Sakuraba, Animal models of inflammatory bowel disease, *J Gastroenterol*, 37 (2002) 409-417.
- [515] B.R. MacPherson, C.J. Pfeiffer, Experimental production of diffuse colitis in rats, *Digestion*, 17 (1978) 135-150.
- [516] T. Yamada, E. Deitch, R.D. Specian, M.A. Perry, R.B. Sartor, M.B. Grisham, Mechanisms of acute and chronic intestinal inflammation induced by indomethacin, *Inflammation*, 17 (1993) 641-662.
- [517] H. Satoh, F. Sato, K. Takami, S. Szabo, New ulcerative colitis model induced by sulfhydryl blockers in rats and the effects of antiinflammatory drugs on the colitis, *Jpn J Pharmacol*, 73 (1997) 299-309.
- [518] Y. Cong, S.L. Brandwein, R.P. McCabe, A. Lazenby, E.H. Birkenmeier, J.P. Sundberg, C.O. Elson, CD4+ T cells reactive to enteric bacterial antigens in spontaneously colitic C3H/HeJBir mice: increased T helper cell type 1 response and ability to transfer disease, *J Exp Med*, 187 (1998) 855-864.
- [519] S. Matsumoto, Y. Okabe, H. Setoyama, K. Takayama, J. Ohtsuka, H. Funahashi, A. Imaoka, Y. Okada, Y. Umesaki, Inflammatory bowel disease-like enteritis and caecitis in a senescence accelerated mouse P1/Yit strain, *Gut*, 43 (1998) 71-78.
- [520] J. Rivera-Nieves, G. Bamias, A. Vidrich, M. Marini, T.T. Pizarro, M.J. McDuffie, C.A. Moskaluk, S.M. Cohn, F. Cominelli, Emergence of perianal fistulizing disease in the SAMP1/YitFc mouse, a spontaneous model of chronic ileitis, *Gastroenterology*, 124 (2003) 972-982.
- [521] M. Watanabe, Y. Ueno, T. Yajima, Y. Iwao, M. Tsuchiya, H. Ishikawa, S. Aiso, T. Hibi, H. Ishii, Interleukin 7 is produced by human intestinal epithelial cells and regulates the proliferation of intestinal mucosal lymphocytes, *J Clin Invest*, 95 (1995) 2945-2953.
- [522] S. Wirtz, S. Finotto, S. Kanzler, A.W. Lohse, M. Blessing, H.A. Lehr, P.R. Galle, M.F. Neurath, Cutting edge: chronic intestinal inflammation in STAT-4 transgenic mice: characterization of disease and adoptive transfer by TNF- plus IFN-gamma-producing CD4+ T cells that respond to bacterial antigens, *J Immunol*, 162 (1999) 1884-1888.
- [523] J.P. Sundberg, C.O. Elson, H. Bedigian, E.H. Birkenmeier, Spontaneous, heritable colitis in a new substrain of C3H/HeJ mice, *Gastroenterology*, 107 (1994) 1726-1735.
- [524] M.M. Kosiewicz, C.C. Nast, A. Krishnan, J. Rivera-Nieves, C.A. Moskaluk, S. Matsumoto, K. Kozaiwa, F. Cominelli, Th1-type responses mediate spontaneous ileitis in a novel murine model of Crohn's disease, *J Clin Invest*, 107 (2001) 695-702.
- [525] M. Watanabe, Y. Ueno, T. Yajima, S. Okamoto, T. Hayashi, M. Yamazaki, Y. Iwao, H. Ishii, S. Habu, M. Uehira, H. Nishimoto, H. Ishikawa, J. Hata, T. Hibi, Interleukin 7 transgenic mice develop chronic colitis with decreased interleukin 7 protein accumulation in the colonic mucosa, *J Exp Med*, 187 (1998) 389-402.
- [526] T.M. Kundig, H. Schorle, M.F. Bachmann, H. Hengartner, R.M. Zinkernagel, I. Horak, Immune responses in interleukin-2-deficient mice, *Science*, 262 (1993) 1059-1061.
- [527] D.M. Spencer, G.M. Veldman, S. Banerjee, J. Willis, A.D. Levine, Distinct inflammatory mechanisms mediate early versus late colitis in mice, *Gastroenterology*, 122 (2002) 94-105.



- [528] K. Takeda, B.E. Clausen, T. Kaisho, T. Tsujimura, N. Terada, I. Forster, S. Akira, Enhanced Th1 activity and development of chronic enterocolitis in mice devoid of Stat3 in macrophages and neutrophils, *Immunity*, 10 (1999) 39-49.
- [529] D. Kontoyiannis, G. Boulougouris, M. Manoloukos, M. Armaka, M. Apostolaki, T. Pizarro, A. Kotlyarov, I. Forster, R. Flavell, M. Gaestel, P. Tschlis, F. Cominelli, G. Kollias, Genetic dissection of the cellular pathways and signaling mechanisms in modeled tumor necrosis factor-induced Crohn's-like inflammatory bowel disease, *J Exp Med*, 196 (2002) 1563-1574.
- [530] B. Sadlack, H. Merz, H. Schorle, A. Schimpl, A.C. Feller, I. Horak, Ulcerative colitis-like disease in mice with a disrupted interleukin-2 gene, *Cell*, 75 (1993) 253-261.
- [531] B. Kneitz, T. Herrmann, S. Yonehara, A. Schimpl, Normal clonal expansion but impaired Fas-mediated cell death and anergy induction in interleukin-2-deficient mice, *Eur J Immunol*, 25 (1995) 2572-2577.
- [532] D.J. Berg, N. Davidson, R. Kuhn, W. Muller, S. Menon, G. Holland, L. Thompson-Snipes, M.W. Leach, D. Rennick, Enterocolitis and colon cancer in interleukin-10-deficient mice are associated with aberrant cytokine production and CD4(+) TH1-like responses, *J Clin Invest*, 98 (1996) 1010-1020.
- [533] R. Kuhn, J. Lohler, D. Rennick, K. Rajewsky, W. Muller, Interleukin-10-deficient mice develop chronic enterocolitis, *Cell*, 75 (1993) 263-274.
- [534] F. Powrie, T cells in inflammatory bowel disease: protective and pathogenic roles, *Immunity*, 3 (1995) 171-174.
- [535] F. Powrie, M.W. Leach, S. Mauze, S. Menon, L.B. Caddle, R.L. Coffman, Inhibition of Th1 responses prevents inflammatory bowel disease in scid mice reconstituted with CD45RBhi CD4+ T cells, *Immunity*, 1 (1994) 553-562.
- [536] R.G. Lorenz, V.J. McCracken, C.O. Elson, Animal models of intestinal inflammation: ineffective communication between coalition members, *Springer Semin Immunopathol*, 27 (2005) 233-247.
- [537] M. Talieri, K. Mathioudaki, P. Prezas, D.K. Alexopoulou, E.P. Diamandis, D. Xynopoulos, A. Ardavanis, N. Arnogiannaki, A. Scorilas, Clinical significance of kallikrein-related peptidase 7 (KLK7) in colorectal cancer, *Thromb Haemost*, 101 (2009) 741-747.
- [538] M. Devetzi, T. Trangas, A. Scorilas, D. Xynopoulos, M. Talieri, Parallel overexpression and clinical significance of kallikrein-related peptidases 7 and 14 (KLK7KLK14) in colon cancer, *Thromb Haemost*, 109 (2013) 716-725.
- [539] S. Danese, M. Sans, C. Fiocchi, The CD40/CD40L costimulatory pathway in inflammatory bowel disease, *Gut*, 53 (2004) 1035-1043.
- [540] D. Spina, PDE4 inhibitors: current status, *Br J Pharmacol*, 155 (2008) 308-315.
- [541] C.P. Page, D. Spina, Phosphodiesterase inhibitors in the treatment of inflammatory diseases, *Handb Exp Pharmacol*, (2011) 391-414.
- [542] L. Vong, J.G. Ferraz, N. Dufton, R. Panaccione, P.L. Beck, P.M. Sherman, M. Perretti, J.L. Wallace, Up-regulation of Annexin-A1 and lipoxin A(4) in individuals with ulcerative colitis may promote mucosal homeostasis, *PLoS One*, 7 (2012) e39244.
- [543] T. Minami, H. Tojo, Y. Shinomura, S. Tarui, M. Okamoto, Raised serum activity of phospholipase A2 immunochemically related to group II enzyme in inflammatory bowel disease: its correlation with disease activity of Crohn's disease and ulcerative colitis, *Gut*, 33 (1992) 914-921.
- [544] M.M. Haapamaki, J.M. Gronroos, H. Nurmi, K. Irjala, K.A. Alanen, T.J. Nevalainen, Phospholipase A2 in serum and colonic mucosa in ulcerative colitis, *Scand J Clin Lab Invest*, 59 (1999) 279-287.



- [545] M.M. Haapamaki, J.M. Gronroos, H. Nurmi, K. Alanen, T.J. Nevalainen, Gene expression of group II phospholipase A2 in intestine in Crohn's disease, *Am J Gastroenterol*, 94 (1999) 713-720.
- [546] Y. Tomita, H. Jyoyama, M. Kobayashi, K. Kuwabara, S. Furue, M. Ueno, K. Yamada, T. Ono, I. Teshirogi, K. Nomura, H. Arita, I. Okayasu, Y. Hori, Role of group IIA phospholipase A2 in rat colitis induced by dextran sulfate sodium, *Eur J Pharmacol*, 472 (2003) 147-158.
- [547] T.M. Woodruff, T.V. Arumugam, I.A. Shiels, M.L. Newman, P.A. Ross, R.C. Reid, D.P. Fairlie, S.M. Taylor, A potent and selective inhibitor of group IIA secretory phospholipase A2 protects rats from TNBS-induced colitis, *Int Immunopharmacol*, 5 (2005) 883-892.
- [548] M. Krinsky, S. Yedgar, L. Aptekar, O. Schwob, G. Goshen, A. Gruzman, S. Sasson, M. Ligumsky, Amelioration of TNBS-induced colon inflammation in rats by phospholipase A2 inhibitor, *Am J Physiol Gastrointest Liver Physiol*, 285 (2003) G586-592.
- [549] F.F. Davidson, E.A. Dennis, M. Powell, J.R. Glenney, Jr., Inhibition of phospholipase A2 by "lipocortins" and calpactins. An effect of binding to substrate phospholipids, *J Biol Chem*, 262 (1987) 1698-1705.
- [550] E.K. Brint, D. Xu, H. Liu, A. Dunne, A.N. McKenzie, L.A. O'Neill, F.Y. Liew, ST2 is an inhibitor of interleukin 1 receptor and Toll-like receptor 4 signaling and maintains endotoxin tolerance, *Nat Immunol*, 5 (2004) 373-379.
- [551] A. Salas, The IL-33/ST2 axis: yet another therapeutic target in inflammatory bowel disease?, *Gut*, 62 (2013) 1392-1393.
- [552] C.J. Beltran, L.E. Nunez, D. Diaz-Jimenez, N. Farfan, E. Candia, C. Heine, F. Lopez, M.J. Gonzalez, R. Quera, M.A. Hermoso, Characterization of the novel ST2/IL-33 system in patients with inflammatory bowel disease, *Inflamm Bowel Dis*, 16 (2010) 1097-1107.
- [553] L. Pastorelli, R.R. Garg, S.B. Hoang, L. Spina, B. Mattioli, M. Scarpa, C. Fiocchi, M. Vecchi, T.T. Pizarro, Epithelial-derived IL-33 and its receptor ST2 are dysregulated in ulcerative colitis and in experimental Th1/Th2 driven enteritis, *Proc Natl Acad Sci U S A*, 107 (2010) 8017-8022.
- [554] M.A. Sedhom, M. Pichery, J.R. Murdoch, B. Foligne, N. Ortega, S. Normand, K. Mertz, D. Sanmugalingam, L. Brault, T. Grandjean, E. Lefrancais, P.G. Fallon, V. Quesniaux, L. Peyrin-Biroulet, G. Cathomas, T. Junt, M. Chamaillard, J.P. Girard, B. Ryffel, Neutralisation of the interleukin-33/ST2 pathway ameliorates experimental colitis through enhancement of mucosal healing in mice, *Gut*, 62 (2013) 1714-1723.
- [555] C.A. Anderson, G. Boucher, C.W. Lees, A. Franke, M. D'Amato, K.D. Taylor, J.C. Lee, P. Goyette, M. Imielinski, A. Latiano, C. Lagace, R. Scott, L. Amininejad, S. Bumpstead, L. Baidoo, R.N. Baldassano, M. Barclay, T.M. Bayless, S. Brand, C. Buning, J.F. Colombel, L.A. Denson, M. De Vos, M. Dubinsky, C. Edwards, D. Ellinghaus, R.S. Fehrmann, J.A. Floyd, T. Florin, D. Franchimont, L. Franke, M. Georges, J. Glas, N.L. Glazer, S.L. Guthery, T. Haritunians, N.K. Hayward, J.P. Hugot, G. Jobin, D. Laukens, I. Lawrance, M. Lemann, A. Levine, C. Libioulle, E. Louis, D.P. McGovern, M. Milla, G.W. Montgomery, K.I. Morley, C. Mowat, A. Ng, W. Newman, R.A. Ophoff, L. Papi, O. Palmieri, L. Peyrin-Biroulet, J. Panes, A. Phillips, N.J. Prescott, D.D. Proctor, R. Roberts, R. Russell, P. Rutgeerts, J. Sanderson, M. Sans, P. Schumm, F. Seibold, Y. Sharma, L.A. Simms, M. Seielstad, A.H. Steinhardt, S.R. Targan, L.H. van den Berg, M. Vatn, H. Verspaget, T. Walters, C. Wijmenga, D.C. Wilson, H.J. Westra, R.J. Xavier, Z.Z. Zhao, C.Y. Ponsioen, V. Andersen, L. Torkvist, M. Gazouli, N.P. Anagnou, T.H. Karlsen, L. Kupcinkas, J. Sventoraityte, J.C. Mansfield, S. Kugathasan, M.S. Silverberg, J. Halfvarson, J.I. Rotter, C.G. Mathew, A.M. Griffiths, R. Garry, T. Ahmad, S.R. Brant, M.

Chamaillard, J. Satsangi, J.H. Cho, S. Schreiber, M.J. Daly, J.C. Barrett, M. Parkes, V. Annese, H. Hakonarson, G. Radford-Smith, R.H. Duerr, S. Vermeire, R.K. Weersma, J.D. Rioux, Meta-analysis identifies 29 additional ulcerative colitis risk loci, increasing the number of confirmed associations to 47, *Nat Genet*, 43 (2011) 246-252.

[556] J. Roman, N. Planell, J.J. Lozano, M. Aceituno, M. Esteller, C. Pontes, D. Balsa, M. Merlos, J. Panes, A. Salas, Evaluation of responsive gene expression as a sensitive and specific biomarker in patients with ulcerative colitis, *Inflamm Bowel Dis*, 19 (2013) 221-229.

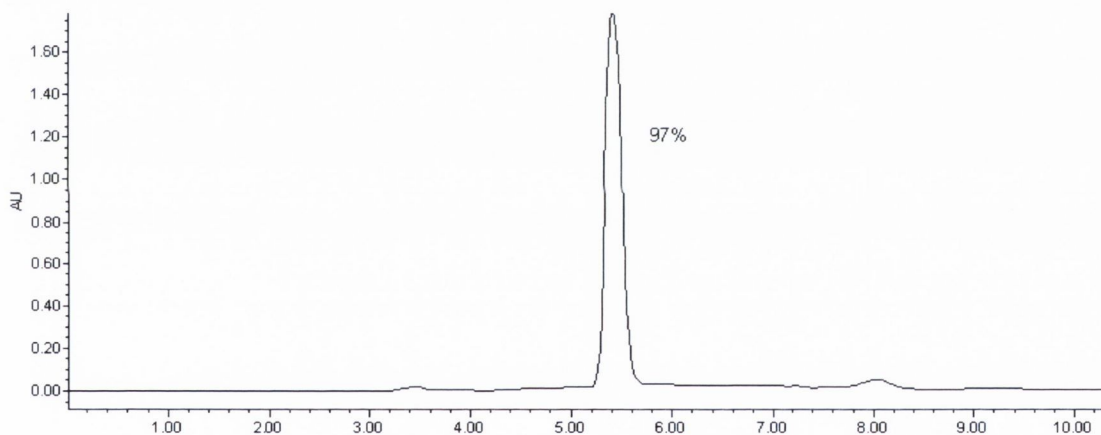
## 8. Appendix I



## 8.1. Compound characterisation

### 8.1.1. 5-(4-phenoxyphenyl)-5-(bis-(2-nitrooxy-ethyl)-amino)pyrimidine-2,4,6(1H,3H,5H)-trione (1a)

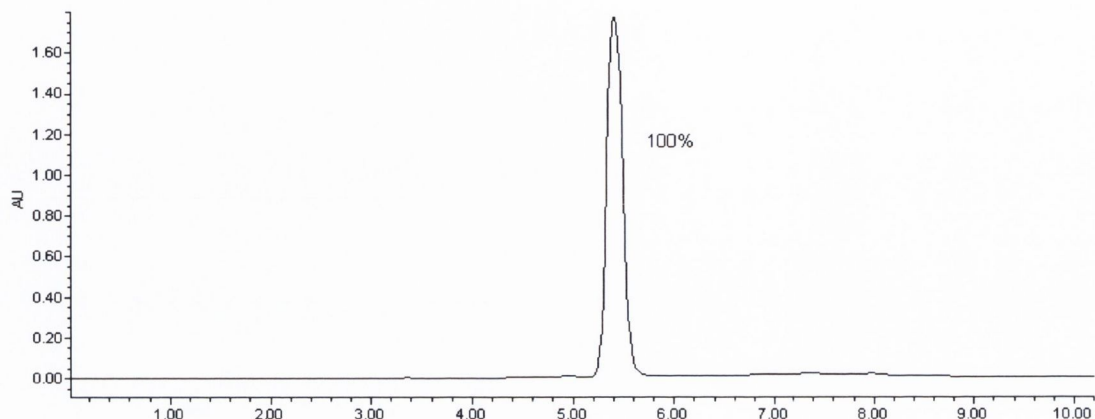
Crude product was purified by flash column chromatography to yield products as off-white solids (194mg, 39.6%). mp 184–186 °C. HRMS: C<sub>20</sub>H<sub>19</sub>N<sub>5</sub>O<sub>10</sub> [M + Na<sup>+</sup>] requires 512.1182; found 512.1168. <sup>1</sup>H NMR δ (MeOH-d<sub>4</sub>) ppm: 2.84–2.87 (t, J = 5.02, 4H), 4.64–4.67 (t, J = 5.02, 4H), 6.91–7.01 (m, 4H), 7.12–7.15 (t, J = 7.53, 1H), 7.34–7.38 (t, J = 7.53, 2H), 7.46–7.51 (m, 2H). <sup>13</sup>C NMR δ (MeOD-d<sub>4</sub>) ppm: 46.7; 72.0; 100.8; 119.3; 120.6; 122.2; 125.2; 128.7; 131.1; 150.6; 157.6; 160.2; 170.5. IR (KBr) ν (cm<sup>-1</sup>): 3068; 1728; 1706; 1648; 1281; 849.



### 8.1.2. 5-(4-phenoxyphenyl)-5-(bis-(2-hydroxyethyl)-amino)pyrimidine-2,4,6(1H,3H,5H)-trione (2a)

Crude products was purified by flash column chromatography to yield products as colourless oil (203 mg, 50.8%). HRMS: C<sub>20</sub>H<sub>21</sub>N<sub>3</sub>O<sub>6</sub> [M + Na<sup>+</sup>] requires 422.1323; found 422.1338. <sup>1</sup>H NMR δ (CDCl<sub>3</sub>) ppm: 3.00–3.05 (m, 4H), 3.85–3.90 (m, 4H), 6.95–6.98 (d, J = 8.53, 2H), 7.03–7.07 (d, J = 8.53, 2H, Ar-H), 7.16–7.20 (t, J = 7.53, 1H), 7.35–7.39 (t, J = 7.53, 2H), 7.46–7.51 (m, 2H, Ar-H). <sup>13</sup>C NMR δ (CDCl<sub>3</sub>) ppm: 50.8; 60.5; 82.2; 118.2;

119.8; 120.4; 121.3; 123.9; 128.7; 131.1; 150.8; 157.6; 160.2; 170.5. IR (CHCl<sub>3</sub>)  $\nu$  (cm<sup>-1</sup>):  
3496; 3266; 3068; 1770; 1717; 1685; 1355.



### 8.1.3. Bis-(2-nitroxy-ethyl)-amine (3a)

Product was precipitated out as white crystalline solids after reaction. (375 mg, 48.1%).

MP: 110–112°C. HRMS: C<sub>4</sub>H<sub>10</sub>N<sub>3</sub>O<sub>6</sub> [M + H<sup>+</sup>] requires 196.0570; found 196.0573. <sup>1</sup>H

NMR  $\delta$  (D<sub>2</sub>O) ppm: 3.52–3.54 (t, *J* = 5.02, 4H, CH<sub>2</sub>), 4.81–4.83 (m, *J* = 5.02, 4H, CH<sub>2</sub>).

<sup>13</sup>C NMR  $\delta$  (D<sub>2</sub>O) ppm: 44.6; 67.5. IR (KBr):  $\nu$  (cm<sup>-1</sup>): 1648, 1283, 925.

### 8.1.4. 5-(4-phenoxyphenyl)-5-(methyl-(2-nitroxy-ethyl)-amino)pyrimidine- 2,4,6(1H,3H,5H)-trione (1b)

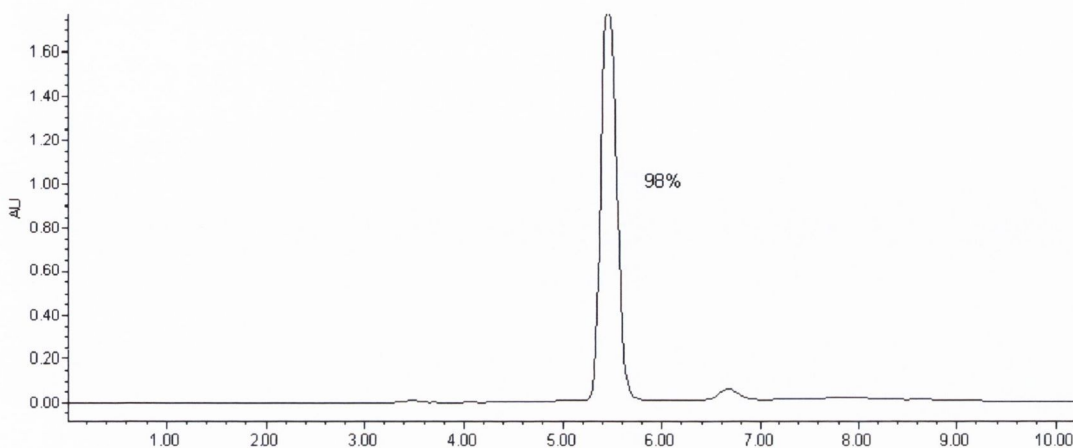
Crude product was purified by flash column chromatography to yield products as off-white solids (134 mg, 32.3%). MP: 143–145 °C. HRMS: C<sub>19</sub>H<sub>18</sub>N<sub>4</sub>O<sub>7</sub> [M + Na<sup>+</sup>] requires

437.1073; found 437.1078. <sup>1</sup>H NMR  $\delta$  (CDCl<sub>3</sub>) ppm: 2.41 (s, 3H), 2.91–2.96 (m, 2H),

4.37–4.42 (m, 2H), 6.90–6.92 (d, *J* = 8.03, 2H), 7.00–7.02 (d, *J* = 8.03, 2H), 7.15–7.18 (t, *J*

= 7.53, 1H), 7.34–7.38 (t, *J* = 7.53, 2H), 7.40–7.46 (m, 2H). <sup>13</sup>C NMR  $\delta$  (CDCl<sub>3</sub>) ppm:

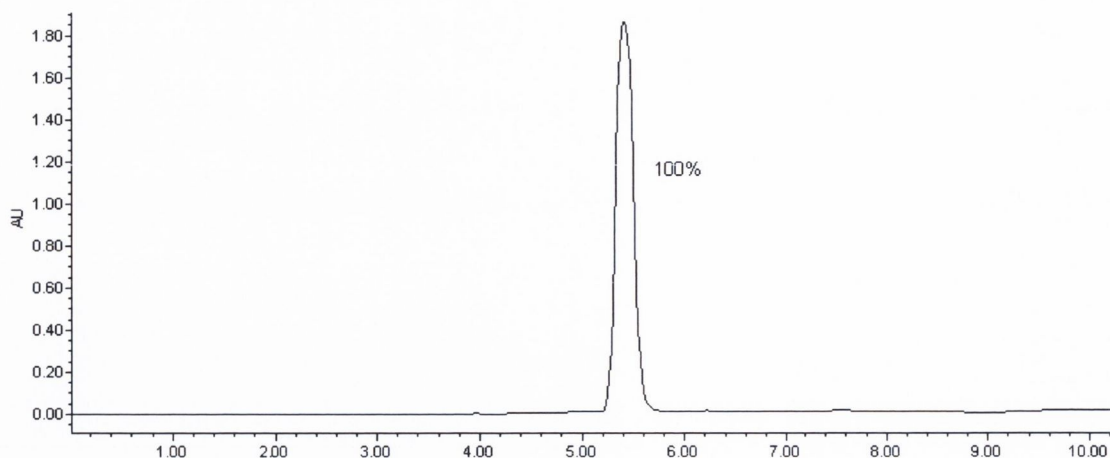
38.2; 49.8; 70.8; 100.8; 118.3; 119.8; 121.4; 124.6; 129.5; 130.0; 150.8; 155.6; 159.1;  
171.2. IR (KBr)  $\nu$  ( $\text{cm}^{-1}$ ): 3066; 1720; 1698; 1644; 1280; 842.



#### 8.1.5. 5-(4-phenoxyphenyl)-5-(N-(2-hydroxyethyl-N-methylamino)pyrimidine-2,4,6(1H,3H,5H)-trione (2b)

Crude product was purified by flash column chromatography to yield products as off-white solids (145 mg, 39.3%). mp 164–166 °C. HRMS:  $\text{C}_{19}\text{H}_{19}\text{N}_3\text{O}_5$  [ $\text{M} + \text{Na}^+$ ] requires 392.1217; found 392.1214.  $^1\text{H}$  NMR  $\delta$  (MeOH- $d_4$ ) ppm: 2.43 (s, 3H), 2.87–2.93 (m, 2H), 3.66–3.69 (m, 2H), 6.96–6.98 (d,  $J = 8.03$ , 2H), 7.00–7.02 (d,  $J = 8.03$ , 2H), 7.15–7.18 (t,  $J = 7.53$ , 1H), 7.34–7.38 (t,  $J = 7.53$ , 2H), 7.44–7.46 (d,  $J = 8.03$ , 2H).  $^{13}\text{C}$  NMR  $\delta$  (MeOH- $d_4$ ) ppm: 32.9; 55.7; 58.4; 76.1; 118.3; 119.8; 121.4; 124.3; 129.7; 130.0; 149.7; 155.5; 159.0; 171.0. IR (KBr)  $\nu$  ( $\text{cm}^{-1}$ ): 3493; 3264; 3073; 1762; 1709; 1676; 1375.



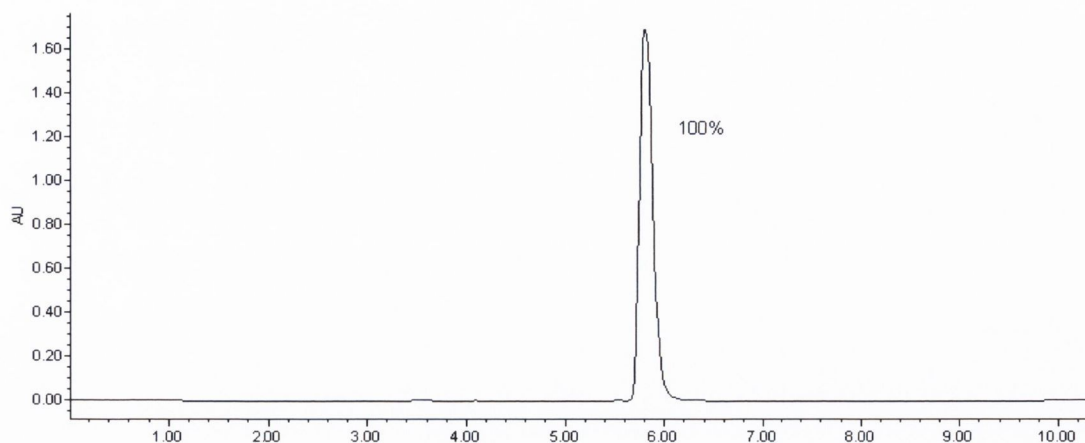


### 8.1.6. Methyl-(2-nitrooxy-ethyl)-amine (3b)

Product precipitated out as white crystalline solids after reaction. (413 mg, 57.3%). mp: 58–60°C. HRMS:  $C_3H_9N_2O_3$   $[M + H^+]$  requires 121.0613; found = 121.0611.  $^1H$  NMR  $\delta$  ( $D_2O$ ) ppm: 2.79 (s, 3H,  $CH_3$ ), 3.49–3.51 (t,  $J = 5.02$ , 2H,  $CH_2$ ), 4.85–4.87 (m,  $J = 5.02$ , 2H,  $CH_2$ ).  $^{13}C$  NMR  $\delta$  ( $D_2O$ ) ppm: 35.1; 48.2; 70.1. IR (KBr):  $\nu$  ( $cm^{-1}$ ): 1646, 1280, 912.

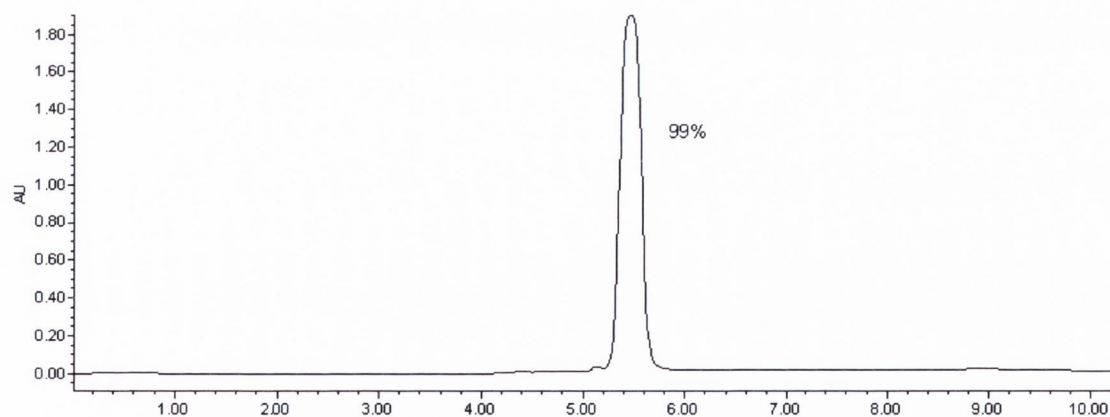
### 8.1.7. 5-(4-phenoxyphenyl)-5-(4-(2-nitrooxy-ethyl)piperazin-1-yl)pyrimidine-2,4,6(1H,3H,5H)-trione (1c)

The resulting crude products were purified by flash column chromatography to yield products as off-white solids (197 mg, 42.0%). mp 206–208 °C. HRMS:  $C_{22}H_{24}N_5O_7$   $[M + H^+]$  requires 470.1676; found 470.1679.  $^1H$  NMR  $\delta$  (DMSO) ppm: 2.47–2.51 (m, 6H); 2.62–2.68 (m, 4H); 4.05–4.08 (m, 2H); 7.02–7.07 (m, 4H); 7.17–7.21 (t,  $J = 7.53$ , 1H); 7.40–7.43 (m, 4H).  $^{13}C$  NMR  $\delta$  (DMSO) ppm: 47.8; 52.8; 57.3; 71.0; 74.0; 118.2; 118.4; 119.2; 121.4; 124.2; 129.6; 130.2; 150.2; 155.9; 159.3. 170.1. IR (KBr)  $\nu$  ( $cm^{-1}$ ): 3066; 1710; 1684; 1640; 1281; 849.



### 8.1.8. 5-(4-phenoxyphenyl)-5-(4-(2-hydroxyethyl)piperazin-1-yl)pyrimidine-2,4,6(1H,3H,5H)-trione (2c)

Crude product was purified by flash column chromatography to yield products as off-white solids (183 mg, 43.2%). mp 175–178 °C. HRMS: C<sub>22</sub>H<sub>25</sub>N<sub>4</sub>O<sub>5</sub> [M + H<sup>+</sup>] requires 425.1819; found 425.1823. <sup>1</sup>H NMR δ (DMSO) ppm: 2.37–2.40 (m, 6H); 2.56–2.59 (m, 4H); 3.44–3.46 (m, 2H); 7.01–7.06 (m, 4H); 7.17–7.21 (t, J = 7.53, 1H); 7.40–7.43 (m, 4H). <sup>13</sup>C NMR δ (DMSO) ppm: 47.3; 53.8; 58.4; 62.2; 73.9; 118.1; 118.4; 119.3; 121.3; 124.1; 129.7; 130.2; 149.5; 155.8; 157.4. 170.0. IR (KBr) ν (cm<sup>-1</sup>): 3490; 3266; 1768; 1708; 1684; 1380.



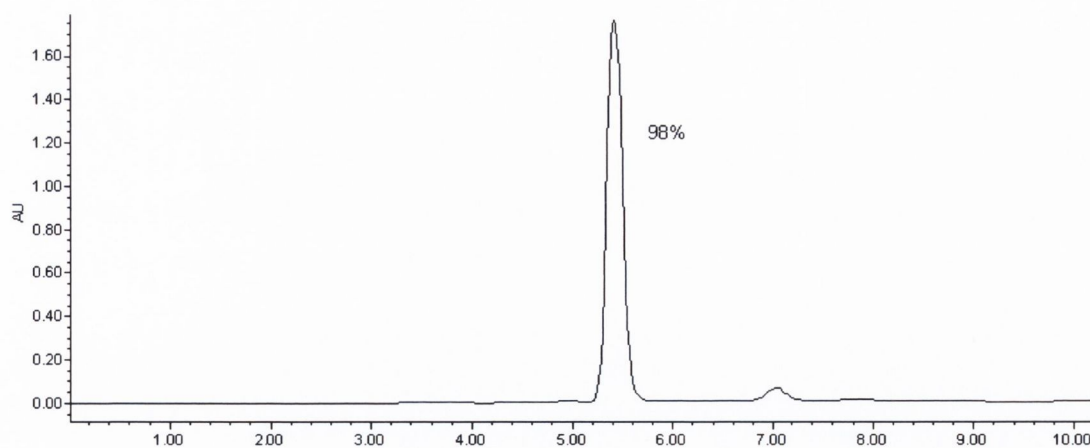
### 8.1.9. (2-nitrooxy-ethyl)-piperazine (3c)

Solvents were removed *in vacuo* to yield product as light yellow oil (324 mg, 46.2%). MS: Calculated for C<sub>6</sub>H<sub>14</sub>N<sub>3</sub>O<sub>3</sub> [M + H<sup>+</sup>] required 176.1035; found 176.1030. <sup>1</sup>H NMR δ (CDCl<sub>3</sub>) ppm: 2.37–2.41 (m, 4H, CH<sub>2</sub>); 2.50–2.53 (m, 2H, CH<sub>2</sub>); 2.62–2.68 (m, 4H, CH<sub>2</sub>); 4.04–4.07 (m, 2H, CH<sub>2</sub>). <sup>13</sup>C NMR δ (CDCl<sub>3</sub>) ppm: 46.3; 53.0; 57.3; 70.7. IR (film) ν (cm<sup>-1</sup>): 1641; 1280; 936.

#### 8.1.10. 5-(4-phenoxyphenyl)-5-(4-(2-nitrooxy-ethyl)piperidin-1-yl)pyrimidine-2,4,6(1H,3H,5H)-trione (1d)

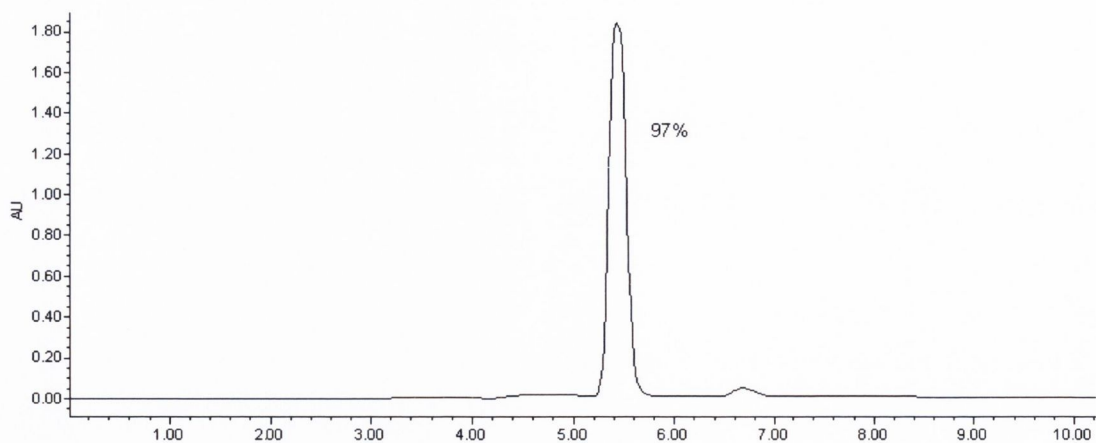
Crude products were purified by flash column chromatography to yield products as off-white solids (145 mg, 30.9%). mp: 201–203°C. HRMS: C<sub>23</sub>H<sub>25</sub>N<sub>4</sub>O<sub>7</sub> [M + H<sup>+</sup>] requires 469.1723; found 469.1723. <sup>1</sup>H NMR δ (CDCl<sub>3</sub>) ppm: 1.33–1.39 (m, 2H, CH<sub>2</sub>) 1.42–1.46 (m, 2H, CH<sub>2</sub>), 1.48–1.51 (m, 1H, CH), 1.73–1.78 (m, 2H, CH<sub>2</sub>), 2.57–2.64 (m, 2H, CH<sub>2</sub>), 2.76–2.79 (m, 2H, CH<sub>2</sub>), 4.78–4.82 (m, 2H, CH<sub>2</sub>), 6.92–6.94 (d, *J* = 8.53, 1H, Ar-H), 6.96–6.98 (d, *J* = 8.53, 2H, Ar-H), 7.03–7.05 (d, *J* = 8.53, 1H, Ar-H), 7.16–7.19 (t, *J* = 7.53, 1H, Ar-H), 7.36–7.40 (t, *J* = 7.53, 2H, Ar-H), 7.45–7.49 (m, 2H, Ar-H), 8.99 (s, 2H, NH). <sup>13</sup>C NMR δ (CDCl<sub>3</sub>) ppm: 21.4; 32.2; 32.6; 48.1; 70.5; 76.0; 118.2; 119.7; 121.2; 124.2; 129.5; 129.9; 148.7; 155.8; 158.1; 169.8 IR (KBr) ν (cm<sup>-1</sup>): 3068; 1732; 1704; 1633; 1285; 849.





### 8.1.11. 5-(4-phenoxyphenyl)-5-(4-(2-hydroxyethyl)piperidin-1-yl)pyrimidine-2,4,6(1H,3H,5H)-trione (2d)

Crude products were purified by flash column chromatography to yield products as off-white solids (171 mg, 40.3%). mp 186–188 °C. HRMS:  $C_{23}H_{25}N_3O_5$  [ $M + Na^+$ ] requires 446.1686; 446.1705.  $^1H$  NMR  $\delta$  (MeOH- $d_4$ ) ppm: 1.27–1.32 (m, 2H), 1.50–1.53 (m, 3H), 1.65–1.68 (m, 2H), 2.54–2.60 (m, 2H), 2.76–2.79 (m, 2H), 3.86–3.89 (d,  $J = 6.53$ , 2H), 6.92–6.94 (d,  $J = 8.53$ , 1H), 6.96–6.98 (d,  $J = 8.53$ , 2H), 7.03–7.05 (d,  $J = 8.53$ , 1H), 7.15–7.18 (t,  $J = 7.53$ , 1H), 7.35–7.39 (t,  $J = 7.53$ , 2H), 7.45–7.47 (m, 2H), 9.02 (s, 2H).  $^{13}C$  NMR  $\delta$  (MeOH- $d_4$ ) ppm: 14.9; 31.9; 35.7; 48.1; 60.0; 75.6; 117.9; 119.3; 120.9; 123.8; 129.2; 129.6; 148.3; 155.6; 158.3; 169.6 IR (KBr)  $\nu$  ( $cm^{-1}$ ): 3496; 3301; 3084; 1776; 1711; 1685; 1386.



### 8.1.12. 4-(2-nitrooxy-ethyl)-piperidine (3d)

The solvents were removed *in vacuo* to yield product as yellow oil (328 mg, 47.1%).

HRMS:  $C_7H_{15}N_2O_3$  [ $M + H^+$ ] required 175.1083; found 175.1077.  $^1H$  NMR  $\delta$  ( $CDCl_3$ )

ppm: 1.08–1.18 (m, 2H,  $CH_2$ ), 1.71–1.78 (m, 5H, CH +  $CH_2$ ), 2.48–2.55 (m, 2H,  $CH_2$ ),

2.99–3.06 (m, 2H,  $CH_2$ ), 3.48–3.52 (m, 2H,  $CH_2$ ), 4.57–4.61 (m, 2H,  $CH_2$ ).  $^{13}C$  NMR  $\delta$

( $CDCl_3$ ) ppm: 21.4; 32.3; 33.9; 46.3; 70.7. IR (film)  $\nu$  ( $cm^{-1}$ ): 1652, 1281, 915

### 8.1.13. 5-(4-phenoxyphenyl)-5-(4-(1-nitrooxy-methyl)piperidin-1-yl)pyrimidine-2,4,6(1H,3H,5H)-trione (1e)

Crude products were purified by flash column chromatography to yield products as off-

white solids (158 mg, 34.8%). mp: 190–192°C. HRMS:  $C_{22}H_{23}N_4O_7$  [ $M + H^+$ ] requires

455.1561; found 455.1567.  $^1H$  NMR  $\delta$  ( $CDCl_3$ ) ppm: 1.16–1.27 (m, 2H,  $CH_2$ ) 1.47–1.58

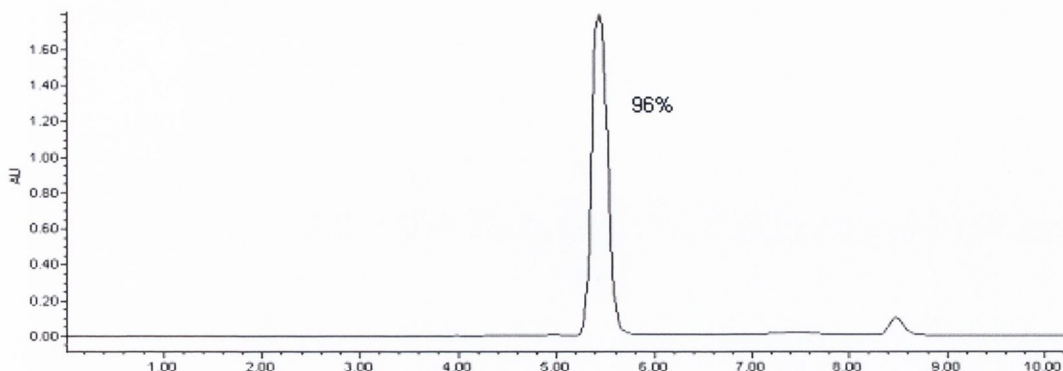
(m, 3H,  $CH_2+CH$ ), 2.32–2.37 (m, 2H,  $CH_2$ ), 2.77–2.83 (m, 2H,  $CH_2$ ), 4.84–4.90 (m, 2H,

$CH_2$ ), 6.92–6.95 (d,  $J = 8.53$ , 1H, Ar-H), 6.97–6.99 (d,  $J = 8.53$ , 2H, Ar-H), 7.01–7.03 (d,  $J$

= 8.53, 1H, Ar-H), 7.15–7.18 (t,  $J = 7.53$ , 1H, Ar-H), 7.37–7.40 (t,  $J = 7.53$ , 2H, Ar-H),

7.43–7.48 (m, 2H, Ar-H).  $^{13}C$  NMR  $\delta$  ( $CDCl_3$ ) ppm: 27.4; 34.2; 49.1; 75.7; 76.1; 118.4;

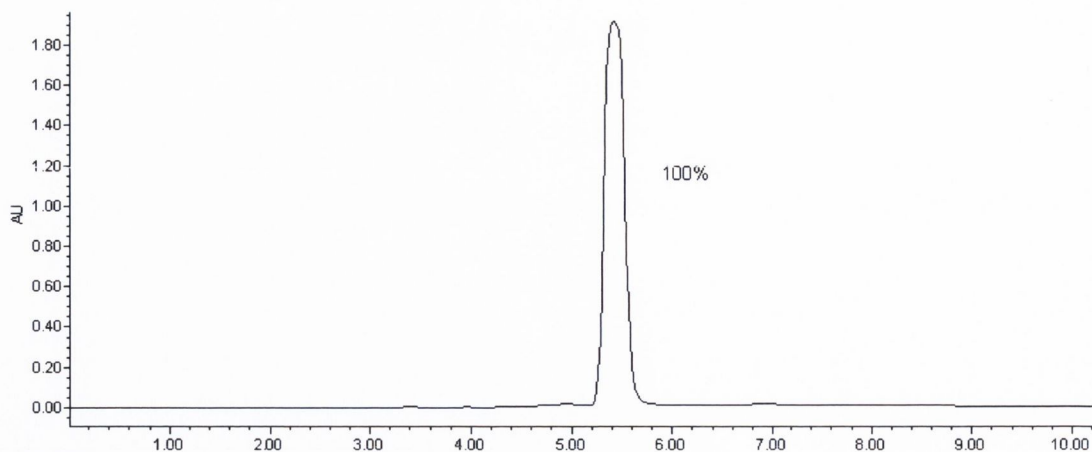
119.8; 121.3; 124.3; 129.6; 130.2; 150.7; 155.9; 159.4; 170.6. IR (KBr)  $\nu$  ( $\text{cm}^{-1}$ ): 3068; 1732; 1694; 1642; 1286; 849.



#### 8.1.14. 5-(4-phenoxyphenyl)-5-(4-(hydroxymethyl)piperidin-1-yl)pyrimidine-2,4,6(1H,3H,5H)-trione (2e)

Crude products were purified by flash column chromatography to yield products as off-white solids (167 mg, 40.8%). mp 171–174 °C. HRMS:  $\text{C}_{22}\text{H}_{24}\text{N}_3\text{O}_5$  [ $\text{M} + \text{H}^+$ ] requires 410.1710; found 410.1743.  $^1\text{H}$  NMR  $\delta$  (acetone- $\text{d}_6$ ) ppm: 1.52–1.56 (m, 2H) 1.62–1.66 (m, 1H), 1.69–1.74 (m, 2H), 2.33–2.38 (m, 2H), 2.52–2.57 (m, 2H), 3.39–3.46 (m, 2H), 7.01–7.08 (m, 4H), 7.17–7.21 (t,  $J = 7.53$ , 1H), 7.41–7.45 (t,  $J = 7.53$ , 2H), 7.57–7.62 (m, 2H).  $^{13}\text{C}$  NMR  $\delta$  (acetone- $\text{d}_6$ ) ppm: 26.5; 35.3; 50.1; 65.9; 76.7; 119.2; 120.6; 122.4; 125.1; 131.1; 131.3; 149.9; 157.1; 158.7; 171.1. IR (KBr)  $\nu$  ( $\text{cm}^{-1}$ ): 3551; 3264; 3042; 1762; 1708; 1675; 1341.





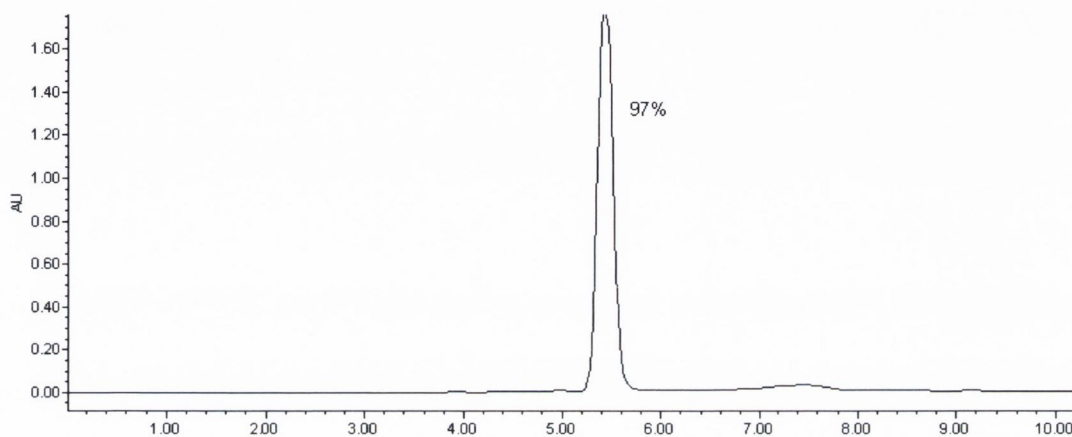
### 8.1.15. 4-(1-nitrooxy-methyl)-piperidine (3e)

Solvents were removed *in vacuo* to yield product as yellow oil (285 mg, 44.5%). HRMS:  $C_6H_{13}N_2O_3$  [ $M + H^+$ ] requires 161.0926; found 161.0921.  $^1H$  NMR  $\delta$  ( $CDCl_3$ ) ppm: 1.10–1.21 (m, 2H,  $CH_2$ ), 1.63–1.71 (m, 3H,  $CH+CH_2$ ), 2.40–2.47 (m, 2H,  $CH_2$ ), 2.92–2.97 (m, 2H,  $CH_2$ ), 4.49–4.52 (m, 2H,  $CH_2$ ).  $^{13}C$  NMR  $\delta$  ( $CDCl_3$ ) ppm: 29.4; 34.6; 46.2; 76.2. IR (film)  $\nu$  ( $cm^{-1}$ ): 1640, 1282, 910

### 8.1.16. 5-(4-phenoxyphenyl)-5-(3-(1-nitrooxy-methyl)piperidin-1-yl)pyrimidine-2,4,6(1H,3H,5H)-trione (1f)

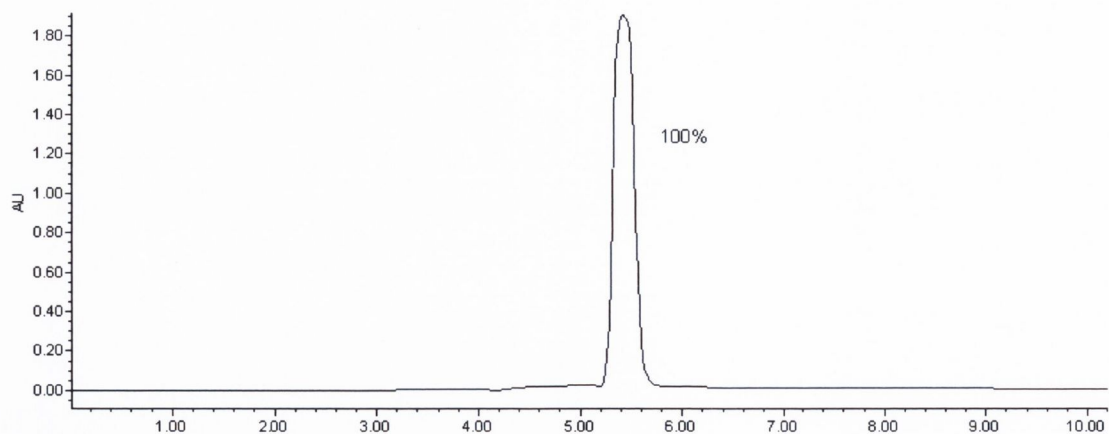
Crude products were purified by flash column chromatography to yield products as off-white solids (181 mg, 39.8%). mp 190–192 °C. HRMS:  $C_{22}H_{23}N_4O_7$  [ $M + H^+$ ] requires 455.1568; found 455.1567.  $^1H$  NMR  $\delta$  ( $CDCl_3$ ) ppm: 1.28–1.30 (m, 1H), 1.3–1.40 (m, 1H), 1.56–1.59 (m, 1H), 1.64–1.68 (m, 1H), 1.71–1.76 (m, 1H, CH), 2.08–2.13 (m, 1H), 2.51–2.57 (m, 1H), 2.61–2.68 (m, 1H), 2.71–2.75 (m, 1H), 4.37–4.41 (m, 1H), 4.52–4.57

(m, 1H), 6.92–6.94 (d,  $J = 8.53$ , 2H), 6.96–6.99 (d,  $J = 8.53$ , 1H), 7.04–7.06 (d,  $J = 8.53$ , 1H), 7.16–7.20 (t,  $J = 7.53$ , 1H), 7.36–7.40 (t,  $J = 7.53$ , 2H), 7.45–7.49 (m, 2H), 9.15 (s, 1H), 9.16 (s, 1H).  $^{13}\text{C}$  NMR  $\delta$  ( $\text{CDCl}_3$ ) ppm: 26.6; 34.2; 48.8; 50.7; 53.7; 73.7; 74.6. 118.5; 119.7; 121.3; 124.2; 129.4; 129.9; 148.9; 155.7; 158.9; 170.0. IR (KBr)  $\nu$  ( $\text{cm}^{-1}$ ): 3066; 1723; 1688; 1640; 1281; 853.



### 8.1.17. 5-(4-phenoxyphenyl)-5-(3-(hydroxymethyl)piperidin-1-yl)pyrimidine-2,4,6(1H,3H,5H)-trione (2f)

Crude products were purified by flash column chromatography to yield off-white solids (149 mg, 36.4%). mp: 166–168 °C. HRMS:  $\text{C}_{22}\text{H}_{24}\text{N}_3\text{O}_5$  [ $\text{M} + \text{H}^+$ ] requires 410.1710; found 410.1747.  $^1\text{H}$  NMR  $\delta$  ( $\text{MeOH-d}_4$ ) ppm: 1.28–1.30 (m, 1H), 1.27–1.33 (m, 1H), 1.48–1.54 (m, 1H), 1.67–1.70 (m, 1H), 1.79–1.85 (m, 1H), 1.99–2.06 (m, 1H), 2.51–2.57 (m, 1H), 2.58–2.64 (m, 1H), 2.78–2.81 (m, 1H), 3.40–3.42 (m, 1H), 3.91–3.93 (m, 1H), 6.96–6.98 (d,  $J = 8.53$ , 2H), 7.02–7.04 (d,  $J = 8.53$ , 2H), 7.14–7.17 (t,  $J = 7.53$ , 1H), 7.36–7.40 (t,  $J = 7.53$ , 2H), 7.48–7.52 (m, 2H).  $^{13}\text{C}$  NMR  $\delta$  ( $\text{MeOH-d}_4$ ) ppm: 24.7; 28.6; 39.8; 48.5; 53.0; 67.8; 76.5. 118.9; 119.4; 120.5; 122.1; 125.0; 130.6; 130.9; 150.7; 157.4; 159.7; 172.0. IR (KBr)  $\nu$  ( $\text{cm}^{-1}$ ): 3498; 3281; 3062; 1766; 1710; 1688; 1351.



### 8.1.18. 3-(1-nitroso-methyl)-piperidine (3f)

Solvents were removed *in vacuo* to yield product as yellow oil (342 mg, 53.4%). HRMS:  $C_6H_{13}N_2O_3$  [ $M + H^+$ ] requires 161.0926; found 161.0924. <sup>1</sup>H NMR  $\delta$  ( $CDCl_3$ ) ppm: 1.07–1.17 (m, 1H,  $CH_2$ ), 1.37–1.47 (m, 1H,  $CH_2$ ), 1.58–1.62 (m, 1H,  $CH_2$ ), 1.71–1.74 (m, 1H,  $CH_2$ ), 1.86–1.92 (m, 1H, CH), 2.32–2.37 (m, 1H,  $CH_2$ ), 2.45–2.52 (m, 1H,  $CH_2$ ), 2.90–2.94 (m, 1H,  $CH_2$ ), 3.02–3.04 (m, 1H,  $CH_2$ ), 4.18–4.25 (m, 2H,  $CH_2$ ). <sup>13</sup>C NMR  $\delta$  ( $CDCl_3$ ) ppm: 24.5; 26.8; 34.2; 33.9; 45.7; 48.4; 75.2. IR (film)  $\nu$  ( $cm^{-1}$ ): 1641, 1277, 910.



## 9. Appendix II

## 9.1. Presentation of work

O'Sullivan S, Wang J, Harmon S, Gilmer JF, Medina C. Novel barbiturate-nitric oxide donor compounds inhibit matrix metalloproteinase-9 upregulation in intestinal inflammation. All Ireland School of Pharmacy 34<sup>th</sup> research seminar, University College Cork, Ireland. 2<sup>nd</sup>-3<sup>rd</sup> April, 2012 (Poster)

O'Sullivan S, Wang J, Harmon S, Gilmer JF, Medina C. Barbiturate-nitrate compounds inhibit matrix metalloproteinase-9 in both in-vitro and in-vivo models of inflammatory bowel disease. All Ireland School of Pharmacy 35<sup>th</sup> research seminar, University of Ulster, Northern Ireland. 25-26<sup>th</sup> March, 2013 (Oral)

O'Sullivan S, Wang J, Gilmer JF, Medina C. Barbiturate-nitrate hybrids inhibit matrix metalloproteinase-9 in intestinal inflammation. The 6<sup>th</sup> annual meeting of the Irish Epithelial Physiology Group (IEPG), Newpark Hotel, Kilkenny, 24-25<sup>th</sup> October, 2013 (Oral)

Hall B, Holleran G, O'Sullivan S, Smith S, Medina C, McNamara D. Crohn's disease in an Irish population – a pilot genotype-phenotype analysis. 9<sup>th</sup> Congress of European Crohn's and Colitis Organisation (ECCO), Bella center, Copenhagen, Denmark. 20<sup>th</sup>-22<sup>nd</sup> February, 2014 (Poster)

O'Sullivan S, Wang J, Gilmer JF, Medina C. Inhibition of matrix metalloproteinase-9 in intestinal inflammation by barbiturate-nitrate hybrids. 9<sup>th</sup> Congress of European Crohn's and Colitis Organisation (ECCO), Bella center, Copenhagen, Denmark. 20<sup>th</sup>-22<sup>nd</sup> February, 2014 (Poster)

## 9.2. Publications

J. Wang, S. O'Sullivan, S. Harmon, R. Keaveny, M.W. Radomski, C. Medina, J.F. Gilmer, Design of barbiturate-nitrate hybrids that inhibit MMP-9 activity and secretion, *J Med Chem*, 55 (2012) 2154-2162.

S. O'Sullivan, C. Medina, M. Ledwidge, M.W. Radomski, J.F. Gilmer, Nitric oxide-matrix metalloproteinase-9 interactions: Biological and pharmacological significance: NO and MMP-9 interactions, *Biochim Biophys Acta*, 1843 (2013) 603-617.

Radziwon-Balicka A, Santos-Martinez MJ, Corbalan JJ, O'Sullivan S, Treumann A, Gilmer JF, Radomski MW, Medina C. Mechanisms of platelet-stimulated colon cancer invasion: role of clusterin and thrombospondin 1 in regulation of the P38MAPK-MMP-9 pathway, *Carcinogenesis*. 2014 Feb;35(2):324-32. Epub 2013 Oct 1.

O'Sullivan S, Medina C. Matrix metalloproteinases in intestinal inflammation (an update). *Mediators Inflamm*, 2014 (Commissioned)

O'Sullivan S, Gilmer JF, Medina C. Barbiturate-nitrate hybrids inhibit MMP-9 gene expression in a sGC/cGMP dependent manner (In preparation)

O'Sullivan S, Gilmer JF, Medina C. Barbiturate-nitrate hybrids reduce the severity of DSS induced colitis in rats through MMP-9 inhibition (In preparation)